Contributions of Fever to Tissue Repair in Teleost Fish

by

Amro M. Soliman Sherif

A thesis submitted in partial fulfillment of the requirements for the degree of

Doctor of Philosophy

in

Physiology, Cell and Developmental Biology

Department of Biological Sciences
University of Alberta

Abstract

Fever is a physiological defense mechanism against infection associated with a rise in host's temperature. Febrile responses are evolutionarily conserved through millions of years, taking place in both warm-blooded and cold-blooded vertebrates that share common biochemical pathways for fever induction. Ectotherms, unlike endotherms, rely entirely on behaviour to raise their body temperatures by translocating to warmer environments. Despite fever's long-standing role in host survival, as displayed in several animal experiments and clinical trials, the underlying mechanisms remain poorly understood. Historically, a shift away from a pathogen's preferred temperature and global activation of the immune system were proposed. However, the reported capability of microbes to thrive at fever-range temperatures and detrimental inflammation-associated tissue damage in case of overall augmentation of immune responses undermine these assumptions. Therefore, a debate on the net value of fever to health continues to permeate the literature, which was further compounded by limitations in available experimental models effectively replicating natural physiological processes driving and maintaining fever. The commonly utilized endothermic models employing fever-range hyperthermia provided valuable insights into the thermal regulation of innate and adaptive immunity. However, physiological stress coupled with mechanical hyperthermia or off-target effects accompanying antipyretics use in these models intervened with intrinsic pathways, altering immune and homeostatic regulatory effects prompted by febrile responses.

In this study, I took advantage of a cold-blooded teleost fish model with the advantage of natural kinetics for fever induction and regulation as well as wide-ranging

tolerated temperatures to investigate the ability of a febrile response to enhance restoration of tissue integrity and homeostasis. A custom swim chamber, combined with high-resolution quantitative positional tracking, demonstrated consistency in the preference of infected fish for higher temperatures. A self-resolving *Aeromonas veronii* cutaneous infection allowed for examination of the impact of fever on inflammatory and subsequent proliferative phase of tissue repair that necessitates proper resolution of inflammation. This was achieved through *in vivo* and *in vitro* assays, including histopathological, gene expression, immune functional and proliferation analyses.

Results reveal a novel intrinsic fever capacity to promote restoration of tissue homeostasis upon infection. Fish exerting behavioural fever demonstrated enhanced kinetics of leukocyte recruitment to the infection site and significantly improved bacterial clearance, despite *A. veronii* growing better at higher temperatures. We further characterized selectivity in the induction of protective immune mechanisms during febrile response that correlated less inflammation-associated collateral injury. Marked differences in the expression of inflammatory mediators were observed under fever and non-fever conditions. Additional robustness of inflammation control and upregulation of pro-resolution cytokines promoted the shift toward proliferation stage. Fever fish showed enhancements of wound closure, re-epithelialization and collagen deposition. These attributes were coupled with remarkable upregulation of growth factors and efficient epidermal and dermal healing. Fever-range hyperthermia, commonly used to study fever, and mechanical replication of behavioural fever's thermal pattern recapitulated some but not all benefits achieved during natural host-driven dynamic thermoregulation.

Together, my findings show that fever is not a by-product of inflammation but an integrative host response that regulates inflammatory and proliferative phases of tissue healing, contributing significantly to restoring tissue homeostasis subsequent to infection. They further underscore the significant role of febrile responses in host defense and provide a better understanding of fever biology and the underlying mechanisms of its survival capacity.

Preface

This thesis is an original work by Amro M. Soliman unless otherwise stated. My research project received ethical approval from the University of Alberta Ethics Board. Animal use and care protocols for this project, including this thesis, can be found under Protocol #706 entitled "Comparative biology of fish phagocytic antimicrobial responses". This research was funded through the following National Sciences and Engineering Research Council of Canada (NSERC) grant awarded to Dr. Barreda (RGPIN-2018-05768).

Parts of the research conducted in this thesis have been published (or in the process of publication) in peer-reviewed journals as follows:

Chapter I:

- **Soliman, A. M.**, & Barreda, D. R. (2023). Acute inflammation in tissue healing. *International Journal of Molecular Sciences*, 24; 641.
- **Soliman, A.M.**, & Barreda, D. R. The acute inflammatory response of teleost fish. Submitted to *Development and Comparative Immunology*.

Chapters II and III:

- **Soliman, A. M.**, Yoon, T., Wang, J., Stafford, J. L., & Barreda, D. R. (2021). Isolation of skin leukocytes uncovers phagocyte inflammatory responses during induction and resolution of cutaneous inflammation in fish. *Frontiers in Immunology*, 12; 725063.
- Haddad, F.*, **Soliman, A. M.***, Wong, M. E., Albers, E. H., Semple, S. L., Torrealba, D., Heimroth, R. D., Nashiry, A., Tierney, K. B., & Barreda, D. R. (2023). Fever integrates

antimicrobial defences, inflammation control, and tissue repair in a cold-blooded vertebrate. *eLife*, 12; e83644.

* *Authors contributed equally to this work, and parts of this paper will be published in Haddad, F. thesis.*

Chapters IV and VI:

- Haddad, F.*, **Soliman, A. M.***, Wong, M. E., Albers, E. H., Semple, S. L., Torrealba, D., Heimroth, R. D., Nashiry, A., Tierney, K. B., & Barreda, D. R. (2023). Fever integrates antimicrobial defences, inflammation control, and tissue repair in a cold-blooded vertebrate. *eLife*, 12; e83644.

  * *Authors contributed equally to this work, and parts of this paper will be published in Haddad, F. thesis.*

Chapters V:

- **Soliman, A. M.**, Haddad, F., & Barreda, D. R. Mechanical fever enhances protection against *Aeromonas* infection in teleost fish. Manuscript in progress.

Other collaborative publications:

- Wang, J., **Soliman, A.M.**, Norlin, J., Barreda, D.R., Stafford J.L. (2023). Expression analysis of Carassius auratus-leukocyte-immune-type receptors (CaLITRs) during goldfish kidney macrophage development and in activated kidney leukocyte cultures. *Immunogenetics,* 75; 171–189.
- Joshi, R., **Soliman, A.M**., Haddad, F., Barreda D.R. Precise evaluation of cell death through a modified annexin V/propidium iodide apoptosis protocol using Flow Cytometry. Submitted to *Methods in Molecular Biology*.

Acknowledgment

The journey through my PhD program has been exciting and so much rewarding. With several challenges and failures along the way in the last few years, it would not have been possible to complete it without the help and support of many people. Therefore, all the appreciation and gratitude to these wonderful individuals, as well as the great University of Alberta with its administration, facilities and generous funding, made my graduate studies an outstanding experience.

I would like to thank my supervisor and mentor, Dr. Daniel Barreda, for his support, guidance, advice, suggestions, funding, opportunities and patience. Since I joined the lab, Dan has always been there for me, guiding me through many steps of the program with not only his rich and great professional research expertise but also a wonderful life experience. With his help, I managed to overcome several challenges and accomplish many achievements, including getting two Alberta Graduate Excellence Scholarships, among other awards. Special thanks to my committee members: Dr. Ted Tredget and Dr. Richard Uwiera, for their treasured support and mentorship that were influential in shaping my experimental methods and critiquing my results. I further extend my thanks and gratitude to the external examiner Dr. Matthew Rise, and the arm-length examiner Dr. Norman Neumann, and the chair Dr. Warren Wakarchuk for their contribution. Also, to my candidacy exam committee members: Dr. Debbie McKenzie, Dr. Ted Allison and Dr. George Owttrim.

I would like to thank my dear friends and lab mates: Farah Haddad, Dr. Shawna Semple, Emilie Albers, Reema Joshi, Matthew Michnik, Wanwei He, Dale Archer, Ethan

Proctor, Dr. Parsa Kamely, Dr. Juan More-Bayona, Dr. Débora Torrealba and Dr. Asif Nashiry. Thank you, guys, for all the wonderful times in the lab and out, your advice and chumminess when things got rough. I couldn't have wished for better company in the lab. Thanks for a beloved time spent together in the lab and in other social settings.

I further had the opportunity to collaborate with great scientists throughout the course of my degree. Special thanks to Farah Haddad for performing the behavioural analysis in this study. Many thanks to Dr. James Stafford and Jacob Wang (UofA) for providing me with an opportunity to expand my research. I also want to thank Taekwan Yoon and Amber Ali for their valuable help and contributions to this project. I would like to extend my gratitude to the aquatic facility staff. Special thanks to Tad Plesowicz, Lauresha Kepuska, Sarah Collard and Carol Boechler for their great effort in maintaining the fish essential for the experiments.

Finally, to my wonderful family, my father, Dr. Mohamed Soliman, my sweet mother, my lovely wife Israa, my son Anas and my brothers Osama and Hisham, thank you for your endless encouragement and support and for keeping me level-headed and motivated. Love you, my sweet family.

Table of Contents

List of Tables

List of Figures

List of Abbreviations

AKT	Protein kinase B
ATPT	Annular thermal preference tank
Ccl	Chemokine (C-C motif) ligand
CCN	Cellular communication network factor
Ccr	CC-chemokine receptor
CFUs	Colony forming units
cGAS	Cyclic GMP-AMP synthase
CLRs	C-type lectin receptors
CNS	Central nervous system
Col1a2	Collagen 1 a2
Col3a1	Collagen 3 a1
COX	Cyclooxygenase
Cxcl	Chemokine (C-X-C motif) Ligand
Cxcr	Chemokine (C-X-C) motif receptor
DAF-FM DA	4-Amino-5-Methylamino-2',7'-Difluorofluorescein Diacetate
DAMPs	Damage-associated molecular patterns
DETCs	Dendritic epidermal T cells
DSBs	Double-strand breaks
DUOX	Dual oxidase
ECM	Extracellular matrix
ECs	Endothelial cells
EDU	2'-Deoxy-5-ethynyluridine
Egf	Epidermal growth factor
ERK	Extracellular signal-regulated kinase
Fgf	Fibroblast growth factor

Gcsf	Granulocyte colony-stimulating factor
Gmcsf	Granulocyte–macrophage colony-stimulating factor
Gpcrs	G-protein coupled receptors
GPI	General paralysis of the insane
H_2O_2	Hydrogen peroxide
Hgf	Hepatocyte growth factor
HR	Homologous recombination
Hsf	Heat shock factor protein
Hsp	heat shock protein
Hspg	Heparan sulfate-carrying proteoglycans
IBD	Inflammatory bowel disease
Ido	Indolamine 2,3 dioxygenase
Ifn	Interferon
Igf	Insulin-like growth factor
Il	Interleukin
IPNV	Infectious pancreatic necrosis virus
Irf	Interferon regulatory factor
JNK	C-Jun N-terminal Kinase
Kgf	Keratinocyte growth factor
LPS	Lipopolysaccharide
MAPK	Mitogen-activated protein kinases
Mcp	Monocyte chemoattractant protein
MGFL-15	Modified goldfish Leibovitz's L-15
MHC	Major histocompatibility complex
Mmp	Matrix metalloprotease
MRTFA	Myocardin related transcription factor A
MT	Masson’s Trichrome
MyD88	Myeloid differentiation primary response 88

NE	Norepinephrine
NF-κB	Nuclear factor-kappa B
Ngf	Nerve growth factor
NLRs	Nucleotide-binding oligomerization domain-like receptors
NO	Nitric oxide
NOS	Nitric oxide synthase
NOX	NADPH oxidase
NSAID	Nonsteroidal anti-inflammatory drug
NTRK1	Tropomyosin-related kinase receptor 1
NTS	Nucleus of the solitary tract
OVLT	Organum vasculosum laminae terminalis
PAMPs	Pathogen-associated molecular patterns
PBS	Phosphate-buffered saline
Pdgf	Platelet-derived growth factor
PG	Prostaglandin
PGES1	Prostaglandin E synthase 1
PI3K	Phosphatidylinositol-3-kinase
PMN	Polymorphonuclear leukocyte
PRRs	Pattern recognition receptors
PSGL	P-selectin glycoprotein ligand
Rac1	RAS-related C3 botulinum toxin substrate 1
RLRs	Retinoic acid-inducible gene I like receptors
RNS	Reactive nitrogen species
ROS	Reactive oxygen species
STAT3	Signal transducer and activator of transcription 3
STING	Stimulator of interferon genes
Tgf	Transforming growth factor
Timps	Tissue inhibitors of Mmps

TLR	Toll-like receptor
TMS	Tricaine Methanesulfonate
Tnf	Tumor necrosis factor
TRAM	TRIF-related adapter molecule
TRIF	Toll/Il1R domain-containing adaptor-inducing INFB
Vegf	Vascular endothelial growth factors
Vegfr	Vascular endothelial growth factor receptor
Viperin	Virus inhibitory protein endoplasmic reticulum-associated interferon-inducible
VSV	Vesicular stomatitis virus

Chapter I

Introduction and literature review[†]

[†] Parts of this chapter have been published or in the process of publication in

- **Soliman, A. M.** & Barreda, D. R. (2023). Acute inflammation in tissue healing. *International Journal of Molecular Sciences*, 24; 641.
- **Soliman, A.M.**, & Barreda, D. R. The acute inflammatory response of teleost fish. Submitted to *Development and Comparative Immunology*.

1.1. Introduction

Fever is a physiological immune mechanism against infection characterized by a rise in body temperature [1]. Febrile response is evolutionarily conserved through millions of years, which supports its value to host survival. Fever was described as early as 400 BC by Hippocrates to possess a superior healing capacity in treating diseases [2]. Additionally, the expanding literature since the mid-1970s has consistently recounted the significant role of fever in reducing morbidity and mortality rates, as exhibited in animal experiments and clinical trials [3,4]. These observations suggested a capacity of fever to enhance immune responses and achieve effective return to homeostasis. Yet, these assumptions and their underlying mechanisms are not fully determined, leading to an ongoing debate as to whether fever is net positive or negative to health. This is further complicated by the current gaps in our understanding of fever's biology compounded by limitations in available experimental models that can effectively recapitulate the natural physiological processes driving and sustaining fever. For instance, although the commonly utilized endothermic mammalian models (e.g., mice, rats and rabbits) have provided valuable insights into the thermal regulation of immune responses [3], these models are associated with physiological stress resulting from mechanically-induced hyperthermia in addition to off-target effects of antipyretics used to suppress fever [3,5,6], which ultimately interfered with the host's intrinsic febrile responses. This, in turn, could skew any immune or homeostatic regulatory effects prompted by fever.

Fever is classically initiated in endotherms through a humoral pathway that involves binding of damage-associated molecular patterns (DAMPs) and/or pathogen-associated

molecular patterns (PAMPs) to pattern recognition receptors (PRRs) on tissue-resident myeloid cells to trigger pro-inflammatory and antimicrobial responses [7]. Endogenous pyrogenic cytokines such as interleukin 1 (Il1), Il6 and tumor necrosis factor alpha (Tnfa) are released into the bloodstream to reach the pre-optic nucleus of the hypothalamus [8]. Pyrogens induce an increase in prostaglandin (PG)E2 levels via upregulating PGE synthase 1 (PGES1) [9]. PGE2 plays a dominant role in fever induction by blocking inhibitory neuronal pathways and initiating excitatory outputs on sympathetic neurons instigating vasocontraction of peripheral blood vessels, muscle shivering and thermogenesis [10]. Since its discovery, fever has been described to exist only in warm-blooded animals. Yet, in 1974, Vaughn *et al.*, followed by other researchers, reported fever in cold-blooded animals (e.g., amphibians, reptiles and fish) [11–17], where they behaviourally translocate to warmer environments to increase their body temperatures, i.e., behavioural fever. Interestingly, mechanisms driving fever, including the engagement of the central nervous systems (CNS) and PGE2, are shared and well-conserved between endotherms and ectotherms [18]. Thereby, behavioural fever models represented a unique opportunity to examine the potential impact of fever on immune responses and restoration of tissue homeostasis via controlling the environmental temperatures surrounding the ectothermic model. These models avoid physiological stresses associated with manipulating hypothalamic temperature set-point. Additionally, they circumvents the pharmacological off-target effects accompanying the use of antipyretics in endotherms [3].

Restoration of tissue homeostasis following an injury induced by physical damage and/or infection is achieved via tissue repair [19], a complex biological process that involves

interactions between immune and connective tissue cells. Together, these cells and several humoral factors accomplish sequential phases, comprising inflammation and proliferation, to restore damaged tissue. Following an injury, tissue is infiltrated with leukocytes recruited by pro-inflammatory cytokines (e.g., Il1b and Tnfa) and chemokines such as Chemokine C-X-C motif Ligand 8 (Cxcl8), also known as Il8 [20]. Immune cells combat pathogens via defense mechanisms, such as phagocytosis and antimicrobial responses, e.g., nitric oxide (NO) and reactive oxygen species (ROS) [21]. Following eradication of infection, tissue-resident cells secrete anti-inflammatory cytokines (e.g., transforming growth factor beta (Tgfb) and Il10 to induce a resolution of inflammation and a shift toward the proliferative phase of tissue repair [20]. Macrophages, among other cells, produce a variety of growth factors, including vascular endothelial growth factor (Vegf), insulin like growth factor 1 (Igf1), fibroblast growth factor (Fgf) and epidermal growth factor (Egf) to initiate rebuilding of damaged tissue [21,22]. These growth factors activate several tissue repair pathways to accomplish re-epithelialization [23–25], granulation tissue formation [22,26], and development of new blood vessels (angiogenesis) [27].

In this study, I utilized a behavioural fever teleost fish model to examine contributions of fever to tissue repair and their underlying mechanisms under host-driven dynamic thermoregulation. This enabled me to closely resemble natural conditions for heating and cooling; and to overcome caveats associated with the use of exogenous drugs, mechanical hyperthermia, or disruption of natural thermoregulatory response in endothermic models. Moreover, using a self-resolving *Aeromonas veronii* cutaneous infection as a tissue repair model allowed me to examine the effects of fever on the inflammatory phase as well

as the proliferation phase that requires proper resolution of inflammation. I hypothesized that fever, along with enhancing immune responses toward infection, would likewise promote restoration of homeostasis and healing of damaged tissue via activation of tissue repair machinery as a part of its advantageous host survival ability.

Results showed that fever modulated both inflammatory and proliferative phases of the repair process. Febrile responses were associated with early recruitment of leukocytes dominated by neutrophils to the infection site, followed by rapid resolution of inflammation. Moreover, recruited cells revealed marked changes in their antimicrobial profile characterized by a significant reduction in oxidative burst. During proliferation phase, I observed activation of various tissue repair pathways that are critical for the development of both epidermis and dermis layers of the skin in fever fish. I further identified a robust intrinsic capacity of fever to enhance re-epithelialization and collagen deposition. Although a manual increase in fish housing temperature to a febrile range or mechanically replicating fever's thermal pattern showed some of its modulatory effects, it did not recapitulate fever's full tissue repair capacity.

1.2. Thesis objectives

The main objective of my thesis was to characterize potential contributions of fever to restoration of homeostasis subsequent to infection by assessing fever's impact on inflammatory and proliferative phases of tissue repair. This was complemented by dissecting underlying mechanisms by which fever can modulate immune and reparative pathways to

influence bacterial clearance, wound closure, development of epidermis and dermis layers of the skin using a behavioural fever model. My research focused explicitly on assessing contributions of dynamic behavioural fever to several tissue repair events compared with a basal static housing temperature and fixed static high (fever-range) temperature in goldfish challenged with *Aeromonas veronii* cutaneous infection. These events, for example, involved expression level of inflammatory cytokines, leukocyte recruitment, inflammation resolution, pathogen clearance, re-epithelialization, mature collagen (type I) deposition and growth factors profile. Specific aims of my thesis were: (1) to characterize kinetics of wound healing and behavioural fever pattern in *A. veronii* infected goldfish; (2) to determine the impact of fever on the inflammatory phase of tissue repair; (3) to determine the effects of fever on the proliferative phase of tissue repair; (4) to determine the feasibility of replicating fever's reparative benefits through mechanical means.

1.3. Thesis outline

My thesis comprises six chapters. The first chapter is an introduction and literature review where I discuss what we know so far about fever and the current gaps in the literature about its biology. Additionally, I briefly highlight the main mechanisms and stages of tissue repair as well as the significant contribution of acute inflammatory response to healing outcomes. The second chapter describes the materials and methods utilized in my thesis. The third chapter focuses on describing wound healing kinetics in goldfish as well as characteristics of behavioural fever response in fish infected with *Aeromonas veronii*. This

chapter provides a foundation for the following chapters, where I discuss fever's modulations of the healing process. The fourth chapter encompasses the core part of my research, where I highlight the impact of fever on inflammatory and proliferative phases of tissue repair. The fifth chapter largely emphases the effects of mechanical replication of fever on tissue repair. The sixth chapter summarizes the main findings and discusses relevance and future directions.

1.4. Literature review: Fever and tissue repair

1.4.1. Introduction

The conservation of fever through millions of years of evolution was supported by the discovery of behavioural fever since most ectothermic vertebrates, representing the majority of animal species, do not have the capacity to increase their body temperature metabolically as in the case of endotherms. The revealed intrinsic ability of ectotherms to migrate to higher temperature environments provided an alternative to achieve a fever state by which ectotherms can enhance their survivability when infected. The evolutionarily conserved deployment of fever in both endotherms and ectotherms in response to infection indicated fever as an essential physiological defense mechanism. This was further supported by several observations showing a fever-associated increase in survival rates in a variety of animals challenged with diverse pathogens [28], in addition to clinical studies correlating the rise in mortality rates with suppression of fever in critically ill patients [4].

Fever-range temperatures were reported to influence inflammatory responses by modulating various components of innate and adaptive immunity [3,4]. These studies utilized endothermic models where mechanical hyperthermia and antipyretics were employed. The utilization of a behavioural fever model in the Barreda lab provided an opportunity to study fever as a widely evolutionarily conserved febrile response and allowed for characterization of significant immunomodulatory effects of fever deprived of dysregulation of normal febrile responses. Still, the host has to ensure an effective return to homeostasis [3]. Therefore, I hypothesized fever to achieve effective restoration of tissue integrity by tightly regulating immune responses avoiding extensive collateral tissue damage and effective tissue healing as a mechanism of its survival capacity.

Tissue repair is a biological process by which a host mediates healing of injured tissue induced by physical damage and/or infection [19]. The process entails an overlapping sequence of cellular and molecular events following a tissue lesion to restore damaged tissue and its function [21]. Wound healing represents a good model of tissue repair since it encompasses the majority of healing events occurring in other parts of the body and the comparatively easy assessment of wound closure and signs of healing. Therefore, I used an *A. veronii* cutaneous infection model to investigate tissue repair under fever and non-fever conditions. The inflammatory and proliferative phases of wound healing are sequential events regulated by a complex network of cytokines and growth factors [29]. Major events involve leukocyte recruitment, inflammation control, fibroblast proliferation, collagen deposition, angiogenesis and re-epithelialization [30].

1.4.2. Fever

Fever, also known as pyrexia, is a state of increased host core temperature beyond its normal range to function as a physiological defensive mechanism against infection [3]. Fever differs from hyperthermia despite both being associated with an elevated body temperature above the host's thermopreferendum. During fever, the temperature rise is regulated centrally by the hypothalamus through thermoregulatory mechanisms in response to infection with a strong association of sickness behaviours. In hyperthermia, the process is induced by excessive heat production, disruption of heat dissipation means or exogenous gain of heat increasing host's temperature that is not regulated by CNS [31,32]. For example, hyperthermia can be triggered due to pharmacological or pathological impairments of thermoregulation pathways mediating heat loss [33]. Another form of hyperthermia, commonly utilized in endothermic models investigating fever, is fever-range hyperthermia, where these animals are exposed to external heat sources [3]. Fever is markedly distinctive from these forms of hyperthermia being induced by pyrogenic cytokines and inhibited by antipyretics. In contrast, hyperthermia lacks these characteristics, indicating that only fever is generated due to an upward displacement of the hypothalamic set point [31,34].

Since antiquity, fever has been considered a hallmark and a cardinal symptom of several inflammatory and infectious diseases. The relationship between infection and host's temperature was even detected in plants, where the temperature of bean plant's leaves was found to increase by approximately 2°C during fungal infection [35]. Great scholars such as Parmenides described fever as early as 500 BC: "Give me the power to produce fever and I'll cure all disease" [2]. Hippocrates also highlighted the fever's beneficial therapeutic effects

on epilepsy; likewise, Galen reported the capacity of fever to cure Melancholia [36]. In 1927, Austrian psychiatrist Julius Wagner-Jauregg won a Nobel prize in medicine and physiology for utilizing fever generated by malaria infection to treat syphilis-induced general paralysis of the insane (GPI). Following that, fever started gaining prevalent interest and attracted the scientific community to investigate its biology and possible contributions to biological processes such as immune responses.

The long-standing conservation of fever despite the associated energy loss [37] and high risk of predation [38], caused by increased metabolism and lethargy/sickness behaviours, suggested its significant role in defense against infection. Yet, fever was viewed for many years as an undesirable sign of inflammation. This is owing to gaps in our understanding of its biology and the lack of valid experimental models to fill those gaps. As a result, fever is commonly suppressed by anti-inflammatory and antipyretic medications by the public as well as in clinical settings [39,40] to avoid distress and discomfort. It is worth mentioning that there are severe pathological forms of fever where body temperature is above the normal febrile range and persists for prolonged durations. Managing these cases via external cooling or antipyretics is essential to avoid neurological complications and other organ failures [41,42]. My focus in this research is on the most common milder forms of febrile responses.

1.4.2.1. Fever in endotherms

Fever is classically induced in endothermic vertebrates metabolically through a humoral pathway along with behavioural changes such as lethargic sickness behaviour and seeking warmth. This comes at a high metabolic cost since a rise in body temperature by 1°C is associated with about a 10% increase in metabolic rate [43]. The initiation and maintenance of fever in response to infection are achieved through complex coordination between the innate immune system and CNS, particularly the hypothalamus [8], in addition to the peripheral nervous system [44].

1.4.2.1.1. Humoral and neuronal regulation of fever

1.4.2.1.1.1. Humoral pathway

Subsequent to infection, recognition of exogenous pyrogens such as PAMPs and DAMPs by PRRs, including toll-like receptors (TLRs) on tissue-resident leukocytes, triggers pro-inflammatory and antimicrobial responses [7,8,45]. These leukocytes involve neutrophils, macrophages and dendritic cells [46]. Upon their activation, these immune cells secrete endogenous pyrogens such as Tnfa, Il1b, Il6 and interferon gamma (Ifng) to be released into the bloodstream [9,47,48]. Il6 levels are enhanced by both Il1b and Tnfa [49], and it was reported to be the primary mediator inducing fever [50]. This was clearly shown in mice challenged with lipopolysaccharide (LPS) that were unable to generate fever, regardless of high levels of Tnfa and Il1b, when Il6 was neutralized either by knockout or antibodies [51,52].

Endogenous pyrogens travel through the bloodstream to CNS, particularly the preoptic-anterior hypothalamic area, via active transendothelial transport or through *organum vasculosum laminae terminalis* (OVLT) that is deficient of a blood-brain barrier [53,54]. Through activation of nuclear factor-kappa B (NF-κB) [55] and signal transducer and activator of transcription-3 (STAT3) [56] in endothelial cells of anterior hypothalamus, pyrogens induce upregulation of cyclooxygenase 2 (COX2) [55] and PGES1 [57] enzymes. These enzymes promote the synthesis of PGE2. Other researchers suggested that PAMPs can directly bind to TLRs on brain endothelial cells, thus increasing PGE2 levels [58,59].

PGE2 retains a key role in inducing and sustaining fever [60]. Injection of PGE2 directly into the ventricles of rabbits and cats led to a rise in their body temperature [61]. Other experiments established the significance of PGE2 in fever induction by utilizing PGE2 inhibitors [62,63]. The biosynthesis of PGE2 involves three successive steps: (1) arachidonic acid is produced by phospholipase A2 enzyme; (2) COX enzyme converts arachidonic acid into PGG2 and then into PGH2; (3) PGES1 enzyme metabolizes PGH2 into PGE2 [64]. While there are two forms of COX enzymes (COX1 and COX2), COX2 is commonly expressed in response to inflammation [65]. PGE2 can also be produced peripherally by tissue-resident macrophages, in addition to being locally generated in the brain, to travel through the bloodstream to reach CNS [62]. Several studies detected peaked levels of PGE2 in fish plasma during behavioural fever [66,67].

PGE2 binds to its receptors located on neurons of the preoptic nucleus. Among several types of PGE2 receptors [68], EP3 is the most crucial [69]. EP3 receptors activate GABAergic neurons that provoke inhibitory functions on the dorsomedial nucleus of the

hypothalamus [10,70]. Blocking downstream neurons of the dorsomedial nucleus generates excitatory outputs towards sympathetic neurons, enhancing the release of norepinephrine (NE) [10]. NE induces peripheral vasoconstriction and intrinsic thermogenesis of brown adipose tissue resulting in heat production and conservation. Furthermore, somatomotor neuron activation promotes acetylcholine release to induce skeletal muscle shivering [71]. Collectively, thermogenesis, vasoconstriction and shivering cause a rise in body core temperature [71].

1.4.2.1.1.2. Neural pathway

A neural pathway was alternatively proposed for fever induction in endotherms, yet to be characterized in ectotherms. PGE2 stimulates peripheral sensory neurons, including Trigeminal [72] and Vagus [73] nerves. These neurons synapse with the nucleus of the solitary tract (NTS), where stimulatory signals reach the ventral noradrenergic part of the preoptic nucleus of anterior hypothalamus to release NE, thus energizing the synthesis of PGE2 [44]. Notably, the neural pathway is suggested to be accountable for the short-term onset of fever [8].

1.4.2.1.2. Thermoregulatory behaviours in endotherms

Despite the classical metabolic induction of fever in endotherms/humans, various accompanying behavioural responses have been documented to be deployed, thus assisting in heat conservation or cooling. These behaviours are likely triggered by the hypothalamus

via temperature sensing [74,75] to achieve comfort based on the hypothalamic set-point of temperature. Searching for warmer environments entails sunbathing, crouching (in animals) and wearing more clothes (in humans), whereas seeking shade, wallowing, panting and bird bathing are utilized to avoid hyperthermia [76].

1.4.2.1.3. Limitations of endothermic fever models

The majority of studies investigating the impact of fever on immune responses largely utilized *in vivo* and *in vitro* mammalian endothermic models. Researchers in these experiments examined thermo-immunomodulation via employing a fever-range whole-body mechanical hyperthermia, i.e., manually increasing the host's temperature to a febrile range using exogenous heat [77,78]. These techniques managed to highlight the significant impact of fever-range hyperthermia on both innate and adaptive immune arms [3]; nevertheless, it does not take into consideration the contributions of cytokines and lipid mediators generated during fever. Another caveat of this approach is the physiological stress induced by external heat and manipulating hypothalamic temperature set-point, which could bias the results [79]. For example, glucocorticoids generated during thermal stress via the hypothalamic-pituitary-adrenal axis have immunosuppressive effects, which can influence leukocyte migration, inflammatory cytokines profile and cell-mediated adaptive immune responses [80,81].

On the other hand, stress-generated sympathetic activation could have additional, premature, or excessive triggering of pro-inflammatory pathways [82]. Moreover, protective cooling mechanisms activated following external heat application ultimately interfere with

various regulatory pathways. Suppression of fever in endothermic models is primarily achieved via pharmacological inhibition using antipyretics. These drugs were shown to have side and off-target effects that could disrupt inflammatory programs, representing another challenge in establishing the adaptive value of fever [83–85]. Likewise, although applying external heat to *in vitro* cell lines can demonstrate the outcome of thermal applications in individual cell types, it neglects other extracellular factors and interplays/crosstalk with other cells. Collectively, stress- or antipyretics-associated alterations of immune responses during hyperthermia in mammalian models led to an unestablished determination of potential immunomodulatory effects of fever.

1.4.2.2. Fever in ectotherms

Cold-blooded animals possess the ability to translocate to environments of higher temperatures, above their final thermal preference, in response to infection [18]. Fever in ectotherms was discovered for the first time by Vaughn *et al*., who described a relocation of *Dipsosaurus dorsalis* (desert iguana) to warmer zones when infected with killed Gram-negative *Aeromonas hydrophila* [11]. Following that, researchers characterized behavioural fever in a variety of other ectothermic vertebrates based on their migration to higher temperature environments using various behavioural assessment systems. The list includes but is not limited to (1) **amphibians**: toads [86,87] and frogs [88]; (2) **reptiles**: lizards [11,89–91] and snakes [13]; (3) **fish**: goldfish [12,16,17,92], zebrafish [66,93] and rainbow trout [94]. Additionally, **invertebrates** such as bees [95,96] showed a fever response.

Surprisingly, some newborn mammals, such as rabbits, were shown to generate fever behaviourally when they lacked the metabolic toolkit [97].

Conflicting data were reported demonstrating that behavioural fever was lacking in some ectotherms challenged with killed bacteria, parasites or pyrogens. This was shown in fish [98], lizards [99], turtles [100] and snakes [101]. A number of factors could have influenced these observations, including the temperature gradient system used in the experiment and doses of the stimulants [43,102]. For instance, alligators (*Alligator mississippiensis*) that were injected intraperitoneally with *A. hydrophila* led to a behavioural increase in their body temperature; though, the administration of the same dose of a Gram-positive bacterium, *Staphylococcus aureus* did not provoke fever [14], which suggested that a higher dose of *S. aureus* might have been required to prompt a febrile response.

1.4.2.2.1. Endogenous and exogenous pyrogens in ectotherms

A number of exogenous pyrogens were used in behavioural fever experiments, and they were shown to induce a febrile response. These include several species of both Gram-positive and Gram-negative bacteria [12,89,103–107], fungi [88,108], viruses [66,67,109] and LPS [16,90,94,110]. Conversely, endogenous pyrogens are not well-characterized in ectotherms. Few studies demonstrated that pyrogenic inducers of fever in cold-blooded animals are produced by leukocytes and found in the bloodstream. This was shown when active supernatant of peritoneal leukocytes, not denatured, isolated from lizards *Dipsosaurus dorsalis* infected with *A. hydrophila* resulted in a fever response when injected into the same

lizard species [111]. Comparably, plasma of frogs (*Rana esculenta*) pre-infected with *M. ranae* bacterium was administered to frogs of the same species, that as a result, developed behavioural fever [112]. These findings indicate a potential role of peripheral prostaglandins and cytokines in fever induction in ectotherms. Yet, these pyrogens are still to be identified.

1.4.2.2.2. Regulatory pathways shared between endotherms and ectotherms

Despite the differences in fever's shape between warm- and cold-blooded animals (predominantly metabolic versus behavioural, respectively), they intriguingly share common pathways inducing febrile responses. This was supported by the attenuation of warm-seeking behaviour of some ectotherms by antipyretics [12,113], indicating joint biochemical processes driving fever in endothermic and ectothermic animals. Similar to endotherms, the preoptic area of anterior hypothalamus is considered the heat regulatory centre in the case of ectotherms, where it contains thermo-sensitive neurons [114–116]. This was established when a group of researchers induced electrolytic lesions in the preoptic nucleus, thereby suppressing behavioural fever in toads [117]. In contrast, lesions away from the area did not impact the febrile responses.

PGE2 was also found to play an important role in ectothermic fever. Injection of PGE2 into the brain of salamanders or frogs resulted in behavioural fever in those animals [112,118]. Others utilized antipyretics such as salicylic acid, indomethacin and acetaminophen to inhibit the synthesis and/or release of PGE2, which, when administered, suppressed fever in lizards, toads and fish [87,107,119]. Additionally, plasma levels of PGE2

were remarkably increased in fish during febrile responses [66,67,109]. Taken together, these results established a shared involvement of PGE2 and hypothalamus in fever induction between ectotherms and endotherms. Still, little is known about endogenous pyrogens in ectothermic animals, in addition to stimulatory neurons activated by PGE2 to trigger behavioural changes.

1.4.2.2.3. Behavioural fever in fish

In 1977, fever was reported to exist in fish (goldfish; *Carassius auratus*) for the first time [92]. Succeeding that, other fish species were shown to deploy behavioural fever in response to various stimuli (refer to **1.4.2.2 Fever in ectotherms** for more information). In parallel to other ectotherms, the body temperature of fish is principally affected by the surrounding environment. Water has a higher conductance, leading to uncontrolled exchanges of thermal energy between fish and the adjacent water through skin and gills [120]. Therefore, it is challenging for fish to maintain a core body temperature above the environmental temperatures. Also, most fish are devoid of brown adipose tissue and metabolic regulatory pathways generating heat during endothermic fever. Thereby, the vast majority of fish species continue to be ectothermic, thus retaining the ability to adapt and survive environmental stresses [121,122]. Still, different fish species have a distinct preferred range of temperatures that they can withstand without experiencing stress. These optimal temperatures further differ within the same species depending on age, season, environmental interactions, and whether they are infected [123]. In spite of their inability to generate heat metabolically in response to infection, fish can increase their body

temperatures behaviourally. This was shown to promote their survival (refer to **1.4.2.3. Fever, survival and impact of antipyretics**).

1.4.2.2.4. Occasional endothermy in ectotherms

In addition to behavioural thermoregulation, some ectotherms, identified as regional or facultative endotherms, have evolved adaptive mechanisms by which they can generate heat to maintain higher temperatures compared to those of surrounding environments. Animals, including tegu lizard [124], pythons [125], and a few fish species such as sharks, tunas, billfish, swordfish, mackerel and lamnid, are able to increase the temperature of specific tissues and/or organs via thermogenesis [121,126,127]. Fish can generate heat using particular muscles located deep and insulated by overlaying fatty tissues during locomotion and further conserve this generated heat via an intricate vascular heat exchange system [128,129]. The system comprises adjacent venules and arterioles to allow heat transfer from the warm venous blood exported from heat-producing muscles and tissues to cold blood in arterioles diverting from gills [130,131]. The heat exchange system preserves heat and foils energy loss. Other fish species, such as marlins, spearfishes and billfishes, were found to possess heat-generating tissues in the cranium along with brown adipose tissue [132,133].

Notably, regional endotherms can only generate and maintain heat for short periods, likely to empower particular vital biological functions such as food digestion, absorption, vision and intellectual functions, especially at depth [134,135]. Nonetheless, these animals lose this capacity over time and are required to exercise behavioural thermoregulation [136].

Interestingly, opah, a mesopelagic fish also known as moonfish, showed the capacity to produce thermal energy using aerobic pectoral muscles to be distributed throughout the entire body [137], representing a rare model of whole-body endothermy in ectotherms. Opahs are additionally characterized by a stacked counter-current exchange system located in fat-insulated gill arches that greatly diminish heat loss between gills and surrounding water [137].

1.4.2.3. Fever, its survival advantage and the impact of antipyretics

1.4.2.3.1. Fever promotes host survival in both endotherms and ectotherms

There is growing evidence supporting the significant role of fever in enhancing host survival subsequent to infection. This is clearly shown at the level of animal experiments, including the warm- and cold-blooded, as well as clinical trials. These experiments either compared a host under fever and non-fever conditions or the impact of inhibiting fever using antipyretics on overall survival. Among these lines of evidence, researchers reported the ability of some pathogens to inhibit fever as a part of their resistance programs. For instance, herpesvirus infection induces soluble decoy Tnf receptors expression to delay the induction of behavioural fever, thus promoting viral replication [138], which indicates a prominent role of febrile responses in disease resistance.

1.4.2.3.1.1. Survival in mammals

An increase in the mortality rate of rabbits infected with the rinderpest virus by about 55% was reported when researchers suppressed fever in those animals using a common antipyretic (acetylsalicylic acid) compared with rabbits who were left to undergo febrile responses [139]. Similarly, New Zealand white rabbits infected with *Pasteurella multocida* showed an improved survival rate when they developed fever with an increase in body temperature to less than 2.25°C. Though, there was an increase in the death rate of animals that developed a high-grade fever (more than 2.25°C) [140]. Administration of antipyretics directly into the anterior hypothalamus of rabbits infected with *P. multocida* suppressed fever, and similarly, these rabbits had a considerable increase in the mortality rate compared to the control group [141]. Others studied the impact of inhibiting fever using flurbiprofen, a nonsteroidal anti-inflammatory drug (NSAID), in goats infected with *Trypanosoma vivax*. Interestingly, most goats with fever survived (n=16); however, all the goats that were given antipyretics died (n=5) [142].

1.4.2.3.1.2. Survival in humans and medical relevance of fever suppression

With regard to clinical trials, fever was shown to be allied with improved prognoses during several bacterial infections. For example, a retrospective study of 218 patients infected with Gram-negative bacteria showed a fever-linked reduction in the death rate [143]. Likewise, in spontaneous bacterial peritonitis, patients with body temperature > 38°C were associated with an increased survival rate [144]. A similar trend was observed in clinical studies involving patients with sepsis and severe infection, where in more than 2000

patients admitted to the ICU, fever was strongly related to shorter hospital stays and lower mortality [145,146]. Recently, better survival rates have been reported in patients with COVID-19-induced acute respiratory distress syndrome when having a fever (≥39°C) [147].

The use of antipyretics to suppress fever correlated with an increased mortality rate of human populations infected with the influenza virus in the United States [148] and in critically ill patients admitted to Intensive Care Units [149,150]. Suppression of fever using paracetamol was linked to prolonged disease and late recovery in patients having chickenpox and malaria [151,152]. Likewise, the administration of NSAIDs in children and adults with respiratory infections (e.g., pneumonia) has been associated with extended hospitalization and empyema [153]. Patients experiencing hypothermia (a body temperature of 35 to 36°C) had a remarkably higher mortality rate than other groups with fever who were associated with better survival regardless of the magnitude of the fever [145,154]. The study included patients with different pulmonary, urinary, cutaneous and intra-abdominal infections. Other research groups reported a similar correlation between hypothermia and mortality in hospital-admitted patients [155,156].

On the contrary, researchers reported that controlling fever via exterior cooling in patients admitted with septic shock has decreased early mortality rates [157]. A systematic review and meta-analysis of five clinical trials reported limited evidence supporting a correlation between fever inhibition and high mortality in critically ill patients without acute neurological injury [158]. Though, authors of the review highlighted that those studies were underpowered to prove any clinically significant differences. The discrepancies in the literature are probably due to difficulties associated with human trials, in addition to several

other factors influencing the findings. For example, patients were not infected with the same or equal doses of pathogens. Moreover, infected patients did not have the same magnitude and duration of fever. Another aspect could be the origin of fever and whether it is induced by infectious or non-infectious disease. Young *et al*. showed that lowering temperature in patients with infectious diseases is likely to have a negative outcome since fever in these patients was associated with a lower risk of death [155]. Meanwhile, it was suggested that antipyretics could enhance survivability in patients with fever of non-infectious origin.

1.4.2.3.1.3. Survival in ectotherms

Cold-blooded vertebrates (amphibians, reptiles and fish) provided a unique opportunity to study the direct effect of fever on host survival and to answer some of the questions concerning fever's adaptive value. These animals can behaviourally raise their body temperatures in response to infection by translocating to warmer environments [18]. An early research attempt to examine behavioural fever's impact on survival was conducted in 1975 by Kluger's group through infecting desert iguana (*Dipsosaurus dorsalis*) with *A. hydrophila*. Researches reported that the survival rate was substantially decreased if lizards were prevented either physically [159] or via antipyretics [119] from behaviourally migrating to warmer environments. Likewise, similar observations were detected in fish. For instance, Covert *et al.* reported that behavioural fever significantly promoted the survival of *Carassius auratus* injected with *A. hydrophila* [92]. Moreover, in zebrafish (*Danio rerio*) with spring viremia of carp infection, fish that were allowed to deploy fever were associated

with a rapid viral clearance along with fewer clinical signs, contrary to fish maintained at a fixed temperature condition [66].

1.4.2.3.2. Currently proposed mechanisms of survival during fever

The expanding literature supporting fever's ability to promote host survival subsequent to infection opened the door toward characterizing the putative underlying mechanisms driving these observations. The suggested hypotheses were as follows (1) an increase in body temperature during fever is directly lethal or inhibitory to infectious microbes; (2) fever accomplishes a global activation of the immune system, including its innate and adaptive arms; (3) fever enhances a rapid and efficient return to homeostasis [3]. Although the first two parts of the hypothesis were explored widely through literature, there is limited research investigating the third part. Also, most studies examining fever focused mainly on the impact of fever-range hyperthermia on various components of innate or adaptive immunity and pathogen clearance.

1.4.2.3.2.1. Thermal restriction of pathogens

Bacteria, fungi, viruses and parasites are directly inhibited by thermal restriction, where these pathogens are exposed to a temperature that reaches or exceeds their maximum tolerated temperatures [160–163]. For instance, high temperatures (40-41°C) result in a substantial reduction in poliovirus replication rate [161] and promote the serum-induced lysis of Gram-negative bacteria [164]. Thereby, fever was suggested to unequivocally

provide a thermal inhibitory environment against microbes. Nevertheless, newly emerging infectious pathogens were shown to have the ability to tolerate a broad thermal range that is likely acquired from encountering previous similar hosts [165]. For instance, mice infected with *Klebsiella pneumoniae* displayed an improved bacterial clearance at a febrile-range temperature of 37°C. Yet, the bacteria were growing at an ideal rate in culture media at the same temperature [166]. This indicated an alternative route by which fever can reduce microbial activity, irrespective of thermal restriction, that potentially involves enhancement of immune responses.

1.4.2.3.2.2. Fever-range temperatures influence innate and adaptive immune responses

Fever is postulated to promote immune-protective mechanisms by influencing different immune system components. In response to infection, activation of acute inflammatory program that incorporates upregulation of pro-inflammatory cytokines and recruitment of innate immune cells to infection site is critical to combat pathogens via phagocytic or antimicrobial activities [167]. Despite the complexity of immune defense mechanisms, fever-range temperatures influenced almost every part of the process. For example, febrile temperature augmented neutrophil recruitment to infection sites in mice [168]. Mechanistically, granulocyte colony stimulating factor (Gcsf) was one of the main factors contributing to heat-induced neutrophil migration in addition to increasing neutrophil progenitor cells in bone marrow [169,170], which had a protective effect in irradiation-generated neutropenia in murine models. Neutrophil recruitment also depends dramatically on the levels of Cxcl8, which happens to be affected by fever-range temperature via

controlling the expression of heat-inducible transcription factor: heat shock factor protein 1 (Hsf1) [171].

The thermal component of fever enhances neutrophil extravasation through diminishing endothelial barrier integrity regulated by extracellular signal-regulated kinase (ERK) and mitogen-activated protein kinases (MAPKs) [172]. In addition to augmenting neutrophil accumulation at the infection site, fever-range hyperthermia empowers their respiratory burst and bactericidal activities Likewise, exposing human neutrophils to fever-scale hyperthermia for a short period increased their released neutrophil extracellular traps (i.e., NETosis) and ROS activity in response to *P. aeruginosa* challenge [173]. RAW 264.7 cells were found to be more protected against vesicular stomatitis virus (VSV)-induced cytotoxicity *in vitro* when exposed to a fever-range temperature of 39.5°C compared with cell lines that were kept at 37°C [174]. Researchers also detected a heat-induced upregulation of cyclic GMP-AMP synthase (cGAS)-stimulator of interferon genes (STING) pathway, resulting in an increased production of interferon beta (Ifnb). Similar results were found *in vivo*, when mice held at 39.5°C were injected with the virus along with an antiviral agent (DMXAA); they showed higher levels of Ifnb and better survival [174].

Added to promoting the innate immune arm, fever-range temperatures can influence the bridging to and the development of adaptive immune responses. For example, higher temperatures markedly enhanced the phagocytic ability of dendritic cells and their Ifng production [175,176]. These data are in accordance with the heat-induced increase in major histocompatibility complex (MHC) class I and II that help activate T helper cells [177–179]. Elevated temperatures further promote the translocation of dendritic cells to lymph nodes via

enhancing the sensitivity of CC-chemokine receptor 7 (Ccr7) to CC-chemokine ligand 21 (Ccl21) [180,181], suggesting a potential role of febrile-range temperatures in positioning dendritic cells in lymphoid organs for antigen presentation. This was clearly shown in the capacity of dendritic cells isolated from heat-exposed mice to stimulate T cells [177].

1.4.2.3.2.3. Currently projected immunomodulation of behavioural fever

Behavioural fever model presented a powerful approach to examine the mechanistic contribution of fever to survival via assessing its impact on immune responses under host-driven thermoregulation. This allowed for a closer resembling of natural heating and cooling conditions and overcoming caveats associated with endothermic models (refer to **1.4.2.1.3. Limitations of endothermic fever models**). Among early studies, Kluger *et al*. reported that behavioural fever in lizards enhanced defense mechanisms and lowered mortality rates [159]. Several research groups then utilized various behavioural fever models, including fish, to study febrile responses [28]. Multiple reports in 1970s revealed enhanced survivability of fish infected with different pathogens, including viruses, when allowed to deploy behavioural fever [92,182,183]. More recently, behavioural fever in *Oncorhynchus mykiss* (rainbow trout) was shown to promote inflammatory responses via upregulating *il1b* in response to LPS injection compared to fish held at a constant temperature [94]. Likewise, Atlantic salmon (*Salmo salar*) challenged with infectious pancreatic necrosis virus (IPNV) revealed a considerable upregulation of pro-inflammatory cytokines, including *tnfa*, *il6* and *il1b* during behavioural fever [109].

Other researchers reported that behavioural fever in zebrafish (*Danio rerio)* challenged with synthetic dsRNA (poly I:C) was associated with significant and temperature-dependent alterations in brain transcriptome. Significant differences in the expression levels of neuroregulatory elements, including acetylcholinesterase and α7 nicotinic acetylcholine receptor, were detected amongst fever and non-fever fish [66]. Investigators concluded that behavioural fever inhibited anti-inflammatory reflex, thereby decreasing inhibitory output and promoting antiviral activity via acting at the gene-environment level. On the other hand, fish not permitted to choose their preferred temperatures demonstrated a reduced survival rate [66]. Temperature shifts during fever significantly affect the inflammatory reflex in CNS by substantially increasing cholinergic neurotransmitters and promoting cholinergic receptors' activity, signifying neuro-immune crosstalk that contributes to regulating antimicrobial responses under fever condition [67].

Similarly, zebrafish larvae infected with dsRNA and added to a continuous thermal gradient preferred higher temperatures as compared to uninfected larvae. Behavioural fever was associated with a remarkable increase in antiviral transcripts such as virus inhibitory protein endoplasmic reticulum-associated interferon-inducible (viperin) and interferon regulatory factor 7 (irf7), suggesting a fever-coupled improvement of the immune response [93]. The impact of behavioural fever was extended to induce epigenetic modulation of immune responses by influencing gene expression regulation [184]. Despite the above-mentioned findings that strongly suggest immunomodulation induced by fever, there are still gaps in the literature concerning inflammation control and successive restoration of homeostasis.

1.4.3. Tissue repair

Throughout millions of years of evolution, multicellular organisms adapted complex systems for recognizing and repairing injured tissues. The process involves interactions between a variety of immune and connective tissue cells. Together, these cells and several humoral factors accomplish sequential phases, comprising inflammation and proliferation to restore damaged tissues [19] (**Figure 1.1**). Subsequent to an injury, there is a constriction of injured blood vessels followed by thrombocyte activation and clot formation to stop bleeding. Fibrin threads in the clot act as a scaffold for infiltrating leukocytes. The cellular migration is largely triggered via activation of an acute inflammatory program that involves upregulation of several cytokines and chemokines [185]. Following eradication of infection and tissue debris, anti-inflammatory mediators and growth factors are released to suppress inflammation and initiate the proliferative phase [186]. At this stage, the repair process aims to fulfill extracellular matrix (ECM) deposition, facilitated by fibroblasts, to fill the wound gap, along with re-epithelialization to cover the wound surface [187]. Cellular proliferation and re-epithelialization rely on developing new blood vessels at the injury site via angiogenesis to supply the newly formed tissue with oxygen and essential nutrients [188].

The regulation of proliferation phase of tissue repair is orchestrated by various cytokines and growth factors released by inflammatory and tissue-resident cells [22]. It is further dependent on efficient clearance of pathogens and proper resolution of inflammation [189]. This is evidently observed in disrupted tissue repair associated with impaired immune

responses and prolonged inflammation instigated by, for example, diabetes, aging and malnutrition [190,191].

Notably, tissue repair is significantly affected by nutrition. For instance, diet changes were demonstrated to intensely influence wound healing in humans [192] and fish [193]. Mechanistically, diet alters pathways important for regulating glycolysis, complement system activity, collagen formation and heat shock protein expression in Atlantic Salmon (*Salmo salar*) [194]. To avoid a potential impact of diet on wound healing in this study, I applied the same standard regular feed typically used in the aquatic facility to all experimental groups.

1.4.3.1. Inflammatory phase

Induction of acute inflammation is critical for efficient healing. This is principally attributed to the early initiation of these inflammatory cascades within a few hours following an injury, in addition to their role in clearing pathogens and regulating subsequent reparative events. However, tight regulation of acute inflammation is required to avoid its excessive perturbations, which ultimately results in defective and delayed healing. Following an injury, DAMPs [195], generated by necrotic cells, as well as PAMPs [46], including conserved motifs of invading pathogens, are recognized by innate receptors (e.g., TLRs) on tissue-resident cells to subsequently trigger an acute inflammatory reaction (**Figure 1.2**) [196]. As a result, various inflammatory mediators are released to promote cellular recruitment and regulate immune responses at the injury site [197]. Subsequent to elimination of infection,

several pathways regulate inflammation resolution (**Figure 1.2**). The following sections summarize the mechanisms of induction and resolution of the inflammatory phase of tissue repair.

1.4.3.1.1. Immune system perception of injury: the role of DAMPs and PAMPs

DAMPs are either passively or actively released by injured host cells. They include patterns that are usually isolated inside cells with limited extracellular exposure. For example, DNA (genomic or mitochondrial), ATP, heat shock proteins (Hsp) and other proteins are released into the extracellular space following cell death or lysis [198]. These patterns provide self-injury detection strategies for the host to activate inflammatory responses in the case of sterile injuries or wounds with restricted PAMPs. Mechanistically, DAMPs function by directly binding to PRRs on resident cells or indirectly by modifying ECM molecules to possess pro-inflammatory stimulating properties [199]. In addition to DAMPs, hydrogen peroxide (H_2O_2) [200] and lipid mediators (e.g., Thromboxane A2, Leukotriene B4 and Hydroxyeicosatetraenoic acid) [201] are released by damaged cells to deliver signals promoting innate immune functions such as leukocyte recruitment. For example, H_2O_2 was found to provoke neutrophil migration toward the injury site for rapid pathogen clearance [200]. On the other hand, PAMPs, also known as microbe-associated molecular patterns (MAMPs), are parts of different invading microbes (e.g., viruses, bacteria, parasites and fungi) that embrace LPS, microbial lipoproteins, β-glucan and double-stranded RNA [202]. Similar to DAMPs, PAMPs have the ability to act as ligands for several PRRs to launch an acute inflammatory program.

1.4.3.1.2. Activation of PRRs and downstream inflammatory pathways

The injury-recognition system markedly relies on innate PRRs located on tissue-resident cells. PRRs include several types, such as TLRs, nucleotide-binding oligomerization domain-like receptors (NLRs), retinoic acid-inducible gene I like receptors (RLRs) and C-type lectin receptors (CLRs) [203]. TLRs were found to play a crucial role in initiating the inflammatory phase of tissue repair [204] via specifically binding to a variety of ligands. Activated TLRs trigger NF-κB and MAPK pathways via adaptor proteins such as Toll/Il1R domain-containing adaptor-inducing Ifnb (TRIF), TRIF-related adapter molecule (TRAM) and myeloid differentiation primary response 88 (MyD88), upregulating the expression of pro-inflammatory cytokines (e.g., *il1b* and *tnfa*) in addition chemokines and adhesion molecules [205]. Other transcription-independent pathways are activated early at the injury site via Ca^{2+} influx, purigenic molecules and ROS to compensate for the delay in induction of transcription machinery [22]. For instance, intracellular Ca^{2+} levels were found to substantially increase within a few minutes at the wound edges and later at the center after an injury [206].

1.4.3.1.3. Inflammatory cytokines

Cytokines are small proteins (~ 10-kDa) characterized by having the amino acid cysteine in their structure. The two most important cytokines involved in tissue repair are (1) CC cytokines which have two adjacent cysteines and (2) CXC cytokines which contain two cysteines separated by another amino acid. Cytokine production is a complex biological

process regulated by several activators and inhibitors depending on the stage of inflammation and other environmental factors, including cellular crosstalk and lipid mediators [207]. Cytokines are essential for induction, propagation and resolution of the inflammatory phase of tissue repair [208]. Moreover, they promote cellular recruitment and regulate their development, proliferation and functions during the healing process, as shown in (**Table 1.1)** [209]. Notably, the majority of tissue-resident cells, including parenchymal cells, fibroblasts, endothelial cells as well as immune cells, can produce various cytokines in response to DAMPs and PAMPs. Furthermore, recruited leukocytes accentuate the release of these cytokines under a pro-inflammatory condition [210]. For instance, despite the critical role of Il6 in induction of acute inflammation and leukocyte chemotaxis [211,212], it is also vital for wound healing by regulating collagen deposition and angiogenesis.[213].

1.4.3.1.4. Mechanisms of cellular recruitment to injury site

Many CC and CXC cytokines act as chemoattractant proteins, identified as chemokines, regulating the migration of several immune and non-immune cells that are critical for the repair process [214]. CXC chemokines containing glutamate–leucine–arginine (ELR) motifs such as Cxcl8, also known as Il8, are more specialized in polymorphonuclear leukocyte (PMN) recruitment [215]. Meanwhile, other CC cytokines, including chemokine C-C motif ligand 1 (Ccl1), act as monocyte [216] and lymphocyte [217] attractants. Expression of these chemokines must be strictly regulated during tissue repair to avoid dysregulation of inflammatory responses. For example, persistent uncontrolled up- or down-regulation of particular chemokines results in the development of a variety of pathological

conditions such as chronic obstruction pulmonary disease and neurological diseases (e.g., multiple sclerosis) [218–220].

Upon their release, chemokines bind to glycosaminoglycans on endothelial cells of blood vessels to be presented to circulating immune cells [221]. Leukocytes bind to these chemokines via their corresponding G-protein coupled receptors (Gpcrs), resulting in extravasation of these cells and their migration towards the injury site [222]. For instance, chemokine (C-X-C motif) Ligand receptor 1 (Cxcr1) and Cxcr2 on PMN bind to Cxcl8, activating downstream signaling pathways and promoting neutrophil recruitment [223]. Intriguingly, several chemokines were shown, as reviewed by Ridiandries *et al*. [224], to contribute not only to inflammatory cell recruitment but also to proliferation and remodeling phases of tissue repair. For example, Cxcl1 and Cxcl7 were involved in angiogenesis [225], while Cxcl12 promotes the differentiation of stem cells into fibroblasts and endothelial cells, enhancing granulation tissue formation [226].

Leukocyte extravasation is achieved through several steps involving adhesion molecules (e.g., selectins and integrins), chemokines and interactions with endothelial cells. Selectins (such as E-, P- and L-selectins), type I transmembrane proteins, are primarily accountable for the initial tethering and adhesive interactions between endothelial cells and circulating leukocytes [227]. Selectins bind to carbohydrate-based ligands such as P-selectin glycoprotein ligand-1 (PSGL-1), which is generally expressed on leukocyte microvilli to secure these cells to endothelial cells of blood vessels at the injury site [228]. After capturing immune cells, leukocytes roll along the surface of endothelium to sense glycosaminoglycan-bound chemokines. Activation of chemokine receptors on leukocytes results in

conformational changes and leukocyte adhesion cascade (diapedesis) [229], where inflammatory cells crawl through endothelial junctions or weak regions of the basement membrane [230].

1.4.3.1.5. Role of inflammatory cells during tissue repair

1.4.3.1.5.1. Neutrophils

Among immune cells involved in the repair process, neutrophils are considered the "first responders" being swiftly recruited to the injury site [231]. In addition to the potent Cxcl8, other cytokines, such as Cxcl4 and Ccl3/4 promote PMN migration [232]. Neutrophils are not commonly detected in healthy skin; instead, they remain in the bone marrow, where they are produced, and in the bloodstream [233], ready to be drafted, as discussed in the previous section. Interestingly, recruited neutrophils can further augment additional PMN infiltration by releasing several chemoattractant factors [231,234].

The primary function of neutrophils at the injury site is to combat invading pathogens via various antimicrobial responses, including phagocytosis, releasing toxic granules, oxidative burst and neutrophil extracellular traps (chromatin filaments that are released extracellularly to immobilize and eliminate microbes known as NETs) [235]. Still, a critical balance must be maintained between these phagocytes' protective functions and their possible contributions to prolonged and exacerbated inflammation [236]. This equilibrium ensures eradication of infection while minimizing collateral tissue damage. Several studies suggested that the prolonged existence of neutrophils at the injury site was detrimental to proper tissue repair [237,238]. This was attributed to PMNs-derived proteases degrading

ECM as well as being allied with deleterious levels of ROS [239,240]. Recently, neutrophils were also found to induce genomic instability via ROS-independent pathways involving the release of microparticles/extracellular vesicles containing pro-inflammatory microRNAs (miR-23a and miR-155) in patients with inflammatory bowel disease (IBD) [241]. These miRNAs promoted the accumulation of double-strand breaks (DSBs) by inhibiting homologous recombination (HR), resulting in impeding resolution of inflammation and overall intestinal healing [241].

Neutrophils are characterized by having distinct granules containing bactericidal agents. These granules either fuse with phagosomes to destroy pathogens intracellularly [242] or undergo exocytosis to combat microbes extracellularly [233]. Antimicrobial agents of these granules include myeloperoxidase, lysozyme, matrix metalloproteases (Mmps), lactoferrin and proteases (e.g., elastase and cathepsin G) [237]. The utilization of proteases by neutrophils is not limited to their antibacterial activity. Proteases are also crucial for neutrophil extravasation via breaking down ECM and basement membrane of endothelial cells directly or indirectly by activating Mmps [243]. Despite their importance for PMN migration and bactericidal actions, an unrestrained increase in proteases induces extensive tissue damage, ensuing impaired healing and chronic wounds. This is attributed to proteolytic enzymes-induced obliteration of growth factors, newly formed blood vessels and granulation tissue [244].

Recent experimental evidence suggested parallel immunomodulatory functions of neutrophils during tissue healing in addition to their bactericidal actions. This was observed in mice with myocardial infarction (a sterile injury model), where researchers have

characterized N2 neutrophils to potentially restore injured tissue irrespective of their antimicrobial functions [245]. Mechanistically, neutrophils were found to modulate macrophage phenotype from a pro-inflammatory to an anti-inflammatory/reparative state following engulfing of apoptotic PMN by these macrophages (efferocytosis) [246]. Modulated macrophages release pro-resolution cytokines (e.g., Il10) and growth factors to promote inflammation control and rebuild damaged tissue [246].

A genetically modified reduction in PMN recruitment (*cxcr2*$^{-/-}$) in injured mice resulted in delayed re-epithelialization at wound sites [247]. Conflicting data showed an accelerated re-epithelialization during neutrophil depletion compared with control mice [248]. Notably, even though differences were observed at the epidermis development level, no significant changes were evidenced regarding collagen deposition [248]. Aging-induced delayed wound healing was postulated to be instigated by downregulation of neutrophil numbers or functions in mice [249] and humans [250]. This was attributed to neutrophil-tempted incompetent pathogen clearance, causing a late inflammation resolution. Still, more research is encouraged to fully characterize the immunomodulatory functions of PMN during tissue repair.

1.4.3.1.5.2. Macrophages

Macrophages play a key role in tissue repair stemming from influencing both the inflammatory and proliferative phases. Contributions of macrophages to immunomodulation, resolution of inflammation and tissue healing have been well-studied [251]. Macrophage numbers increase gradually and peak 48-72 hours after an injury [252]. Influenced by

chemokines such as Ccl1 and Cxcl12 [253], monocytes migrate from bone marrow and adjacent blood vessels to the injury site and differentiate into macrophages. Additionally, recruited macrophages can amplify the relocation of additional monocytes via releasing monocyte chemoattractant protein (Mcp1) [254].

Several macrophage phenotypes with distinctive functions were characterized during tissue repair [255]. It is worth mentioning that these phenotypes are not distinctively represented by particular macrophage subsets or a subject of on/off switch but rather a dynamic continuation of macrophage polarization based on environmental stimuli and interplay with other cells [256,257]. During the early phases of tissue repair, a classically activated macrophage phenotype, also known as M1, was shown to induce pro-inflammatory and bactericidal activities via expressing *il1b* and *tnfa* in addition to mediating phagocytosis [258]. Later during the repair process, macrophages transition to becoming alternatively activated (M2) macrophages in order to suppress inflammation and promote the healing of damaged tissues [259]. Interestingly, recent reports indicated that M2 activation has expanded, triggered by various stimuli, to involve other phenotypes such as M2a, M2b, M2c and M2d [255]. For example, M2a is activated by Il4 and Il13; while exposure to Il10 and glucocorticoids stimulates M2c phenotype [255]. These M2 phenotypes largely possess anti-inflammatory, pro-resolution and healing activities [260].

Moreover, the expanding literature supports the crucial role of macrophages in tissue repair. For instance, depletion of macrophages in wounds of murine models was associated with delayed healing induced by impaired angiogenesis, collagen synthesis and growth factors expression [261,262]. These observations supported the significant engagement of

macrophages in various tissue repair events. **Table 1.2** summarizes macrophage phenotypes' potential functions and contributions during the repair process. Notably, macrophage phenotypes are not limited to the previously mentioned categories. There are likely several other phenotypes that are continuously activated depending on the differentiation stage, type and duration of stimulus as well as the overall biochemical milieu [257,263].

1.4.3.1.6. Antimicrobial defense mechanisms

1.4.3.1.6.1. Reactive oxygen species (ROS)

In addition to its crucial role in intracellular signaling, ROS is considered one of the evolutionarily conserved microbicidal agents utilized by immune cells during inflammatory responses [264]. The process involves generating various by-products of molecular oxygen during aerobic metabolism either inside or outside the mitochondria; thereby, ROS generation is also known as oxidative or respiratory burst. These molecules can induce permanent oxidative damage to cellular structures, e.g., lipids, DNA and proteins, ultimately resulting in cell death [265]. The most common forms of ROS include non-radical H_2O_2, hydroxyl radicals (HO•) and superoxide anion (O_2^-), and they are produced by NADPH oxidase (NOX) enzymes [266].

NOX is activated in neutrophils following their exposure to microbes to generate non-mitochondrial ROS, while it remains inactive in resting PMN [267]. Mechanistically, NOX is composed of a membrane-bound cytochrome b558 in addition to cytosolic factors (p40phox, p47phox and p67phox), which during enzyme activation, translocate to the membrane component. Through transferring an electron to molecular oxygen, O_2^- and other

types of ROS are generated [265]. Dual oxidase (DUOX) enzyme was identified as one of the NOX homologues. DUOX, in addition to the other six members, are known as the NOX/DUOX family [268]. It was reported that DUOX possesses potential roles in cell signaling, immune functions and H_2O_2 production [269].

1.4.3.1.6.2. Nitric oxide (NO)

NO is generated by nitric oxide synthase (NOS) enzyme through metabolizing L-arginine [270]. There are three types of NOS: inducible (i), neuronal (n) and endothelial (e)NOS. Both nNOS and eNOS are constitutively producing NO to maintain tissue homeostasis, while iNOS was found to generate immunologic NO in response to pro-inflammatory stimuli in mammals [270] and fish [271]. NO can induce damage to cellular components (e.g., DNA and proteins) either directly or via developing reactive nitrogen species (RNS) molecules such as peroxynitrite and superoxide anions [272]. Moreover, NO is capable of inducing deamination of nucleotides and total fragmentation of DNA [273].

NO functions are not limited to combating pathogens but further, extend to regulate resolution of inflammation and tissue repair events. For instance, although NO and its RNS molecules possess microbicidal properties [274], NO mediates antioxidant and anti-inflammatory activities [275] that involve reducing ROS levels. NO regulates the activity of NOX and minimizes the reactivity of O_2^- and H_2O_2 [273]. Moreover, NO restricts ROS distribution to specific locations to help eliminate pathogens while minimizing ROS-associated cellular damage [273]. NO can further impede PMN adhesion [276], in addition

to downregulating *il8* [277] and *il1b* [278], thus contributing to inflammation control. A positive contribution of NO to several healing mechanisms, such as cellular proliferation, collagen deposition and wound closure, was likewise demonstrated [279].

1.4.3.1.7. Suppression of inflammation

Following eradication of infection and exclusion of cellular debris, a transition towards an anti-inflammatory program is essential for activating reparative pathways that restore the structure and function of damaged tissue. The process is achieved through various suppressive signals prompting a reduction in pro-inflammatory mediators and infiltrating leukocytes in addition to upregulation of pro-resolution molecules, including Il10 and Tgfb [280]. Several pathways were reported to regulate resolution of inflammation that relies largely on effective elimination of pathogens [281]. Defects in pathogen clearance necessitate a continuation of a pro-inflammatory reaction that ultimately results in delayed healing. The process further involves crosstalk and interplay between immune and non-immune cells at the injury site.

Pathways regulating control of inflammation can be categorized into cell- and cytokine-mediated mechanisms. The launch of resolution of acute inflammatory responses is generally timely mapped with the disappearance of PMN from the injury site [22]. Downregulation of PMN can be achieved through two main mechanisms: (1) apoptosis followed by efferocytosis and (2) reverse migration. The Barreda lab has previously highlighted the role of neutrophils in resolving inflammation via their efferocytosis by

macrophages [282]. The process is accomplished by binding cellular communication network factor 1 (CCN1), present on phosphatidylserine of apoptotic PMN, to integrins of macrophages [283]. Engulfing apoptotic neutrophils is critical to avoid their secondary necrosis, which ultimately leads to a substantial release of detrimental pro-inflammatory cytokines and ROS [282], and to transform macrophages into anti-inflammatory phenotypes [311]. On the other hand, recent data indicates a retrograde migration of neutrophils back into circulation as a pathway of PMN resolution [231,284]. This was shown in various models of mice, zebrafish, and *in vitro* human neutrophils [231,284]. Notably, prolonged inflammatory conditions have been commonly associated with extensive and prolonged neutrophil infiltration, resulting in chronic wounds [285].

Additionally, M2 macrophages contribute to controlling inflammation by secreting various anti-inflammatory mediators such as Il10 and Tgfb. Other cell types at the injury site, including T cells and fibroblasts were reported to express pro-resolution cytokines e.g., Il4, Il13 and Il35 [286]. These cytokines suppress inflammation by inhibiting the synthesis of pro-inflammatory cytokines and chemokines [281]. Furthermore, they reduce cellular infiltration by repressing the expression of adhesion molecules on endothelial cells and diminishing chemokine-mediated leukocyte recruitment [281,287].

1.4.3.1.8. Dysregulation of inflammatory phase and its outcome on tissue repair

Tight regulation of acute inflammation is critical for normal tissue repair. Dysregulation of inflammatory responses eventually disrupts the repair process due to failing to transition to the proliferative phase (**Figure 1.3**). This is primarily attributed to the

impairment of pathways involved in resolution of inflammation, instigating prolongation and exaggeration of immune mechanisms such as leukocyte recruitment and production of pro-inflammatory mediators (**Figure 1.3**). I previously highlighted the significance of cellular and cytokine effectors in the induction of acute inflammation. Though a balance has to be maintained, and resolution must be achieved in a timely manner to avoid collateral tissue damage associated with sustained inflammatory processes or exaggerated responses such as cytokine storms .

Non-healing injuries are commonly accompanied by persistent inflammation. Mechanistically, extensive and persistent neutrophil infiltration at the injury site, along with their compromised resolution, is escorted by detrimental levels of ROS and proteases, causing damage to cell membranes, ECM and crucial tissue repair mediators such as Tgfb and platelet-derived growth factor (Pdgf) [288,289]. Likewise, macrophages in chronic wounds are associated with reduced levels of tissue inhibitors of Mmps (Timps); thus, augmenting ECM degradation and delaying healing [290]. Indeed, there are many types of Mmps contributing significantly to various tissue repair mechanisms such as re-epithelialization and angiogenesis as reviewed by Kandhwal *et al* [291]. Mmps are engaged in all phases of wound healing [291]. For instance, during acute inflammation, specific Mmps (e.g., Mmp2 and Mmp9) are accountable for removing damaged proteins and transepithelial migration of leukocytes [291]. Whereas, during the proliferation phase, Mmp1, Mmp8 and Mmp13 mediate detachment of keratinocytes from the basement membrane during re-epithelialization and enhance fibroblast migration [291]. In fish, there are twenty-six protease genes that have been identified where they show homologous

functions compared with their mammalian counterparts [292]. In this study, I examined the gene expression of two conserved Mmps (Mmp1 and Mmp9) that are well-recognized to play important roles in inflammatory and proliferative phases of wound healing in fish [292]. Dysregulated proteolytic activities associated with overproduction of Mmps in uncontrolled inflammatory reactions can devastate the protective repair mechanisms, including cleaving growth factors [293]. Therefore, during chronic inflammation, the activity and expression of Mmps (e.g., Mmp1 and Mmp3) were shown to be substantially upregulated in humans [294]; while levels of Mmp9 and Mmp13 were increased in fish [292].

Macrophages also tend to present a profile of deregulated expression of anti-inflammatory mediators and growth factors in non-healing injuries [186]. This is further complicated by an imbalance in M1/M2 phenotype transition, where alternatively activated (M2) macrophages are significantly diminished [295]. Conversely, keratinocytes show impaired migration and proliferation abilities in chronic injuries [296,297]. Likewise, fibroblasts suffer the loss of their proliferative potentials due to being less responsive to growth factors [298]. Based on the previously mentioned observations, it is generally agreed that a pro-inflammatory cycle must be broken for non-healing injuries to heal properly.

1.4.3.2. Proliferative phase

1.4.3.2.1. Re-epithelialization

Keratinocytes differentiate and migrate through the provisional matrix [299], composed of plasma fibronectin, fibrin and thrombocytes, to form a basal layer of cells migrating from wound edges toward the centre to cover the wound surface. Keratinocyte

cell-cell connections and adhesion to the basement membrane are weakened to allow for their translocating across the temporary fibrin scaffold [300]. Cellular migration continues until keratinocytes from opposing edges come in contact, completing the basal layer that develops new adhesions with the underlying matrix [301]. Keratinocytes then rebuild the basement membrane [301]. Notably, Mmps, specifically Mmp1 and Mmp9, are reported to be critical for keratinocyte migration by cleaving various ECM and/or diminishing integrin:matrix adhesion [302]. Meanwhile, suprabasal keratinocytes proliferate to provide multiple overlying layers of keratinocytes filling the gap between wound edges [303]. Re-epithelialization is regulated via several cytokines and growth factors as well as crosstalk between keratinocytes and inflammatory cells, fibroblasts and endothelial cells [304]. For instance, keratinocytes were found to activate fibroblasts to release growth factors, thus promoting keratinocyte proliferation [305].

Various mediators activate re-epithelialization, such as macrophage-released NO [279], Egf, hepatocyte growth factor (Hgf), Fgf, Tgfb, Igf1, nerve growth factor (Ngf), and epidermal granulocyte macrophage colony stimulating factor (Gmcsf) [208,306]. Several cell types secrete all these pleiotropic growth factors in a spatio-temporal manner to play a crucial role in regulating epidermal development at different stages with overlapping contributions (refer to **1.4.3.2.4 Growth factors in tissue repair**).

1.4.3.2.2. Granulation tissue formation

During the proliferation phase, new connective tissue is formed simultaneously with other healing events, such as re-epithelialization and neovascularization. Fibroblast is the key cell accountable for constructing this granulation tissue to fill in the wound gap. In response to various signaling molecules that are released from tissue-resident macrophages, thrombocytes, keratinocytes and endothelial cells following an injury (e.g., Tgfb, Egf, Fgf and Pdgf) [305,307,308], fibroblasts proliferate, migrate and become pro-fibrotic, depositing ECM proteins [309] (refer to **1.4.3.2.4 Growth factors in tissue repair**). Prior to laying ECM proteins by fibroblasts, they obliterate the provisional matrix by secreting Mmps, to be substituted by soft granulation tissue rich in immature collagen (collagen type III), fibronectin, glycoproteins and proteoglycans [310]. While the newly formed ECM works as a scaffold helping the migration of various cells through the injury site, it ultimately gets replaced by mature ECM with abundant collagen type I, synthesized by fibroblasts, providing strength and support to the dermis layer [311].

It is worth mentioning that fibroblasts in wound repair demonstrate functional diversity, stemming from their contribution to many other healing events [312]. For example, fibroblasts were further found to assist in re-epithelialization [313]. Additionally, they exhibit heterogeneity depending on their activation status and throughout different developmental stages [314], resulting in significant phenotypic/subpopulation functional differences as previously reviewed [315]. These phenotypes mediate varying functions in wound repair, including secretion of growth factors, immunomodulation, ECM synthesis and organization [316].

1.4.3.2.3. Angiogenesis

The newly formed granulation tissue and epidermis require an adequate supply of nutrients and oxygen to maintain homeostasis and promote further healing. This is achieved by developing new blood vessels at the wound area to compensate for those lost during the injury. The process is known as neovascularization or angiogenesis, accomplished via activating local endothelial cells (ECs) lining the inner surface of neighboring blood vessels [317]. In response to hypoxia-responsive growth factors (e.g., Vegf), ECs migrate, proliferate, and form new cell-to-cell junctions to develop new capillaries branching out from the existing blood vessels. Migrating ECs degrade ECM while traversing across granulation tissue through secreting Mmps, such as Mmp2 and Mmp9 [310,318].

Angiogenesis is regulated by angiogenic molecules other than Vegf, such as Pdgf, Fgf, angiopoietins and Tgfb [319]. Interestingly, ECs showed heterogeneity in response to these molecules by functioning as either lead tip or trailing stalk cells. Lead tip cells migrate towards angiogenic factors in response to positive and negative regulators. On the other hand, stalk cells preserve the structure of existing blood vessels [320]. The role of Vegf in angiogenesis is conserved in numerous species, including fish [321–323]. Vegf initiates neovascularization by promoting the migration of lead tip cells and proliferation of stalk cells [321].

1.4.3.2.4. Growth factors in tissue repair

1.4.3.2.4.1. Tgfb

Transforming growth factor beta (Tgfb) is an immune-regulatory cytokine and growth factor conserved throughout vertebrates and invertebrates [324,325]. There are three functional isoforms (Tgfb1, 2 and 3) that were reported to have similar effects *in vitro* [324]. However, other researchers revealed opposing functions, where Tgfb3, unlike Tgfb1, possesses an anti-fibrotic effect in cutaneous healing [326]. This can be explained by the distinctive temporal and spatial expression pattern of these isoforms during tissue repair [327,328]. Amongst the three variants, Tgfb1 has been found to be the most influential thru the repair process [329]. Subsequent to an injury, Tgfb is secreted by a variety of cells, such as fibroblasts and macrophages [330]. The growth factor is typically synthesized in a proprotein form that is cleaved later into a bioactive molecule to be released extracellularly [331].

Bioactive Tgfb binds to Type 1 and 2 Tgfb receptors to induce immunomodulatory and tissue repair functions [332]. Mice with Tgfb1 deficiency developed prolonged and persistent inflammation [332], indicating its remarkable anti-inflammatory effects. In mammals, Tgfb participates in resolution of inflammation via activation of myriad regulatory processes, including T cell differentiation to Th2 or T_{reg}, antagonizing PMN chemoattractants (e.g., Il8) and suppressing recruitment of inflammatory cells [332,333]. Likewise in fish, Tgfb1 controls the acute inflammatory response via inhibiting pro-inflammatory cytokine expression [325,334] and their bioavailability [335]. Moreover, Tgfb contributes significantly to cellular recruitment, angiogenesis and re-epithelialization

[336,337]. Tgfb was also found to enhance ECM development via promoting fibroblast proliferation and collagen deposition [338].

1.4.3.2.4.2. Fgf

Fibroblast growth factor (Fgf) is a potent mitogen critical for tissue repair [339], released by keratinocytes, fibroblasts and mast cells/eosinophilic granule cells [337]. It has an established role in epithelial and mesenchymal proliferation and angiogenesis [340]. Among several isoforms of Fgf, Fgf2, also known as basic (b)Fgf, has been shown to substantially enhance wound healing when applied exogenously to burn wounds and ulcers in clinical trials [341,342]. Fgf2 interacts with four cell surface receptors (Fgfr1-4) [343]. Effects of Fgf2 are largely attributed to the activation of intrinsic tyrosine kinase [344] or dephosphorylation heparan sulfate-carrying proteoglycans (Hspg) syndecan-4 protein [345]. Fgf2 enhances granulation tissue formation and re-epithelialization via synthesis and deposition of several components of ECM (e.g., collagen), promoting migration and proliferation of fibroblasts in addition to boosting keratinocyte motility [346,347]. *fgf2* levels were shown to be substantially decreased in human chronic wounds [340].

1.4.3.2.4.3. Egf

Epidermal growth factor (Egf) is produced and secreted by macrophages and fibroblasts to be localized mainly in the epidermis layer [348]. It is well known for its ability to facilitate re-epithelialization through enhancing keratinocyte migration and proliferation

[348]. Therefore, Egf has been utilized to accelerate wound closure in partial-thickness burns [349]. Likewise, it increases the re-epithelialization rate and incidence of diabetic ulcers [350,351]. Through binding Egf receptor (Egfr), a tyrosine kinase transmembrane protein, Egf induces an autophosphorylation or tyrosine phosphorylation of downstream proteins [352]. Similar to many other growth factors, chronic wounds display reduced *egf* levels [353] caused by highly upregulated Mmps at the site of chronic inflammation that degrade ECM proteins and essential growth factors [290,340]. Furthermore, extensive expression and activation of other proteases, such as stromelysins, elastases and a disintegrin and metalloproteinase (ADAMs) were demonstrated in chronic cutaneous wounds associated with delayed healing [354].

1.4.3.2.4.4. Igf1

Insulin like growth factor 1 (Igf1), previously known as somatomedin C, structurally resembles proinsulin and possesses similar metabolic effects of insulin [355]. Although Igf1 is mainly released by hepatocytes, several studies reported other tissues synthesizing Igf1, including the skin [337,356], where it mediates its effects via binding to type I IGF receptor (Igf1r) [357]. In response to an injury, *igf1* is remarkably expressed to contribute to epidermal healing [358], displaying mitogenic effects on keratinocytes [359,360]. Dermal cells producing Igf1 include keratinocytes [361], macrophages [362], and cultured fibroblasts [363]. Igf1r has been shown to present throughout the epidermis, predominantly in the basal layer, while its expression was remarkably downregulated in diabetic wounds [337]. In addition to binding Igf1r, Igf1 concurrently with Egf can activate Egfr to stimulate

mitogen-activated protein kinase (MAPK) and posphatidylinositol-3-kinase (PI3K) pathways, inducing a synergistic effect on keratinocyte migration and proliferation [24].

1.4.3.2.4.5. Pdgf

Platelet derived growth factor (Pdgf) is a potent mitogen secreted by platelets, endothelial cells, macrophages, keratinocytes and fibroblasts [330]. Pdgf regulates cell growth and proliferation, thereby significantly contributing to several tissue repair events [208]. This is supported by low Pdgf levels detected in chronic wounds [340], induced by its high susceptibility to proteolytic enzymes [290]. Following an injury, Pdgf is released to trigger PMN, fibroblast and macrophage recruitment [364]. Pdgf activates macrophages to generate other growth factors (e.g., Tgfb), thus enhancing granulation tissue formation [365]. Additionally, it directly activates fibroblasts to produce collagen [366]. Pdgf further promotes the expression of *vegf*, an important mediator of angiogenesis [367]. It was also shown to upregulate *igf1*, thereby positively contributing to the re-epithelialization process [208]. Numerous clinical trials have demonstrated the effectiveness of topical administration of Pdgf in treating chronic wounds [368–370]. As a result, Pdgf was the first recombinant growth factor approved for managing diabetic ulcers in the United States [353].

1.4.3.2.4.6. Ngf

Although nerve growth factor (Ngf) is primarily involved in neural development, growing evidence indicates its role in regulating tissue repair [371]. For instance, Ngf was

found to enhance keratinocyte proliferation, fibroblast activation, production of ECM and angiogenesis [371–374]. The growth factor mediates its functions via binding to nerve growth factor receptor (Ngfr) and tropomyosin-related kinase receptor 1 (NTRK1), which are expressed on the surface of various cell types in the skin [375]. Ngf is constitutively expressed by tissue-resident cells, such as keratinocytes and fibroblasts, to maintain tissue homeostasis [376,377]. However, upon injury, *ngf* expression is remarkably upregulated at the injury site [371,378]. Topical administration of Ngf improved the healing of diabetic wounds [379]. Mechanistically, Ngf aids re-epithelialization via enhancing keratinocyte migration [371] as well as neovascularization by activating of Vegf-Akt-NO pathway [380]. Recently, the FDA has authorized Ngf eye drops to manage neurotrophic keratitis [381].

1.4.3.2.4.7. Vegf

Vascular endothelial growth factor is a homodimer glycoprotein that almost resembles the structure of Pdgf [382]. It is synthesized and secreted by various cells involved in tissue repair, including macrophages [383], endothelial cells [384], thrombocytes [385] and fibroblasts [386]. Vegf binds to Vegfr1 and Vegfr2, which are high-affinity receptors belonging to type 3 tyrosine kinase family [387], and are found mainly on the surface of mature and developing blood vessels [388]. The primary function of Vegf in the repair process is activating and promoting angiogenesis. The formation of new blood vessels at the injury site is accomplished through several steps that include vasodilation, basement membrane degradation, migration and proliferation of endothelial cells. Interestingly, Vegf contributes significantly to all these steps [27]. Moreover, it has been shown to enhance the

recruitment of additional macrophages and the development of new lymphatic vessels [389]. In fish, Vegf has been characterized to play a critical role in angiogenesis [390,391], with a high level of amino acid homology between mammalian and fish Vegf [392].

1.4.4. Anatomy of fish skin

Fish skin is a dense coherent layer protecting underlying tissue from external environments. It is composed mainly of 3 parts: (1) Outer epithelial layer (epidermis), entailing multilayers of keratinocytes together with mucus-secreting cells resting on a basement membrane; (2) Intermediate layer of connective tissue containing collagen, glycoproteins, proteoglycans and fibronectin; (3) Inner hypodermis or subcutaneous layer encompassing nerves, adipose tissue as well as blood and lymphatic vessels [393]. Fish skin retains unique structures and features that have evolved to adapt to the surrounding watery environment. Among them, the mucus layer covering epidermis provides immunological and mechanical protection against microbes. Likewise, dermal scales, alarm substance glands, venom glands and pigment-containing cells deliver distinctive functions, such as deterring predation [394].

Initial experiments confirmed basal anatomical structures of the goldfish skin. Histological analysis of cutaneous sections showed that goldfish skin typically consists of three layers, as shown in (**Figure 1.4**). The epidermis comprises layers of keratinocytes (cuboidal cells with rounded nuclei) resting on basal layer of columnar cells (**Figure 1.4**). Mucus-secreting cells (M) are frequently found between keratinocytes (**Figure 1.4**). A well-

defined basement membrane separates the epidermis and dermis layers (arrowheads; **Figure 1.4**). The dermis is composed of two layers: loose and dense connective tissue (LCT and DCT, respectively) (**Figure 1.4**). In addition to offering structural strength, these layers provide a matrix for nerves as well as blood and lymphatic vessels [395]. LCT, also known as "stratum spongiosum" contains loose sparse collagen fibers, sensory papillae, chromatophores and other ECM components [489,490]. The deeper layer of dermis (DCT) or stratum compactum consists of relatively acellular dense, parallel and well-organized collagen fibers with fibroblasts lying between collagen bundles. The innermost layer of the skin is the hypodermis or subcutaneous layer (**Figure 1.4**). It is situated underneath the dermis and immediately above the muscles. It is formed of loose connective tissue containing blood and lymphatic vessels, adipocytes, fibroblasts, as well as neural tissues [393].

1.4.5. Wound healing in fish

In response to skin injury in fish, an acute inflammatory response is critical for microbe clearance and regulation of subsequent reparative responses [396]. This is achieved via activation of innate immune programs to enhance inflammatory cell recruitment [396]. Cellular migration rate varies considerably based on the wound type (sterile or infected), fish species and the surrounding temperature [395,397]. Inflammatory mediators driving leukocyte relocation to wound area are still not fully characterized in goldfish. Additionally, little is known about antimicrobial responses excreted by these leukocytes in addition to the molecular and cellular mechanisms prompting the resolution of cutaneous inflammation.

1.4.5.1. Re-epithelialization

In superficial cutaneous wounds, re-epithelialization starts immediately by migrating keratinocytes as a collective sheet to cover the exposed wound surface [398]. Notably, re-epithelialization kinetics and characteristics show differences in other tissues, such as gut and gills owing to histological structural and functional distinctions [399–401]. Extensive recruitment of keratinocytes from wound edges ensures their rapid rearrangements [402]. Though, in deep wounds, keratinocyte migration and mucus cell development are relatively delayed due to extending of the injury to reach the inter-scale pockets, indicated to be the main reservoir of epidermal cells [402]. Notably, the initiation of re-epithelialization was found to be independent of other inflammatory or proliferative events [396,403]. This makes sense considering the importance of rapid re-establishment of epidermal layers protecting against potential osmotic shock and pathogens [404]. Cellular movement stops when keratinocytes from wound edges meet at the centre, followed by keratinocyte proliferation and differentiation to increase the thickness of epidermis [405]. Yet, others suggested that mucus cell differentiation occurs simultaneously with keratinocyte migration [406]. Reconstruction of epidermis continues throughout the wound healing process to restore a fully mature and functioning epidermis [406].

1.4.5.2. Granulation tissue formation

Similar to mammals, generation of granulation tissue in fish is accomplished by fibroblasts, the key cells producing ECM components and collagen. Notably, kinetics of the process varies significantly depending on fish species and wound depth. For instance, zebrafish showed a relatively rapid granulation tissue formation at 4 days post wounding (dpw) [396], while it was achieved later at 14 dpw in Atlantic salmon [406]. The critical role of acute inflammation in wound healing is conserved between mammals and fish [406]. This was clearly shown in compromised granulation tissue formation in zebrafish treated with hydrocortisone [396,407], where researchers indicated the importance of fibroblast-stimulating signals released by immune cells. Similarly, transgenic suppression of Fgf signal in zebrafish supports its conserved role in re-establishing the dermis layer in fish [408]. Collectively, these data shed light on evolutionary conserved molecular mechanisms regulating the proliferative phase of tissue repair in fish. However, wound healing in fish still differs from mammalian healing in terms of the ability of fish to heal with minimal scarring, where, unlike mammals, the entire granulation tissue resolves, and the skin regenerates [396].

1.4.6. *Aeromonas veronii* bacterium

Aeromonas spp. is ubiquitous Gram-negative bacilli causing disease in several hosts, including humans and fish [409]. It is also one of the well-recognized fish pathogens characterized more than 100 years ago [410]. The bacterium is known for its detrimental effects on the aquaculture industry by inducing cutaneous and systemic infections in a

variety of fish species [411–413]. Originally, two major groups of *Aeromonas* were identified: the non-motile psychrophilic group, typically infecting fish at an optimal growth temperature of 22-25°C, and the motile mesophilic group causing infections in mammals/humans [410]. Currently, eighteen genetically different species of *Aeromonas* have been identified using molecular methodologies, including DNA hybridization, PCR and sequencing [410]. The Barreda lab has previously isolated a wild strain of *Aeromonas veronii* from natural lesions found on goldfish held at the aquatic facility, Department of Biological Sciences, University of Alberta [414]. Analysis of *A. veronii* genomes demonstrated this species to possess several virulence factors [415,416], including toxins, adhesion molecules, lytic enzymes and quorum sensing.

1.4.6.1. Furunculosis and its impact on fish industry

Furunculosis, cutaneous ulcers, is among the most common forms of infection induced by *Aeromonas* spp., representing a worldwide disease affecting the aquaculture industry and causing enormous economic losses [417–419]. Beside cutaneous lesions, other common signs of *Aeromonas* infection include exophthalmia, ascites, and hemorrhages of internal organs [420]. Interestingly, particular fish species, such as trout, may not show any signs of infection and act as healthy carriers transmitting the disease [421]. Though, outbreaks are common in these animals during spawning season or stressful conditions [422,423]. In goldfish, *Aeromonas* spp. induces cutaneous furunculosis called “goldfish ulcer disease”. Bacteria bind to dead/injured skin cells and invade tissues while proliferating,

resulting in the development of necrotic purulent exudate and hemorrhages [424]. Sloughing of necrotic tissue is associated with the exposure of underlying degenerated muscle layers.

1.4.6.2. Public health relevance

In humans, *Aeromonas* spp. was reported to be associated with a number of diseases affecting the skin, gastrointestinal tract and blood [409]. The severity of infection varies greatly from a mild form of disease to extremely severe and life-threatening conditions. For instance, while *Aeromonas* spp. can cause slight cutaneous lesions and acute gastroenteritis, it is presented in some cases with fatal necrotizing fasciitis and septicemia [425]. *Aeromonas* spp. is also linked to several eye, joint, urogenital and respiratory tract infections [409,425]. The incidence of *Aeromonas* infections was reported to increase significantly with warmer temperatures in summer and spring [426,427]. Immunocompromised people are at a higher risk of acquiring the infection when compared to healthy individuals who showed less morbidity and mortality rates [409,428].

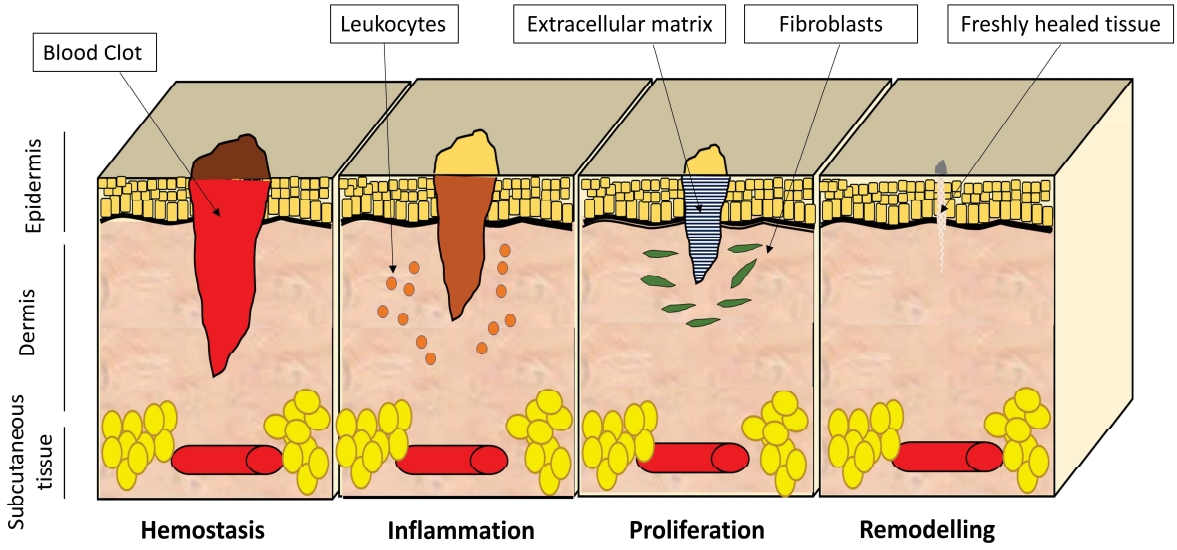

Figure 1.1. Stages of tissue repair. A schematic diagram illustrating healing phases. Following an injury, blood clot formation is formed to stop the bleeding (hemostasis). Within a few hours, leukocytes infiltrate the injury site, indicating the progression of acute inflammatory response. Subsequent to the resolution of inflammation, the proliferation phase commences rebuilding of damaged tissue with the help of fibroblasts, which lay down various components of extracellular matrix. Finally, the newly formed tissue undergoes remodeling.

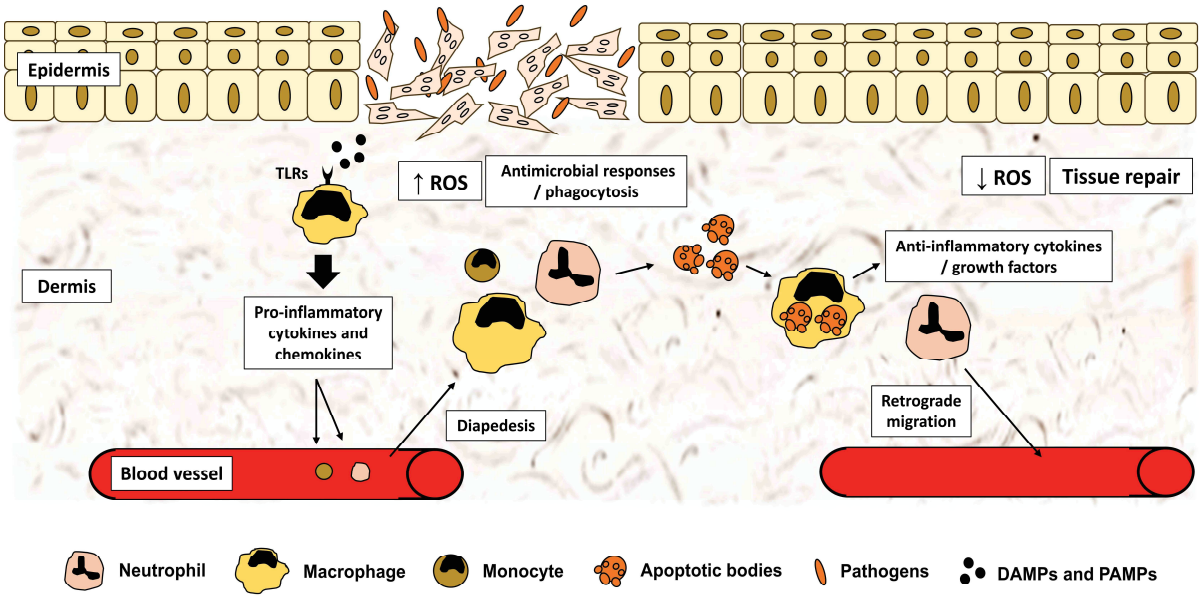

Figure 1.2. Induction and resolution of acute inflammation during wound healing. Pathogen/Damage Associated Molecular Patterns (PAMPs/DAMPs) associated with an injury bind Toll-like receptors (TLRs) expressed by tissue-resident cells, including macrophages. These cells release pro-inflammatory mediators and chemokines to activate an acute inflammatory program, recruiting leukocytes from nearby blood vessels. Neutrophils and monocytes gradually infiltrate the injury site to exert antimicrobial mechanisms, including increased reactive oxygen species (ROS) production. Following the eradication of pathogens, neutrophils undergo apoptosis to be engulfed by macrophages (efferocytosis). Activated macrophages undergo polarization to release anti-inflammatory cytokines leading to resolution of inflammation and reduction in ROS levels. A retrograde migration of neutrophils aids in decreasing infiltrating leukocytes. Additionally, macrophages release various growth factors to trigger tissue repair machinery.

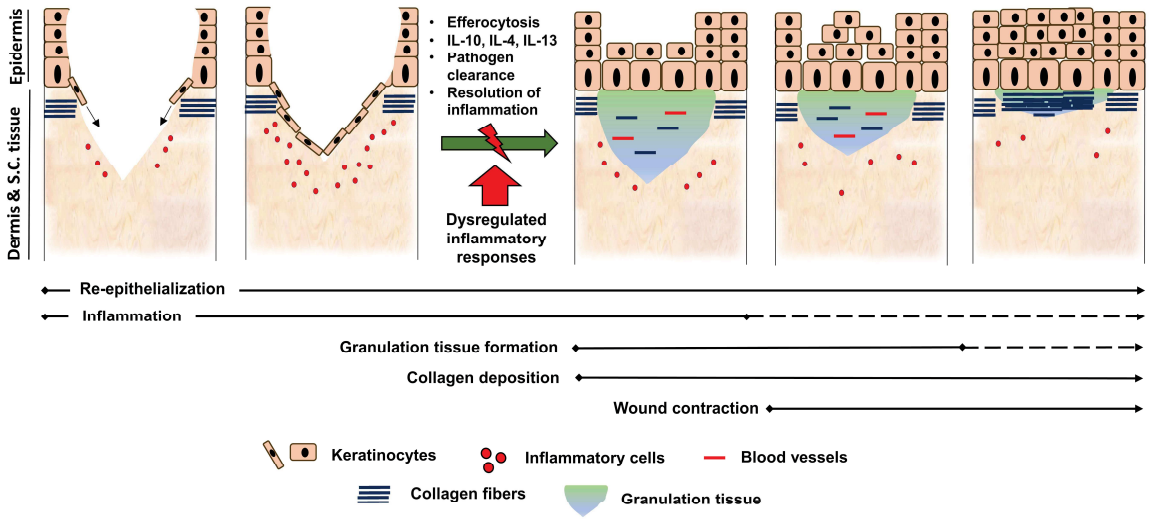

Figure 1.3. A classic wound healing model shows the importance of transitioning from the inflammatory to proliferative phases during the repair process. A schematic diagram shows that wound healing typically progresses via activation of an innate immune program involving inflammatory cell recruitment. Anti-inflammatory responses are triggered through several mechanisms, including efferocytosis, to suppress inflammation and initiate repair events. These reparative phases comprise re-epithelialization, granulation tissue formation, angiogenesis and collagen deposition. Dysregulation of inflammatory responses in case of, for example, diabetes, aging and immunosuppressive diseases result in failure to transition to the proliferation phase, thereby inducing delayed wound healing or chronic injuries. S.C.: subcutaneous.

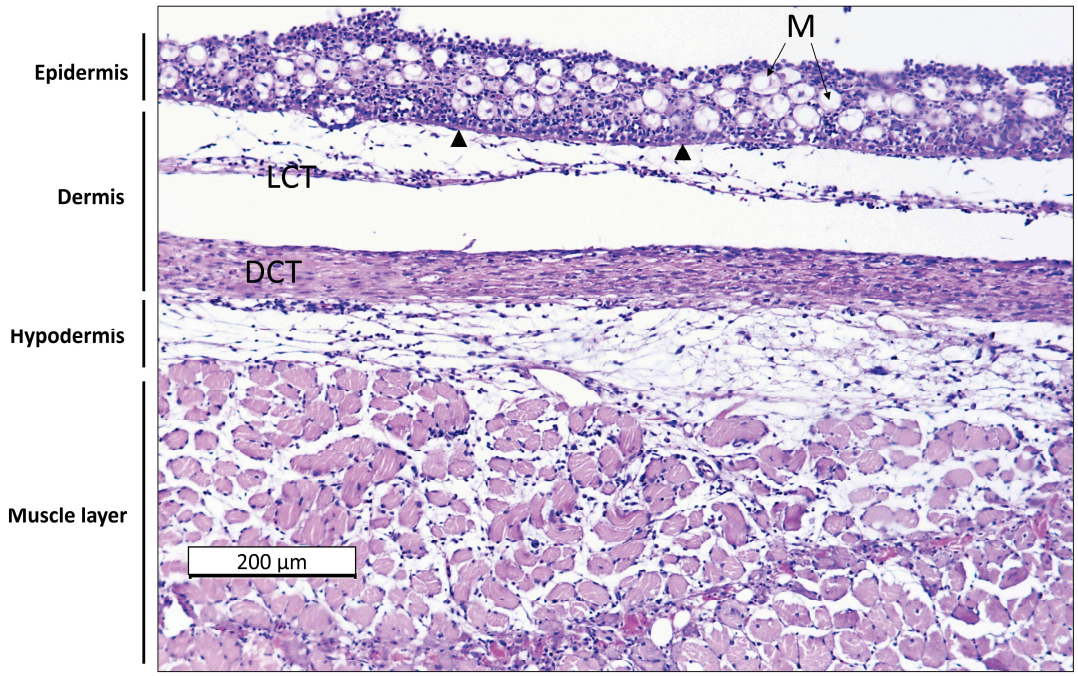

Figure 1.4. Histological structure of goldfish skin. A cross-section of the skin stained with hematoxylin and eosin shows three main layers situated on top of a muscle layer: (1) Epidermis consisting of a basal layer of keratinocytes resting on a basement membrane (arrowheads) with overlying layers of keratinocytes. Mucus-secreting cells (M) are observed among epidermal cells; (2) Dermis consisting of loss connective tissue (LCT) and dense connective tissue (DCT); (3) Hypodermis layer. Scale: 200 µm.

Table 1.1. Cytokines involved in tissue repair and their potential biological functions

Cytokine	Receptor	Source	Functions
Tnfa	Tnfr1 (p55) & Tnfr2 (p75)	PMN, macrophages & mast cells	‣ Increases synthesis of adhesion molecules to augment PMN recruitment [429] ‣ Promotes angiogenesis [430] ‣ Enhances keratinocyte proliferation and expression of adhesion molecules [76 ‣ Mast cell-released Tnfa activates DCs migration and maturation [431]
Il1	Il1r1, Il1r2 & Il1rAcP (Il1r3)	keratinocytes, PMN & macrophages	‣ Augments producing pro-inflammatory cytokines (e.g., Tnfa and Il6) [432] ‣ Increases fibroblast-secreted Kgf and Fgf7 to promote keratinocyte migration and proliferation [208,433,434] ‣ Triggers skin stem cell proliferation and activates gamma delta (γδ) T cells [435]
Cxcl8	Cxcr1	Platelets, PMN & macrophages	‣ A potent chemoattractant of neutrophils [436,437] ‣ Upregulates integrins and PMN-endothelium interactions to facilitate diapedesis [438] ‣ Enhances anti-microbial mechanisms of PMN (ROS production and release of neutrophilic granules) [439]
Il6	gp130 & Il6r	Myeloid cells, lymphocytes & fibroblasts	‣ Induces Th2 and Th17 differentiation in $CD4^+$ T-cells [440] ‣ Il6-stimulated Th2 cells release Il4 and Il13 to activate M2 polarization [441] ‣ Promotes Tgfb expression and re-epithelialization [442] ‣ Enhances fibroblast proliferation, activation and migration [443] ‣ Augments wound closure and granulation tissue formation in glucocorticoid-induced immunosuppressed mice [444] ‣ Activates fibroblasts, macrophages and keratinocytes to secrete Vegf, promoting angiogenesis [445]
Ifng	Ifngr1 & Ifngr2	Natural killer (NK) cells,	‣ Antiviral activities [429]

		plasmacytoid DCs & T cells	‣ Activates macrophage to produce pro-inflammatory cytokines and enhances phagocytosis [446] ‣ Regulates differentiation of $CD4^+$ T cells into Th1 effectors [446]
Il10	Il10r	Macrophages, DCs, PMN, mast cells & T cells	‣ Inhibits expression of pro-inflammatory cytokines, chemokines, adhesion molecules in macrophages and neutrophils [447] ‣ Suppresses NO and ROS production [447]
Tgfb	type II Tgfb receptor	Macrophages, keratinocytes fibroblasts & platelets	‣ Antagonizes PMN chemoattractants (e.g., Il8) and suppresses migration of inflammatory cells to the injury site [332,333] ‣ Enhances the expression of ECM components (collagen and fibronectin) by fibroblasts [208] and inhibits Mmps [448] ‣ Promotes angiogenic activities of endothelial progenitor cells [449] ‣ Augments keratinocyte migration and overall re-epithelialization [450]

Tnfa: tumor necrosis factor-alpha; Tnfr: tumor necrosis factor receptor; PMN: polymorphonuclear leukocytes; Il: interleukin; Kgf: keratinocyte growth factor; Fgf: fibroblast growth factor; Cxcl8: C-X-C motif chemokine ligand 8; Tgfb: transforming growth factor-beta; Ifng: interferon gamma; DCs: dendritic cells; NO: nitric oxide; ROS: reactive oxygen species; ECM: extracellular matrix; Mmps: matrix metalloproteinase.

Table 1.2. Functions of macrophage phenotypes during tissue repair

Phenotype	Receptors	Functions
M1 (classically activated or pro-inflammatory)	CD68 CD86 CD80	‣ Induces microbicidal activities (NO, ROS and phagocytosis) [258]. ‣ Releases pro-inflammatory cytokines (Tnfa, Il1b and Il6) [251,451] ‣ Enhances neutrophil recruitment by expressing chemokines [451,452] and synthesizing Mmps to degrade ECM [453] ‣ Clears apoptotic and necrotic PMN [454]
M2a (alternatively activated or wound healing)	CD163 CD206 CD209 Ym1	‣ Activated by Il4/Il13 [455] ‣ Produces chemokines: Ccl17, Ccl18, Ccl22 and growth factors: Igf1, fibronectin, Tgfb and Pdgf [456,457] ‣ Promotes ECM formation and angiogenesis [458]
M2b (regulatory or type 2)	CD86	‣ Activated *in vitro* by phagocytosing apoptotic neutrophils [459] ‣ Inhibits inflammation by releasing Il10 [459] ‣ Expresses Il6, Ccl1 and high levels of iNOS [456,460]
M2c (pro-resolving or deactivated)	CD86 CD163 CD206	‣ Stimulated by Il10 via STAT3 pathway ‣ Releases Il10 and Tgfb to exhibit anti-inflammatory responses [186,461] ‣ increases Mer receptor tyrosine kinase (MerTK) essential for efferocytosis [462]
M2d (tumor-associated macrophages)	-	‣ Activated by Il6 or both TLR ligands and A2 adenosine receptor agonists [463,464] ‣ Secretes Vegf, Il10, Tgfb and downregulates Tnfa, Il12 and Il1b [465,466]

Tnfa: tumor necrosis factor-alpha; PMN: polymorphonuclear leukocytes; Il: interleukin; Tgfb: transforming growth factor-beta; NO: nitric oxide; ROS: reactive oxygen species; Mmps: matrix metalloproteinases; ECM: extracellular matrix; Ccl: chemokine (C-C motif) ligand; Igf1: insulin growth factor 1; Pdgf: platelet-derived growth factor; iNOS: inducible nitric oxide synthase; STAT3: signal transducer and activator of transcription 3; TLR: Toll-like receptors; Vegf: vascular endothelial growth factor.

Chapter II

Materials and Methods[†]

[†] Parts of this chapter have been published in

- **Soliman, A. M.**, Yoon, T., Wang, J., Stafford, J. L., & Barreda, D. R. (2021). Isolation of skin leukocytes uncovers phagocyte inflammatory responses during induction and resolution of cutaneous inflammation in fish. *Frontiers in Immunology*, 12; 725063.
- Haddad, F.*, **Soliman, A. M.***, Wong, M. E., Albers, E. H., Semple, S. L., Torrealba, D., Heimroth, R. D., Nashiry, A., Tierney, K. B., & Barreda, D. R. (2023). Fever integrates antimicrobial defences, inflammation control, and tissue repair in a cold-blooded vertebrate. *eLife*, 12; e83644.
  ** Authors contributed equally to this work, and parts of this paper will be published in Haddad, F. thesis.*

2.1. Ethics statement

All animals were utilized according to the Canadian Council of Animal Care guidelines and the University of Alberta Animal Care and Use Committee (ACUC-Biosciences protocols 706 and 355303). Goldfish were anesthetized using tricaine methane sulfonate (TMS; 02168510; Syndel, WA, USA) solution at a concentration of 40-50 mg/L and pH of 7.4 to 7.6, then euthanized by cervical dislocation. All efforts were made to minimize animal stress and to ensure that termination procedures were efficiently performed.

2.2. Animals

Common goldfish (*Carassius auratus auratus*), 10-15 cm in length, were purchased from Mt. Parnell Fisheries (Mercersburg, PA) and imported to Canada via Aquatic Imports (Calgary, Canada). Fish were kept at 16°C continuous flow tanks at the Aquatic Facility of the Department of Biological Sciences, University of Alberta, on a simulated natural photoperiod of 12 hours of light alternating with 12 hours of dark. The water quality parameters throughout the experiment were maintained: pH at 7.2–8.0 and dissolved oxygen at 5.5–6.5 PPM. Fish were fed daily with 1.5 mm floating pellets containing crude protein, fat, fibers, vitamins and minerals (0060832; Mazuri Exotic Animal Nutrition, St. Louis, MO, USA). Fish were acclimated for at least fourteen days preceding their use in the experiments.

2.3. Bacteria: *Aeromonas veronii*

Aeromonas veronii was isolated and identified by previous lab members (Dr. Jeff Havixbeck and Dr. Aja Rieger) from natural cutaneous infections detected in goldfish held in the Aquatics facility [467]. The isolated bacterium was identified through sequencing as *Aeromonas veronii* biovar sobria (NCBI Taxonomy ID: 114517). A stock of bacteria was made and stored in glycerol solution at -80°C for future use. To generate a bacterial culture broth, frozen bacteria were inoculated into a sterile trypticase soy media (BD Biosciences, Franklin Lakes, NJ) (formula per 1 L of milli-Q water: 17 g pancreatic digest of casein; 3 g papaic digest of soybean; 2.5 g dextrose; 5 g sodium chloride, 2.5 g dipotassium phosphate) and added to a tube shaker to grow fresh overnight before each experiment. Quantifying the bacteria was attained using spectrophotometry (*A. veronii* growth curve is shown in **Figure 2.1**).

2.4. Cutaneous *A. veronii* infection: a tissue repair model

Fish were anesthetized using TMS and placed on a bench coat. Approximately 1x1 cm of scales were removed from the centre of the mid-line on the left side of the fish. A 5x5 mm scratch wound was inflicted via a sterile fine sanding screen (120 Grit). The wound was inoculated with *A. veronii* log-phase culture broth (concentration of 4.1×10^8 CFU/mL) via a sterile swab and then allowed to absorb the bacteria for 5 sec before reviving the fish in regular 16°C water with air bubblers. Wounds in control fish were inoculated with phosphate-buffered saline (PBS). Fish were randomly assigned to different temperature

categories (refer to **1.6. Experimental groups and study design**) and randomly picked at indicated time points for further downstream experiments. Fish were monitored throughout the experiments, and at indicated time points, fish were euthanized. *Aeromonas* load was assessed by swabbing the wound surface with a sterile cotton tip to streak trypticase soy agar plate, prepared by adding 15 g agar (BD Biosciences, Franklin Lakes, NJ) to 1 L of trypticase soy media then autoclaved. Plates were incubated overnight at room temperature and colony-forming units (CFUs) were assessed. Wound or hypothalamus tissues, depending on the experiment, were isolated for further downstream analysis.

2.5. Behavioural analysis

2.5.1. Annular thermal preference tank (ATPT)

ATPT was initially designed by Myrick *et al.* as an advanced tool for characterizing behavioural thermoregulation in fish [468]. As shown in (**Figure 2.2A, B)**, ATPT is composed of three rings: (1) an outer inflow ring consisting of eight segments (2) a middle barrierless continuous swim chamber, where fish is placed, and (3) an innermost circle controlling water outflow as well as depth. Water flows smoothly from the outermost ring to the swimming chamber and lastly to the drain through pores, generating eight temperature zones sustained by fluid dynamics (one zone of 16°C, two zones of 19°C, 21°C, 23°C and one zone of 26°C) (**Figure 2.2B)**, providing an environment for infected fish to deploy behavioural fever responses by translocating to higher temperature zones. The temperature of each zone was found to be maintained throughout the fourteen days of the experiments

with minimal mixing (**Figure 2.2C)** via thermal monitoring of these zones every minute using a HOBOware U30 data-logger (Onset Computer Corporation, MA, USA).

2.5.2. Tracking fish behaviour

Through advanced camera systems equipped with infrared lighting, fish movements in the ATPT were tracked with continuous high-resolution video recording during day and night cycles (**Figure 2.2D**) over 14 days. A tracking analysis software, Ethovision XT, Version 11 (Noldus Information Technology, Wageningen, the Netherlands), helped transform fish movement videos into numerical data. The software quantified fish behaviours based on placement and migration with an outstanding temporal resolution. Data analyses provided an accurate determination of preferred temperature zone, velocity and zone transitions displayed by individual fish on a per-second basis. These raw data were exported and compiled to calculate mean hourly temperature preference, total hourly zone transitions and velocity, thereby characterizing behavioural fever responses in *A. veronii*-infected goldfish.

2.6. Experimental groups and study design

Subsequent to infecting the fish with *A. veronii*, they were allocated to different temperature categories depending on the experiment. In the first part of the study, I aimed to evaluate the impact of behavioural fever on tissue repair. Therefore, I used these three temperature categories: 1) Fixed 16°C (T_{16}) group, representing control (the basal

temperature that fish are acclimatized to in the aquatic facility), where fish are held at a mezzanine tank of 16°C; 2) Fixed 26°C (T_{26}) group, representing fever-range hyperthermia where we manually increased fish housing temperature to 26°C (the highest temperature that fish move to if they are allowed to exert behavioural fever). 3) Dynamic Fever (T_D) group, representing the naturally occurring dynamic fever by allowing fish to freely swim to higher temperature zones of ATPT, deploying behavioural fever.

In the second part of the study, my objectives were to assess whether a manual/mechanical replication of fever would have a similar impact of the dynamic fever response on tissue repair. I used the following temperature categories: 1) Fixed 16°C (T_{16}) group (representing control); 2) Mechanical Fever (*MF*) group in which fish were added to a mezzanine tank, where housing temperature was changed manually according to the pattern of thermal preference observed during behavioural fever (**Figure 2.3**); 3) Short Truncated (*ST*) group, where the temperature pattern of fever was truncated at 4 dpi to return to basal condition (16°C) (**Figure 2.3**); 4) Long Truncated (*LT*) group at which fever's thermal pattern was truncated at 9 dpi to return to basal condition (16°C) (**Figure 2.3**).

2.7. Histopathological analysis

Wound tissues were collected and fixed in 10% neutral-buffered formalin (SF98-4; Thermo Fisher Scientific, Waltham, MA, USA). Following processing tissues overnight in a series of ethanol, toluene, and wax washes using a Leica TP1020 benchtop tissue processor (Leica Biosystems, ON, Canada), they were paraffin-embedded and sectioned (7 µm in

thickness) on slides using a Leica RM2125 RTS microtome (Leica Biosystems, ON, Canada). In this study, I used hematoxylin & eosin (H&E) stain to characterize cellular infiltration during the early part of tissue repair as well as Masson's Trichrome (MT) stain to evaluate collagen content in the dermis layer (collagen fibers are stained in blue).

2.7.1. Haematoxylin and Eosin (H&E) stain

Tissue sections on slides were deparaffinized and washed using two rounds of toluene (T324-1; Thermo Fisher Scientific, Waltham, MA, USA) (5 min each) followed by rounds of 100%, 90%, 70%, and 50% ethanol (2 min each) at room temperature. Slides were placed in Surgipath Hematoxylin Gill III (3801542; Leica Biosystems, ON, Canada) for 2 min and washed with running cold tap water for 15 min followed by 70% ethanol for 2 min, then in Surgipath Eosin solution (3801602; Leica Biosystems, ON, Canada) for 30 sec at room temperature. Slides were washed, dehydrated in a series of alcohol, cleared in toluene and mounted with DPX Mountant (50-980-370; Thermo Fisher Scientific, Waltham, MA, USA) at room temperature. Stained slides were viewed, and images were obtained using AxioScope A1 microscope (Zeiss, Oberkochen, Germany).

2.7.2. Masson's Trichrome (MT) stain

Slides bearing tissue sections were deparaffinized and washed using two rounds of toluene (T324-1; Thermo Fisher Scientific, Waltham, MA, USA) (5 min each) followed by rounds of 100%, 90%, 70%, and 50% ethanol (2 min each) at room temperature. Slides were

placed in Surgipath Hematoxylin Gill III (3801542; Leica Biosystems, ON, Canada) for 1 min and washed with running cold tap water for 15 min. Slides were stained with ponceau-fuchsin (AC400211000; Thermo Fisher Scientific, Waltham, MA, USA) for 2 min, rinsed in distilled water, differentiated in mordant in 1% phosphomolybdic acid (19400; Electron Microscope Sciences, Hatfield, PA, USA) for 5 min at room temperature. Slides were stained with Aniline Blue solution (A967-25; Thermo Fisher Scientific, Waltham, MA, USA) for 3 min and incubated in 1% phosphomolybdic acid then acetic acid solution (A38C-212; Thermo Fisher Scientific, Waltham, MA, USA) for 5 min and 3 min, respectively at room temperature. Slides were dehydrated in 95% ethanol and 100% ethanol for 2 min, cleared in toluene, mounted with DPX (50-980-370; Thermo Fisher Scientific, Waltham, MA, USA) at room temperature. Stained slides were viewed, and images were obtained using AxioScope A1 microscope (Zeiss, Oberkochen, Germany).

2.8. Isolation of skin leukocytes

Several protocols for leukocyte isolation from fish skin were previously reported [469–471]. Herein, I used a modified protocol that utilizes enzymatic digestion and gradient centrifugation to extract immune cells from fish skin [472]. In this protocol, I used modified goldfish Leibovitz's L-15 (MGFL-15) medium developed explicitly for *in vitro* cultivation of carp and goldfish primary cells (**Table 2.1**), in addition to collagenase D (11088858001; Sigma Aldrich, St. Louis, MO, USA) for tissue digestion to maintain cell viability and

maximize yield. Approximately 90% of isolated leukocytes were viable (**Figure 2.4**) (refer to **2.8.1. Assessment of cell viability**). The protocol is as follows:

Wound area was dissected, and skin tissue was added into a petri dish containing cold sterile 1x $PBS^{-/-}$ (no calcium/no magnesium). Using sterile scissors, skin was cut into small pieces (~ $2mm^2$) and washed with cold 1x $PBS^{-/-}$ to avoid blood contamination. Skin pieces were moved into a 50 mL tube containing 10 mL of complete MGFL-15 media that was added to a shaker for 30 min at room temperature. Content of the tube was strained through a sterile 70 µm cell strainer (BAH136800070; Sigma Aldrich, St. Louis, MO, USA). Skin pieces were collected and added into a new 50 mL tube with 10 mL of complete MGFL-15 media containing collagenase D (0.18 mg/mL). The tube was added to a shaker for 120 min at room temperature. Content of the tube was strained through a sterile 70 µm cell strainer, and flow-through containing cells was collected and washed with incomplete MGFL-15 media. Collected cell suspension was layered into a 51/34% discontinuous Percoll density gradient (GE Healthcare Chicago, IL, USA) and centrifuged at 400 x g for 25 min at 4°C. Using electronic pipette, the upper layer was discarded, and the interface was collected carefully into a new 15 mL tube. Cells were washed twice with incomplete MGFL-15 media, ready for downstream analysis.

2.8.1. Assessment of cell viability

Leukocytes isolated from skin were added to a 5 mL round bottom tube at a density of $5x10^5$ cells per 2 mL of incomplete MGFL-15 media and centrifuged at 350 x g for 8 min

at 4°C. Cells were washed twice with 1x Annexin V Binding Buffer (556454; BD Biosciences, Franklin Lakes, NJ, USA), resuspended in 200 µL 1x Annexin V binding buffer, and incubated for 30 min in the dark with 5 µL FITC Annexin V (560931; BD Biosciences, Franklin Lakes, NJ, USA) and 4 µL propidium iodide (PI; P4864; Sigma Aldrich, St. Louis, MO, USA) diluted 1:10 in 1x Annexin V binding buffer. Annexin V FITC binds phosphatidyl serine that is translocated from the inner to the outer surface of the cell membrane during apoptosis. PI, on the other hand, binds to DNA of necrotic cells by intercalating between base pairs. Finally, leukocytes were washed with 500 µL of 1x Annexin V Binding Buffer and fixed with 1% formaldehyde (47608; Sigma Aldrich, St. Louis, MO, USA). Prior to analysis, leukocytes were washed twice with 1x $PBS^{-/-}$, centrifuged at 350 x g for 5 min at 4°C, and the supernatant was decanted. Data was acquired using ImageStream Mk II Imaging Flow Cytometer (Amnis, Seattle, WA, USA) and analyzed using IDEAS Image Data Exploration and Analysis Software (Amnis, Seattle, WA, USA). A minimum of $1x10^4$ events was acquired. Cells were gated based on the normalized frequency of a fluorescent minus one sample (**Figure 2.4**).

2.8.2. Quantification of leukocytes

Leukocyte count per mL extracted from skin tissues was tallied using a hemocytometer (Thermo Fisher Scientific, Waltham, MA, USA) and a light microscope (Nikon Eclipse TS100, Tokyo, Japan). Total leukocyte count was calculated based on the total volume of each extraction. Cell subpopulations were identified using cytochemical staining.

2.8.3. Quantification of leukocyte subsets

A 100 μL volume of cell suspension was centrifuged onto a glass slide at 40 x g for 6 min using a Shandon Cytospin 4 cytocentrifuge (Thermo Fisher Scientific, Waltham, MA, USA). After staining the slides with Sudan Black and Hema3 stains, they were visualized at 1000x magnification (with oil immersion) on a Leica DM1000 confocal microscope (Leica Biosystems, ON, Canada). Cellular subpopulations were counted based on the cellular morphology and Sudan Black staining (**Figure 2.5**) [473]. At least 200 cells were counted per sample. Total number of neutrophil, lymphocyte and macrophage/monocyte subpopulations was calculated by multiplying the percentage of these subsets by the total isolated leukocyte number per each sample.

2.8.3.1. Hema3 stain

Cells were stained according to the manufacturer's specifications (23-122929; Fisher HealthCare -Hema3 Fixative and Solutions, Thermo Fisher Scientific, Waltham, MA, USA). Briefly, cells on slides were fixed in 70% methanol and stained with H&E. Slides were rinsed with cold running tap water and left to dry prior to microscopic visualization.

2.8.3.2. Sudan black stain

Cells were stained according to the manufacturer's protocol (199664; Sudan black B, Sigma Aldrich, St. Louis, MO, USA). Briefly, cells were fixed in a cold glutaraldehyde

fixative solution for 60 sec. Slides were rinsed with distilled water and incubated with Sudan black B staining solution for 5 min with intermittent agitation. Slides were rinsed, counter-stained in Hematoxylin solution Gill No. 3 for 5 min, then rinsed with cold running tap water. Slides were left to airdry before visualization and cell counting.

2.9. Immune functional leukocyte bioassays

2.9.1. Assessing cellular reactive oxygen species (ROS) and nitric oxide (NO) activity

Cells were added to a 5 mL round bottom tube at a density of $5x10^5$ cells per 2 mL of incomplete MGFL-15 media and centrifuged at 350 x g for 8 min at 4°C, then resuspended carefully into 500 µL incomplete MGFL-15 media. Cells were incubated in the dark for 30 min with 0.5 µL of CellROX Deep Red Reagent (C10491; Thermo Fisher Scientific, Waltham, MA, USA), 1 µM 4-Amino-5-Methylamino-2',7'-Difluorofluorescein Diacetate (DAF-FM DA) (D23844; Invitrogen, Waltham, MA, USA), and 4 µL of PI (P4864; Sigma Aldrich, St. Louis, MO, USA) diluted 1:10 in incomplete MGFL-15 media. CellROX and DAF-FM interact with ROS and NO molecules, respectively, and become fluorescent. Cells were washed two times with 1x $PBS^{-/-}$ and fixed with 1% formaldehyde (47608; Sigma Aldrich, St. Louis, MO, USA) for 10 min at 4°C. Cells were centrifuged at 311 x g for 5 min at 4°C and supernatant was removed. Data was acquired using ImageStream Mk II Imaging Flow Cytometer (Amnis, Seattle, WA, USA) and analyzed using IDEAS Image Data Exploration and Analysis Software (Amnis, Seattle, WA, USA). A minimum of $1x10^4$

events was acquired. Cells were gated based on the normalized frequency of a fluorescent minus one sample (**Figure 2.6**).

2.10. Cell culture

2.10.1. Cell lines: Fin fibroblast cell line (CCL71)

Goldfish fin fibroblast cell line (CAR-ATCC, CCL71) was maintained in complete MGFL-15 at room temperature without CO_2. This cell line is adherent. Cells were passaged when reaching 80-90% confluency, generally every 3-4 days, at a 1:10 dilution in fresh complete MGFL-15 media. To passage cells, culture media was decanted, and cells were washed carefully with 1x $PBS^{-/-}$ to remove any serum residues. Cells were incubated for 3 min at 37°C with 1 mL of trypsin-EDTA (25200056; Thermo Fisher Scientific, Waltham, MA, USA), followed by detaching cells by gentle tapping. Complete MGFL-15 media was added to cells to inactivate trypsin. Cell suspension was collected and centrifuged at 311 x g for 8 min. Supernatant was discarded and pelleted cells were resuspended in 10 mL of fresh complete MGFL-15 media. One milliliter of resuspended cells was added to a culture flask containing fresh complete MGFL-15 media. Cell line was stored in liquid phase of liquid nitrogen in MGFL-15 media with sterile 5% (vol/vol) Dimethyl sulfoxide (DMSO) (J66650.AK; Thermo Fisher Scientific, Waltham, MA, USA).

2.10.2. Cell culture media

Modified goldfish Lebovitz-15 (MGFL-15) media is commonly used to culture primary isolated fish cells [474]. Components of the medium can be found in (**Table 2.1**). Briefly, Dulbecco's Modified Eagle Medium (DMEM) (12100046; Thermo Fisher Scientific, Waltham, MA, USA) and Lebovitz-15 medium (L-15) (41300039; Thermo Fisher Scientific, Waltham, MA, USA) (one packet each) are dissolved in 2 L of milli-Q water. The solution was supplemented by vitamins, MEM amino acid, non-essential amino acid (11120052, 11130051, 11140050, Thermo Fisher Scientific, Waltham, MA, USA), bovine insulin (I-035; Sigma Aldrich, St. Louis, MO, USA), sodium pyruvate (11360070; Thermo Fisher Scientific, Waltham, MA, USA) as well as nucleic acid precursor (**Table 2.2**) and 10x Hank's balanced salt (**Table 2.3**) solutions. Hank's balanced salt solution was primarily added to MGFL-15 to retain high viability of primary isolated fish cells and provide a great value in flow cytometric analysis due to its lack of fluorescent phenol red. pH of the media was adjusted to a value of 7.3-7.4. Prepared media were filter sterilized and kept at 4°C. To prepare complete MGFL-15 media, 10% (vol/vol) heat-inactivated newborn calf serum, 100 U/mL penicillin and 100 μg/mL streptomycin were added.

2.10.3. Fibroblast proliferation assay

Wound tissue was dissected and homogenized in 3 mL of incomplete MGFL-15 media. The supernatant containing growth factors was collected following centrifugation at 350 x g for 8 min at 4°C. Goldfish fin fibroblast cell line (CAR-ATCC, CCL71) was

cultured, at a starting population of one million cells, for 48 h at room temperature with complete MGFL-15 media containing 25% (vol/vol) collected growth factors solution. For controls, the growth factors solution was replaced by incomplete MGFL15 media. 2'-Deoxy-5-ethynyluridine (5-EdU) (NE08701; Biosynth Carbosynth, Staad, Switzerland), thymidine analog used to assay DNA synthesis, was added to cells at a final concentration of 20 μM followed by a 2 hour-incubation. Cells were washed with 1x $PBS^{-/-}$, then fixed with 1% formaldehyde (47608; Sigma Aldrich, St. Louis, MO, USA). Cells were washed again and permeabilized in 0.1% Triton X-100 (93443; Sigma Aldrich, St. Louis, MO, USA). Cells were incubated with 1 mL of label mix [one hundred microliters of freshly prepared Ascorbic acid (200 mg/mL) (12050; Lumiprobe, Hunt Valley, MD, USA), 2 μL of Sulfo-Cyanine5 azide (final concentration of 2 μM) (13030; Lumiprobe, Hunt Valley, MD, USA), 5 μL of Copper (II)-TBTA complex (21050; Lumiprobe, Hunt Valley, MD, USA), and 893μL of $PBS^{-/-}$] for 30 min in the dark. Cells were washed and incubated with 5 μL NucBlue Live ReadyProbe Reagent-Hoechst 33342 (R37605; Thermo Fisher Scientific, Waltham, MA, USA) for 20 min at 4°C. Data was acquired using ImageStream Mk II Imaging Flow Cytometer (Amnis, Seattle, WA, USA) and analyzed using IDEAS Image Data Exploration and Analysis Software (Amnis, Seattle, WA, USA). A minimum of $1x10^4$ events was acquired. Cells were gated based on the normalized frequency of a fluorescent minus one sample.

2.11. Gene expression analysis

2.11.1. RNA extraction (skin and hypothalamus)

Goldfish skin and hypothalamus tissues were collected following euthanizing the fish. Tissues were homogenized in 1 mL of Trizol Reagent (15596026; Thermo Fisher Scientific, Waltham, MA, USA) using a PRO Scientific Bio-Gen PRO200 double insulated blade disruption homogenizer (Pro Scientific; Oxford, CT, USA). Homogenized tissue was transferred to respective microfuge tubes along with 100 µL of 1-bromo-3-chloropropane (B62404; Sigma Aldrich, St. Louis, MO, USA). Samples were vortexed and centrifuged at 12,000 x g for 15 min at 4°C. The aqueous layer was collected in a new tube. One hundred microliters of isopropanol were added to each tube and mixed by inversion before being stored at -80°C overnight. Tubes were centrifuged at 12,000 x g at 4°C for 10 min, supernatant was removed, and RNA pellet was washed twice with 75% ethanol. After centrifugation at 7,500 x g for 5 min at 4°C, the supernatant was discarded. The pellet was left to dry and resuspended in nuclease-free water (W4502; Sigma Aldrich, St. Louis, MO, USA). RNA quantity and quality were evaluated using Nanodrop ND-1000 microvolume spectrophotometer (Thermo Fisher Scientific, Waltham, MA, USA) (the range of A260/280 and A260/230 was from 1.8 - 2.2 with average values of 2.0 and 1.9, respectively); and Bioanalyzer-2100 equipped with an RNA 6000 Nano Kit (5067-1511; Agilent Technologies, Santa Clara, CA, USA) (the range of RNA integrity number (RIN) was from 7 to 9 with an average value of 7.9). RNA samples were stored at -80°C for either cDNA synthesis or Nanostring analysis.

2.11.2. Quantitative PCR analysis

2.11.2.1. cDNA synthesis

cDNA was synthesized from RNA samples using iScript cDNA synthesis kit (1708891; BioRad, Mississauga, Canada) according to manufacturer's protocol. Total RNA was standardized by molecular weight (1 µg for both skin and hypothalamus samples) through diluting RNA in nuclease-free water (W4502; Sigma Aldrich, St. Louis, MO, USA) and mixed with 1 µL with iScript reverse transcriptase enzyme and 4 µL of 5x reaction mix. Samples were then incubated in a thermal cycler for priming (5 min at 25°C), reverse transcription (20 min at 46°C) and finally, reverse transcription inactivation (1 min at 95°C). cDNA samples were stored at -20°C or used immediately for qPCR analysis.

2.11.2.2. Quantitative (q)PCR conditions

qPCR of cDNA was performed using QuantStudio 6 Flex Real-Time PCR System (Applied Biosystems, Waltham, MA, USA). In a 10 µL reaction mix, 5 µL SYBR green reagent mix (prepared by Molecular Biology Services Unit staff at the University of Alberta), 0.5 µL of both forward and reverse primers (final concentration is 0.5 µM) and 2.5 µL of cDNA (representing 12.5 ng of input total RNA) were added. Reaction mix was loaded into a 384-well plate with 3 technical replicates for each sample. Plates were heated to 95°C for 10 min and cycled 40 times between 60°C for 60 sec and 95°C for 15 sec. Raw qPCR data were analyzed through QuantStudio 6 Flex Real-Time software (Applied Biosystems, Waltham, MA, USA) to generate cycle threshold (Ct) values. Ct represents the number of cycles necessary for the fluorescent signal to exceed the background level.

Relative quantification (RQ) analysis was performed [475] using *actb* as an endogenous control. *actb* was chosen based on its superior gene expression stability under different experimental conditions compared to other housekeeping genes. RQ values were normalized against gene expression on day 0.

2.11.2.3. Primers

Primers used in qPCR analysis are listed in **Table 2.4**. Primers were previously validated in goldfish models [414,476,477] and further tested through melt curve results in addition to controls where no-reverse transcriptase and no-templet were added to qPCR reaction mix.

2.11.3. Nanostring analysis

Nanostring technology delivers direct profiling of individual mRNAs in a highly multiplexed single reaction devoid of the need for amplification. RNA from wound tissue was hybridized on nCounter multiplex analysis system (Nanostring Technologies; Seattle, WA, USA) to quantify the expression of 33 genes, including two housekeeping genes in purified RNA of these experimental groups: T_{16}, T_D, T_{26}, *MF*. The expression of housekeeping genes was stable at different time points under all experimental conditions and passed the quality control checks conducted by Nanostring Technologies. Reporter probe raw counts (the number of times the color-coded barcode for a target gene is detected) were normalized to the geometric mean of housekeeping genes; *beta actin* (*actb*) and *elongation*

factor 1 alpha (*ef1a*) according to manufacturer's protocol, then log_2-transformed using nSolver software package v4.0.72 and nSolver Advanced Analysis module v2.0.134 (Nanostring technologies; Seattle, WA, USA). The library and CodeSet used in the analysis involving target genes and accession numbers can be found through this link: https://figshare.com/s/68d0a5f2c88074656fed

2.11.3.1. Sample preparation

The recommended RNA input (60 ng) was prepared by standardizing the molecular weight of RNA samples by diluting RNA in nuclease-free water (W4502; Sigma Aldrich, St. Louis, MO, USA). For analysis, samples were shipped on dry ice to Nanostring in Seattle, USA. Nanostring technologies rechecked the quality and quantity of RNA samples before commencing the analysis with no reported quality control flags.

2.11.3.2. Quality controls

The performance of nCounter assay is determined based on assessing data quality at every step of the analysis to detect any QC flags (**Figure 2.7**). The process starts with evaluating imaging and binding density QC metrics to spot any issues with imaging performance or whether data collection was compromised due to image saturation with too many overlapping codes. Additionally, six positive controls (synthetic DNA targets) are included in each assay to measure the efficacy of the hybridization reaction. Finally, overall

visual inspections of data are conducted to weigh the severity of QC flags, if applicable. All nCounter gene expression assays in this study reported no QC flags throughout the analysis.

2.11.3.3. Pro-inflammatory pathway score

Pro-inflammatory pathway score was generated using the Pathway Scoring Module in nSolver Advanced Analysis software (Nanostring Technologies; Seattle, WA, USA). The score was calculated as the first principal component of the pathway genes' normalized expression. The pathways score engaged pro-inflammatory mediators, as well as neutrophil/macrophage phenotypes genes (*csf1r*, *cxcl8*, *il6*, *ccl1*, *csf1*, *tnfa*, *ifng*, *gcsfr*, *grn* and *il1b*).

2.12. Statistics

Data were statistically analyzed and graphed using GraphPad v9.3.1 (GraphPad Software, San Diego, CA, USA) For statistics involving more than two comparisons (where the variable factor is time) in the same experimental group, non-parametric Kruskal–Wallis followed by Dunn's test for multiple comparisons were used. One-way ANOVA was used to compare the variance in the means of three or more categorical independent groups, considering a single independent factor or variable in the analysis. Data had a normally distributed population, and each sample was drawn independently of the other samples. Additionally, the dependent variable was continuous. Two-way ANOVA was utilized to compare the effect of two independent categorical factors on a dependent variable, such as

fold change. The dependent variable was continuous, and each sample was drawn independently of the other samples. All statistical results correspond to a significance level of $p<0.05$. Mean values and correlations for behavioural data were calculated in Excel (Microsoft, Redmond, WA, USA). R (version 3.3, The R Foundation for Statistical Computing, Vienna, Austria) was used to calculate multivariate statistics, including principal component analysis (standard R package) and permutational multivariate analysis of variance using distance matrices ('vegan' community ecology package).

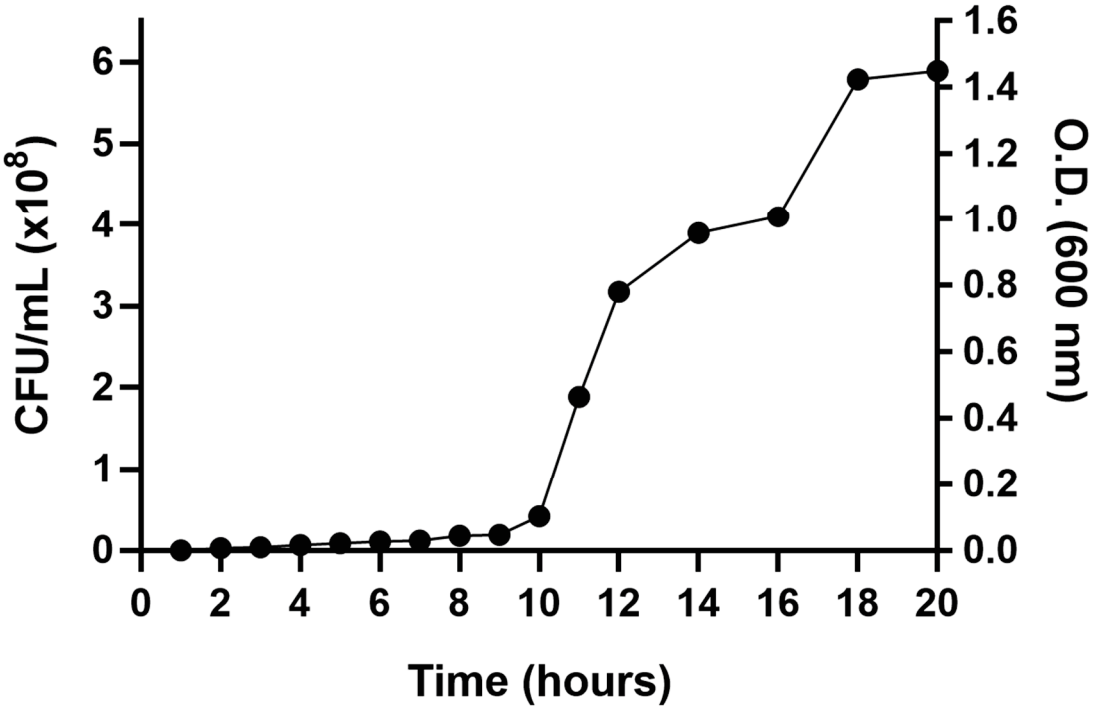

Figure 2.1. Growth curve of *Aeromonas veronii* bacterium. *A. veronii* was grown from a frozen stock at room temperature in trypticase soy medium. Optical density of the culture at 600nm was assessed by spectrophotometry. At the same time points, aliquots of culture were plated on agar plates and incubated overnight at room temperature, then CFUs were counted.

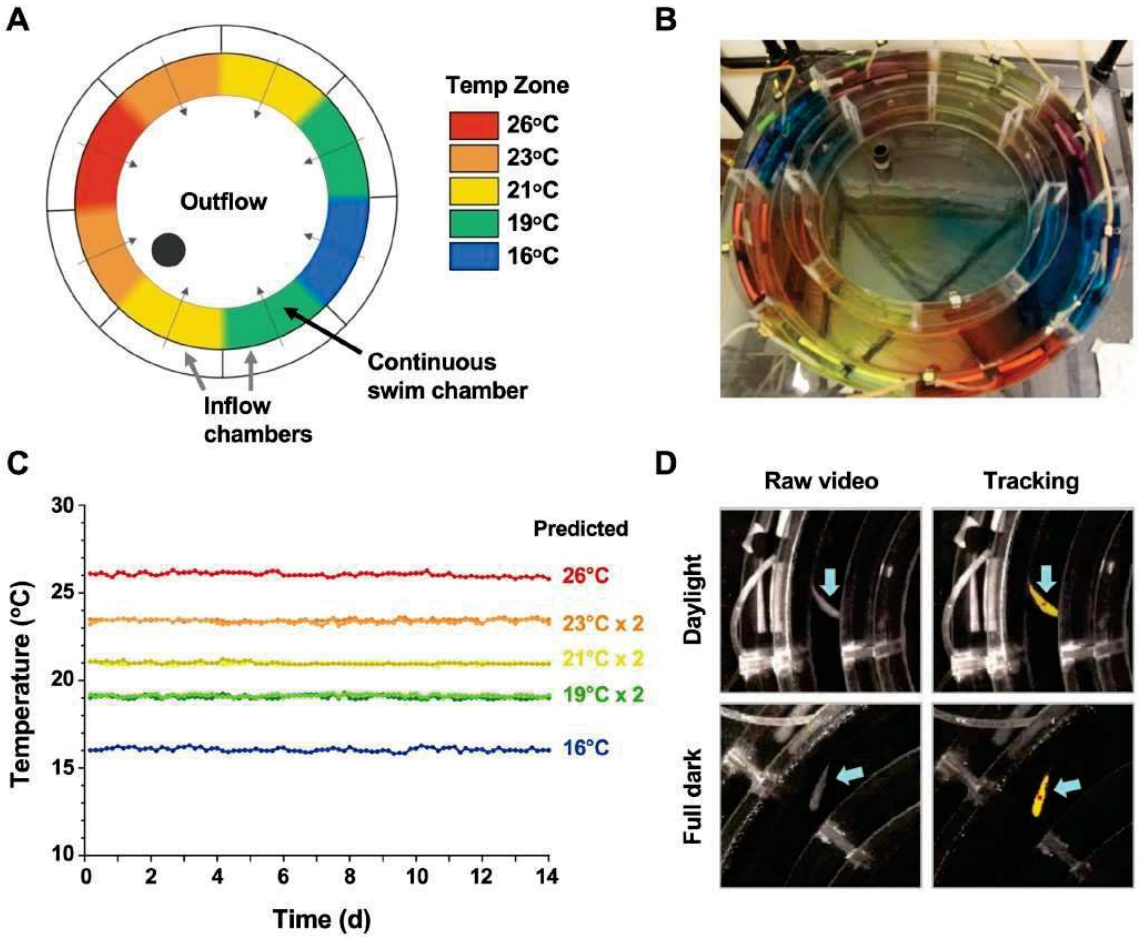

Figure 2.2. Annular thermal preference tank design, validation and fish tracking. (**A**) The ATPT established a continuous ring-shaped swim chamber that offered distinct temperature environments separated by fluid dynamics instead of physical barriers. (**B**) Dye flow test highlights eight distinct thermal zones created using concentric flow directed toward the center of the apparatus. (**C**) Analysis of temperature stability for established thermal zones. Single lines correspond to highest (26°C) and lowest (16°C) temperatures. Double lines denote values from equivalent zones on opposing sides of the apparatus for 19°C, 21°C, and 23°C target temperatures. (**D**) Representative images of a fish (blue arrows) in raw infrared and processed video, under simulated daylight and night (full dark) conditions. Yellow identifier denotes strong tracking signal achieved for experimental setup. Red dot denotes centre point used to set coordinates for raw behavioural data.

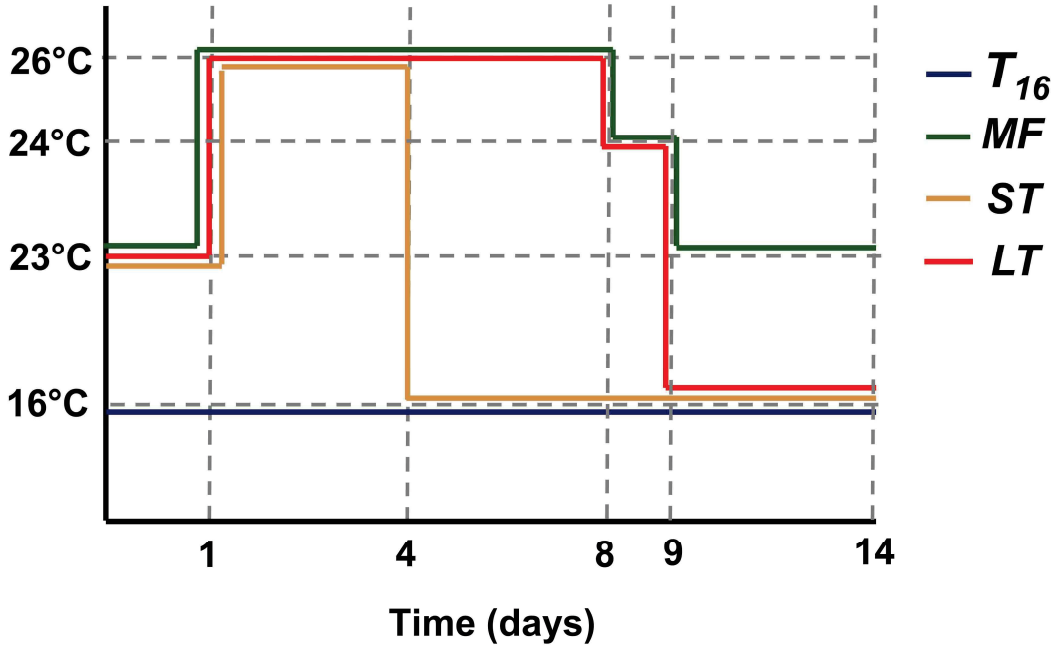

Figure 2.3. Temperature patterns of fixed basal temperature (T_{16}); mechanical fever (*MF*); short truncated (*ST*) and long truncated (*LT*).

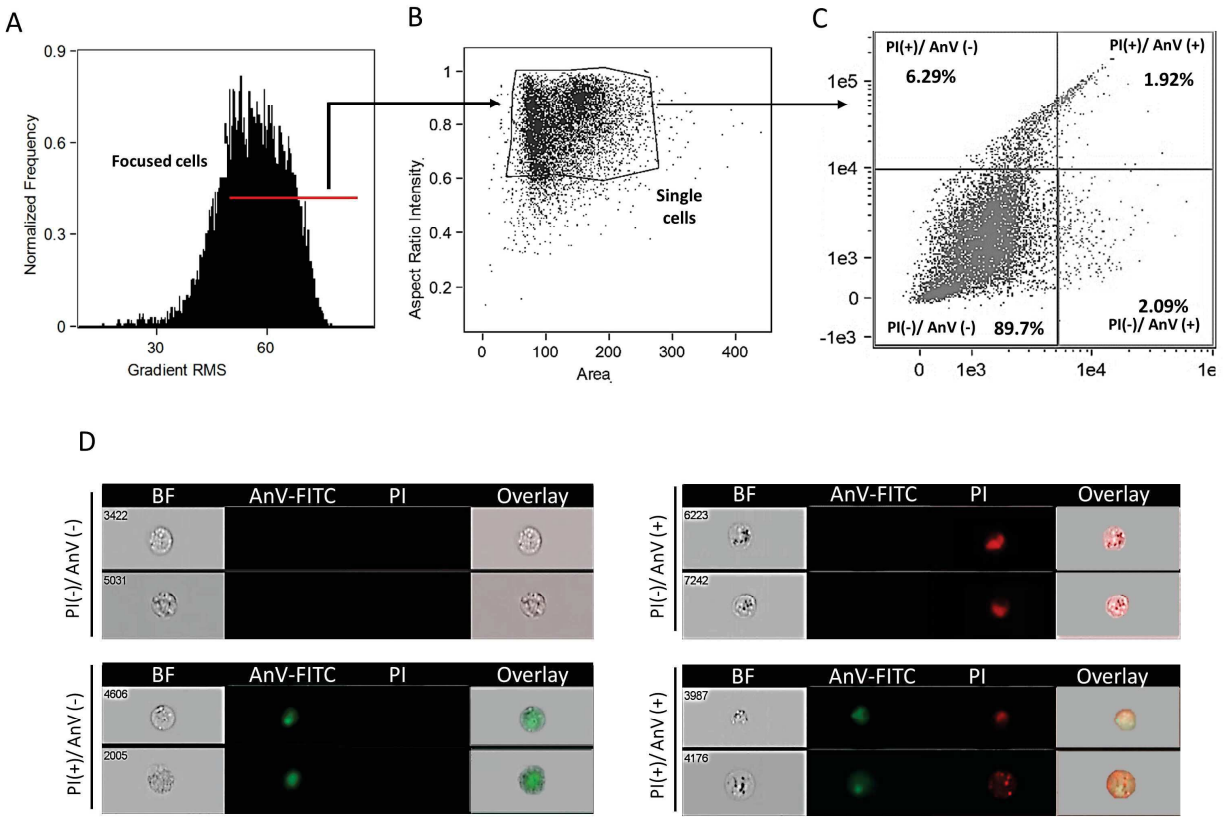

Figure 2.4. Leukocytes isolated from *A. veronii* infected skin showed ~90% viability. (**A**) Cells evaluated by ImageStream Mk II Imaging Flow Cytometer (Amnis) were gated using gradient RMS to identify focused cells. (**B**) Single cells were subsequently evaluated for (**C**) cell death based on propidium iodide (PI) and annexin V (AnxV FITC) staining. (**D**) Representative images show healthy cells [PI(-)/AnxV(-)], as well as those undergoing apoptosis or necrosis [PI(+)/AnxV(-)], [PI(-)/AnxV(+)], [PI(+)/AnxV(+)]. BF, bright field.

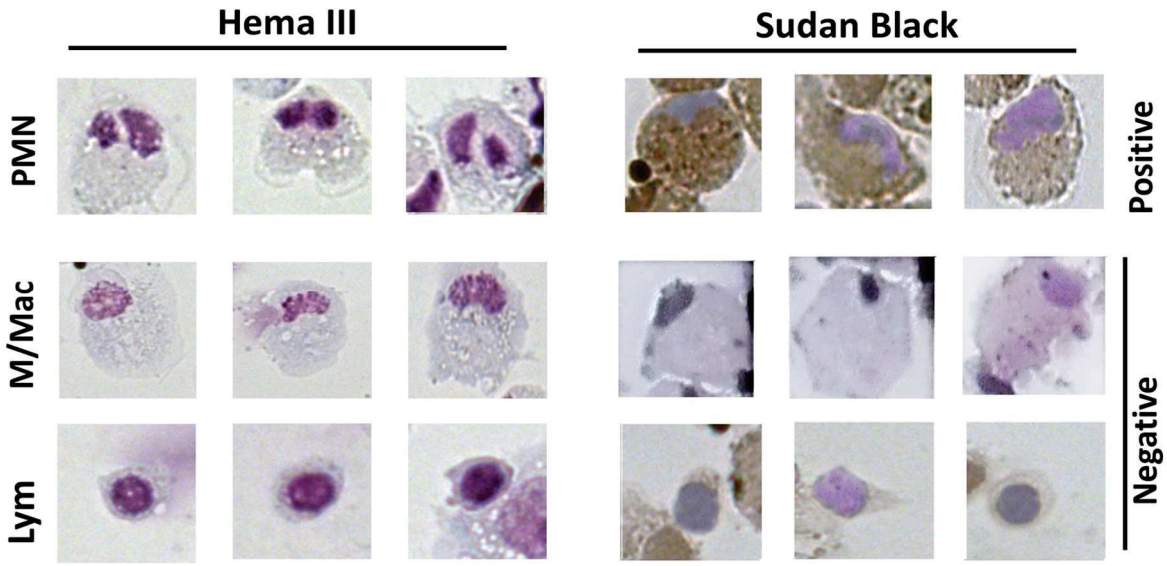

Figure 2.5. Staining of isolated leukocytes from fish skin. Representative images show leukocytes stained with both Hema3 and Sudan Black stains. PMN (polymorph nuclear leukocytes)/Neutrophils are positive for Sudan Black staining, while monocytes/macrophages (M/Mac) and lymphocytes (Lym) are Sudan Black negative.

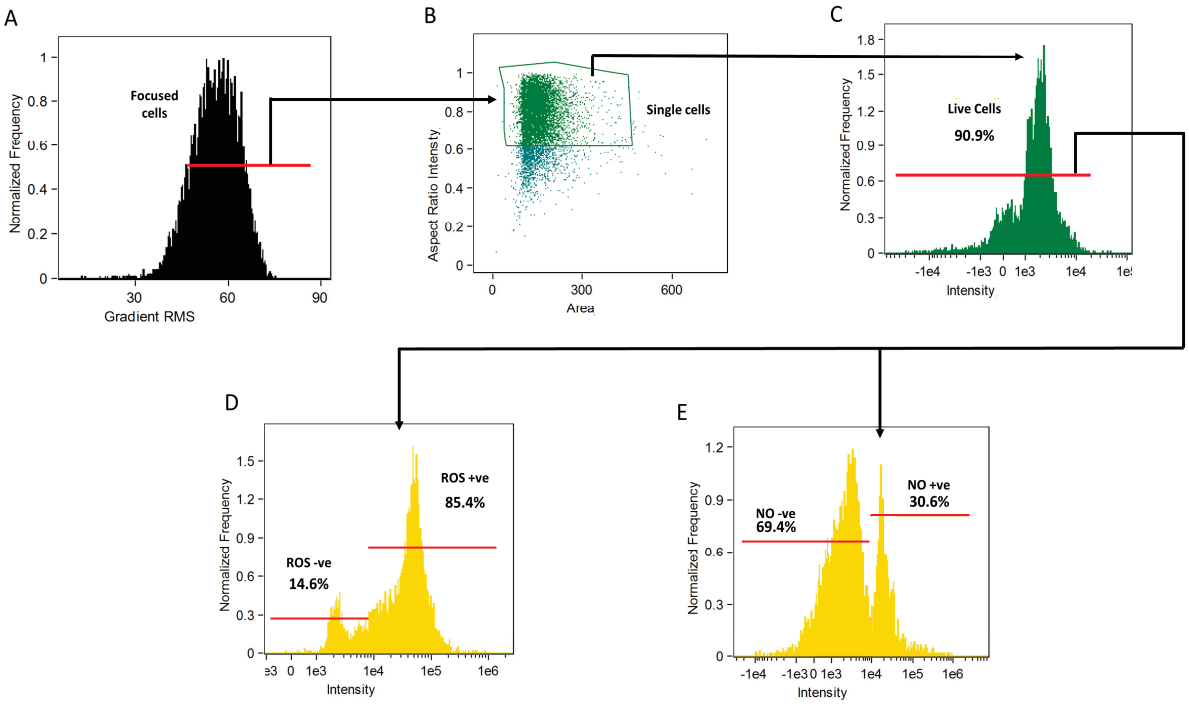

Figure 2.6. Gating strategy to evaluate the production of reactive oxygen species (ROS) and nitric oxide (NO). (**A**) Events acquired by ImageStream Mk II Imaging Flow Cytometer were gated using gradient RMS to identify focused cells. (**B**) Single cells were subsequently evaluated for (**C**) viability based on propidium iodide (PI) staining. (**D**) ROS and (**E**) NO production were examined based on CellROX and DAF-FM staining, respectively. BF, bright field.

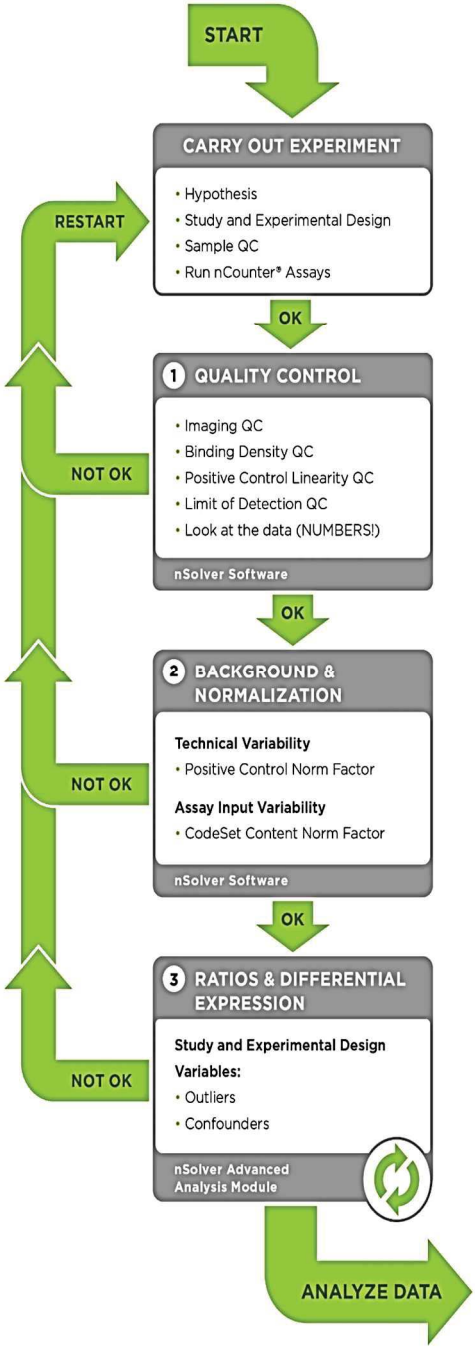

Figure 2.7. Steps of Nanostring analysis including quality controls and data normalization.
Source: nanostring.com

Table 2.1. Components of MGFL-15 media.

Component	Quantity
KH_2PO_4	0.69 g
K_2HPO_4	0.57 g
NaOH	0.75 g
$NaHCO_3$	0.34 g
HEPES	7 g
L-glutamine	0.584 g
Bovine Insulin	0.01 g
GFL-15 [§]	1L
10x Hank's Balanced Salt Solution	80 mL
Nucleic acid precursor solution	20 mL
MEM amino acid solution	25 mL
MEM non-essential amino acid solution	25 mL
Sodium pyruvate solution	25 mL
MEM vitamin solution	20 mL
β-mercapto-ethanol	7 μL
Milli-Q water	fill to 2L

[§] GFL contains DMEM and L-15 (one pack each) dissolved in 2 L of milli-Q water.

To prepare complete MGFL-15 media, 10% (vol/vol) heat-inactivated newborn calf serum, 100 U/mL penicillin and 100 μg/mL streptomycin were added.

Table 2.2. Components of nucleic acid precursor solution.

Component	Quantity
Cytidine	0.061 g
Adenosine	0.067 g
Thymidine	0.061 g
Hypoxanthine	0.034 g
Uridine	0.061 g
Milli-Q water	100 mL

Table 2.3. Components of 10x Hank's Balanced Salt Solution.

Component	Quantity
$NaHPO_4 \bullet 7H_2O$	2 g
KCl	2 g
Phenol red	0.05 g
KH_2PO_4	0.3 g
NaCl	40 g
D-glucose	0.05 g
Milli-Q water	500 mL

Table 2.4. Primer sequences and accession numbers used in quantitative PCR analysis.

Primer	Sequence (5'-3')	GenBank Accession numbers	Expected amplicon size (bp)
actb FW	GACCAACCCAAACCTCTCAA	AB039726	75
actb RV	AGTCAATGCGCCAAACAGA		
il10 FW	CAAGGAGCTCCG TTCTGCAT	HQ259106	73
il10 RV	TCGAGTAATGGTGCCAAGTCATCA		
tnfa FW	TCATTCCTTACGACGGCATTT	EU069817	126
tnfa RV	CAGTCACGTCAGCCTTGCAG		
il1b FW	GATGCGCTGCTCAGCTTCT	AJ249137	76
il1b RV	AGTGGGTGCTACATTAACCATACG		
tgfb FW	GTACACTACGGCGGAGGATTG	EU086521	74
tgfb RV	CGCTTCGATTCGCTTTCTCT		
nos2 FW	TTGGTACATGGGCACTGAGATT	AY904362	74
nos2 RV	CCAACCCGCTCAAGAACATT		
vegf FW	ATGAGAACCACACAGGACGGGATG TA	XM026228403	79
vegf RV	CGAGAGCTGCTGGTAGACATCATT		
cxcl8 FW	CTG AGA GTC GAC GCA TTG GAA	HM355573	73
cxcl8 RV	TGGTGTCTTTACAGTGTGAGTTTGG		
hsp27 FW	GATTCCACCAGACATCGCCA	DQ872651	185
hsp27 RV	ATTCCCAACTCCACCATGTG		
hsp70 FW	GCTGGCTGACAAAGAGGAGT	AB092839	93
hsp70 RV	TGGCATCCCTCCCTGATACA		
igf1 FW	ATGTACTGTGCGCCCGTAAA	AF001005	198
igf1 RV	CCATTCGCCCTACTGTCCTC		
col1a2 FW	AAGAACCCTGCCCGTACTTG	AB275455	155
col1a2 RV	AGAGAGCATCCCACGCAAAA		
il6 FW	CAGATAGCGGACGGAGGGGC	XM019073058	190
il6 RV	GCGGGTCTCTTCGTGTCTT		

FW: forward; RV: reverse

Chapter III

Characterization of wound healing kinetics and behavioural fever response in goldfish with *Aeromonas veronii* cutaneous infection†

---

† Parts of this chapter have been published in

- **Soliman, A. M.**, Yoon, T., Wang, J., Stafford, J. L., & Barreda, D. R. (2021). Isolation of skin leukocytes uncovers phagocyte inflammatory responses during induction and resolution of cutaneous inflammation in fish. *Frontiers in Immunology*, 12; 725063.
- Haddad, F.*, **Soliman, A. M.***, Wong, M. E., Albers, E. H., Semple, S. L., Torrealba, D., Heimroth, R. D., Nashiry, A., Tierney, K. B., & Barreda, D. R. (2023). Fever integrates antimicrobial defences, inflammation control, and tissue repair in a cold-blooded vertebrate. *eLife*, 12; e83644.
  * *Authors contributed equally to this work, and parts of this paper will be published in Haddad, F. thesis.*

3.1. Introduction

Initial characterization of wound healing kinetics in goldfish with a focus on the particulars of the inflammatory and proliferative phases under a static 16°C condition is discussed in this chapter. This was necessary to provide a foundation for identifying possible differences at various levels of the healing process under fever and static 26°C conditions. Skin lesions are common in fish, and they are induced either mechanically or through infection. Wound healing studies in fish utilizing zebrafish, Atlantic salmon, African catfish and rainbow trout show conservation of classical wound repair events (e.g., inflammation, granulation tissue formation and re-epithelialization) [396]. The Barreda lab has previously highlighted the capacity of *A. veronii* to induce cutaneous lesions in goldfish characterized by ulcers associated with extensive necrosis of subcutaneous tissues [467]. Fish were wounded and inoculated with either *A. veronii* or PBS (as a control), as previously described in (refer to **Section 2.3**), to be subsequently added to a mezzanine tank of 16°C temperature for 21 days. Kinetics of wound healing in *A. veronii* infected goldfish were identified in the first part of this chapter. Various methodologies, including histopathology, gene expression analysis and immune functional assays of isolated skin leukocytes, assisted in characterizing cutaneous immune responses against *Aeromonas* and kinetics of reparative events.

Additionally, confirming a behavioural fever response in goldfish infected with *A. veronii* was essential to link fever to tissue repair developments. This was achieved by analyzing fish behaviours, including their thermal preference, velocity and zone transitions, using a custom ATPT and high-resolution monitoring of fish movement. The second part of

this chapter identifies these behavioural thermoregulations and confirms engagement of CNS and systemic pyrogens during febrile responses.

3.2. Results

3.2.1. Wound healing in goldfish

Examining wound pathology across different time points provided insights into timelines for inflammation induction, resolution and wound closure. At 1 and 2 dpw, there was a gradual increase in the size of wounds with surrounding pale whitish areas (arrows; **Figure 3.1**) in fish inoculated with PBS or *A. veronii*. These white spots are called "macerations" and are mainly induced by edematous swelling of tissues around the injury site. Although there were no significant differences in the wound pathology between the two groups on the first 2 days after wounding, I detected signs of inflammation and purulent exudate only in *Aeromonas*-inoculated fish at 4 dpw (circle; **Figure 3.1**). This was followed by formation of sores that erupted, showing underlying necrotic subcutaneous tissue in the center at 7 dpw (**Figure 3.1**).

Pus formation is a sign of an acute inflammatory response that involves neutrophil recruitment and cellular apoptosis. The absence of purulent exudate and ulcer formation in PBS group indicated these observations to be *A. veronii*-induced. The detrimental tissue necrosis and sore formation significantly delayed wound closure in infected fish to be nearly completed at 21 dpw, while it was seen earlier at 14 dpw in PBS group (**Figure 3.1**).

3.2.1.1. Inflammation phase of wound healing

As previously mentioned, induction of the inflammatory phase of tissue repair is achieved by upregulation of pro-inflammatory mediators along with recruitment of immune cells to combat pathogens. Herein, I examined cytokines gene expression, kinetics of cellular migration and their antimicrobial responses during an acute inflammatory program in goldfish infected with *A. veronii* while kept at 16°C.

3.2.1.1.1. A. veronii cutaneous infection triggers an acute inflammatory response characterized by upregulation of pro-inflammatory mediators and neutrophil-dominant leukocyte recruitment

Histopathological analysis showed that leukocytes were gradually recruited to the infection site to reach a peak at 48 hours post-infection (hpi) (**Figure 3.2**). Cellular recruitment correlated with upregulation of classical pro-inflammatory cytokines and chemokines. For example, *tnfa* and *il1b* were markedly upregulated between 24 and 48 hpi (**Figure 3.3**). To gain added resolution into the infiltration kinetics of different leukocyte subpopulations, I isolated leukocytes from wound tissue. Consistent with the histopathological analyses above, the total number of isolated leukocytes gradually increased to reach maximum levels between 36 to 48 hpi (**Figure 3.4**). Among recruited cells, neutrophils accounted for the majority of infiltrating leukocytes (> 56%) compared to monocytes/macrophages (~ 29 %) during the first 48 hpi (**Figure 3.4**). Limited number of neutrophils existed at the injury site at 0 hpi; though, they increased significantly to ~ 29 x 10^4 at 24 hpi and then to ~ 45 x 10^4 at 36 and 48 hpi, making neutrophils the main cells to

respond and to be recruited. Characterization of gene expression profiles at the wound site showed an upregulation of neutrophil chemoattractant *cxcl8* at 36-48 hpi (**Figure 3.3**), correlating well with PMN recruitment.

Other leukocytes, such as monocyte/macrophage increased at the wound site at a relatively slower rate than neutrophils. For instance, I observed an increase in the number of monocytes/macrophages by ~ 17 x 10^4, while there was a marked rise in neutrophil number by ~ 44 x 10^4 at 36 hpi compared with the basal levels (**Figure 3.4**). Notably, macrophages also dominated the leukocyte population residing in the skin (~75 %) at 0 hpi (**Figure 3.4**). Lastly, lymphocytes infiltrated the wound site gradually to reach a significant number at 48 and 72 hpi (**Figure 3.4**).

3.2.1.1.2. Activation of anti-inflammatory program was associated with a neutrophil-dominated decline in recruited leukocytes and resolution of inflammation

Resolution of inflammation is critical to prevent chronic inflammatory conditions and to initiate reparative responses. Inflammation control is principally accomplished by downregulation of pro-inflammatory cytokines and leukocyte recruitment. Histopathological analyses and cell counts showed a reduction in leukocyte number in the wound area at 72 hpi (**Figures 3.2** and **3.4**), which was driven by a sharp decline in neutrophils (**Figure 3.4**). I further observed a substantial decrease in the gene expression of pro-inflammatory cytokines (*tnfa* and *il1b*) and chemokines (*cxcl8*) at 72 and 96 hpi (**Figure 3.3**). This was associated with a remarkable upregulation of crucial anti-inflammatory cytokines, such as *tgfb* and *il10* (**Figure 3.3**). Tgfb and Il10 mediate robust pro-resolution functions by suppressing pro-

inflammatory cytokines and chemokines expression [325,334,478]. Macrophages/monocytes and lymphocytes were the dominant populations of leukocytes residing in the wound tissue at 72 hpi (~ 40% and ~ 35%, respectively).

3.2.1.1.3. Recruited leukocytes exert differential antimicrobial responses during induction and resolution of inflammation characterized by dramatic changes in ROS levels

I was also interested in examining antimicrobial defenses exerted by recruited leukocytes at the wound site in response to *A. veronii* infection. Both ROS and NO represent evolutionarily conserved defense mechanisms deployed by leukocytes against invading pathogens [479]. While there was no increase in ROS levels at 12 hpi, a significantly higher percentage of leukocytes showed evidence of ROS activity at 24 and 48 hpi (**Figure 3.5**). This was followed by a sudden drop in ROS at 72 hpi (**Figure 3.5**). The upsurge in ROS production was correlated with upregulation of pro-inflammatory cytokines (*tnfa* and *il1b*) (**Figure 3.3**) along with the increase in neutrophil-centric leukocytic infiltration (**Figure 3.4**) between 24 and 48 hpi. Additionally, a neutrophil-mediated decline in leukocyte numbers (**Figure 3.4**), as well as upregulation of *il10* and *tgfb* (**Figure 3.3**), were associated with a substantial drop in ROS at 72 hpi, suggesting a shift from pro-inflammatory to anti-inflammatory program.

On the other hand, levels of another antimicrobial mechanism, NO, were relatively lower than ROS at 24 and 48 hpi (**Figure 3.5**). NO is a signaling molecule that mediates antimicrobial activities [480–484], and regulates cellular and biological functions such as

angiogenesis and chemotaxis [26,279,485]. The percentage of leukocytes with NO activity increased gradually to peak at 24 hpi (**Figure 3.5**). NO is synthesized by three different nitric oxide synthases (NOS): endothelial NOS (eNOS), neuronal NOS (nNOS) and inducible NOS (iNOS). Both eNOS and nNOS are constitutively expressed in endothelial cells and neurons, respectively. Meanwhile, iNOS expression is regulated in various cells, e.g., macrophages, monocytes, and mast cells, in response to inflammatory mediators [26,486]. My data showed that *nos2* (coding for iNOS enzyme) expression was significantly upregulated at 24 hpi (**Figure 3.3**).

3.2.1.2. Proliferation phase of wound healing

Following eradication of infection and resolution of inflammation, several reparative pathways are activated to restore damaged tissues [22]. These pathways are orchestrated by a variety of growth factors and crosstalk between immune and connective tissue cells to mediate re-epithelialization, angiogenesis and granulation tissue formation.

3.2.1.2.1. Re-epithelialization

Histopathological analysis revealed evidence of epidermis development at 4 days post-infection (dpi) (**Figure 3.6**). Epidermal layer was classically composed of basal layer (arrows; **Figure 3.6**) and overlaying thick low-density layer of keratinocytes. Full maturation of epidermis was reached at 21 dpi, indicated by the presence of mucus-secreting cells (circles; **Figure 3.6**). Skin mucus, particularly in fish, is an essential component of innate

immune mechanisms against invading pathogens; therefore, mucus-secreting cells are a critical part of a fully mature and functional epidermis [487]. The re-epithelialization process is regulated by a number of growth mediators, where Igf1 plays a key role in migration and proliferation of keratinocytes [306]. My data shows increased expression levels of *igf1* at 72-96 hpi (**Figure 3.7**).

3.2.1.2.2. Granulation tissue formation and angiogenesis

With regard to dermis healing, I focused on assessing collagen deposition and formation of new blood vessels in the wound area. Granulation tissue formation is a critical step in wound healing, aiming to fill the gap with ECM elements e.g., fibronectin, elastin, proteoglycans, glycoproteins and collagen type III fibers that get replaced later with collagen type I to provide tensile strength [29]. Through utilizing Masson's Trichrome stain, stains collagen with blue, small traces of collagen fibers were detected in the dermis layer at 4 and 7 dpi with a substantial amount of loose connective tissue (**Figure 3.6**); though, relatively abundant collagen was observed in the dermal layer at 14 dpi. By the end of the 21 days, dense, parallel and well-organized collagen fibres were detected. Expression of collagen gene (*col1a2*: *collagen type 1 alpha 2*) increased gradually to reach a peak at 336 hpi (14 dpi) (**Figure 3.7**).

Neovascularization was evidenced to occur in the dermis at 4 dpi (**Figure 3.6**). The angiogenesis process is regulated mainly by Vegf [27], which exhibited a significant upregulation between 48 and 96 hpi (**Figure 3.7**). Vegf is among several growth mediators

released by macrophages and other tissue-resident cells. Likewise, these cells also express Hsps to protect tissue against stress-induced misfolded proteins during the repair process [488]. I observed a significant upregulation of *hsp27* and *hsp70* at 24-48 hpi (**Figure 3.7**).

3.2.2. Behavioural fever in goldfish

Conventional models for studying behavioural fever in fish, such as shuttle box are well known to produce significant variability between individual animals. This is attributed to differential preference of fish for cover, swim depth and activity level. Other contributing factors include schooling, dominance and territorial grouping [489]. Herein, we utilized customized ATPT to reduce this variability and achieve robust analytical depth to behavioural outputs [468]. ATPT takes advantage of fluid dynamics rather than physical barriers to establish distinctive temperature zones (refer to **1.5.1. Annular thermal preference tank**). Under this setup, fish were free to choose their preferred environmental temperatures while avoiding heterogeneity induced by the previously mentioned factors. Distinct temperature set points (16, 19, 21, 23, 26^{o}C) were chosen and used to create a barrier-free environmental housing temperature gradient that spanned a 10^{o}C range. Directional flow rates across the swim chamber were adjusted to create smaller temperature gradients between each of the primary thermal zones. This ensured less abrupt changes in water temperature between zones that may impact fish choice to move among adjacent thermal zones.

Next, updated ATPT was coupled to an automated monitoring system with a per-second temporal resolution for effectively tracking fish through day and night cycles. We then challenged individual goldfish with an *Aeromonas* cutaneous infection *in vivo*. As eurythermal ectotherms, goldfish offered an opportunity to examine absolute changes to thermo-preference in response to an immune challenge while minimizing the potential for thermal stress. This is because the natural range of tolerated environmental temperatures for these fish (1.3^{o}C to 34.5^{o}C) was broader than those temperatures expected in a febrile response. Individual goldfish were wounded and inoculated with either *A. veronii* or PBS (control) to be subsequently added to ATPT over a timeframe of 14 days to determine their thermal preference, swimming velocity and rate of transitions between temperature zones. The ability of goldfish body temperature to equalize with surrounding water temperature within 2.5 min was established (data not shown). This supported the correlation between behavioural thermoregulation and its effect on tissue repair. Data presented in the following **subsections 3.2.2.1** and **3.2.2.2** are generated and analyzed in collaborative work with Farah Haddad and Dr. Shawna Semple.

3.2.2.1. *A. veronii* cutaneous infection induces febrile responses associated with two lethargy behaviours

Behavioural examination identified four distinct phases of the fever response among groups of fish challenged *in vivo* with *Aeromonas veronii* (**Figure 3.8A**) [490]. Thermal selection patterns across challenged fish were remarkably reproducible, even when fish were placed individually in the annular swim chamber (**Figure 3.8B**) [490]. A distinct period from

1 to 8 days dpi emerged, where *Aeromonas* challenged fish displayed a ~2.8°C increase in thermal preference (purple line in **Figure 3.8B**) compared to mock-infected (saline) controls (green line in **Figure 3.8B**) (25.57 ±SEM 0.1°C vs. 22.79 ±SEM 0.27°C, respectively). Variance analysis confirmed the consistency in environmental temperature selected by individual animals within this 1-8 dpi time window (**Figure 3.8B**). Outside of this window, no significant difference was found in thermal selection between challenged and control individuals, with both *Aeromonas* and saline-treated groups also shifting to large fluctuations both temporally and among individual fish (**Figure 3.8B**) [490].

Two new measurable lethargy-associated outcomes were further observed in teleost fish, which add to the similarities between ectotherm and endotherm fever. The first was defined by a decrease in swimming velocity (V) among *Aeromonas*-challenged fish (1-8 dpi; **Figure 3.8C**) [490].. In contrast, velocity among control fish remained high and variable across individuals during the same timeframe (**Figure 3.8C**). The second lethargy parameter was based on changes to temperature-seeking behaviour, defined by the rate of transitions a fish made between distinct ATPT thermal zones. Whereas control fish continued to show one hundred or more zone transitions (ZT) per hour, *Aeromonas*-treated fish displayed a dramatic decrease in the number of ZT during the same 1-8 dpi window (**Figure 3.8D**) [490]. As with temperature preference and velocity measurements, ZT values within this behavioural fever window were remarkably consistent across individual *Aeromonas*-challenged fish, increasing in variance after 8 dpi (**Figure 3.8D**). In sharp contrast, control fish displayed significant heterogeneity throughout the entire observation period. These two lethargy-associated metrics are consistent with established sickness behaviours of metabolic

fever in humans and other endotherms (immobility, fatigue, and malaise) and help to further define the behavioural fever response of teleost fish.

Hourly values for *Aeromonas*-challenged and saline control groups were evaluated simultaneously during the established fever window (1-8 dpi) and across the broader 14-day observation period. Between 1-8 dpi, marked segregation was identified in the responses elicited by fish in these two groups (**Figure 3.8E**) [490]. For *Aeromonas*-challenged fish, V and ZT values remained exclusively low during the febrile period (**Figure 3.8E**). In contrast, saline control fish exhibited a wider range of movement profiles, dominated by high V and ZT values (**Figure 3.8E**).

3.2.2.2. Behavioural fever in goldfish is associated with classical hypothalamic and PGE2 engagement

To confirm classic fever engagement of the central nervous system and assess potential differences with mechanical fever-range hyperthermia, hypothalamic tissue was isolated from *Aeromonas*-challenged fish and examined for local expression of pyrogenic cytokines. The selected genes, *il1b*, *tnfa* and *il6*, showed more robust local induction of gene expression under dynamic fever conditions (T_D group), where fish had been allowed to swim freely through the established 10^{o}C temperature gradient within the ATPT (**Figure 3.9**) [490]. Two cytoprotective elements (*hsp70* and *hsp90*) further displayed the highest levels of expression in the hypothalamus under these dynamic thermal conditions (**Figure 3.9**). Additional evaluation of PGE2 concentrations in circulation showed an early peak at 24 hpi for T_D fish [490], consistent with its role as a significant pyrogenic mediator of fever. These

responses were distinct from those fish placed under 26°C (T_{26}; mechanical fever-range hyperthermia) or 16°C static thermal conditions ($T_{16;}$ basal acclimated temperature) following infection. Mechanical hyperthermia promoted upregulation of cytokine and cytoprotective genes in our panel, but to lower levels than those fish allowed to exert dynamic fever. Circulating PGE2 concentrations remained near basal levels for both T_{26} and T_{16} groups [490].

Administration of an antipyretic offered added support for the shared biochemical pathways directing fever in ectotherms and endotherms. Ketorolac was chosen as a nonsteroidal anti-inflammatory drug (NSAID) with the capacity to inhibit COX1 and COX2 [491]. This drug has been successfully used in a range of animal species [492] and can be injected [491,493], thereby ensuring consistent dosing. In humans, a dose of 0.5 mg/kg is effective, and results in a 15-20 min onset with a 6-8 h duration of action [491]. Similarly, injection of ketorolac to *Aeromonas*-infected fish inhibited fever at a dose of 0.5 mg/kg [490]. This was based on a comparison of thermal preference between fish infected with *Aeromonas*, and those where ketorolac was administered to *Aeromonas*-infected fish.

3.3. Discussion

Aeromonas veronii is a freshwater pathogen that is well-known for its ability to induce severe cutaneous tissue damage, recognized as furunculosis (necrotic skin ulcers) [494–497]. Wound pathology of *A. veronii* infected fish showed skin lesions erupting white necrotic tissue (purulent exudate) that progresses to a complete loss of the tissue at the centre

of the lesion and exposing the underlying musculature. These observations were not detected in wounded fish inoculated with PBS. Additionally, infected fish experienced a behavioural fever response that was not seen in control fish. This implied that *Aeromonas* cutaneous infection, not solely a scratch wound, is required to trigger a febrile response in goldfish. My data highlights cutaneous immune reactions to an ubiquitous microbe that is reported to infect humans in addition to other mammals and fish [498] by exploring the regulatory procedures inducing and resolving acute inflammation during wound healing. Furthermore, kinetics and possible molecular pathways driving re-epithelialization, granulation tissue formation and angiogenesis were characterized.

The inflammatory response following skin injury is crucial for eradicating infection and normal wound healing [451]. Induction of acute inflammatory response involves upregulation of pro-inflammatory cytokines and leukocyte migration to the infection site [20]. Crucial to pathogen clearance and subsequent tissue repair is the recruitment of leukocytes from nearby blood vessels to wound area [479,499–501]. My data revealed a significant increase in leukocytes infiltrating the infection site at 36-48 hpi. Among infiltrating cells, neutrophils accounted for a considerable portion compared to monocyte/macrophage. Neutrophils are usually the first line of defense since they infiltrate the infection site rapidly to become the dominant leukocyte in earlier stages of acute inflammation [451]. In mammals and fish, neutrophils exist in the bloodstream and within hematopoietic tissue, ready to relocate toward a microbial challenge [414,502–504]. Previously, the Barreda lab has shown a rapid mobilization of neutrophils from hematopoietic tissue to the circulation in response to *A. veronii* cutaneous infection [467].

Though, kinetics of neutrophil recruitment to wound area were not established. Herein, I observed neutrophil-centric leukocyte recruitment to the infection site, which is consistent with the period of neutrophilia detected during the first 48 hpi [467].

Neutrophil recruitment was associated with a remarkable upregulation of pro-inflammatory cytokines (*tnfa* and *il1b*) and a potent neutrophil chemoattractant (*cxcl8*). Pro-inflammatory cytokines enhance the migration of immune cells, including neutrophils, to the infection site and further increase the level of chemoattractants to augment their recruitment [451]. Downregulation of pro-inflammatory mediators and upregulation of anti-inflammatory cytokines were coupled with an abrupt decline in neutrophil numbers at 72 hpi. Reduction in neutrophils at the infection site is possibly induced by their retrograde migration to the circulation [505] and cellular apoptosis [414]. These apoptotic neutrophils further contribute to resolution of inflammation via being internalized by macrophages to initiate anti-inflammatory/pro-resolution programs [414].

Macrophages/monocytes were the primary cells occupying the skin tissue at 0 hpi, suggesting their role in immune surveillance, pathogen detection, induction of acute inflammatory responses and recruitment of other leukocytes. I observed a relatively less increase in macrophage/monocyte numbers at 24-48 hpi when compared with neutrophils. This could be explained by the necessity of early neutrophil recruitment, thereby contributing to the majority of leukocytes infiltrating the wound area during early phases of acute inflammation, which was largely at the expense of monocytes/macrophages. *A. veronii* cutaneous infection is associated with low levels of blood monocytes [467], in addition to their capacity to induce high levels of apoptosis in macrophage populations [497,506], which

may explain the relatively low numbers of monocytes/macrophages at the infection site. The substantially low monocyte number in the peripheral circulation was attributed to an *A. veronii*-mediated selective recruitment of neutrophils [467], suggesting that the vascular route may not be the only path for monocyte recruitment to wound area. Recent studies indicated that monocyte migration to infection site could be achieved through visceral organs [507]. Moreover, a local proliferation of macrophages could contribute to an increased macrophage population [508,509].

Concomitantly with the significant drop in neutrophil numbers at 72 hpi, monocytes/macrophages remained the dominant population of leukocytes at the wound area. Macrophages contribute significantly to resolution of inflammation and subsequent tissue repair via upregulating anti-inflammatory cytokines, Hsps and growth factors [186]. Activation of tissue repair machinery is critical for restoring tissue integrity and homeostasis following an injury. The process involves crosstalk between several pathways and growth factors [510]. Among these factors, the pleiotropic Vegf is considered crucial for several wound healing processes, such as angiogenesis, re-epithelialization and collagen deposition, in addition to enhancing vascular permeability to promote cellular chemotaxis [27,511]. qPCR analysis showed a significant increase in *vegf* gene expression at 72 and 96 hpi, suggesting a shift from an inflammatory to a proliferative phase. Lymphocytes, on the other hand, infiltrated wound area at 48-72 hpi to mediate antigen-specific responses that activate adaptive immune responses. Previous studies reported lymphocyte infiltration during the late inflammatory phase of wound healing to play a role in resolution of inflammation and tissue remodeling [512,513].

Resolution of cutaneous inflammation commenced at 72 hpi, indicated by a neutrophil-driven reduction in leukocytes, downregulation of pro-inflammatory mediators and decreased ROS. These pro-resolution events were potentially driven by anti-inflammatory cytokines (*tgfb* and *il10*) that were upregulated at 72 and 96 hpi. Il10 was found to downregulate NADPH oxidase essential for ROS generation [478]. Meanwhile, Tgfb reduces levels of pro-inflammatory cytokines that potentiate leukocyte recruitment and ROS production [325,334]. Even though it is crucial for pathogen killing and intracellular signaling, ROS induce cellular damage if released extracellularly in large quantities, resulting in chronic inflammation and impaired wound healing [514]. Therefore, a balance between pro-inflammatory and anti-inflammatory mediators is crucial for effective pathogen clearance along with minimal collateral tissue injury [515]. Resolution of inflammation is further suggested to be mediated by several mechanisms. For instance, macrophages internalize apoptotic neutrophils, followed by downregulation of their pro-inflammatory profile [516–518]. Additionally, activated neutrophils *ex vivo* also showed the capacity to engulf apoptotic cells, leading to inflammation control and a substantial reduction in ROS [518,519].

Redox molecules, including NO and ROS, as well as their products, e.g., hydrogen peroxide (H_2O_2), superoxide anion (O_2^-), and reactive nitrogenous species (RNS) are essential for regulating inflammatory responses and eradication of infection [273]. ROS is critical for intracellular signaling pathways and antimicrobial activities [264]. In response to inflammatory mediators and phagocytosis, ROS is generated by NADPH oxidase (NOX) enzyme complex [520]. At the inner wall of the phagosome, NOX produces O_2^- and H_2O_2 to

destroy pathogens through damaging proteins, lipids and/or DNA [264,521]. High ROS levels were coupled to a significant increase in neutrophil-dominated leukocytes as well as an upsurge in the gene expression of pro-inflammatory cytokines. Likewise, a reduction in neutrophil numbers correlated with a marked decline in ROS at 72 hpi. NO level, in contrast, was relatively lower than ROS. NO possesses antimicrobial properties, including suppression of bacterial DNA repair and enzymes [480–484]. Furthermore, NO enhances respiratory burst-induced cytotoxicity in bacterial cells [522] and protects against oxidative stress-associated cellular injury [523] via controlling ROS production and minimizing the reactivity of O_2^- and H_2O_2 [273].

Taken together, my data suggests that subsequent to *A. veronii* cutaneous infection, an acute inflammatory response peaked at 36-48 hpi, identified by a neutrophil-dominated migration of leukocytes to infection site, where they deployed antimicrobial defenses to combat pathogens (**Figure 3.10A**). The acute inflammatory response and leukocyte recruitment are likely triggered and regulated via pro-inflammatory cytokines as well as chemokines [20,524] (**Figure 3.10A**). A shift from pro-inflammatory to pro-resolution state was noted at 72 hpi, evident by a substantial drop in neutrophils, which was possibly induced by a retrograde migration of PMN back into the circulation [505] and neutrophil apoptosis [414] (**Figure 3.10A**). PMN undergo apoptosis and produce chemotactic factors to attract macrophages [505,525], which in turn engulf apoptotic bodies and secrete pro-resolution/anti-inflammatory cytokines, as well as growth factors [526]. Anti-inflammatory cytokines provoke a reduction in pro-inflammatory mediators and ROS production to control

inflammation [334] (**Figure 3.10A**). Meanwhile, growth factors are critical for activating tissue repair machinery to restore integrity and homeostasis.

In order to examine the proliferation phase of wound healing, I focused on assessing re-epithelization, granulation tissue formation and angiogenesis. Regulation of these repair events is achieved through pleiotropic growth factors and cytokines along with crosstalk between various cellular effectors; thereby, it is challenging to determine exclusive contributors to a single process. Nonetheless, I investigated gene expression of the most prominent growth factors involved in each healing event. My results revealed an upregulation *tgfb* necessary for fibroblast activation and biosynthesis of granulation tissue components [527]. The granulation tissue is firstly composed of a loose connective tissue substance entailing tissue-resident cells, delicate small blood vessels and fibrin threads in ECM. The loose granulation tissue gets replaced largely with collagen synthesized by fibroblasts [19]. Hence, I examined collagen content in wound area at different time points. Collagen deposition increased gradually to replace granulation tissue at 21 dpi. Notably, expression levels of *col1a2* were substantially increased at 14 dpi. Likewise, progressive development and maturation of the epidermis layer were detected. Re-epithelialization is a crucial event that occurs early during the healing process to shield damaged and newly formed tissue against threats from the surrounding environments, especially in aquatic organisms. The gradual increase in *igf1*, among other factors, likely enhanced keratinocytes migration from wound edges and proliferation to cover the wound surface [306].

Collectively, histopathological and gene expression analyses suggest that the inflammatory phase of tissue repair starts principally at 24 hpi to reach a peak at 48 hpi,

demonstrated by significant cellular infiltration (**Figure 3.10B**). Resolution of inflammation begins at 72 hpi, followed by initiation of granulation tissue formation and collagen deposition observed at 4 dpi. Replacement of newly developed loose connective tissue by collagen fibres progressively continues to fill the wound gap at 21 dpi (**Figure 3.10B**). Given the significance of re-epithelialization, the process starts early with migrating keratinocytes from wound edges to cover the wound surface. Keratinocytes continue proliferation and differentiation to reach full maturation at 21 dpi, indicated by the presence of mucus-secreting cells (**Figure 3.10B**). Despite several studies examining wound healing in fish, significant differences regarding the outline of repair events and wound closure were reported [396,406,528]. These differences depend primarily on fish species, developmental stages, skin microbiota [528], superficial or deep wounds [393,402] and housing temperatures [193]. However, these models of tissue repair share conserved healing mechanisms [396,402]. For example, wound healing in Atlantic salmon (*Salmo salar* L.) demonstrated the same healing steps reported here; however, timelines were extended, where full maturation of the dermis layer was detected at 36 dpw [406].

My results demonstrate that *A. veronii* cutaneous infection stimulated behavioural fever in goldfish, represented by an increase in their thermal preference. Additionally, the febrile response was in conjunction with lethargy behaviours resembling sickness behaviours in mammals. The ATPT system allowed for high-resolution tracking of fish individually at in addition to avoiding possible interventions of territorial behaviours and schooling. The analyses revealed a fever window of 7 days, after which animals started to move to lower temperature zones and gain increased movement. Moreover, the increase of *tnfa*, *il6* and *il1b*

expression within the hypothalamus and ketorolac-induced fever suppression concur with growing evidence of conserved pathways of fever induction between endothermic and ectothermic vertebrates [18] and thereby advocating the use of behavioural fever as a comparative model to study fever [60,69].

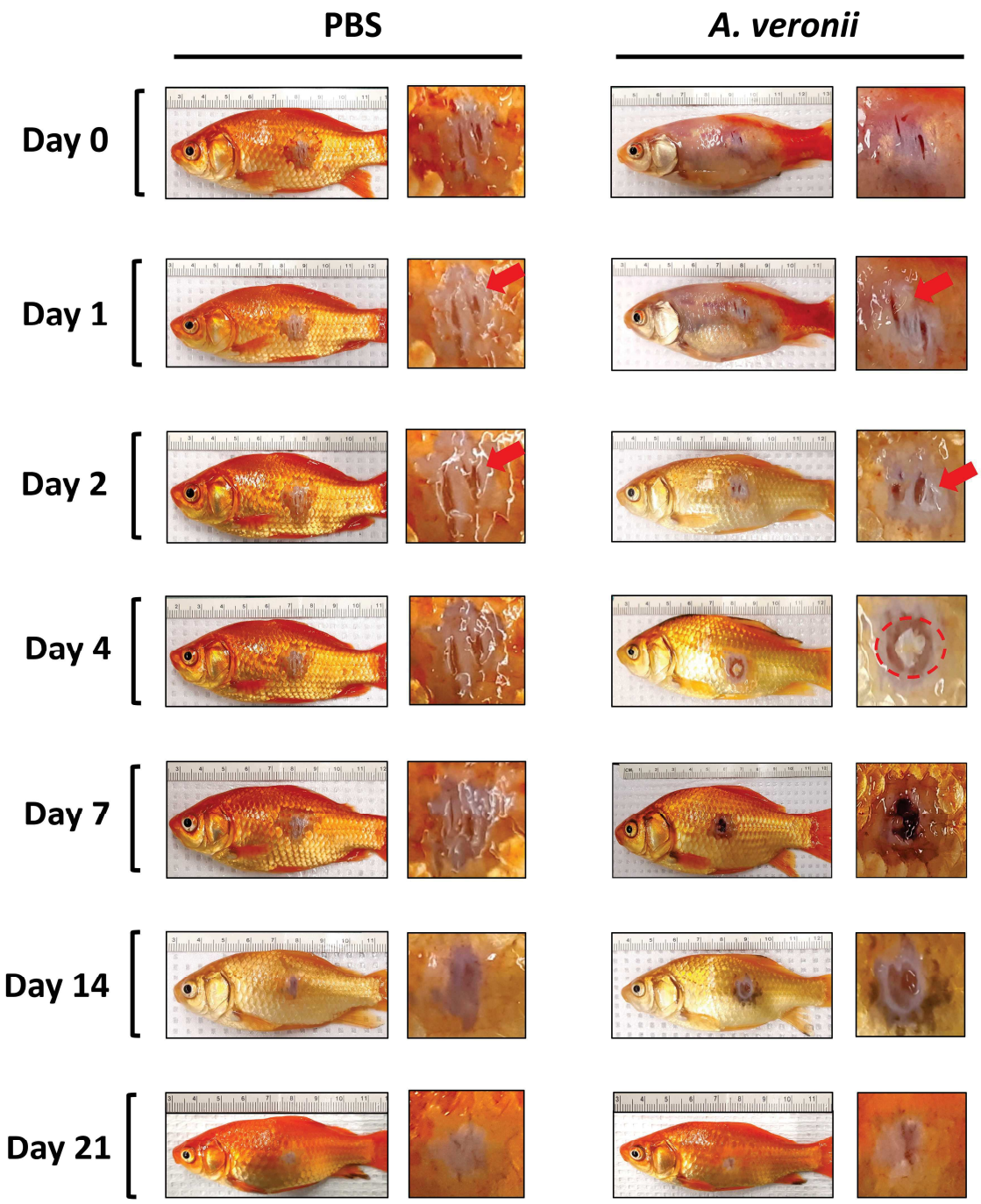

Figure 3.1. Representative images showing the progression of wound healing. Fish were wounded and inoculated with PBS or *A. veronii* and housed at fixed 16^{o}C. Arrows show macerations development in both PBS and *A. veronii* inoculated fish; circle highlights purulent exudate observed only in infected fish.

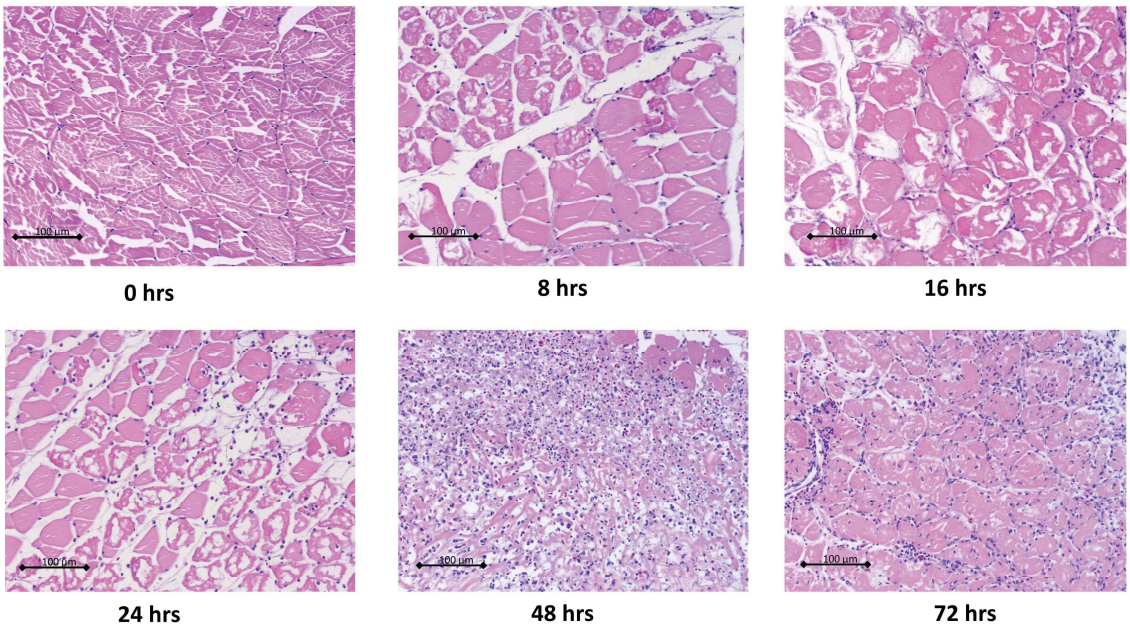

Figure 3.2. Histopathological analysis of wound tissue showed a gradual recruitment of leukocytes to the injury site. Fish were infected with *A. veronii* and housed at fixed 16^{o}C. Representative Hematoxylin & Eosin stained wound sections. Goldfish were wounded and inoculated with *A. veronii*. Wound tissues were collected at indicated time points. Tissues were fixed in 10% formalin then sectioned, stained and imaged (n=3).

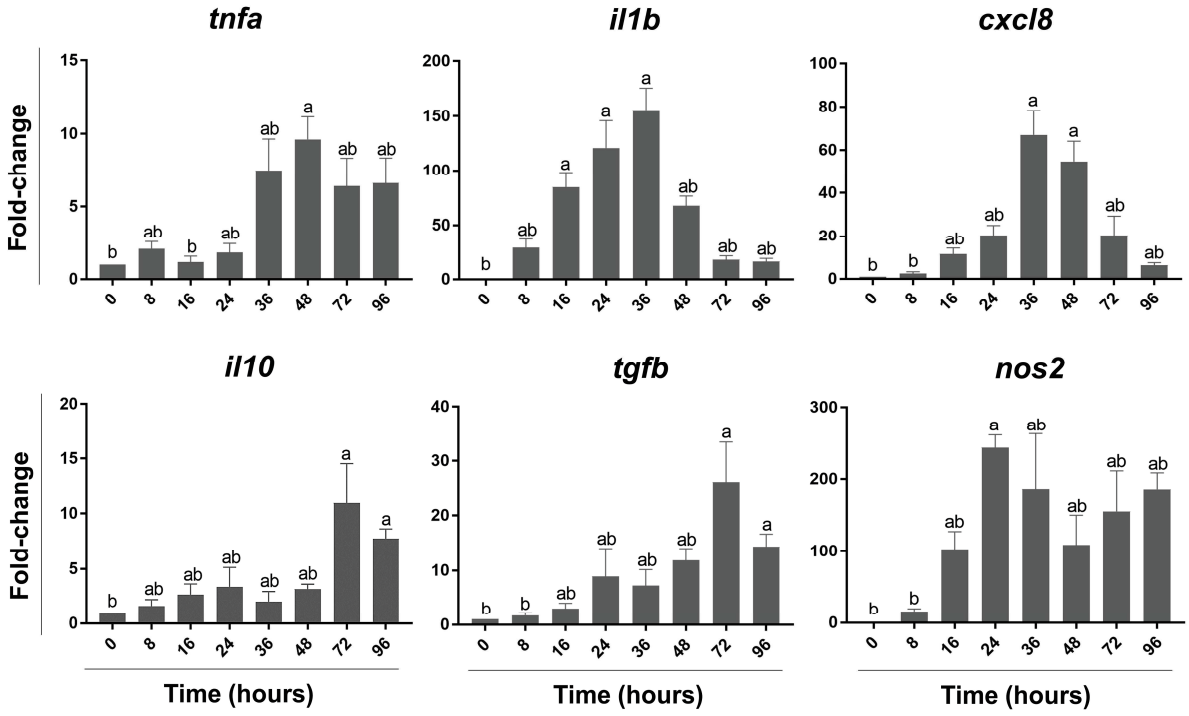

Figure 3.3. Quantitative PCR analysis of wound tissue in *A. veronii* infected fish revealed gene expression kinetics of classical pro-inflammatory and pro-resolution mediators. At each of the indicated time points, wound tissue was collected, RNA extracted, and cDNA synthesized. qPCR was used to evaluate the expression levels of pro-inflammatory cytokines: *tnfa* & *il1b*; anti-inflammatory cytokines: *tgfb* & *il10*; chemokines: *cxcl8*; growth factors: *vegf*; and *inducible nitric oxide synthase*: *nos2*. All statistical results correspond to a significance level of $p<0.05$ using Kruskal–Wallis test followed by Dunn's test for multiple comparison. Bars represent the mean with error bars representing SEM; n=5 per time point. Different letters indicate statistical differences between groups. *actb* was used as an endogenous control; RQ values were normalized against gene expression at day 0.

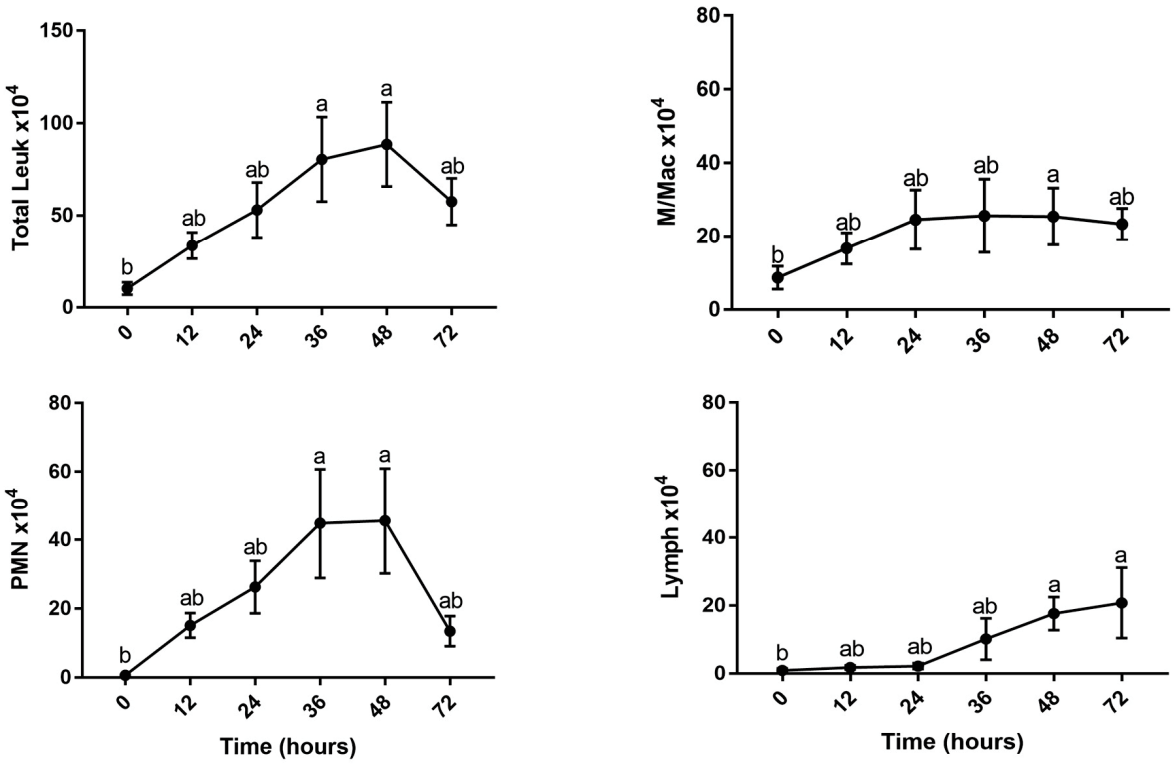

Figure 3.4. Kinetics for neutrophil, monocyte/macrophage, and lymphocyte recruitment to wound area. Fish were infected with *A. veronii* and housed at fixed 16^{o}C. Total leukocytes, PMN (polymorph nuclear leukocytes), M/Mac (macrophages/monocytes), and Lymph (lymphocytes) isolated from wound tissue. At each indicated time point, leukocytes were isolated and counted using a hemocytometer. Cells were fixed on slides using Cytospin and stained with Sudan Black stain. At least 200 cells were counted to determine the proportion of individual leukocyte subsets, which was used to determine total cell numbers. All statistical results correspond to a significance level of $p<0.05$ using Kruskal–Wallis test followed by Dunn's test for multiple comparison. Points represent the mean with error bars representing ±SEM; n=5 per time point. Different letters indicate statistical differences between groups.

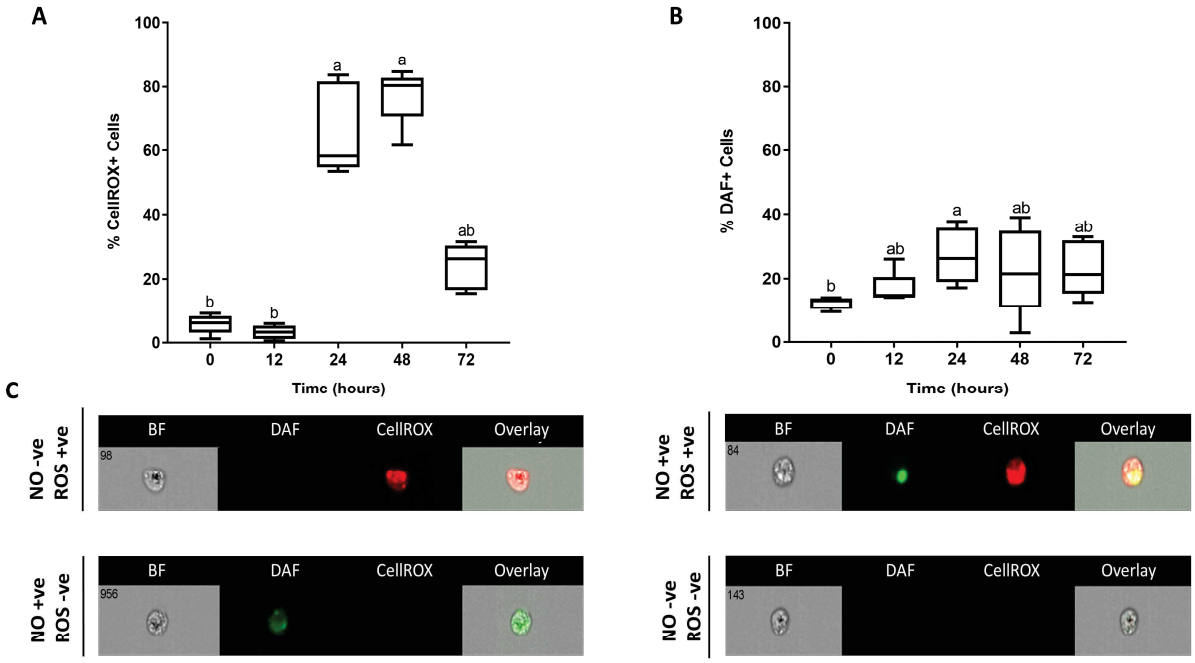

Figure 3.5. Kinetics of ROS and NO antimicrobial responses exerted by skin leukocytes during induction and resolution of cutaneous inflammation. Fish were infected with *A. veronii* and housed at fixed 16^{o}C. At indicated time points, leukocytes were isolated from wound tissues, then incubated with DAF-FM dictate (detects NO) and CellROX (detects ROS) for 30 min. Using image flow cytometry, intensity of DAF-FM and CellROX was detected. The percentage of cells associated with (**A**) reactive oxygen species (ROS) and (**B**) nitric oxide (NO) are shown. All statistical results correspond to a significance level of $p<0.05$ using Kruskal–Wallis test followed by Dunn's test for multiple comparison. Boxplots show spread of data with their median; n=5 per time point. Different letters indicate statistical differences between groups. (**C**) Representative images from ImageStream MKII flow cytometer denote positive or negative DAF-FM and/or CellROX events.

Day 3

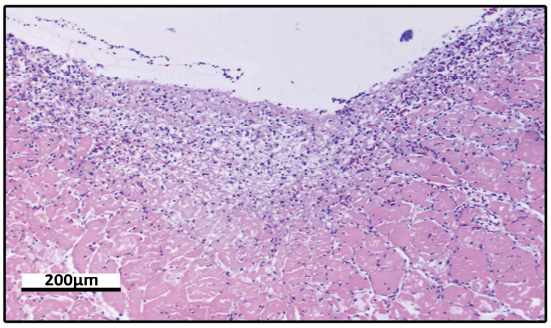

Day 4

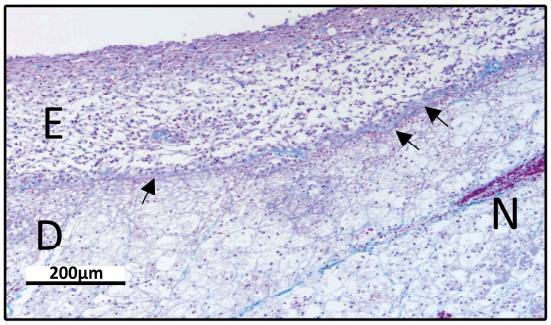

Day 7

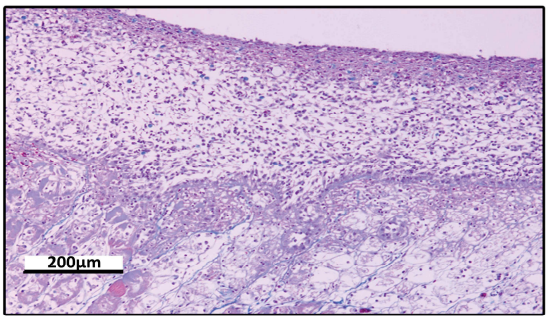

Day 14

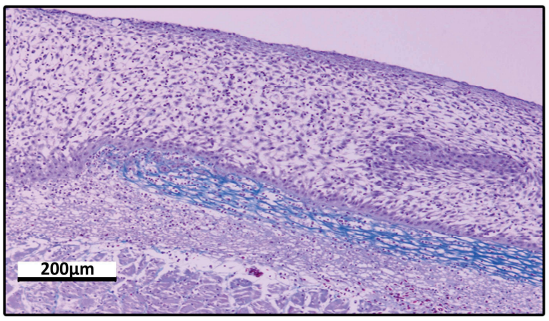

Day 21

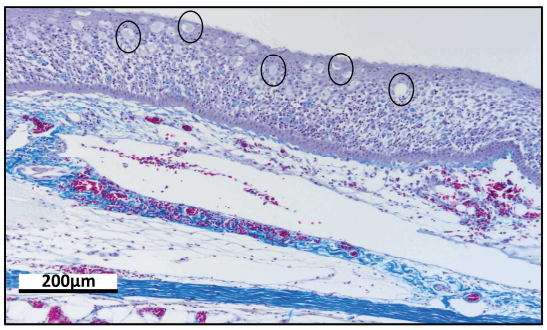

Figure 3.6. Kinetics of wound healing proliferative events in fish infected with *A. veronii*. Fish were infected with *A. veronii* and housed at fixed 16^{o}C. Wound tissues were collected at indicated time points, fixed in 10% formalin, sectioned, stained with Masson's Trichrome stain (n=3). Evidence of epidermis, including the development of basal layer (arrows) and overlying keratinocyte, as well as signs of new blood vessels formation (N) are detected at 4 dpi. Collagen fibers are deposited at wound area gradually starting on day 4 to reach full maturation at 21 dpi when mucus-secreting cells (circles) are also observed in the epidermis layer.

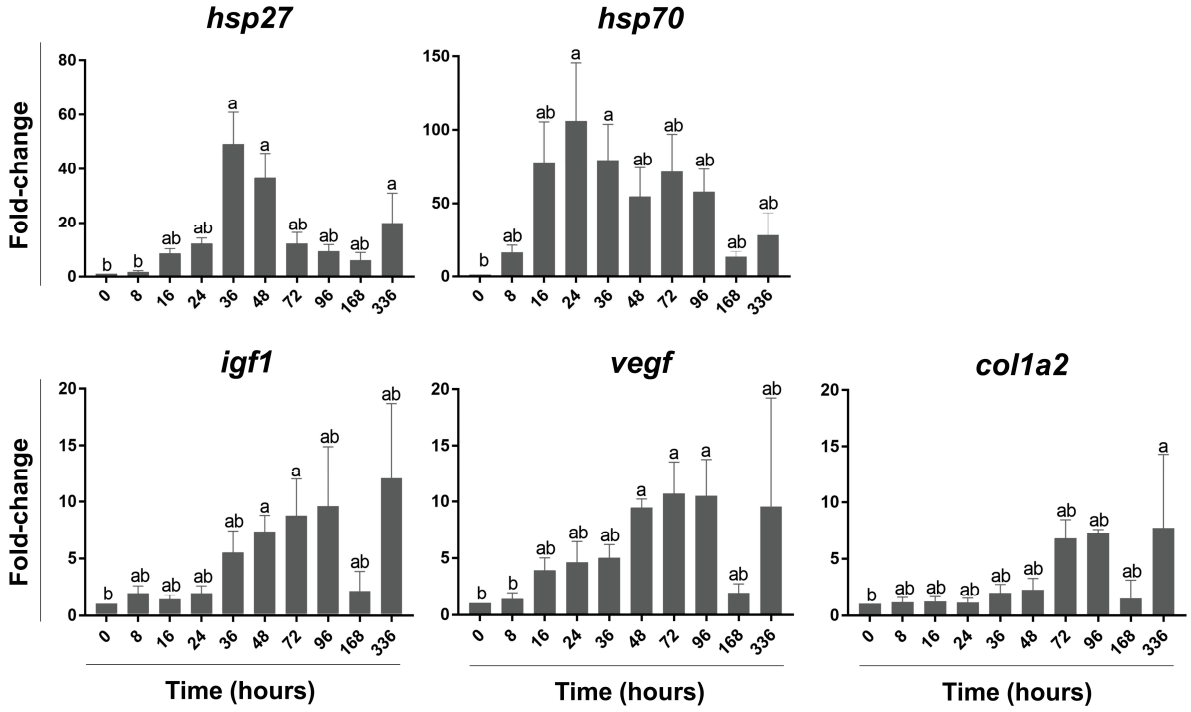

Figure 3.7. Quantitative PCR analysis of wound tissue revealed gene expression kinetics of classical tissue repair mediators and markers. Fish were infected with *A. veronii* and housed at fixed 16^{o}C. At each of the indicated time points, wound tissue was collected, RNA extracted, and cDNA synthesized. qPCR was used to evaluate the expression levels of *heat shock protein*: *hsp27* and *hsp70*; *insulin growth factor 1*(*igf1*); *vascular endothelial growth factor* (*vegf*); and *collagen type 1 alpha 2* (*col1a2*). All statistical results correspond to a significance level of $p<0.05$ using Kruskal–Wallis test followed by Dunn's test for multiple comparison. Bars represent the mean with error bars representing SEM; n=5 per time point. Different letters indicate statistical differences between groups. *actb* was used as an endogenous control; RQ values were normalized against gene expression at day 0.

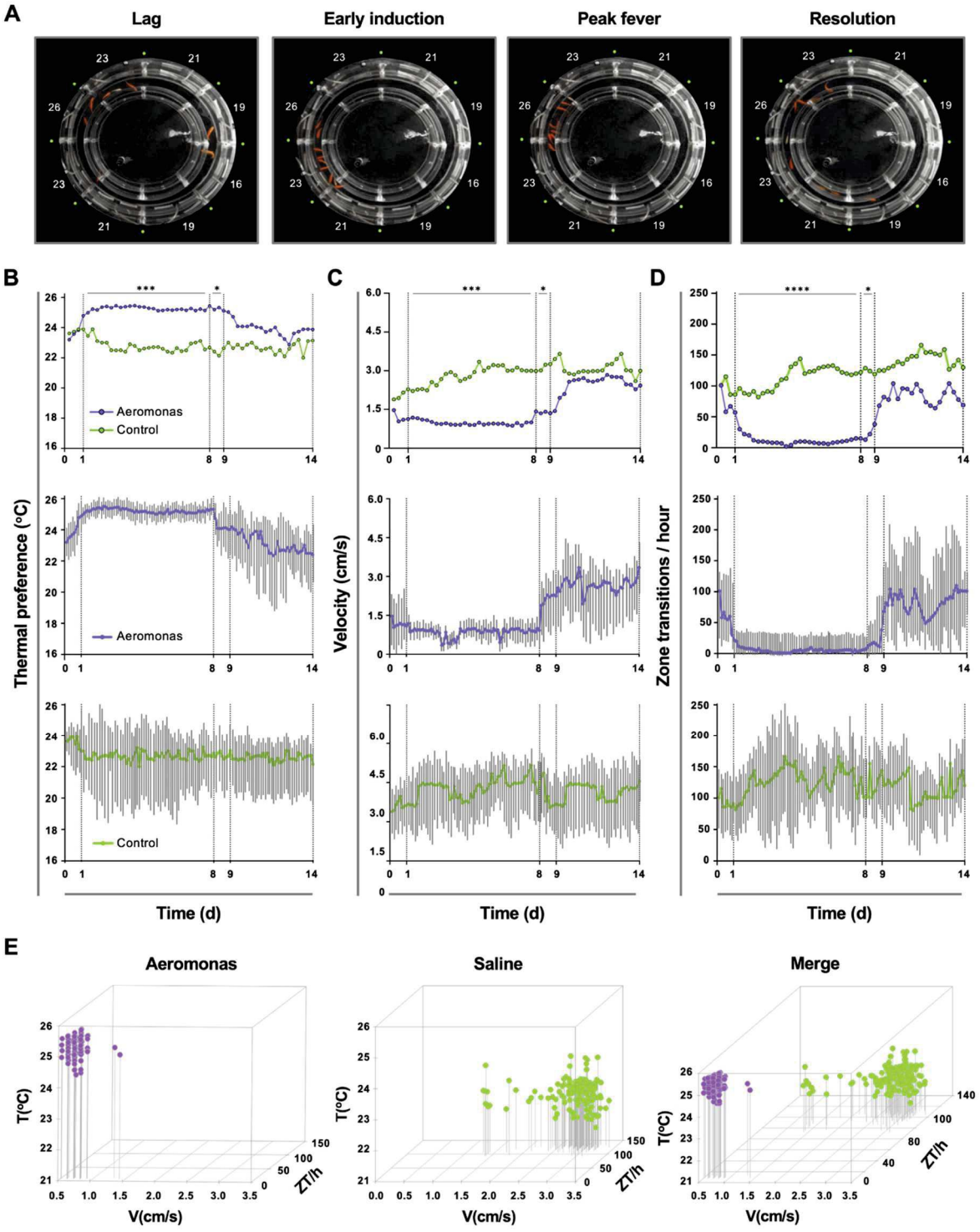
A
Lag
Early induction
Peak fever
Resolution
B
C
D
Thermal preference (°C)
Velocity (cm/s)
Zone transitions / hour
Aeromonas
Control
Time (d)
E
Aeromonas
Saline
Merge
T(°C)
V(cm/s)
ZT/h

Figure 3.8. Homogeneity in thermal preference and sickness behaviours among fish eliciting fever. (**A**) Fish were infected with *Aeromonas* and were free to select a range of environmental temperatures within the ATPT. Video still images show collective positioning of fish during distinct phases of this fever response (lag, early induction, peak fever and resolution). Labels correspond to mean temperature for each ATPT thermal zone. (**B**) temperature preference, (**C**) velocity and (**D**) total transitions across thermal zones for fish infected with *Aeromonas* (n=5) or mock-infected with saline (n=5). Fish were placed separately in the ATPT and individually monitored for 2 weeks. Evaluation of behavioural variance identified distinct periods of marked consistency in temperature preference, swimming velocity and thermal zone transitions in *Aeromonas*-infected fish. Solid lines represent mean hourly values and vertical grey bars correspond to standard deviation at each time point. Results were analyzed using a one-way ANOVA and Tukey's multiple comparisons test (*$p < 0.05$, ** $p< 0.01$, ***$p<0.001$ and **** $p< 0.0001$). (**E**) Simultaneous three-parameter representation of behaviour hourly data points for *Aeromonas*-infected and saline control fish (168 points and n=5 fish per group). 3D plots correspond to 1-8 dpi febrile period. Merged graph highlights segregation of behavioural responses.

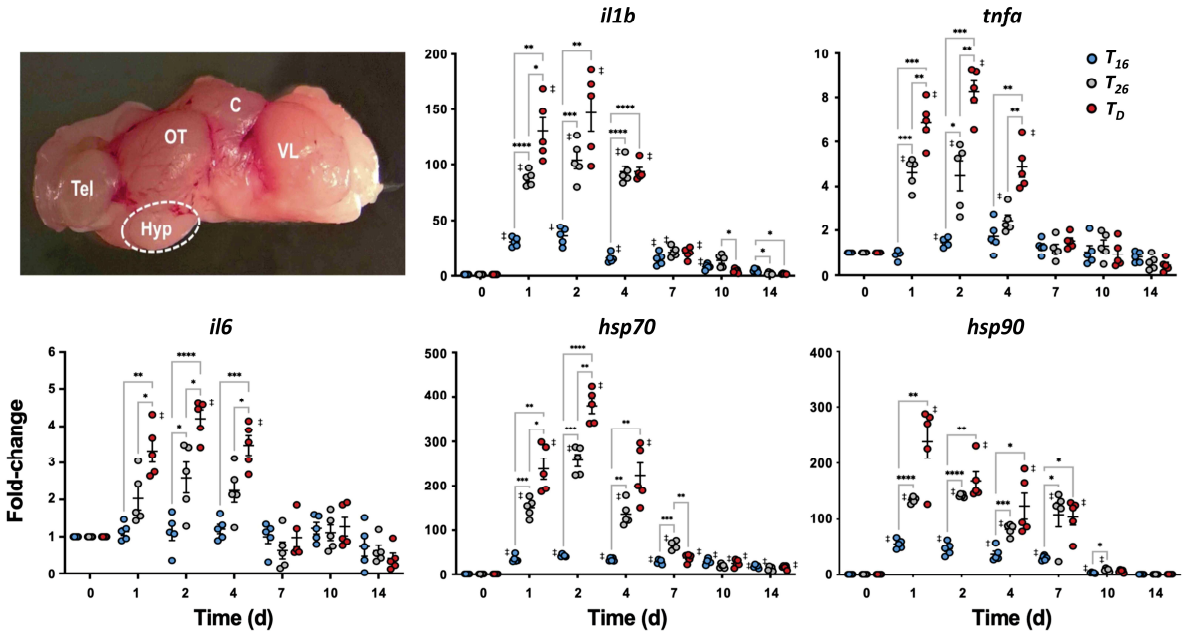

Figure 3.9. Molecular analysis confirms CNS engagement during behavioural fever. Fish were inoculated with *Aeromonas* and placed in static 16°C (basal acclimated temperature; T_{16}), static 26°C (mechanical hyperthermia; maximum temperature that fish selected during behavioural fever; T_{26}), or dynamic fever (where fish could move freely between thermal zones; T_D). qPCR evaluated gene expression in the hypothalamus following infection (n=5 per group per time point). Symbols correspond to individual samples and lines represent the mean ± SEM. Results were analyzed by an ordinary two-way ANOVA using Tukey's post-hoc test. *p< 0.05, **p< 0.01, ***p< 0.001, ****p< 0.0001; ‡ denotes significant difference from time 0, p< 0.05. *actb* was used as an endogenous control; RQ values were normalized against gene expression at day 0.

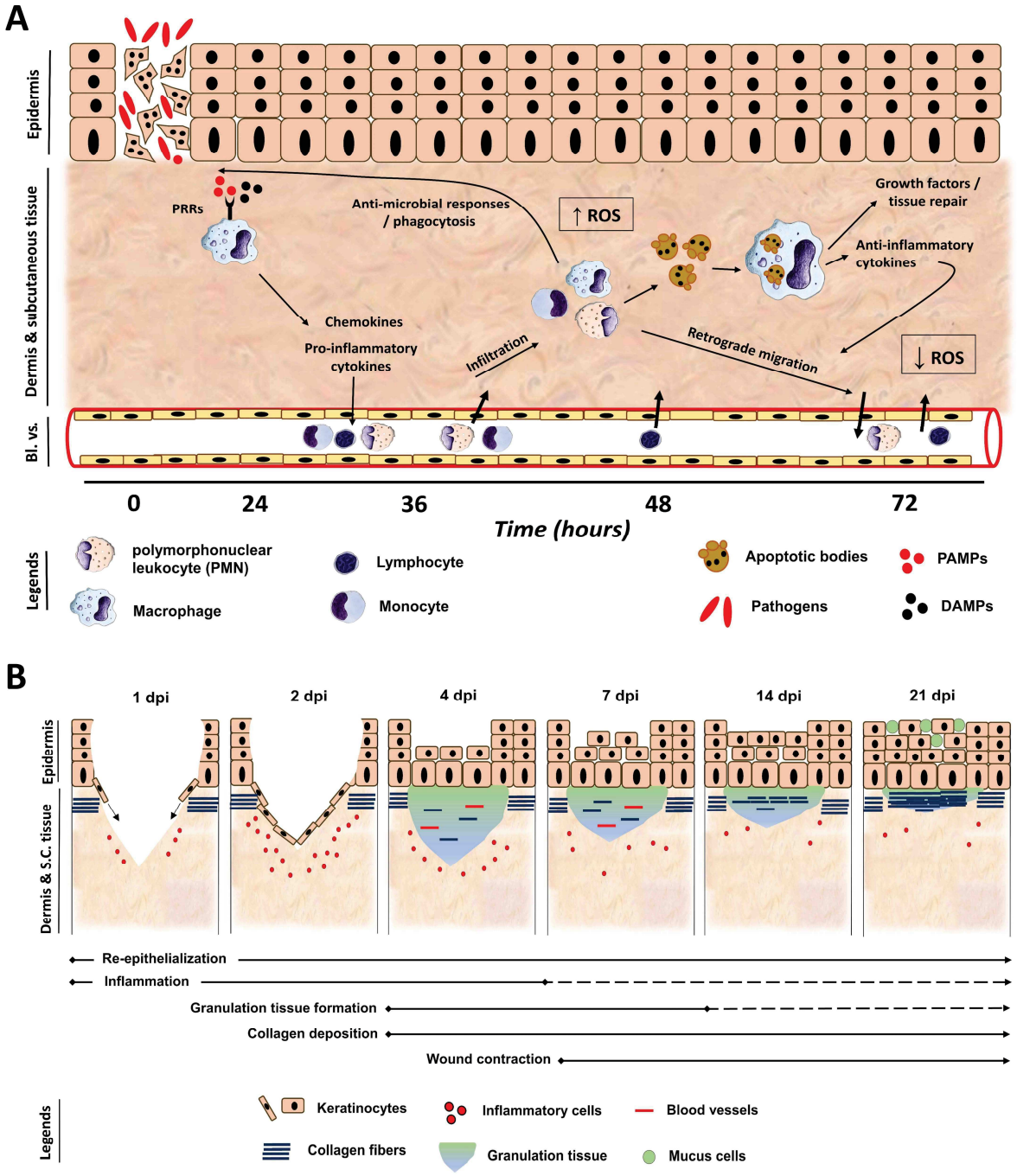

Figure 3.10. Kinetics of the inflammatory and proliferative phases of wound healing in goldfish infected with *A. veronii* and housed at fixed 16°C. (**A**) Damage/Pathogen Associated Molecular Patterns (DAMPs/PAMPs) induced by an injury and/or infection bind to pattern recognition receptors (PRRs) expressed by tissue-resident macrophages, which in turn release pro-inflammatory cytokines and chemokines to trigger an acute inflammatory

response and recruit leukocytes to the injury site from nearby blood vessels (Bl. vs.). Polymorphonuclear leukocytes/neutrophils infiltrate the wound site gradually to reach a peak at 36-48 hpi, where they and macrophages exert antimicrobial defense mechanisms, including reactive oxygen species (ROS), to combat pathogens. The peak of ROS was at 24-48 hpi, which was coupled to an increase in PMN number at the wound site. Lymphocytes were noticed to infiltrate the injury site at 48 and 72 hpi. Following elimination of pathogens, PMN undergo cellular apoptosis to release chemoattractant to attract macrophages, which engulf apoptotic neutrophils. Activated macrophages release anti-inflammatory cytokines to provoke the resolution of inflammation via suppression of ROS production and a retrograde migration of PMN back to circulation at 72 hpi. Furthermore, macrophages release growth factors to activate tissue repair machinery and restore homeostasis. (**B**) The inflammatory phase of tissue repair starts principally at 24 hpi to reach a peak at 48 hpi, demonstrated by significant cellular infiltration. Resolution of inflammation starts at 72 hpi to be followed by initiation of granulation tissue formation and collagen deposition observed at 4 dpi that progressively continues to fill the wound gap completely at 21 dpi. Re-epithelialization starts early by migration of keratinocytes from wound edges to cover the wound surface and an intact basal layer of epidermis and overlaying keratinocytes were noted on 4 dpi where they continue proliferation and differentiation to reach full maturation at 21 dpi, indicated by the presence of mucus-secreting cells.

Chapter IV

Impact of fever on inflammatory and proliferative phases of tissue repair†

---

† Parts of this chapter have been published in

- Haddad, F.*, **Soliman, A. M.***, Wong, M. E., Albers, E. H., Semple, S. L., Torrealba, D., Heimroth, R. D., Nashiry, A., Tierney, K. B., & Barreda, D. R. (2023). Fever integrates antimicrobial defences, inflammation control, and tissue repair in a cold-blooded vertebrate. *eLife*, 12; e83644.
  * *Authors contributed equally to this work, and parts of this paper will be published in Haddad, F. thesis.*

4.1. Introduction

The consistently reported survival advantage of fever across endothermic and ectothermic vertebrates [28,92,140] proposed positive contributions to immune responses and restoration of tissue homeostasis [3]. Though, the mechanisms behind these contributions remain poorly understood. Early assessments into the benefits of fever suffered from temporal deviations where, for example, fever was artificially induced before infection [529]. In other cases, thermal ranges outside those usually provoked by fever were used, or peak temperatures were sustained for extended periods [159]. *In vitro* and *in vivo* mammalian models of fever-range hyperthermia continue to provide valuable insights and confirmed improvements in host survival induced by the increased core body temperatures [3]. Unfortunately, exogenous and mechanical manipulation of temperature is well established to cause physiological stress and fails to replicate the host's intrinsic thermoregulatory machinery tempted during natural febrile responses [119]. Additionally, pharmacological use of antipyretics in these models inhibits inflammatory pathways at multiple points along with off-target effects [148].

In this study, I used a cold-blooded teleost model to gain additional insights into fever biology. I examined febrile response under host-driven dynamic thermoregulation to investigate its impact on tissue repair as a mechanism of restoring tissue homeostasis. This helped me to avoid common caveats encountered with exogenous drugs, temporal deviations of innate thermoregulatory programs, or forcing animals beyond thermal ranges typically elicited through fever. An *in vivo Aeromonas* cutaneous infection model was tailored to focus on the most common moderate self-resolving form of this natural biological process

rather than severe pathological fever. Under these experimental conditions, fever was transient and self-limiting, enabling interrogation of its potential contributions during induction and resolution of the inflammatory phase of wound healing and the succeeding activated tissue repair events. Our results demonstrate that fever is an essential regulator of induction and control of acute inflammation. The functional attributes of fever are caused by earlier and selective rather than stronger induction of innate antimicrobial programs that was historically proposed. These are further integrated with efficient control of inflammation and promotion of various reparative responses to restore homeostasis.

4.2. Results

Goldfish challenged with *A. veronii* cutaneous infection were added to fixed 16°C (T_{16}), fixed 26°C (T_{26}) and ATPT to exert behavioural fever (dynamic fever: T_D) for 14 days (**Figure 4.1**). While T_{16} represented the basal acclimation temperature, T_{26} group was added to investigate the effects of fever-range hyperthermia on tissue repair. Examining wound pathology showed fever's capacity to influence both inflammatory and proliferative phases of wound healing. For instance, similar levels of inflammation were evident in wounds of all groups one day after cutaneous infection (**Figure 4.2**); however, T_D and T_{26} fish showed accelerated kinetics of purulent exudate formation by 2 dpi that was later detected at 4 dpi in T_{16} (**Figure 4.2; red boxes**). Development of purulent exudate indicates cellular recruitment, neutrophil activation and pathogen killing [530]. Fish exerting dynamic fever subsequently progressed most rapidly, displaying early signs of tissue repair and scale regeneration by 7

dpi and advanced stages of wound healing by 14 dpi (**Figure 4.2; green boxes**). Comparatively, T_{16} and T_{26} furuncles did not reach equivalent stages of wound closure. Thus, fish allowed to exert fever resolved *Aeromonas* infection and repaired the associated skin barrier damage faster than those maintained under mechanical fever-range hyperthermia or static 16°C temperature conditions. Even though T_{26} showed indications of rapid resolution of inflammation, wound closure was at a slower rate when compared to T_D.

Together, I hypothesized fever to have a robust wound healing capacity via promoting early immune responses, bacterial killing, effective resolution of inflammation, granulation tissue formation and re-epithelialization. To test this hypothesis, I examined kinetics of cellular recruitment and their antimicrobial responses. Additionally, histopathological analysis of wound tissues was conducted to evaluate healing of both epidermis and dermis layers of the skin, as well as gene expression analysis to identify the possible underlying molecular pathways. The following sections discuss how febrile response influences different components of inflammatory and proliferative phases of wound healing while comparing these outcomes to basal thermal condition and fever-range hyperthermia.

4.2.1. Fever prompts an early and selective innate immune program

Early signs of inflammation detected in fish employing behavioural fever suggested marked changes concerning the inflammatory profile and associated cutaneous immune

responses. Herein, I assessed the effects of febrile response on leukocyte recruitment and their antimicrobial responses.

4.2.1.1. Early inflammatory response is associated with rapid leukocyte recruitment and efficient pathogen clearance

A histopathological examination and ImageJ analysis of wound sections revealed earlier and markedly faster leukocyte recruitment in both T_D and T_{26} compared to T_{16}. Leukocyte infiltration was observed at 8 hours post-infection (hpi) and increased gradually to reach a peak at 24 hpi in both T_D and T_{26} (**Figure 4.3, 4.4A**). In sharp contrast, minimal leukocyte infiltration was observed in T_{16} during the first 24 hpi and peaked at 48 hpi (**Figure 4.3, 4.4A**). A detailed examination of recruited cells was necessary to understand in-depth immunomodulatory effects of fever. Therefore, I used a modified protocol to isolate skin leukocytes to be categorized based on cytochemical staining. This allowed me to characterize kinetics of differential leukocyte recruitment and identify subsets contributing to early cellular infiltration during fever. My results showed that PMNs were the primary cells causing the fever-induced rapid shift in infiltrating cells by dominating recruited cells. Neutrophil counts at 24 hpi were significantly higher in T_D and T_{26} than T_{16} (**Figure 4.4B**), while there were no significant differences in macrophage/monocyte and lymphocyte populations during the first 36 hpi among all groups (**Figure 4.4C, D**). On the other hand, neutrophils were recruited at a relatively slower rate in T_{16} to peak at 36-48 hpi (**Figure 4.4B**). At 48-72 hpi, I detected considerably larger numbers of monocytes/macrophages in T_{16} compared to T_D and T_{26} (**Figure 4.4C**). This could be explained by high PMN numbers at

48 hpi in T_{16}, where macrophages are essential for efferocytosis of apoptotic cells and mediating other antimicrobial functions [531]. Although levels of lymphocytes were not significantly different in all groups across the first 36 hpi, I observed a significant rise in their number at 48 hpi in fever fish only (**Figure 4.4D**), suggesting an early engagement of adaptive immune responses.

Overall enhancements in cellular recruitment induced by fever could have offered an advantage of rapid eradication of infection. Therefore, we assessed the presence of *A. veronii* on the wound surface as a measure of pathogen load and shedding potential. During the course of infection, furuncles caused by *Aeromonas* species can shed up to 10^7 bacteria per hour in fish [467]. Infected fish held at 16^{o}C static thermal conditions displayed heavy bacterial loads through the first 2 days after infection, with a gradual reduction in CFU to reach undetectable levels by 14 dpi (**Figure 4.5A**). Fish in the dynamic fever group also showed heavy initial bacterial burden, but these decreased markedly faster than T_{16} fish to reach below detectable levels by 7 dpi (**Figure 4.5A**). Meanwhile, mechanical hyperthermia (T_{26}) yielded an intermediate response, achieving *Aeromonas* clearance after 10 days. Thus, fish allowed to exert dynamic fever cleared *A. veronii* in half the time than fish maintained in static 16^{o}C conditions. Notably, this enhancement in clearance could not be explained by the current thermal restriction model since *A. veronii* showed faster growth as incubation temperatures increased from 16 to 26°C [490]. Early bacterial clearance suggested enhancement of antimicrobial responses and subsequent swift resolution of inflammation and initiation of cellular proliferation.

4.2.1.2. Behavioural fever alters antimicrobial mechanisms of recruited leukocytes

To determine if fever's enhancement of cellular recruitment and efficient pathogen killing were paired with activation of antimicrobial pathogen-killing mechanisms, we examined cellular production of ROS, as a prominent, effective, and evolutionarily conserved innate defense mechanism [265]. As previously shown, leukocytes derived from fish housed under basal thermal static conditions display a strong capacity for generation of ROS [414,532]. Over 75% of isolated skin leukocytes were positive for ROS production in T_{16}, and similarly in T_{26} (**Figure 4.5B**). Surprisingly, the proportion of ROS-producing leukocytes was significantly reduced under febrile conditions ($T_{D;}$ **Figure 4.5B**) despite the enhanced kinetics in leukocyte recruitment outlined above (**Figure 4.3 and 4.4A**).

Given the long-established contributions of fever to host survival and enhancement of pathogen clearance, I hypothesized that fever promoted innate antimicrobial responses that do not include a strong ROS production component. Thus, we also evaluated leukocyte NO production as an alternative evolutionarily conserved innate response to pathogen attack [532,533]. Contrary to results for ROS, we identified greater overall levels as well as accelerated kinetics of NO production under fever conditions (**Figure 4.5C**). Leukocytes infiltrating the furuncle of T_D fish showed significant upregulation, with peak NO production observed at 24-36 hpi (**Figure 4.5C**). This was further supported by a marked, earlier upregulation of *nos2* expression, which is necessary to produce immune NO (**Figure 4.5D**) [533]. In sharp contrast, both T_{16} and T_{26} displayed lower levels of *nos2* expression and lower overall capacity to produce NO (**Figure 4.5D**). Hence, fever differentially regulated ROS and NO leukocyte antimicrobial mechanisms in *Aeromonas*-challenged fish.

4.2.1.3. Fever promotes early upregulation of pro-inflammatory cytokines and chemokines

The alterations in cellular recruitment kinetics suggested a change in inflammatory cytokines and chemokines levels between treatment groups. Previously, febrile-range temperatures were found to promote the production and release of Tnfa [177] and enhance Cxcl8-mediated neutrophil relocation to infection sites [171,172]. Though, little is known about inflammatory mediators driving cutaneous immune responses during fever. A qPCR analysis of wound tissues revealed an early upregulation of a classical pro-inflammatory cytokine (*tnfa*) in T_D and T_{26} at 16 hpi with no significant changes in the levels of *il1b* during the first 24 hpi (**Figure 4.6**). Meanwhile, in basal thermal condition, *il1b* and *tnfa* were substantially upregulated later at 36 and 48 hpi, respectively (**Figure 4.6**), correlating with delayed cellular recruitment reported earlier. These results further implied the selective nature of fever in activating antimicrobial mechanisms contrary to the historically proposed global activation of immune responses. Moreover, levels of *cxcl8* (a critical chemokine for neutrophil recruitment) were remarkably upregulated in T_D and T_{26} at 16 hpi and later at 36-48 hpi in T_{16} (**Figure 4.6**), which follows the pattern of PMNs migration to the wound area in all groups (**Figure 4.5**), and thereby likely driving early neutrophil recruitment in fever. Notably, the fever-induced changes in cellular recruitment and expression levels of inflammatory mediators were similar to that of the static 26°C condition.

4.2.2. Fever induces an early resolution of inflammation and rapid shift toward proliferation

Studies looking at the basis for host survival due to fever have primarily focused on the activation of immune defense mechanisms with less emphasis on the resolution of inflammation. The self-resolving nature of our teleost model allowed me to characterize immunological changes during the transition between induction and resolution phases of acute inflammation. Given that prolonged inflammation results in impaired healing [534], immune responses must be tightly regulated to prevent extensive tissue damage. And while considering the better wound healing shown during the febrile response, I hypothesized fever to enhance effective control of inflammation, preventing collateral inflammation-associated damage.

Comparison of cellular responses following *Aeromonas* infection showed differences in the control of leukocyte recruitment to wound site. For instance, fever fish reached the peak of infiltration at 24 hpi, subsequently decreasing and nearing basal levels by 48 hpi (**Figure 4.4A**). This was consistent with faster kinetics of induction and control of local *tnfa*, *il1b*, and *cxcl8* gene expression observed in T_D (**Figure 4.5**). In contrast, slower kinetics of leukocyte recruitment in T_{16} did not reach this peak until 48 hpi and were sustained beyond 72 hpi (**Figure 4.4A**), consistent with delayed upregulation of pro-inflammatory cytokines gene expression (**Figure 4.6**) and pathogen clearance (**Figure 4.5A**). The rapid resolution of inflammation during fever suggested alterations in the levels of pro-resolution cytokines. A qPCR analysis showed that *tgfb* was considerably upregulated in T_D and T_{26} at 24-36 hpi compared with T_{16} (**Figure 4.6**). Nevertheless, levels of another critical anti-inflammatory

cytokine (*il10*) were similar among all groups (**Figure 4.6**), which again supports the capacity of fever to selectively upregulate cytokines to modulate immune responses.

A broader gene expression study of other regulators of acute inflammation was conducted using Nanostring technology. This technology delivers direct profiling of individual mRNAs in a highly multiplexed single reaction, devoid of the need for amplification. Overall, the analysis supported the observations above, where a drop in pro-inflammatory genes pathway score was observed at 2 dpi in T_D and T_{26} and later at 4 dpi in T_{16} (**Figure 4.7A**). This was induced by persistent higher expression levels of pro-inflammatory cytokines (*tnfa*, *il1b* and *il6*) (**Figure 4.7B**), in addition to neutrophil chemoattractant (*cxcl8*) and *granulocyte colony stimulating factor receptor* (*gcsfr*) (**Figure 4.7C**) in basal thermal condition compared with fever and mechanical hyperthermia. These observations mirrored late pathogen clearance noted in T_{16}. Notably, the inflammatory stage of wound healing would persist until all excessive pathogens are cleared [534]. Still, extended inflammation can result in immense collateral tissue damage and delayed wound healing [534]. Collectively, my data indicates that behavioural fever promotes a rapid resolution of inflammation, thereby allowing early engagement of growth factors, such as *vegf* in the repair process (**Figure 4.6**), resulting in a better healing outcome.

Despite being upregulated in all groups, I observed significantly higher expression levels of *progranulin* (*grn*) in T_{16} at 1 dpi (**Figure 4.7D**). Progranulin is released as precursor glycoproteins to be cleaved by proteolytic enzymes into smaller peptides called granulin, which possess immunomodulatory effects [535,536]. A balance must be maintained between progranulin and the generated granulin to avoid exacerbation of inflammation [535]. On the

other hand, levels of *colony stimulating factor 1* (*csf1*) and its receptor (*csf1r*) were upregulated in fever fish at 4 dpi (**Figure 4.7E**). Csf1 is one of the primary growth factors regulating macrophage and monocyte differentiation, survival and functions [537]. Administration of Csf1 was found to promote clearance of necrotic cells and tissue repair [537]. Similarly, *ccl1*, a potent chemoattract of both monocytes [216] and lymphocytes [217], was substantially upregulated in T_D at 2 and 4 dpi (**Figure 4.7F**). In addition to being reported to enhance monocyte and lymphocyte recruitment, Ccl1 further supports resolution of inflammation by activating immunosuppressive functions of T_{reg} [538].

Consistent with previous indications of early inflammation resolution, another pro-resolution mediator, indolamine 2,3 dioxygenase (*ido*), was considerably upregulated in fever fish only (**Figure 4.7G**). Ido mediates immunomodulatory functions by impairing inflammatory cell proliferation and activation [29,30], promoting T_{reg} differentiation and activating immunosuppressing activity of mature T_{reg} [539,540]. The higher expression level of *ido* along with *tgfb* (**Figure 4.6**) at 24-48 hpi could be driving early control of inflammation and downregulation of pro-inflammatory mediators (e.g., *il1b*, *tnfa* and *cxcl8*). Fever fish, likewise, demonstrated superior *ifng* expression (**Figure 4.7H**). Ifng is a pleiotropic molecule that is well-known for its capacity to induce cellular apoptosis [541], macrophage activation [542] and resolution of inflammation *in vivo* [543]. Additionally, Ifng is projected to promote wound healing [544,545] via enhancing wound closure, neutrophil resolution and collagen deposition [543].

4.2.3. Fever activates tissue repair pathways to enhance healing of epidermal and dermal layers

Fever's impact on tissue repair was not limited to modulating inflammatory phase. Yet, it was further extended to influence the proliferation phase that involves crosstalk between several healing pathways regulated by pleiotropic growth factors. The process incorporates re-epithelialization, angiogenesis and granulation tissue formation, which occur concurrently [187]. Preliminary macroscopic examination of wound pathology revealed dramatic differences between fever and non-fever conditions in terms of tissue healing and wound closure rate (**Figure 4.2**). Although both T_D and T_{26} conditions exhibited clear indications of early resolution of inflammation, wound was almost closed in T_D and, to a lesser extent, in T_{26} by the end of the 14 days (**Figure 4.2**). At the same time point, limited progress in wound healing was detected in T_{16}, where the wound was still relatively open (**Figure 4.2**). Using ImageJ, wound area at 14 dpi was measured to be 2.24 ±SEM 0.23 mm^2 in T_D, 11.34 ±SEM 0.95 mm^2 in $T_{26,}$ and 22.38 ±SEM 1.57 mm^2 in T_{16}. This indicated changes at the level of granulation tissue formation and re-epithelialization.

4.2.3.1. Febrile response promotes collagen deposition

Fibroblasts play a pivotal role in wound healing, being accountable for new granulation tissue formation and deposition. Following tissue injury, fibroblasts migrate to wound area and proliferate to produce and lay down different components of ECM [546,547]. Among them, collagen is considered the key element constituting the major part and providing strength. Therefore, to identify contributions of fever to granulation tissue

formation, I assessed collagen content at wound site via histopathological examination. Early and relatively abundant collagen (blue color) deposition was detected at 4 and 7 dpi day in T_D compared to T_{26} and T_{16} (**Figure 4.8**). Additionally, collagen fibers were arranged in a parallel well-organized manner under fever condition (**Figure 4.8**).

The marked increase in collagen deposition observed in T_D indicated fever to promote fibroblast proliferation. Hence, I examined the proliferative rate of fibroblasts under fever and non-fever conditions. Surprisingly, I observed limited changes in fibroblast proliferation rate in T_D (**Figure 4.9**). Data showed a gradual increase in fibroblast proliferation to peak at 2-4 dpi in all groups, followed by a steady decline (**Figure 4.9**). Consequently, I hypothesized that the dramatic differences in collagen deposition were attributed to a fever-associated robust fibroblast activation that involved a substantial upregulation of ECM elements, including collagen. Intriguingly, collagen type III (*col3a1*) and type I (*col1a2*) were dramatically upregulated in fever fish when compared to other groups (**Figure 4.10A, B**, respectively). Fibroblasts are mainly activated by Fgf and Tgfb, while their proliferation is primarily stimulated by Pdgf [187]. These growth mediators trigger intracellular signaling pathways to promote the expression of various components of ECM [22]. Fever remarkably upregulated *fgf2* and *tgfb* compared with T_{16} and T_{26} (**Figure 4.10C**). Though, there were no significant differences in the expression level of *pdgf* (**Figure 4.10C**), which is in accordance with a comparable fibroblast proliferation rate in all groups. The development of new blood vessels required for oxygens and nutrient supply is necessary for granulation tissue formation. Dynamic fever exhibited a greater expression level of an essential mediator of angiogenesis, *vegf* (**Figure 4.10E**).

4.2.3.2. Fever improves re-epithelialization

Re-epithelialization is crucial to protect damaged or newly formed tissue against potential threats from surrounding environments, particularly in aquatic organisms. Interestingly, at 3 dpi, I detected an early development of the basal layer of epidermis (arrows) along with overlying layers of keratinocytes in T_D and T_{26} (**Figure 4.8**). Meanwhile, evidence of epidermis development was observed 24 hours later in T_{16} (**Figure 4.8**). The fever-induced dramatic shift in kinetics of re-epithelialization was expanded to achieve a rapid maturation of epidermis by 14 dpi. This was demonstrated by high-density layers of keratinocytes and mucus-secreting cells (arrowheads) observed in T_D (**Figure 4.8**). Mucus is an essential component of cutaneous innate immune mechanisms in fish; thus, mucus-secreting cells are an important part of a mature and functional epidermis [487]. In contrast, T_{16} showed a thick low cell-density epidermis with limited mucus cells (**Figure 4.8**). Although T_{26} demonstrated an early development of epidermis layer, it did not show the same maturation level observed in fever condition at 14 dpi, as evidenced by the sparsity of mucus-secreting cells (**Figure 4.8**). Regeneration of mucus-secreting cells is important for re-establishment of skin barrier functionality. Thus, fever promoted superior levels of wound repair and regained original structural features required for restoration of skin barrier functionality after cutaneous infection. Conversely, the absence of fever caused delayed resolution of the inflammatory response, re-epithelialization, and the appearance of ECM components.

The rapid epidermis development in fever fish indicated effective cellular migration and proliferation. Keratinocytes translocate from wound edges, facilitated by Mmp1 [22], and proliferate to cover wound surface under the influence of several growth factors, e.g., Ngf, Igf1 and Egf [306]. Gene expression analysis showed a significant and early upregulation of *igf1* at 1 dpi in T_D and T_{26} compared to T_{16} (**Figure 4.10D**). Though, on day 2 and 4, high levels of *igf1* were maintained exclusively in fever condition (**Figure 4.10D**). Likewise, *egf* and *ngf* were remarkably upregulated in T_D, which could have contributed to the fever-associated rapid and efficient re-epithelialization complemented by highly expressed *mmp1* detected in wound tissue (**Figure 4.10F**).

Although Mmps are critical for keratinocyte migration via degrading various ECM and weakening integrin:matrix adhesion [302], their unrestrained upregulation provokes extensive tissue damage and obliterates growth factors, thereby causing impaired wound healing [244]. Despite similar expression levels of *mmp9* at 1 dpi in all groups (**Figure 4.10F**), I detected a maintained upregulation of *mmp9* across the 14 days in T_{16} (**Figure 4.10F**). Additionally, I observed limited differences in the gene expression levels of Hsps (*hsp27* and *hsp70*) between fever and non-fever conditions (**Figure 4.11**), despite their positive contributions to molecular chaperoning and repairing misfolded proteins.

4.3. Discussion

Fever is a hallmark of acute inflammation that has been evolutionarily conserved through millions of years. Despite its long-standing role in host survival, there are still gaps

in our understanding of fever biology leading to uncertainty about whether febrile responses are net positive or negative to health. This has resulted in limitations of existing guidelines for fever management in addition to the unregulated use of antipyretics [40]. Indeed, fever has been consistently reported to lower morbidity and mortality rates following infections [119,140,150,548–551], suggesting its potential role in restoring tissue homeostasis [3]. Though, underlying mechanisms remain unestablished. Herein, we demonstrate a novel intrinsic capacity of fever to restore tissue integrity and homeostasis subsequent to a challenge. In addition to presenting a fever-range hyperthermia model, we utilized a behavioural fever model to examine fever under host-driven dynamic thermoregulation. Both models allowed characterization of differences between dynamic fever and mechanical hyperthermia that has commonly been employed to study fever [173,552,553]. My results show that fever induced an early acute inflammatory program driven by selective upregulation of classical pro-inflammatory mediators followed by rapid control of inflammation. Although a static increase in temperature demonstrated parallel effects, it did not recapitulate all of the immunomodulatory impacts of dynamic fever. The influence of fever on tissue repair was more apparent during proliferation, where it was associated with marked enhancements of re-epithelialization and granulation tissue formation. Notably, as shown in epidermis and dermis healing, T_{26} did not reach the full healing potential of a natural febrile response.

An acute inflammatory response associated with PMNs and macrophage migration to the wound area is essential for pathogen and debris clearance. However, a critical balance must be maintained between phagocytes protective functions and their possible contributions

to prolonged and exacerbated inflammation [236]. This balance ensures eradication of infection while minimizing collateral tissue damage. My data demonstrated a fever-induced early neutrophil-centric leukocyte recruitment followed by their rapid resolution. This rapid shift in the acute inflammatory program achieved a remarkably faster bacterial clearance coupled with a reduction in the time PMNs existed at the wound site, thus less inflammation-linked collateral tissue injury. Several studies suggested that prolonged existence of neutrophils in wound area was detrimental to proper tissue repair [237,238]. This was attributed to PMNs-derived proteases degrading ECM and being allied with deleterious levels of ROS [239,240]. Fever by inducing an early innate immune program followed by rapid inflammation control aided in reducing collateral tissue damage and thus indirectly promoting the repair process.

Fever modulated antimicrobial responses exerted by cutaneous leukocytes, where we observed, unlike fixed thermal conditions, a marked reduction in ROS levels accompanied by high levels of NO. Both ROS and NO are evolutionarily conserved antimicrobial defenses employed by phagocytes to combat pathogens. Though, recent research has identified differences in their functions and implications. For instance, although NO and its reactive nitrogen species (RNS) possess microbicidal properties [274,554], NO was also reported to possess anti-oxidant and anti-inflammatory assets [275], including influencing ROS levels and activity. For instance, production of ROS is arbitrated by several mechanisms (e.g., activation of NADPH oxidase), where NO regulates many of them in addition to minimizing the reactivity of O_2^- and H_2O_2 [273]. NO limits the distribution of ROS to specific sites to help eliminate pathogens while minimizing ROS-associated cellular

injury [273]. Likewise, NO was reported to contribute to better inflammation control via impeding PMN adhesion to vascular endothelium [276,555], in addition to downregulating *il8* [277] and *il1b* [278]. Additionally, a positive contribution of NO to several tissue repair events, such as collagen deposition, cell proliferation and wound closure, was shown [279], and supported by the tissue-protective effects observed as a result of NO administration [556,557]. Although a reduction in ROS activity seems contradictory to fever-associated efficient bacterial clearance, an enhanced NO activity was found to promote bacterial killing while suppressing ROS and concomitantly reducing tissue injury coupled with respiratory burst [558]. Our results suggest that fever promotes NO levels to control ROS activity to the level where pathogen clearance and modifications of intracellular signaling pathways essential for host defense are maintained, along with minimizing collateral tissue damage.

A proper transition from inflammatory to proliferative phase is vital for the healing process, which ultimately hinges on efficient resolution of inflammation. Early and robust inflammation control in fever condition was associated with engagement of tissue repair pathways, evidenced by significant upregulation of a variety of growth factors. This was in contrast with persistent expression of pro-inflammatory cytokines until 4 dpi and remarkably lower expression levels of growth mediators in T_{16}. Notably, while fish at a fixed 26°C demonstrated a relatively similar inflammatory profile to that of dynamic fever, there were significant differences concerning activation of tissue healing pathways. This was highlighted by the superior capacity of fever to upregulate growth factors and promote healing of epidermis and dermis layers. Notably, mechanical hyperthermia revealed a better healing outcome when compared to basal thermal condition, evidenced by early

downregulation of pro-inflammatory cytokines and relatively higher expression of a number of growth factors.

Among various wound healing events, I focused on assessing re-epithelialization, angiogenesis and granulation tissue formation. Remarkably, fever contributed positively to all of them. The complex regulation of these events is accomplished via pleiotropic growth factors, cytokines, and crosstalk between various pathways. Herein, I examined the gene expression of growth factors involved in each reparative event to characterize possible molecular pathways driving the superior healing capacity of fever. For instance, I observed a considerable upregulation of *fgf2* and *tgfb* necessary for fibroblast activation and biosynthesis of ECM components [527], which was mirrored by enhanced collagen deposition. Likewise, high mRNA levels of *igf1*, *egf* and *ngf* supported enhanced re-epithelialization under fever condition. My data showed a limited impact of fever on fibroblast proliferation, though fibroblast proliferation assay had some limitations being *in vitro* and utilizing cell lines, not primary cells, which could have provided a higher baseline of cellular proliferation that should be taken into consideration.

Since control/non-infected fish preferred a mean temperature of 23°C during behavioural analysis, despite the marked heterogeneity (**Figure 3.8B**), it was necessary to examine the effects of housing *A. veronii*-infected fish at 23°C on wound healing. Overall, fish at 23°C displayed similar wound healing kinetics to those held at T_{16}. Wound pathology exhibited delayed signs of purulent exudate and didn't reach equivalent stages of wound closure achieved by fever (**Figure 4.12A**). Moreover, histopathological examination revealed late leukocyte recruitment (**Figure 4.12B**) and a slower progression of re-

epithelialization and collagen deposition (**Figure 4.12C**). The data indicates the necessity of reaching a particular degree of temperature (i.e., ~25.5°C) to accomplish fever's significant modulation of tissue repair. The results are in accordance with previous data from our lab (not published) showing enhanced leukocyte recruitment in fish injected intraperitoneally with zymosan (fungal mimic) at 26°C with limited changes reported in their kinetics at lower temperatures (16, 21, 23°C).

A fixed increase in temperature to febrile levels is commonly associated with improved wound healing. For instance, the rate of wound healing in teleost fish was proportional to temperature levels, while temperature-associated stress had diminutive effects on healing [559]. Likewise, Atlantic salmon maintained at 12°C demonstrated faster wound healing than those at 4°C [193]. Other researchers reported high temperatures to enhance the positive healing effects of topical medical-grade honey in carp [560]. With regard to clinical trials, emerging data indicate that local warming of surgical wounds enhances wound healing [561–563]. For example, postoperative application of local water-filtered infrared-A resulted in a wound temperature increase associated with superior oxygen perfusion and overall wound healing [564]. Additional preliminary indications of thermal regulation of tissue repair were shown via increasing wound temperature utilizing a topical radiant heat or sodium nitrite [565,566], where wounds of higher temperatures had a better blood flow and healing outcome. Collectively, these findings support my results, though herein, I characterized some of the mechanistic modulations of febrile-range temperatures to inflammatory and proliferative phases of the repair process, contributing to enhanced wound healing. Furthermore, I revealed for the first time a greater intrinsic healing capacity of

natural dynamic fever compared to mechanical hyperthermia, thus, providing a better understating of fever biology and its essential contribution to host survival.

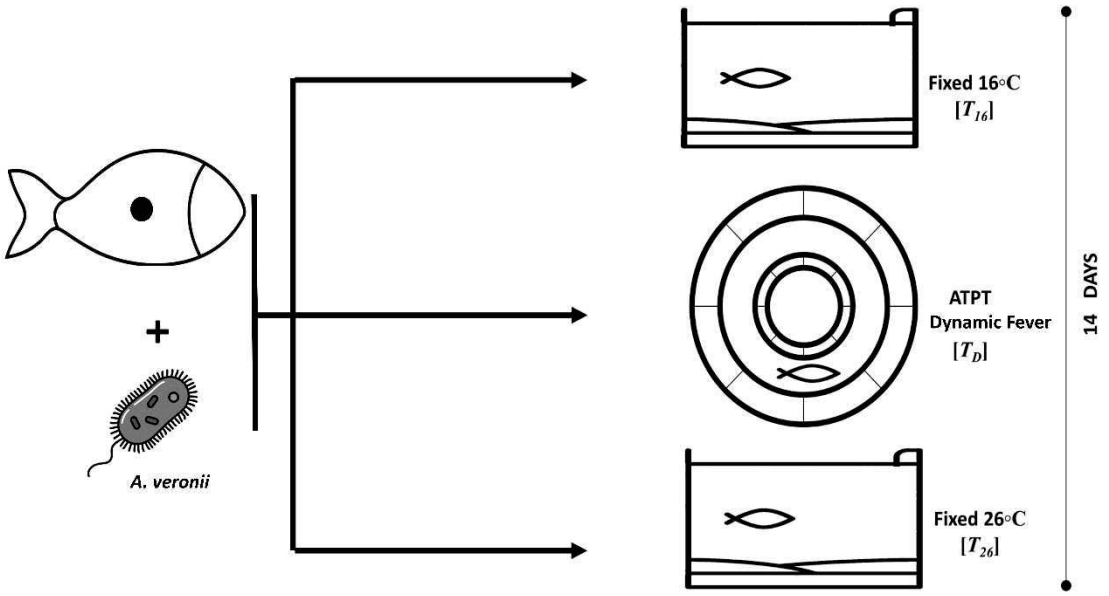

Figure 4.1. Experimental design and groups. ATPT: annular thermal preference tank.

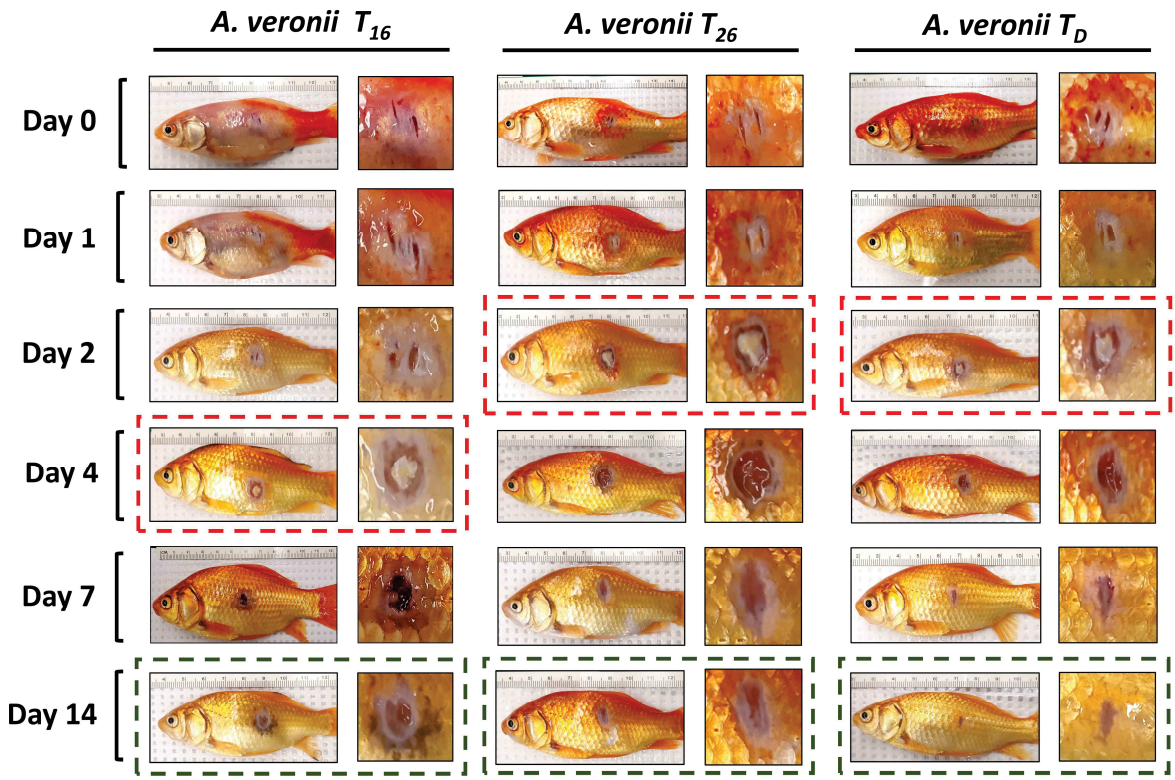

Figure 4.2. Progression of wound pathology in *Aeromonas*-infected fish held at different temperature categories. Representative images show wound pathology for fish inoculated with *Aeromonas veronii*. Timepoints capture progression from initial infection to advanced stages of wound repair. Red boxes highlight differential kinetics of whitish purulent exudate formation. Green boxes showcase distinct degrees of wound closure achieved across *Aeromonas*-infected groups by 14 dpi. T_{16}: fixed 16°C; T_{26}: fixed 26°C; T_D: behavioural fever. Wound images of T_{16} fish were added to this figure to compare wound pathology with T_D and T_{26} groups.

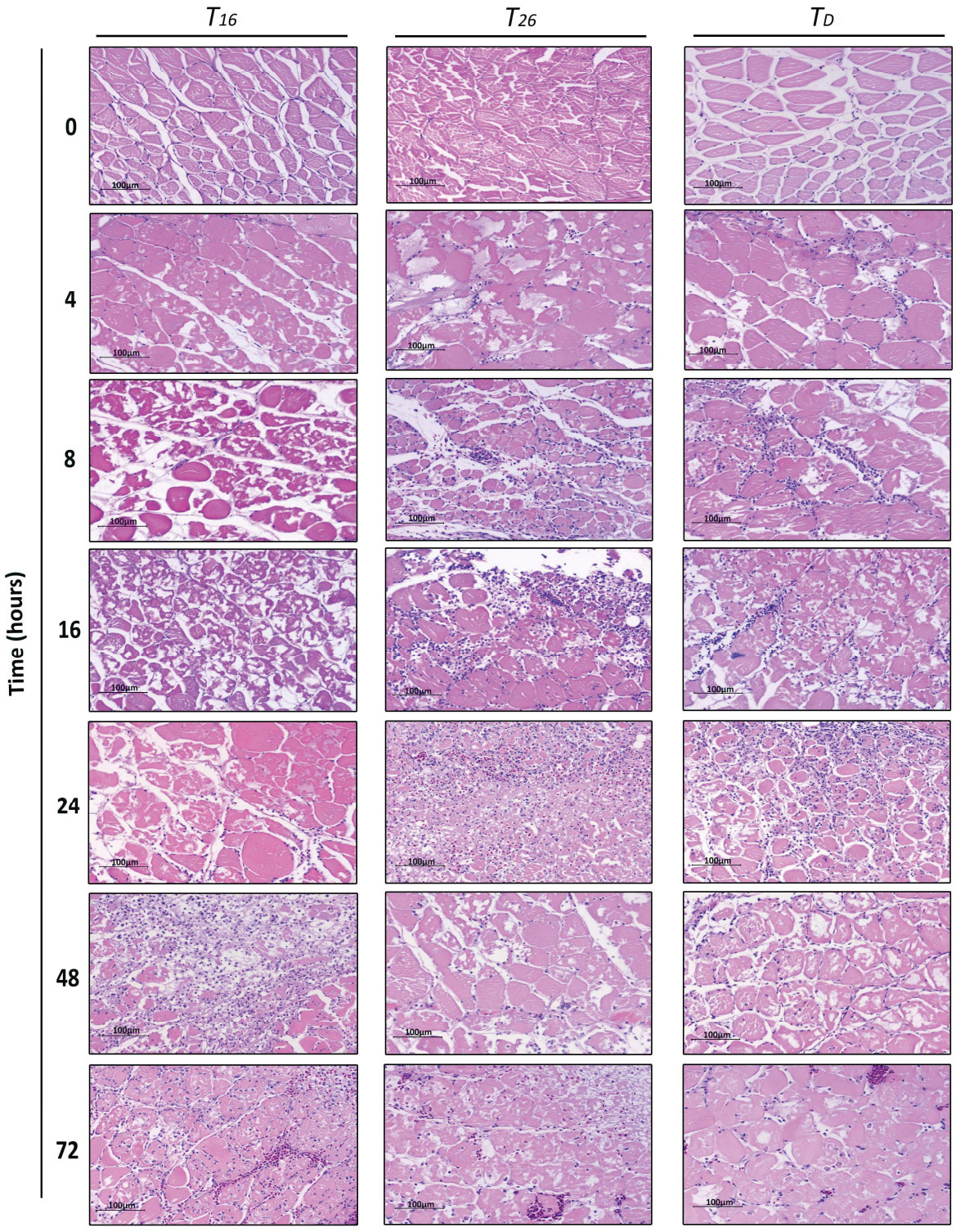
T_{16}
T_{26}
T_D
Time (hours)
0
4
8
16
24
48
72
100µm

Figure 4.3. Thermal promotion of leukocyte recruitment to wound area in *Aeromonas* infected fish. Hematoxylin and eosin stained tissue sections at different time points demonstrate early leukocyte recruitment (observed at 8 hpi and peaks at 24 hpi) and their rapid resolution (noted at 48 hpi) in fish exerting fever (right column) and fish held at 26^{o}C (middle column) compared to static 16^{o}C (left column) showing cellular migration that peaks at 48 hpi. Timepoints capture initial 0-72 h of acute inflammation; n=3 per time point and per group. Scale bar: 100 µm; T_{16}: fixed 16^{o}C; T_{26}: fixed 26^{o}C; T_{D}: behavioural fever.

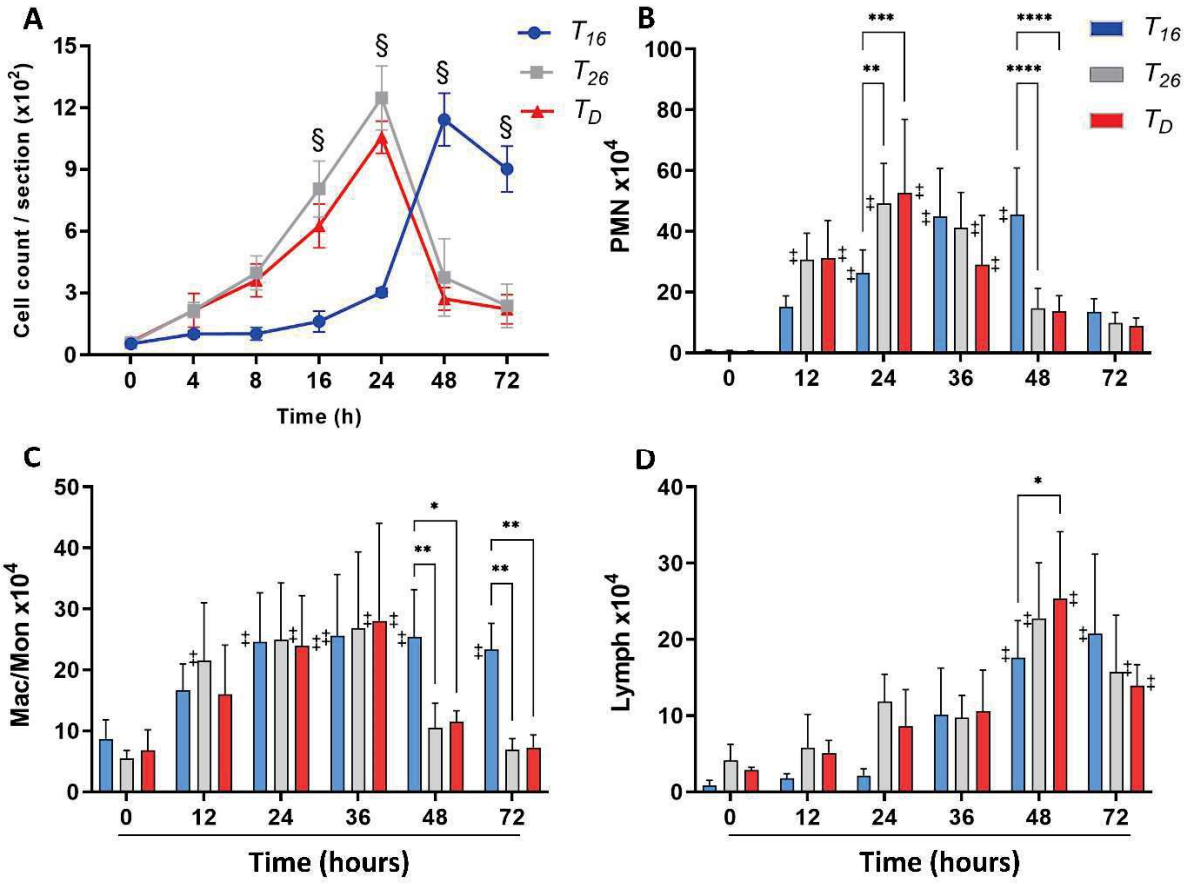

Figure 4.4. Fever induced marked changes in kinetics of leukocyte recruitment. Fish were infected with *A. veronii* and placed under experimental conditions (T_{16}: fixed 16°C; T_{26}: fixed 26°C; T_D: behavioural fever). (**A**) Hematoxylin and eosin were used to stain wound sections. ImageJ analysis assessed cellular recruitment; points represent the mean with error bars representing ± SEM; n=3 per time point per group; refer to **Figure 4.3** for source data. Results were analyzed by an ordinary two-way ANOVA using Tukey's post-hoc test. § corresponds to a statistical significance of $p<0.05$ when dynamic and static 26°C groups were compared to 16°C static conditions. No significant differences were found between dynamic and static 26°C groups at any time point. Leukocytes were isolated from wound tissue of individual fish and cellular subsets, including (**B**) PMN (polymorph nuclear leukocytes), (**C**) Mac/Mon (macrophages/monocytes) and (**D**) Lymph (lymphocytes) were quantified using Sudan black staining. Bars represent the mean with error bars representing SEM; n=5 per time point per group. All data were analyzed using a two-way ANOVA followed by Tukey's post-hoc test (*$p<0.05$, ** $p<0.01$, ***$p<0.001$ and **** $p<0.0001$, ‡ denotes difference from time=0 at $p<0.05$).

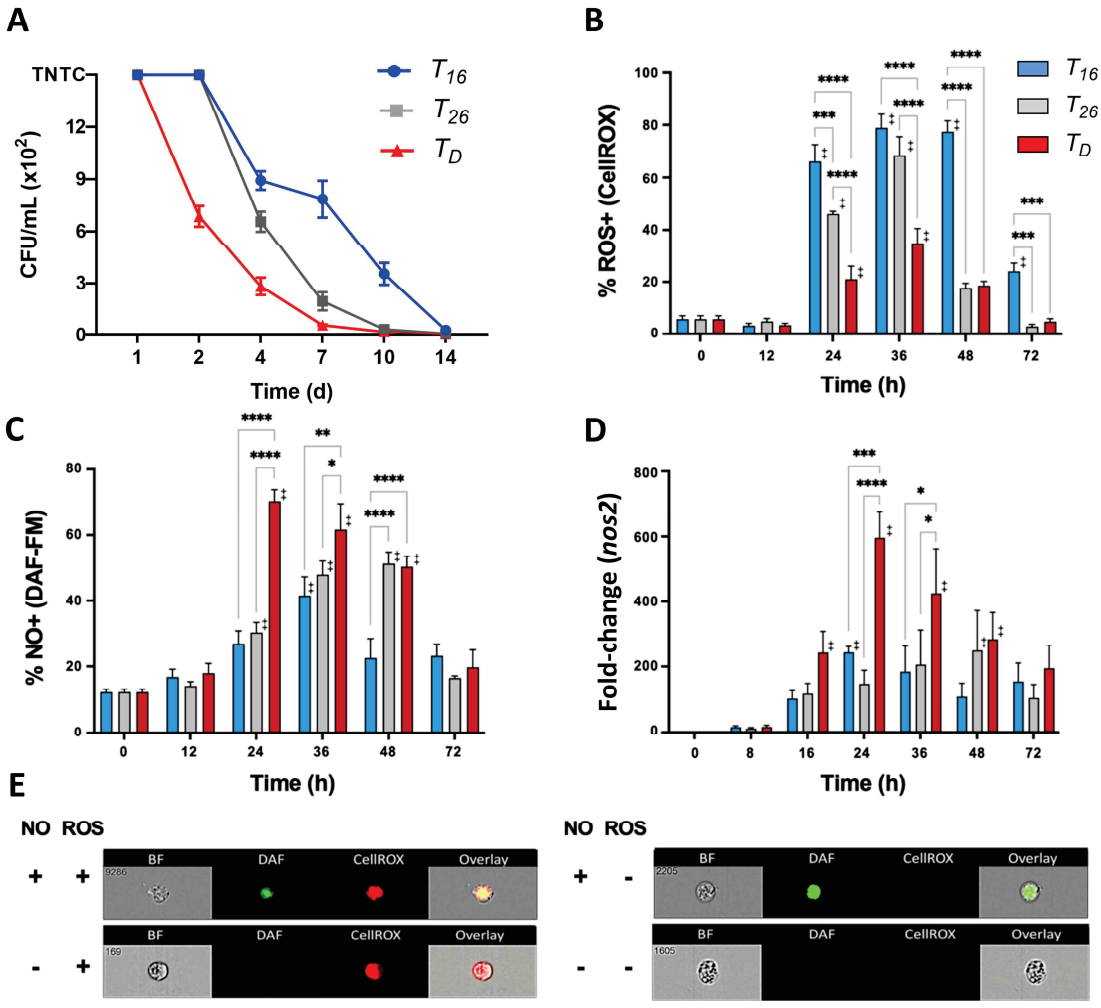

Figure 4.5. Fever enhances pathogen clearance and shows selectivity in induction of ROS and NO antimicrobial defenses. Fish were infected with *A. veronii* and placed under different experimental conditions (T_{16}: fixed 16°C; T_{26}: fixed 26°C; T_D: behavioural fever). (**A**) Bacterial loads and pathogen shedding potential were assessed following sampling of wound surface; n=5 per time point per group. Cutaneous leukocytes were isolated and imaging flow cytometry evaluated their production of (**B**) reactive oxygen species (ROS) via CellROX, and (**C**) nitric oxide production via DAF-FM-DA ; n=5 per group per time point. (**D**) qPCR analysis of wound tissue shows the kinetics of *nos2* gene expression; n=5 per group per time point. (**E**) Representative ImageStream MKII flow cytometer images show positive and negative cells following staining with CellROX and DAF-FM-DA. Results were analyzed using a two-way ANOVA followed by Tukey's post-hoc test. *p< 0.05, **p< 0.01, ***p< 0.001, ****p< 0.0001; ‡ denotes significant difference from time 0 at p< 0.05; points or bars represent the mean with error bars representing SEM.

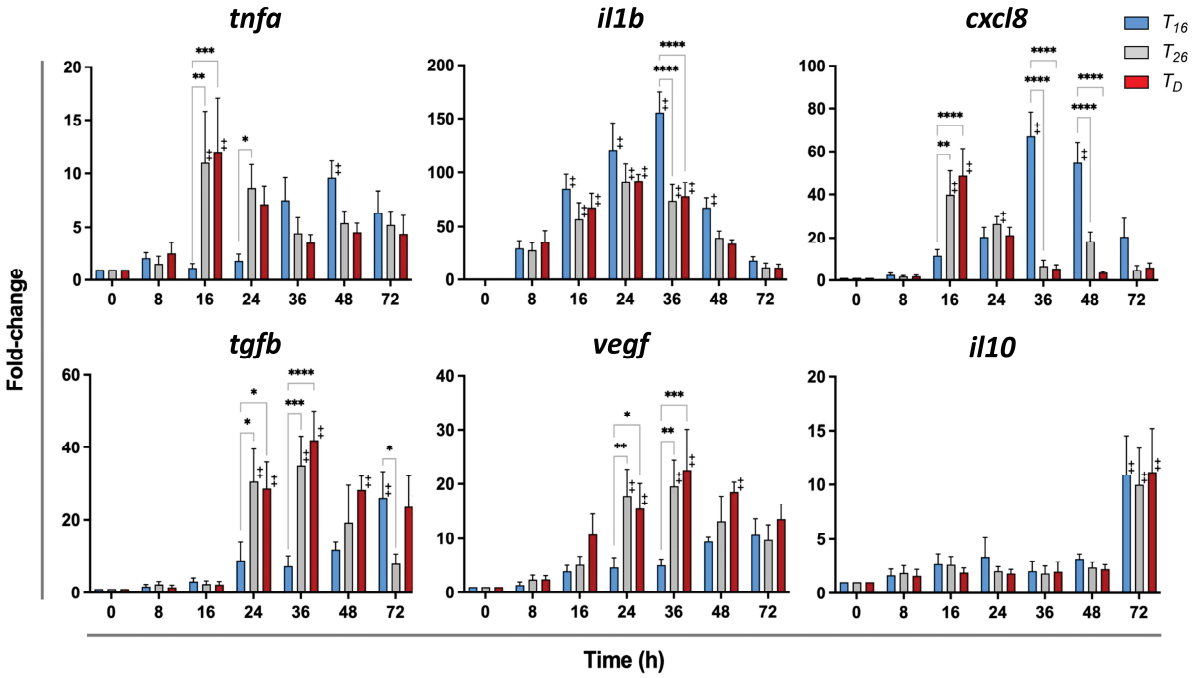

Figure 4.6. Fever selectively induces early upregulation of pro-inflammatory and pro-resolution cytokines. Fish were infected with *A. veronii* and placed under experimental conditions (T_{16}: fixed 16°C; T_{26}: fixed 26°C; T_D: behavioural fever). Quantitative PCR was used to analyze RNA extracted from wound tissue to determine gene expression of pro-inflammatory cytokines (*tnfa* and *il1b*), chemokine (*cxcl8*), anti-inflammatory cytokines (*tgfb* and *il10*) and growth factor (*vegf*). Bars represent the mean with error bars representing SEM; n=5 per time point per group. Data were analyzed using a two-way ANOVA followed by Tukey's post-hoc test (*p<0.05, **p<0.01, ***p<0.001 and ****p<0.0001, ‡ denotes difference from time=0 at p<0.05). *actb* was used as an endogenous control; RQ values were normalized against gene expression on day 0.

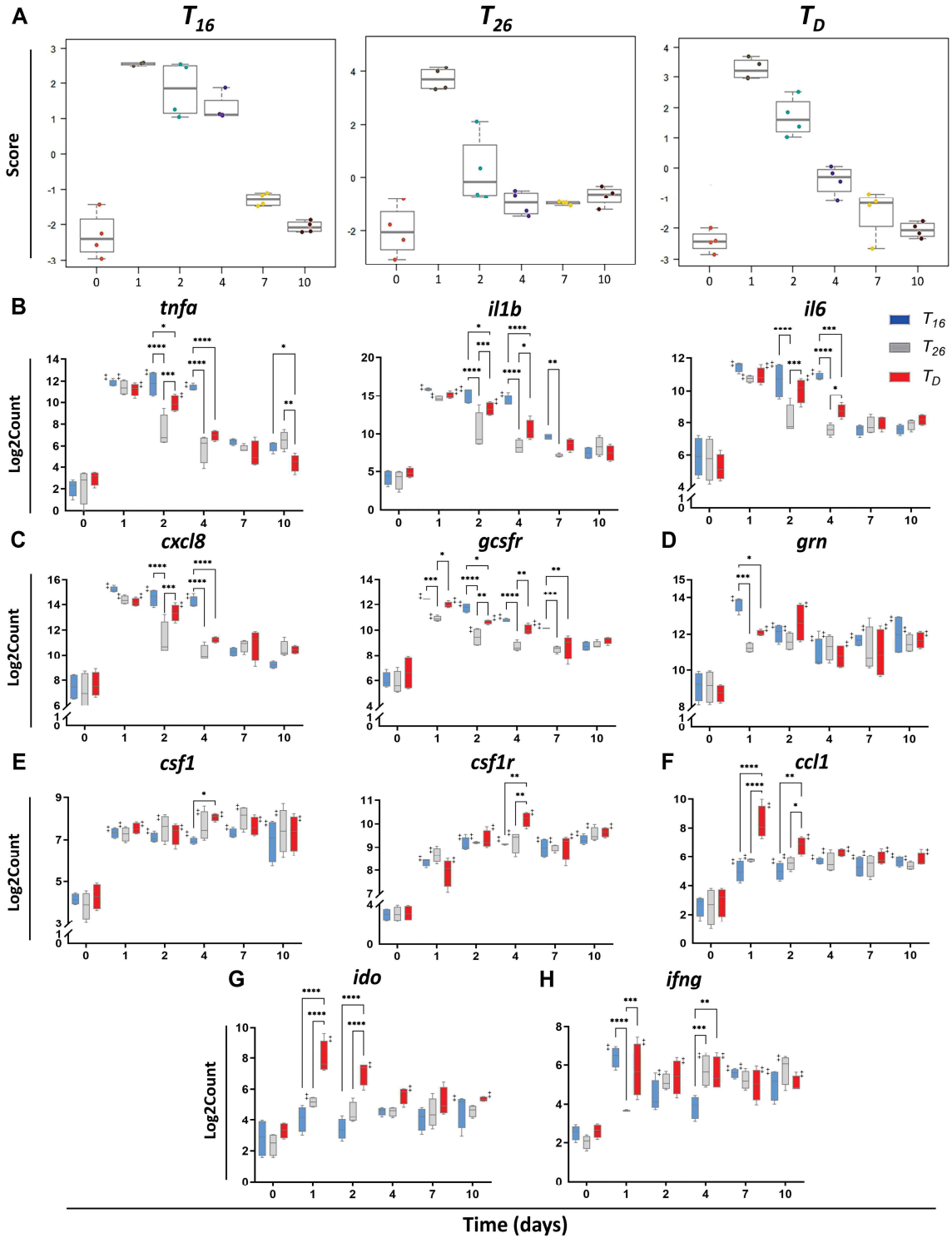
A
T_{16}
T_{26}
T_D
Score
B
tnfa
il1b
il6
T_{16}
T_{26}
T_D
Log2Count
C
cxcl8
gcsfr
D
grn
Log2Count
E
csf1
csf1r
F
ccl1
Log2Count
G
ido
H
ifng
Log2Count
Time (days)

Figure 4.7. Fever alters the gene expression of several inflammatory mediators. Fish were infected with *A. veronii* and placed under experimental conditions (T_{16}: fixed 16°C; T_{26}: fixed 26°C; T_D: behavioural fever). (**A**) Pro-inflammatory pathway score shows a rapid downregulation of genes involved in induction and maintenance of acute inflammation in fever and fixed 26°C conditions compared to fixed 16°C. The score was calculated as the first principal component of genes' normalized expression using Pathway Scoring Module in nSolver Advanced Analysis software. Genes involved in the analysis include pro-inflammatory mediators as well as neutrophil/macrophages phenotypes genes (*csf1r*, *cxcl8*, *il6*, *ccl1*, *csf1*, *tnfa*, *ifng*, *gcsfr*, *grn* and *il1b*). Differential gene expression involved in (**B**) induction of acute inflammation; (**C**) neutrophil recruitment and phenotype; (**D**) granulin synthesis; (**E**) macrophage activation; (**F**) lymphocyte recruitment; (**G**) indolamine 2-3 dioxygenase pathway and (**H**) *interferon gamma*. Gene expression was analyzed using nCounter hybridized multiplex analysis system to quantify mRNA in total RNA extracted from wound tissue. Raw mRNA counts were normalized to geometric mean of housekeeping genes (*actb* and *ef1a*) then log2-transformed; boxplots show spread of data with solid line representing the median; n=4 per time point per group. Data were analyzed using a two-way ANOVA followed by Tukey's post-hoc test (*p<0.05, **p<0.01, ***p<0.001 and ****p<0.0001, ‡ denotes difference from time=0 at p<0.05).

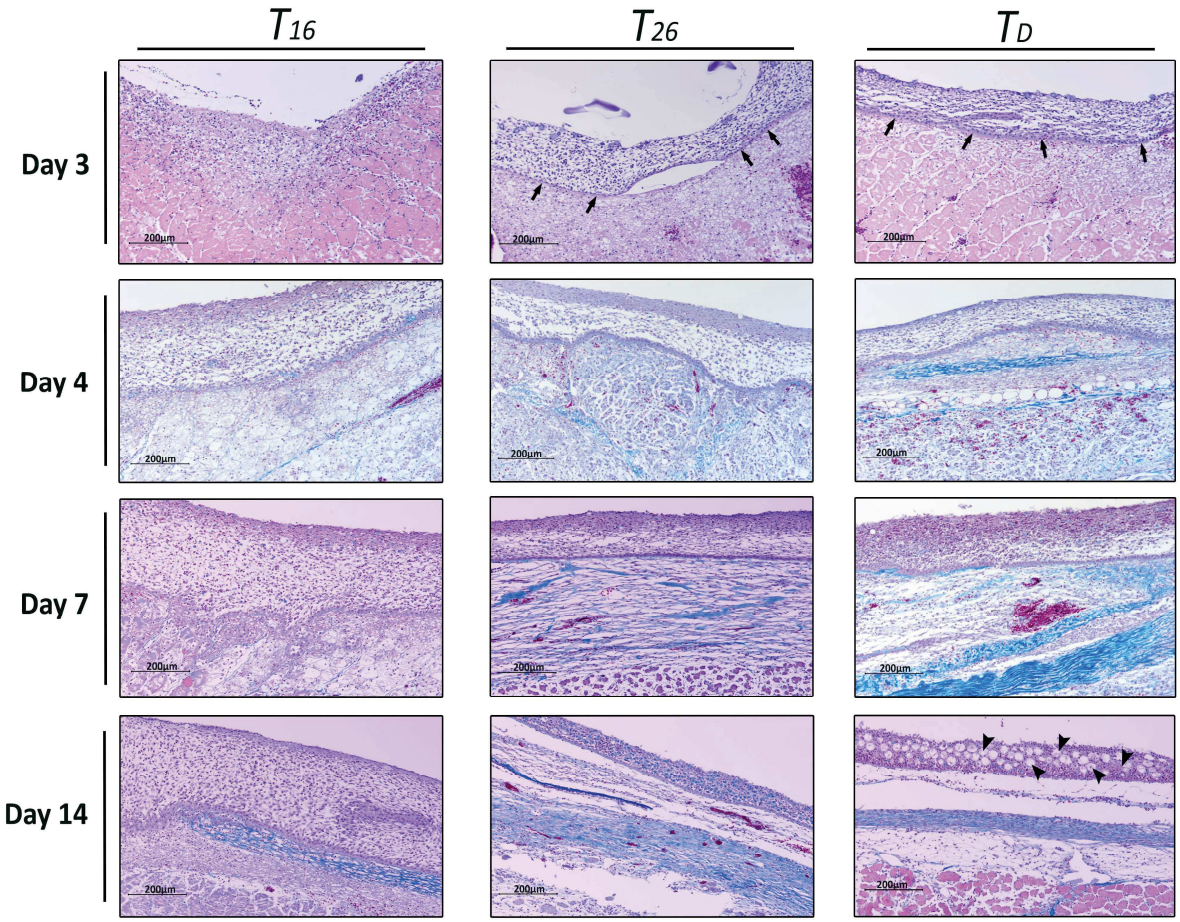

Figure 4.8. Fever enhances re-epithelialization and collagen deposition. Wound tissues from *Aeromonas*-infected fish were collected at the indicated time points, sectioned and stained with Masson's Trichrome stain; n=3 per group per time point. The wound area shows early development of the basal layer of epidermis (arrows) and overlying layers of keratinocytes in fever (right column) and 26°C (middle column) conditions at 3 dpi. In comparison, evidence of epidermis is observed at 4 dpi in fish held at 16°C (left column). At 14 dpi, the epidermis shows developed mucus-secreting cells (arrowheads) in fever fish only. Relatively abundant collagen fibers (blue) are detected at wound area in dynamic fever on day 4 and day 7 compared to other groups. Scale bar: 200 µm.

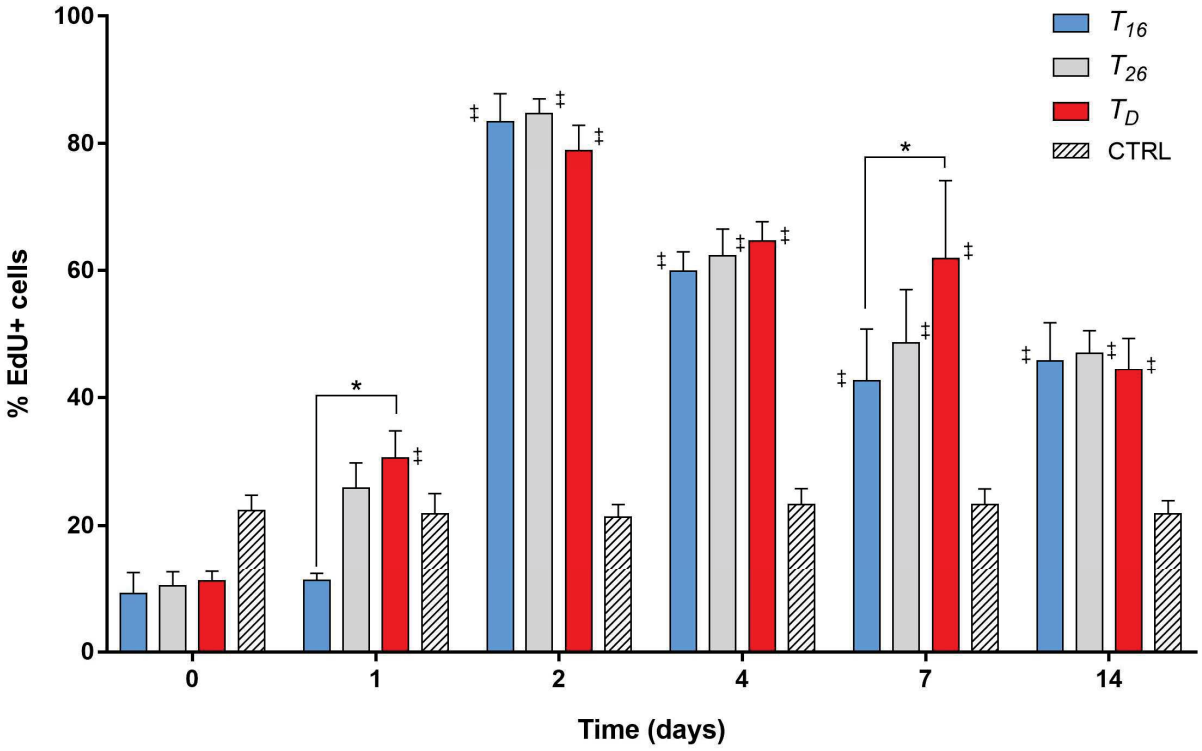

Figure 4.9. Fever possesses a limited impact on fibroblast proliferation. Goldfish fin fibroblasts (CCL71) were incubated for 48 hours with growth factor suspension collected from wound tissue of different experimental groups at indicated time points. Cells were assessed for their proliferation rate via EDU assay on a flow cytometer. Control group was treated with MGFL15 media devoid of growth factor. Bars represent the mean with error bars representing SEM; n=5 per time point per all groups except for control; n=3. Data were analyzed using a two-way ANOVA followed by Tukey's post-hoc test (*p<0.05, **p<0.01, ***p<0.001 and ****p< 0.0001, ‡ denotes difference from time=0 at p<0.05). T_{16}: fixed 16^{o}C; T_{26}: fixed 26^{o}C; T_D: behavioural fever; CTRL: control.

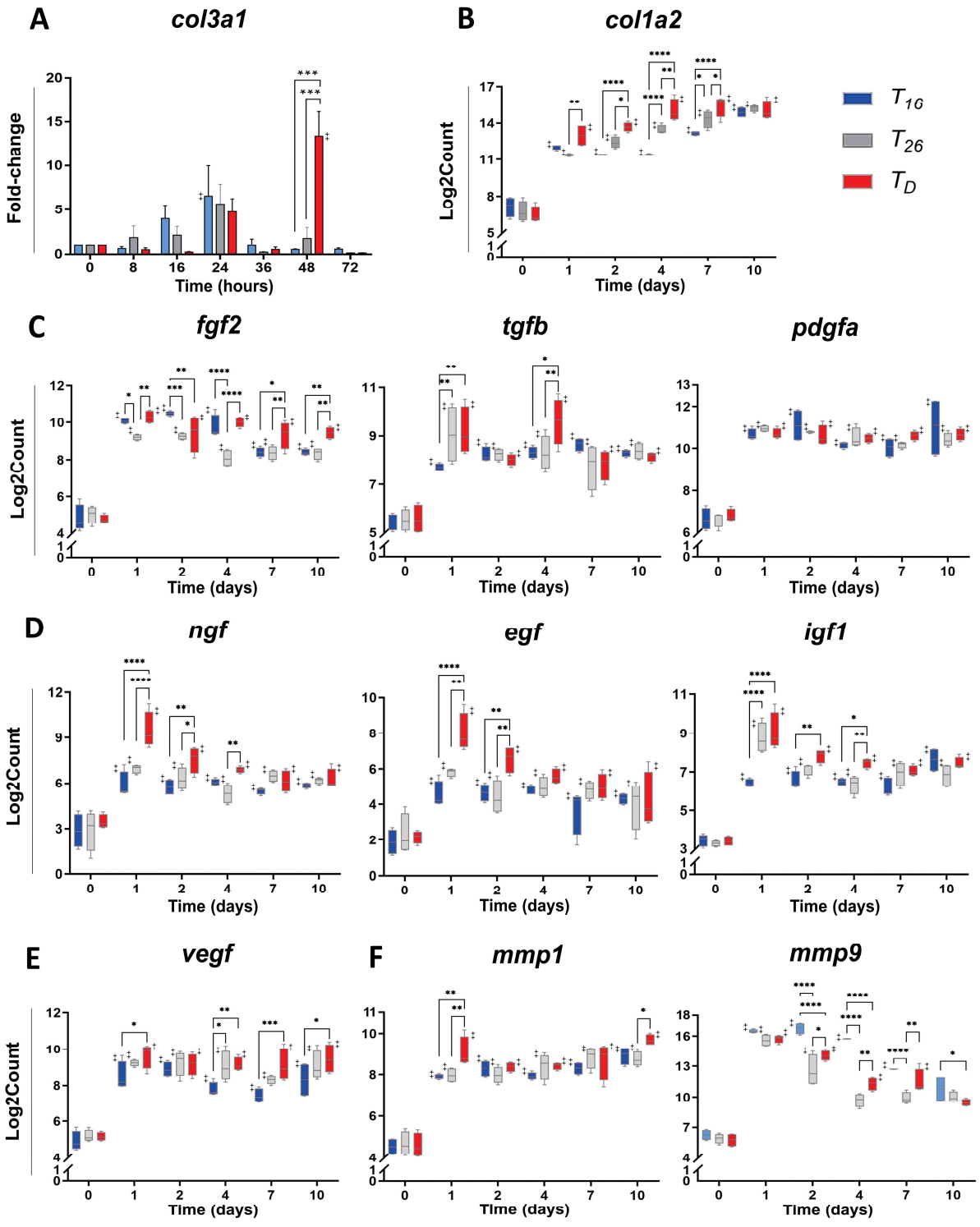
A
col3a1
Fold-change
Time (hours)
B
col1a2
Log2Count
Time (days)
T_{16}
T_{26}
T_D
C
fgf2
tgfb
pdgfa
D
ngf
egf
igf1
E
vegf
F
mmp1
mmp9

Figure 4.10. Febrile response promotes the gene expression of growth mediators involved in re-epithelialization, collagen deposition and angiogenesis. Fish were infected with *A. veronii* and placed under experimental conditions (T_{16}: fixed 16^{o}C; T_{26}: fixed 26^{o}C; T_{D}: behavioural fever). (**A**) Quantitative PCR was used to analyze RNA extracted from wound tissue to determine gene expression of *collagen type 3 alpha 1* (*col3a1*); bars represent the mean with error bars representing SEM; n=5 per time point per group. Differential gene expression of (**B**) *collagen type 1 alpha 2* (*col1a2*); growth factors involved in (**C**) collagen synthesis and deposition (*fgf2*, *tgfb* and *pdgfa*); (**D**) re-epithelialization (*ngf*, *egf* and *igf1*; and (**E**) angiogenesis (*vegf*); as well as (**F**) *matrix metalloproteinase* (*mmp1* and *mmp9*). Gene expression was analyzed using nCounter hybridized multiplex analysis system to quantify mRNA in total RNA extracted from wound tissue. Raw mRNA counts were normalized to geometric mean of housekeeping genes (*actb* and *ef1a*), then log2-transformed; boxplots show spread of data with solid line representing the median; n=4 per time point per group. Data were analyzed using a two-way ANOVA followed by Tukey's post-hoc test (*p<0.05, **p<0.01, ***p<0.001 and ****p<0.0001, ‡ denotes difference from time=0 at p<0.05).

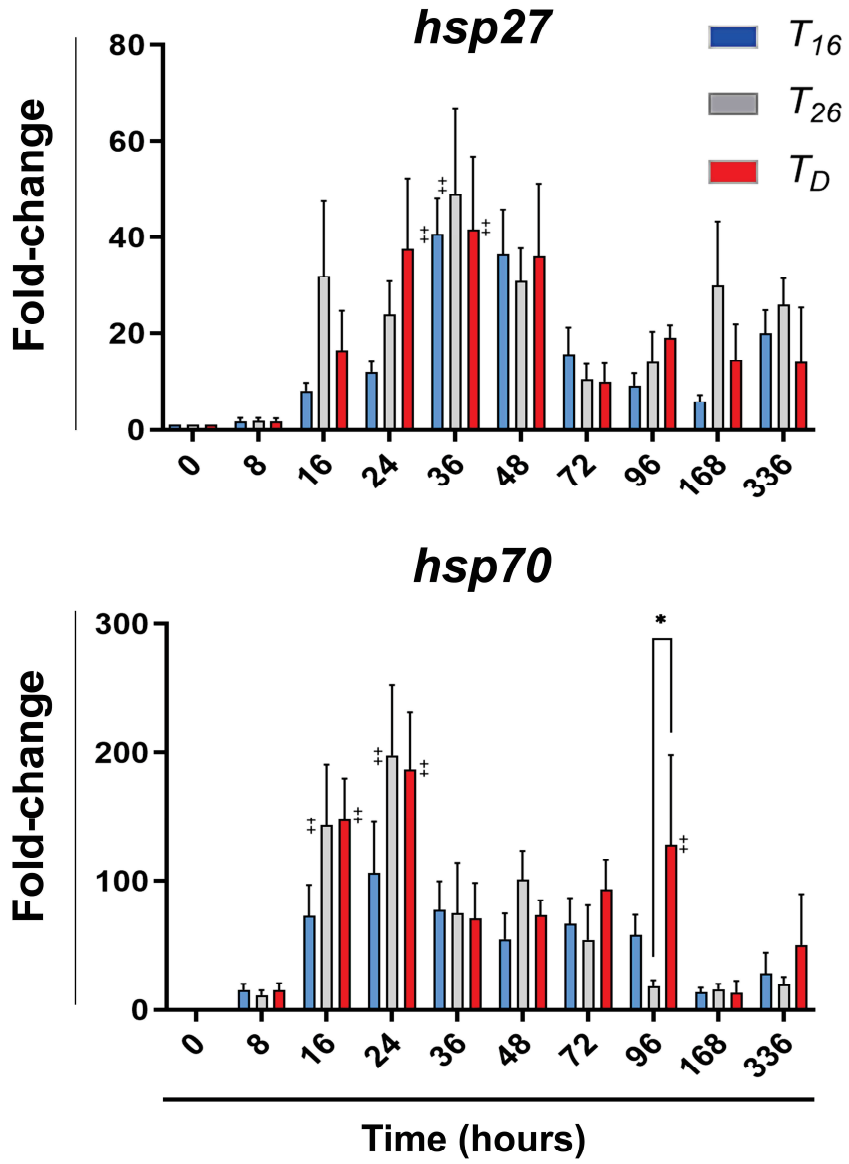

Figure 4.11. Limited changes in the expression of cytoprotective heat shock proteins were shown under fever condition. Fish were infected with *A. veronii* and placed under experimental conditions (T_{16}: fixed 16°C; T_{26}: fixed 26°C; T_D: behavioural fever). Quantitative PCR was used to analyze RNA extracted from wound tissue to determine gene expression of *heat shock protein* (*hsp27* and *hsp70*). Bars represent the mean with error bars representing SEM; n=5 per time point per group. Data were analyzed using a two-way ANOVA followed by Tukey's post-hoc test (*p<0.05, **p<0.01, ***p<0.001 and ****p<0.0001, ‡ denotes difference from time=0 at p<0.05). *actb* was used as an endogenous control; RQ values were normalized against gene expression on day 0.

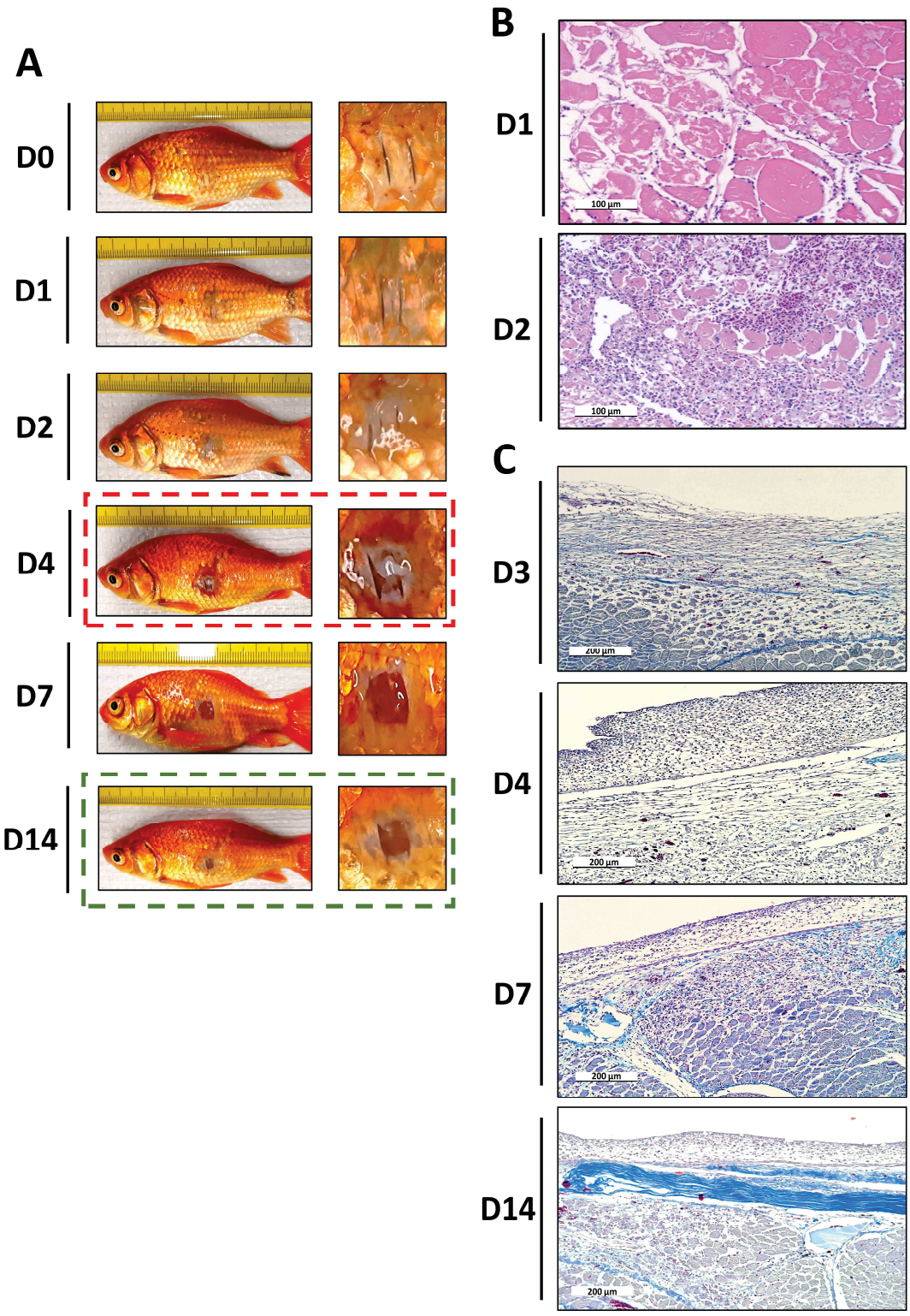
A
D0
D1
D2
D4
D7
D14
B
D1
D2
C
D3
D4
D7
D14
100 µm
100 µm
200 µm
200 µm
200 µm

Figure 4.12. The effects of housing *A. veronii* infected fish at 23^{o}C on tissue repair. Fish were infected with *A. veronii* and placed in fixed 23^{o}C. (**A**) Representative images showing the progression of wound healing. (**B**) H&E stained wound sections showing leukocyte recruitment. (**C**) Masson's Trichrome stained wound sections demonstrate the progression of re-epithelialization and collagen deposition; D: day.

Chapter V

Effects of mechanical replication of fever on tissue repair

5.1. Introduction

Given the previously highlighted beneficial impact of fever on tissue repair, I was interested in assessing whether mechanical replication of fever (*MF*), by manually changing fish housing temperature (as shown in **Figure 5.1A**) to replicate behavioural fever thermal pattern (**Figure 3.8**), would reveal the same benefits. *MF* allowed simulating of thermal components of febrile responses compared with fixed high-temperature group (T_{26}), previously examined in chapter IV. Several research groups investigated the impact of fixed hyperthermia on immune responses, particularly in endothermic models (refer to **1.4.2.3.2.2. Fever-range temperatures influence innate and adaptive immune responses**). Unlike these mechanical hyperthermia studies, our strategy captured distinct thermal levels naturally selected by fish at different points of the febrile response. Importantly, these considered thermal periods tied to the induction and resolution of acute inflammation. The latter was particularly interesting to me and links this work to tissue repair processes. Goldfish were infected with *A. veronii* (refer to **2.4. Cutaneous *A. veronii* infection: a tissue repair model**) and assigned into three different experimental categories: (1) behavioural fever (T_D); (2) mechanical fever (*MF*); and (3) fixed basal acclimated temperature condition (T_{16}). Wound healing parameters were compared between groups with a focus on wound pathology, bacterial clearance and gene expression analysis of inflammatory and growth mediators. In the first part of this chapter, I discuss the impact of mechanical replication of fever on the inflammatory and proliferative phases of wound healing in comparison to natural dynamic fever.

Additionally, I was interested if distinct periods of the fever response are relevant to tissue repair process. Therefore, in the second part of the chapter, I focus on determining if deploying the whole mechanical fever pattern (14 days) is required for fish infected with *A. veronii* to display the reparative effects or whether employing part of it would suffice. Fish were infected and assigned to two temperature categories: (1) short truanted (*ST*) group, where the temperature pattern of fever was truncated at 4 dpi to return to basal temperature (16°C), and (2) long truncated (*LT*) group at which the pattern was truncated at 9 dpi to return to 16°C. Given the importance of thermal component of febrile responses in regulating parts of their functional attributes, I hypothesized that mechanical fever would significantly enhance pathogen clearance and promote tissue repair. Additionally, truncating fever's thermal pattern would inhibit some of these benefits.

5.2. Results

5.2.1. Mechanical fever enhances bacterial clearance and overall wound healing

Analyzing bacterial load from the wound surface displayed a significant difference in CFU/mL between *MF* and T_{16}, where mechanical fever fish demonstrated a superior capacity to clear pathogens (**Figure 5.1B**). Although both groups showed too numerous to count CFUs at 1 and 2 dpi, bacterial load was remarkably reduced in *MF* at 4 dpi compared with T_{16}, which showed substantially higher loads of bacteria at the wound surface till 10 dpi (**Figure 5.1B**). Though, *MF* failed to achieve a similar pathogen-killing ability observed in

dynamic fever (**Figure 5.1B**). The rapid bacterial clearance induced by mechanical fever suggested enhanced kinetics of inflammatory responses. This was supported by early signs of purulent exudate noted in *MF* at 2 dpi (similar to T_{26} fish); however, these signs were exhibited 48 hours later by fish at basal temperature condition (red boxes; **Figure 5.1C**). By the end of the fourteen days, the wound was almost closed in *MF* and T_{26}, yet it was still relatively open in T_{16} (green boxes; **Figure 5.1C**), indicating that mechanical fever significantly improved healing associated with faster wound closure. Histopathological and Nanostring analyses were conducted for a more in-depth analysis of mechanisms underlying these differences in repair outcomes.

5.2.2. Mechanical fever induced an early acute inflammatory program reminiscent of dynamic fever

Signs of acute inflammation and purulent exudate demonstrated concurrently at 2 dpi in both *MF* and T_D indicated a comparable induction pattern of acute inflammatory responses. To analyze these observations, we examined the gene expression of pro-inflammatory mediators using Nanostring technologies. Overall, the pro-inflammatory pathway score peaked at 1 dpi, dropping at 2 dpi (**Figure 5.2**), indicating a similar timeline of induction of acute inflammation in dynamic and mechanical fever that was, in contrast, delayed in T_{16}, as previously shown (refer to **Section 4.2.1.)** The score was calculated as the first principal component of genes' normalized expression involving pro-inflammatory cytokines as well as neutrophil/macrophage phenotypes genes (*csf1r*, *cxcl8*, *il6*, *ccl1*, *csf1*, *tnfa*, *ifng*, *gcsfr*, *grn* and *il1b*). Most of the mediators involved in activation of acute

inflammation, such as *il1b*, *tnfa*, *il6* and *cxcl8* showed no significant differences in their expression levels between *MF* and T_D at 1 and 2 dpi (data not shown). Notably, expression kinetics of molecular inducers of acute inflammation in *MF* were the same under fixed 26°C (**Figure 4.7A**).

5.2.3. Mechanical fever failed to promote collagen deposition and efficient resolution of inflammation attained by febrile responses

The differences in wound closure rate observed by the end of the fourteen days in both T_D and *MF* (**Figure 5.1C**) indicated possible distinctions in epidermal and dermal healing. Therefore, I did histopathological and gene expression analyses to characterize these differences. At 7 dpi, wound sections revealed abundant, parallel and well-organized collagen fibers in dynamic fever compared to mechanical fever (blue color; **Figure 5.3A**). Collagen is the main component of ECM, synthesized by fibroblasts, forming the dermis layer and providing strength [311].

Earlier collagen deposition indicated rapid engagement of tissue repair pathways that necessitate effective inflammation resolution [236], achieved via several regulatory mechanisms (refer to **1.4.3.1.7. Suppression of inflammation**) aiming at downregulating cellular recruitment and pro-inflammatory mediators. Although mechanical fever was associated with a similar expression pattern of pro-inflammatory cytokines presented in behavioural fever during the first 48 hours after infection, I observed significant differences regarding their downregulation at later time points. For instance, at 7 dpi, mRNA levels of

cxcl8 were upregulated in mechanical fever fish compared to those allowed to deploy behavioural fever (**Figure 5.3B**). Furthermore, the substantially higher *progranulin* (*grn*) expression observed in *MF* (**Figure 5.3B**) could have augmented acute inflammation and delayed its control. Progranulin is released as precursor glycoproteins containing granulin-like domains by epithelial and infiltrating hematopoietic cells [535]. It is then cleaved by proteolytic enzymes such as Mmp9 into smaller peptides called granulin [536]. Although progranulin possesses an essential modulatory role in tissue repair, a balance has to be maintained between progranulin and its protease-generated granulins to avoid aggravation of inflammation [535]. Granulin A and B were reported to stimulate epithelial cells to secrete Cxcl8, thus enhancing neutrophil recruitment [567]. Notably, mice with secretory leukocyte peptidase inhibitor (*slpi*$^{-/-}$) knockout displayed prolonged inflammation and impaired wound healing triggered by superfluous granulins generated by the high level of protease activity [568]. We later report a remarkably upregulated *mmp9* in *MF* at the same time point (**Section 5.2.4**), which correlates augmented levels of granulins and *cxcl8*.

We detected a considerable upregulation of *ido*, a pro-resolution mediator, in mechanical fever fish (**Figure 5.3B**). Ido is a rate-limiting enzyme converting tryptophan to kynurenine [569]. Ido mediates immunomodulatory functions during tissue repair by impairing inflammatory cell proliferation and activation [21,22], promoting T_{reg} differentiation and activating their immunosuppressing activity [539,540]. The high expression level of *ido* is suggested to be a compensatory mechanism to suppress augmented inflammation potentially induced by upregulated pro-inflammatory mediators as well as Mmp9-generated granulins at 7 dpi. Additionally, a significant upregulation of *arginase 2*

(*arg2*) enzyme was detected in *MF* (**Figure 5.3B**). Arginase is a metalloenzyme that primarily converts L-arginine, the primary source for NO production, to L-ornithine and urea [570]. Although, L-ornithine is important for proline and subsequent collagen formation, excessive consumption of arginine by increased levels of *arg2* results in uncoupling of NOS that is further associated with a significant reduction in NO [571] and a rise in superoxide [570].

On the other hand, *csf1* and *csf1r* were remarkably upregulated in dynamic fever compared to *MF* (**Figure 5.3C**). Csf1, also known as macrophage colony stimulating factor (Mcsf), is an essential regulator of macrophage proliferation, differentiation, survival and biological functions [572], which is critical for the healing process (refer to **1.4.3.1.5.2. Macrophages**). This indicated a significant contribution of Csf1 to better wound healing by functioning during the early inflammatory and later proliferative phase. The increased expression of *csf1* was revealed to be beneficial to wound healing [573–575]. Mechanistically, Csf1 promotes macrophage activation [575] and increases Tgfb levels [576]. Moreover, Csf1 contributes to dedifferentiating hematopoietic cells into stem cells [573].

Slower downregulation of pro-inflammatory mediators in mechanical fever fish was associated with interrupted tissue repair machinery and collagen deficiency in the dermis layer. Collagen synthesis and release are regulated by a variety of growth factors regulating fibroblast proliferation, migration and activation [310,311] (refer to **1.4.3.2.4. Growth factors in tissue repair**). Among them, we examined the expression of *tgfb*, where we detected a significant upregulation at 7 dpi in dynamic fever (**Figure 5.3D**). A concomitant

higher mRNA levels of collagen (*col1a2*) in T_D (**Figure 5.3D**) was in accordance with histopathological findings and increased *tgfb*.

5.2.4. Mechanical fever enhances re-epithelialization

Assessing re-epithelialization via histological analysis revealed little differences between mechanical and dynamic fever. Both groups showed evidence of epidermis development at 7 dpi that progress toward a mature epidermal layer characterized by high-density keratinocytes and mucus-secreting cells at 14 dpi (**Figure 5.4A**), though relatively more mucus-secreting cells were observed in T_D. Critical for the development of epidermis following an injury is the migration, proliferation and differentiation of keratinocytes [301], activated by various mediators, including Egf, Igf1 and Ngf [208,304,306,337,577] (refer to **1.4.3.2.1. Re-epithelialization**). Nanostring analysis uncovered a similar expression level of these growth factors in T_D and *MF* (**Figure 5.4B**). *ngf* and *egf* are upregulated during early time points, while mRNA levels of *igf1* remain high throughout the 10 days after infection, proposing these pleiotropic growth factors to be produced in a spatio-temporal manner with overlapping contributions regulating epidermal development at different stages. For example, Ngf and Egf seem more related to the initiation of epithelial cell migration and proliferation to rapidly cover the wound surface, whereas Igf1 regulates subsequent cellular proliferation and differentiation crucial for epidermal maturation.

Quantification of mucus-secreting cells showed that dynamic fever fish had a higher number of these cells in the epidermis (**Figure 5.4C**). Skin mucus is an essential component

of cutaneous innate immune mechanisms of fish against invading pathogens; therefore, mucus cells are vital for a functional epidermis [487]. Examining differential gene expression of other pleiotropic growth factors (*fgf2* and *pdgfa*) revealed differences between mechanical and dynamic fever (**Figure 5.4D**). These growth mediators are involved in various tissue repair pathways regulating re-epithelialization, fibroblast activation and collagen synthesis (refer to **1.4.3.2.4. Growth factors in tissue repair**). Significant upregulation of these factors in T_D could have contributed to enhanced collagen deposition and epidermis maturation. Notably, *fgf2* was substantially upregulated at 4 dpi in *MF* (**Figure 5.4D**). Likewise, mechanical fever managed to enhance the expression of most growth factors (compared to a basal expression at 0 dpi) at most of the time points. However, it failed to replicate a similar pattern at 7 dpi. Also, there was no significant difference in the expression level of *vegf*, a potent mediator of neovascularization, between mechanical and dynamic fever (**Figure 5.4E**), which further supports *MF*'s capacity to replicate some of the tissue repair benefits of dynamic fever.

Mmps are critical for several tissue repair events, such as re-epithelization [302], angiogenesis and granulation tissue formation [310]. They function by cleaving ECM and integrin:matrix adhesion, thus facilitating cellular migration [302]. Tight regulation of these proteinases is essential to avoid collateral tissue injury in addition to the annihilation of growth factors and newly formed granulation tissue [365–367]. Examining mRNA level of *mmp9* revealed similar kinetics of expression during the first 4 days in both groups, though there was a persistent upregulation of *mmp9* at 7 dpi in *MF* compared with T_D (**Figure 5.4E**).

High levels of *mmp9* could have contributed to more tissue damage in mechanical fever associated with delayed collagen deposition and augmented granulin levels.

5.2.5. Truncation of mechanical fever pattern displayed similar inflammatory program with restrictions on wound repair

To determine if applying mechanical fever thoroughly (14 days) is necessary to induce tissue repair benefits, we examined the impact of truncating mechanical fever pattern after 4 days (*ST*) and 9 days (*LT*), as shown in (**Figure 5.5A)**. Interestingly, both short and long truncation showed a remarkably rapid bacterial clearance compared to T_{16} (**Figure 5.5B**). Similar to *MF*, early signs of inflammation and purulent exudate were detected at *ST* and *LT* at 2 dpi, while they were observed at 4 dpi in T_{16} (**Figure 5.5C**). This indicates that applying a mechanical fever pattern until day 4 was sufficient to activate an early acute inflammatory response associated with rapid bacterial killing. However, wound pathology at 14 dpi showed differences in wound closure rate between groups (**Figure 5.5C**). *LT* group showed a relatively faster wound closure than *ST*; however, it was slower than *MF* (**Figure 5.5C**). Yet, *ST* and *LT* demonstrated improved overall wound healing compared to fish held at static 16°C (**Figure 5.5C**). While truncating mechanical fever pattern has shown similar effects of *MF* during the inflammation phase of tissue repair, it did not recapitulate the same impact on the proliferative phase.

A qPCR analysis of genes involved in both inflammatory and proliferative parts of the repair process was conducted. Pro-inflammatory cytokines (*tnfa* and *il1b*) showed the

same expression pattern in *MF*, *ST* and *LT*. Still, *tnfa* was early and significantly upregulated in these groups compared to T_{16} (**Figure 5.6A**), with no differences in *il1b* expression levels between the four groups, indicating a potential contribution of *tnfa* rather than *il1b* to the early induction of inflammation. Truncation of mechanical fever also did not impact *nos2* expression levels that remained remarkably high at 2 dpi in *MF*, *ST* and *LT* groups compared with basal static condition (**Figure 5.6A**). Although all four groups showed almost levels of *cd4*, a substantial increase in *cd8* expression was identified only in *MF* and *LT* at 10 dpi (**Figure 5.6B**). Gene expression levels of molecular chaperones (*hsp27*, *hsp70*) were similar in all groups (**Figure 5.6C**). Though growth factors such as *igf1* and *vegf* were significantly upregulated in *MF*, *ST* and *LT* at 1 and 4 dpi, respectively (**Figure 5.6C**). Similarly, expression of *tgfb* was remarkably higher in *MF*, *ST* and *LT* when compared to 0 dpi, which was not observed in basal acclimated temperature (**Figure 5.6C**). *col1a2* was another example where short truncation impacted its expression at 7 dpi (**Figure 5.6C**). Collectively, my data propose the importance of deploying the whole fever window by fish to achieve the full potential of mechanical fever, especially reparative and adaptive immune responses. Yet, applying a part of the fever window still enhanced innate immune responses and, to a lesser extent, improved healing.

5.3. Discussion

In chapter IV, I highlighted dynamic fever's significant and beneficial contributions to reparative responses. However, a question remained on the feasibility of mechanically

replicating the thermal pattern of febrile responses to achieve similar effects of dynamic thermoregulation. It was also essential to characterize the impact of fever's thermal component on tissue repair and to rule out other factors associated with dynamic fever that would induce a superior healing capacity compared to mechanical fever. Our data show that mechanical replication of fever's thermal pattern accomplished remarkable advantageous healing effects compared to control (fish held at 16°C). Yet, it did not recapitulate all repair benefits observed during dynamic fever. Two main factors can explain these findings: (1) fish during behavioural fever response are allowed to freely choose their preferred temperature, providing them with the flexibility to utilize higher temperatures to their benefit when needed; (2) additional possible positively contributing neuronal and metabolic factors that are only activated during natural febrile responses.

Wound pathological examination revealed early signs of purulent exudate, indicating enhanced kinetics of acute inflammatory response in both *MF* and T_D. However, there were differences in wound closure rate between the two groups induced by dynamic fever's robustness in promoting reparative responses such as collagen deposition. Collectively, the data suggest some similarities in inflammatory and proliferative profiles but not a complete reiteration. Fish in *MF* condition were able to clear pathogens at a remarkably faster rate which was still slower compared to these experiencing behavioural fever. All these observations proposed parallels in some aspects of the underlying molecular mechanisms, especially the early expression of pro-inflammatory cytokines.

The delayed downregulation of some pro-inflammatory mediators at 7 dpi explained previously and summarized in (**Figure 5.7**) in mechanical fever fish indicated a late

resolution of inflammation. A proper transition from inflammatory to proliferative phase is vital for the healing process, which ultimately depends on efficient resolve of inflammation [236]. Early and robust inflammation control in dynamic fever, aided by rapid bacterial clearance and downregulation of pro-inflammatory cytokines, was associated with early engagement of tissue repair pathways as shown by upregulation of various growth factors at 7 dpi (**Figure 5.7**); thus, better healing outcomes.

The results match findings illustrated in chapter IV, where fish held at 26°C (the highest temperature fish migrate to during behavioural fever) failed to recapitulate all the effects offered by dynamic fever. However, mechanical fever displayed additional robustness compared to T_{26}, especially regarding wound closure and maturation of epidermis layer. The development of mucus-secreting cells was detected in *MF* group at 14 dpi, but it was not observed in the case of 26°C condition. This signals the importance of distinctive behavioural thermoregulation of infected fish, which are time and temperature specific, and that a fixed increase in housing temperature negates these conditions, abolishing some of the healing benefits. Additionally, infected fish tend to stay at a preferred higher temperature for particular durations, depending on the challenge, sufficient to help fish overcome the infection and restore homeostasis. Hence, truncation of fever's thermal pattern likely disrupted some immunomodulatory and tissue repair benefits orchestrated by these behavioural thermoregulations.

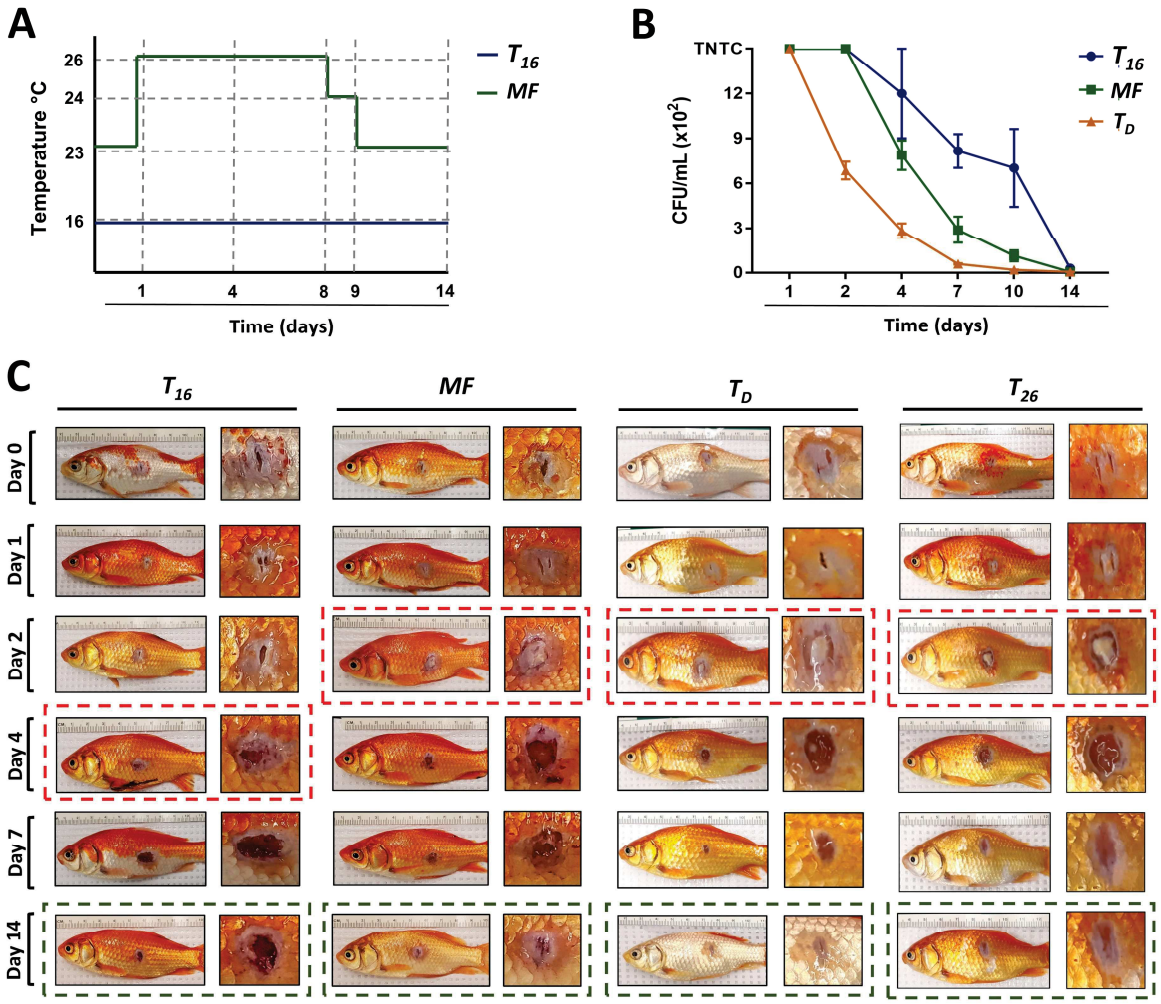

Figure 5.1. Mechanical fever enhances bacterial clearance and overall wound healing. (**A**) Temperature pattern of mechanical fever (*MF*) and fixed basal temperature condition (T_{16}). (**B**) Bacterial load was assessed by collecting and plating surface bacteria from wound surface; points represent the mean with error bars representing ± SEM; n=5 per group per time point. (**C**) Representative photographs at different time points of goldfish with inflicted wounds inoculated with *A. veronii* and placed at 16°C (control, T_{16}); mechanical fever (*MF*), dynamic fever (T_D) and fever-range hyperthermia (T_{26}). Red boxes highlight kinetics of purulent exudate development. Green boxes emphasis distinct degrees of wound closure achieved by 14 dpi. Wound images of T_{26} fish were added to this figure to compare wound pathology with *MF* group.

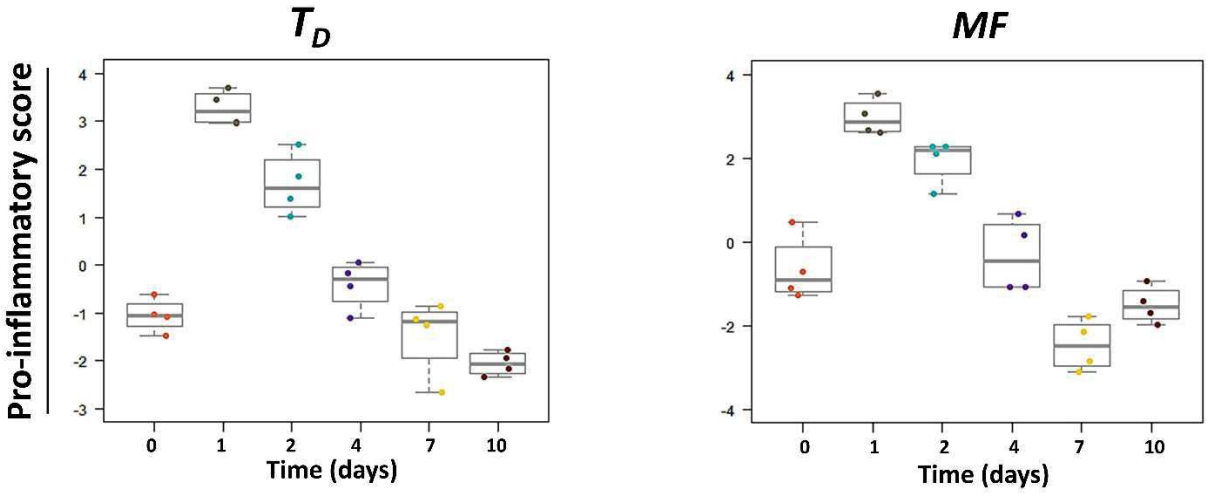

Figure 5.2. Mechanical fever induced an early acute inflammatory program similar to dynamic fever. Fish were infected with *A. veronii* and placed under experimental conditions (T_D: dynamic fever; *MF*: mechanical fever). RNA was isolated from wound tissues and analyzed using Nanostring technologies. Pro-inflammatory pathway score demonstrates a peak of acute inflammatory response at 1 dpi in T_D and *MF*. The pathway was calculated as the first principal component of genes' normalized expression using Pathway Scoring Module in nSolver Advanced Analysis software. Genes involved in the analysis include pro-inflammatory mediators as well as neutrophil/macrophage phenotypes genes (*csf1r*, *cxcl8*, *il6*, *ccl1*, *csf1*, *tnfa*, *ifng*, *gcsfr*, *grn* and *il1b*).

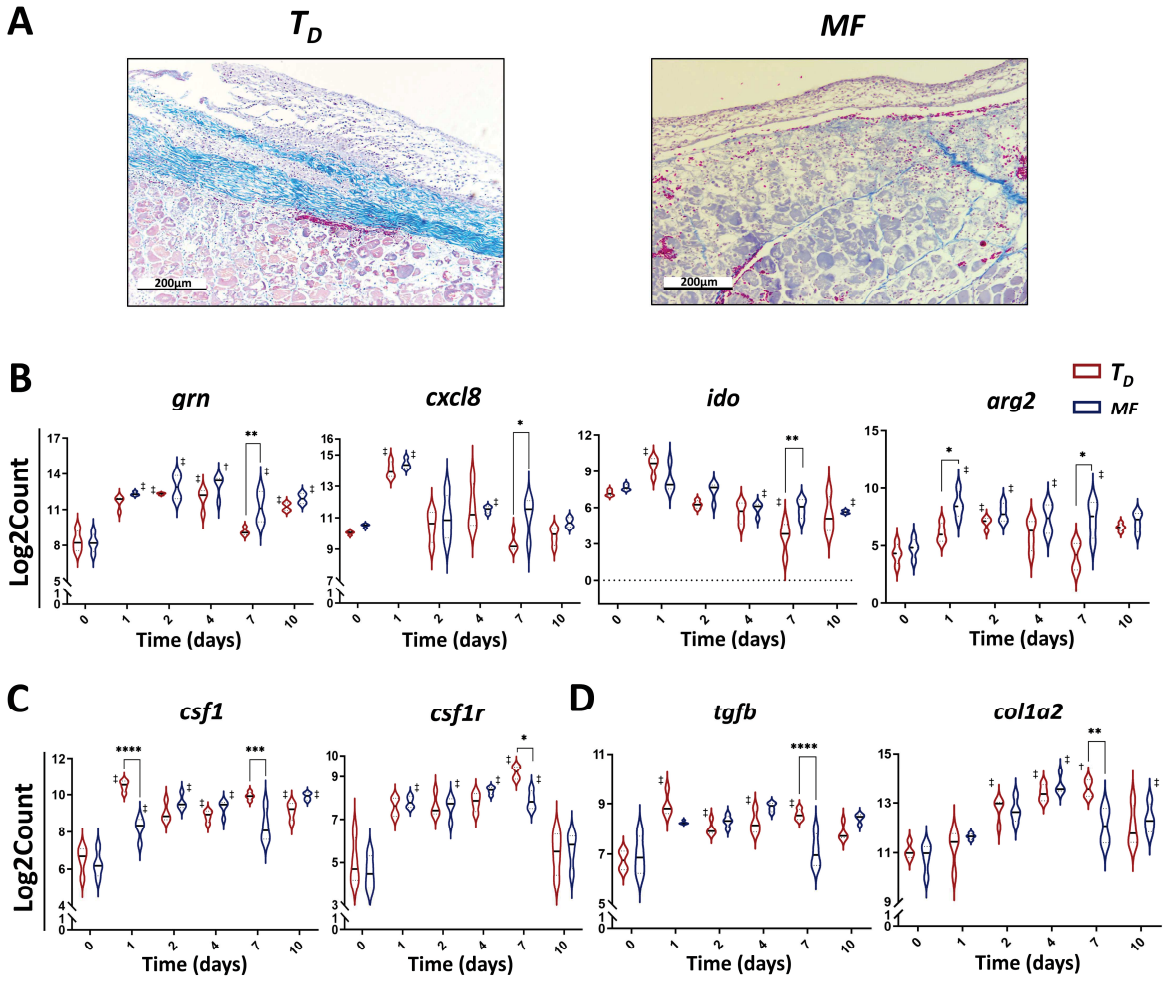

Figure 5.3. Mechanical fever fails to promote collagen deposition and efficient resolution of inflammation achieved by dynamic fever. Fish were infected with *A. veronii* and placed under experimental conditions (T_D: dynamic fever; *MF*: mechanical fever). (**A**) Wound tissues were collected at 7 dpi, sectioned and stained with Masson's Trichrome stain; n=3 per group per time point. Wound sections show relatively abundant collagen fibers (blue) in T_D compared with *MF*. Differential expression of several genes involved in (**B**) regulation of inflammation phase of tissue repair, (**C**) macrophage activation and (**D**) fibroblast proliferation and collagen synthesis. Gene expression was analyzed using nCounter hybridized multiplex analysis system to quantify mRNA counts in RNA extracted from wound tissue. Raw mRNA counts were normalized to geometric mean of housekeeping genes (*actb* and *ef1a*), then log2-transformed; all data were analyzed using a two-way ANOVA followed by Tukey's post-hoc test (*p< 0.05, ** p< 0.01, ***p<0.001 and **** p< 0.0001, ‡ denotes difference from time = 0 at p <0.05); violin plots show spread of data with solid line representing the median; n=4 per group per time point.

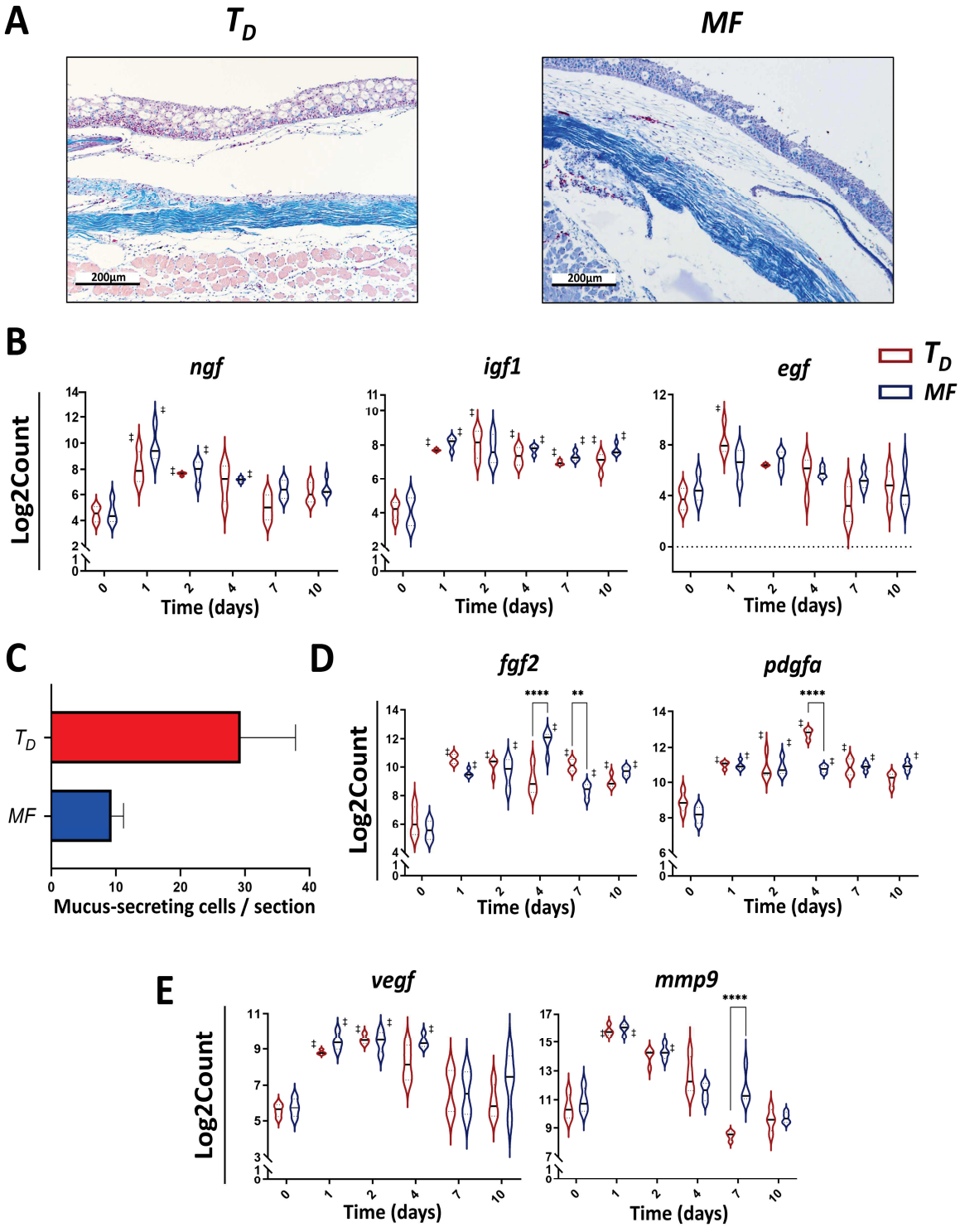
A
T_D
MF
200µm
200µm
B
ngf
igf1
egf
T_D
MF
Log2Count
Time (days)
C
T_D
MF
Mucus-secreting cells / section
D
fgf2
pdgfa
****
**
****
Log2Count
Time (days)
E
vegf
mmp9
****
Log2Count
Time (days)

Figure 5.4. Mechanical fever enhances re-epithelialization. Fish were infected with *A. veronii* and placed under experimental conditions (T_D: dynamic fever; *MF*: mechanical fever). (**A**) Wound tissues were collected at 14 dpi, sectioned and stained with Masson's Trichrome stain; n=3 per group per time point. Sections show evidence of mucus-secreting cells in both groups. (**B**) Differential expression of genes involved in re-epithelialization. (**C**) Quantification of mucus-secreting cells in the epidermis at 14 dpi; bars represent the mean with error bars representing SEM; n=3 per group per time point. Differential expression of (**D**) pleiotropic growth factors engaged in re-epithelialization and collagen synthesis, (**D**) *vegf*; angiogenic factor and matrix metalloproteinase. Gene expression was analyzed using nCounter hybridized multiplex analysis system to quantify mRNA counts in RNA extracted from wound tissue. Raw mRNA counts were normalized to geometric mean of housekeeping genes (*actb* and *ef1a*), then log2-transformed; all data were analyzed using a two-way ANOVA followed by Tukey's post-hoc test (*p< 0.05, ** p< 0.01, ***p<0.001 and **** p< 0.0001, ‡ denotes difference from time = 0 at p <0.05); violin plots show spread of data with solid line representing the median; n=4 per group per time point.

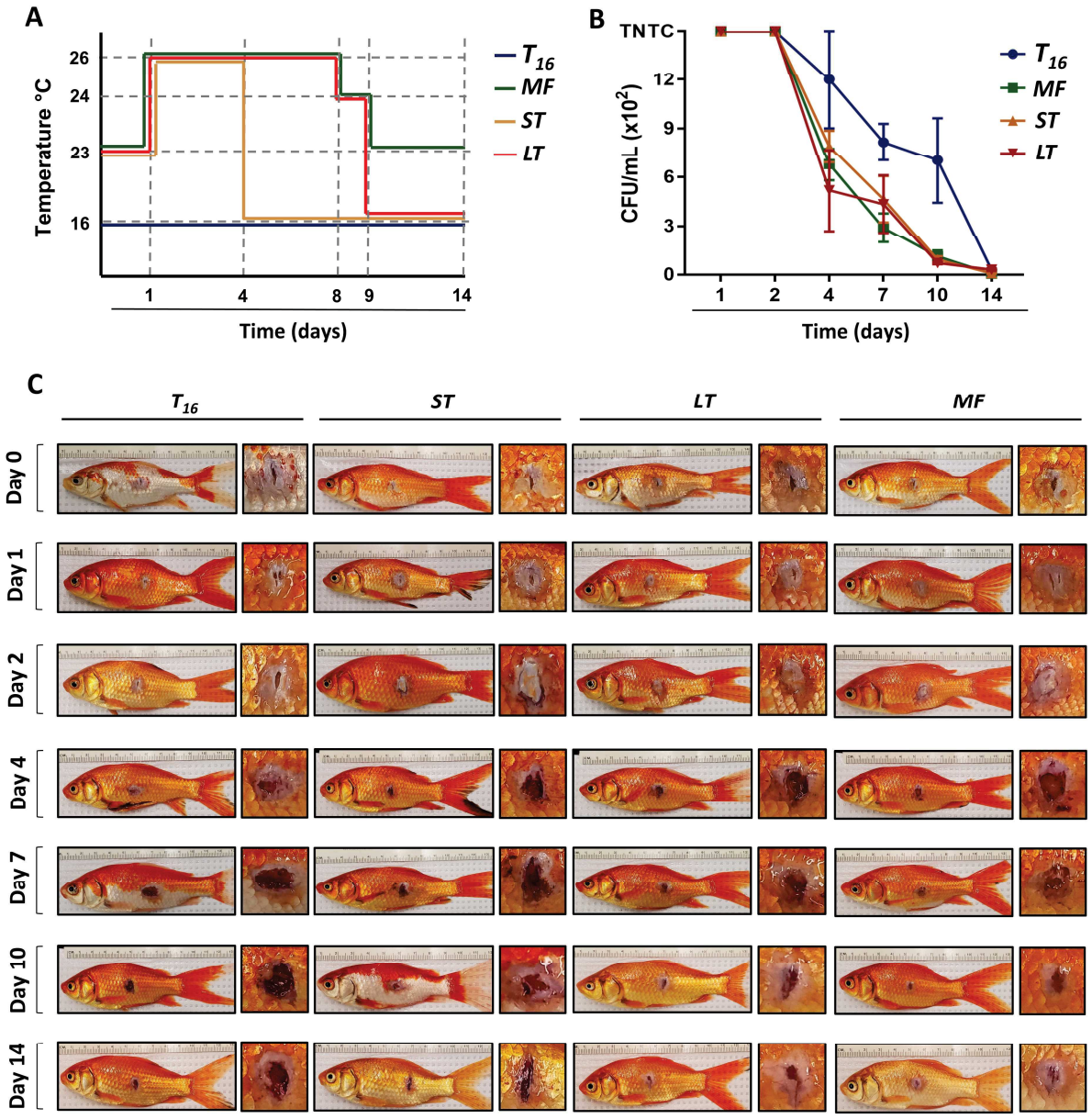

Figure 5.5. Truncation of mechanical fever pattern displayed some parallels at the inflammatory phase and bacterial clearance yet failed to recapitulate all healing benefits. (**A**) Temperature patterns of fixed basal temperature (T_{16}); mechanical fever (*MF*); short truncated (*ST*) and long truncated (*LT*) groups. Fish were infected with *A. veronii* and placed under experimental conditions (T_{16}; *MF*; *ST*; *LT*). (**B**) Bacterial loads and pathogen shedding potential were assessed by collecting and plating bacteria of wound surface; points represent the mean with error bars representing ± SEM; n=5 per time point per group. (**C**) Representative photographs showing the progression of wound pathology.

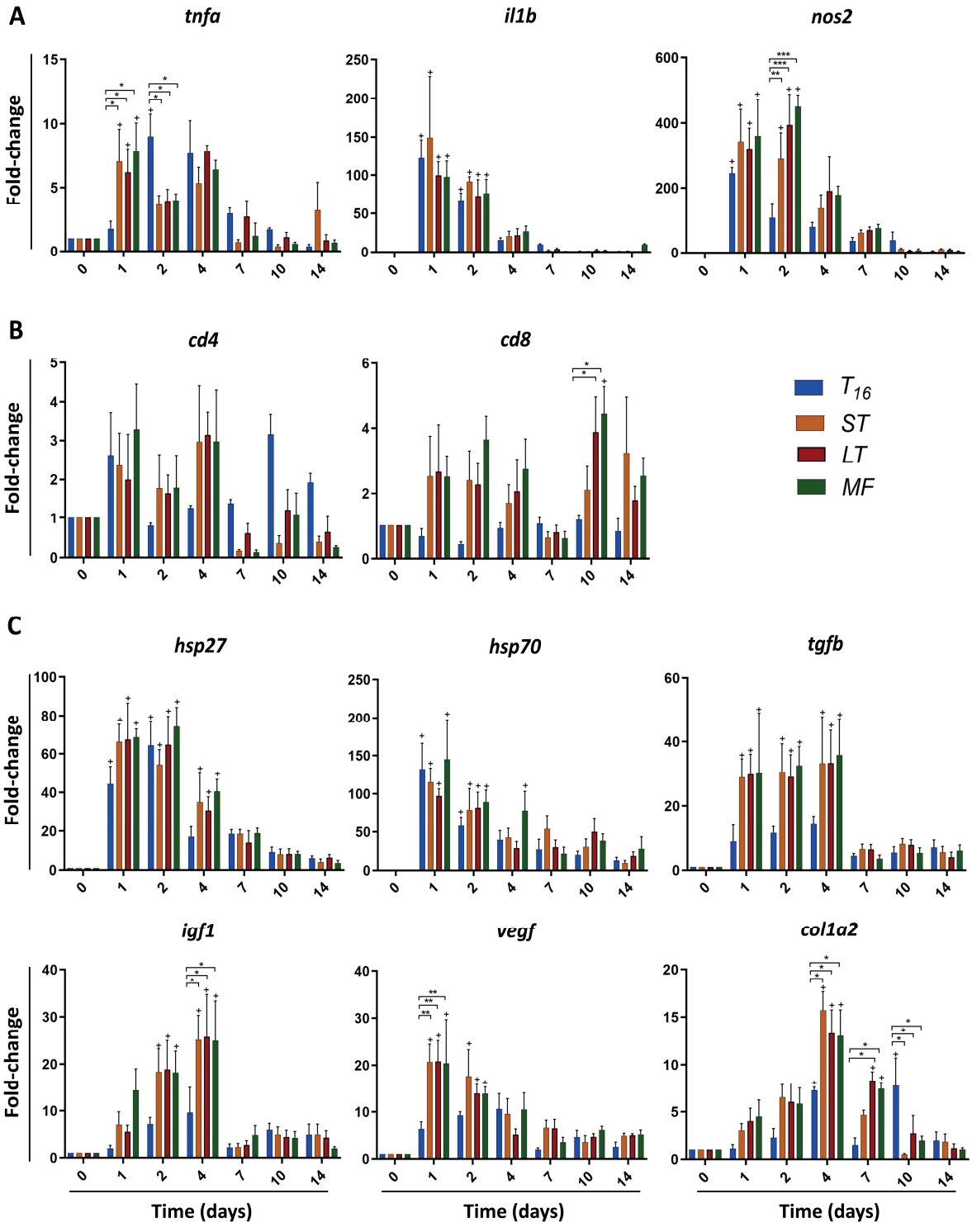
A
tnfa
il1b
nos2
B
cd4
cd8
C
hsp27
hsp70
tgfb
igf1
vegf
col1a2
Fold-change
Time (days)
T_{16}
ST
LT
MF

Figure 5.6. Quantitative PCR analysis of wound tissue reveals that truncation of mechanical fever pattern impacted the expression of genes involved in adaptive immunity and tissue proliferation. Fish were infected with *A. veronii* and placed under experimental conditions (T_{16}: fixed basal temperature; *MF*: mechanical fever; *ST*: short truncated and *LT*: long truncated). At each of the indicated time points, wound tissue was collected, RNA extracted, and cDNA synthesized. qPCR was used to evaluate the expression levels of (**A)** pro-inflammatory cytokines: *tnfa* & *il1b* and *inducible nitric oxide synthase* (*nos2*); (**B)** genes of adaptive immune response: *cd4* & *cd8*; (**C**) genes involved in tissue healing events: *heat shock protein* (*hsp70* & *hsp27*), growth factors (*tgfb*, *igf1*, *vegf*) and collagen (*col1a2*). All data were analyzed using a two-way ANOVA followed by Tukey's post-hoc test (**p*<0.05, ** *p*<0.01, ****p*<0.001 and **** *p*<0.0001, $^{+}$ denotes difference from time = 0 at *p* <0.05); bars represent the mean with error bars representing SEM; n=5 per time point per group. *actb* was used as an endogenous control; RQ values were normalized against gene expression at day 0.

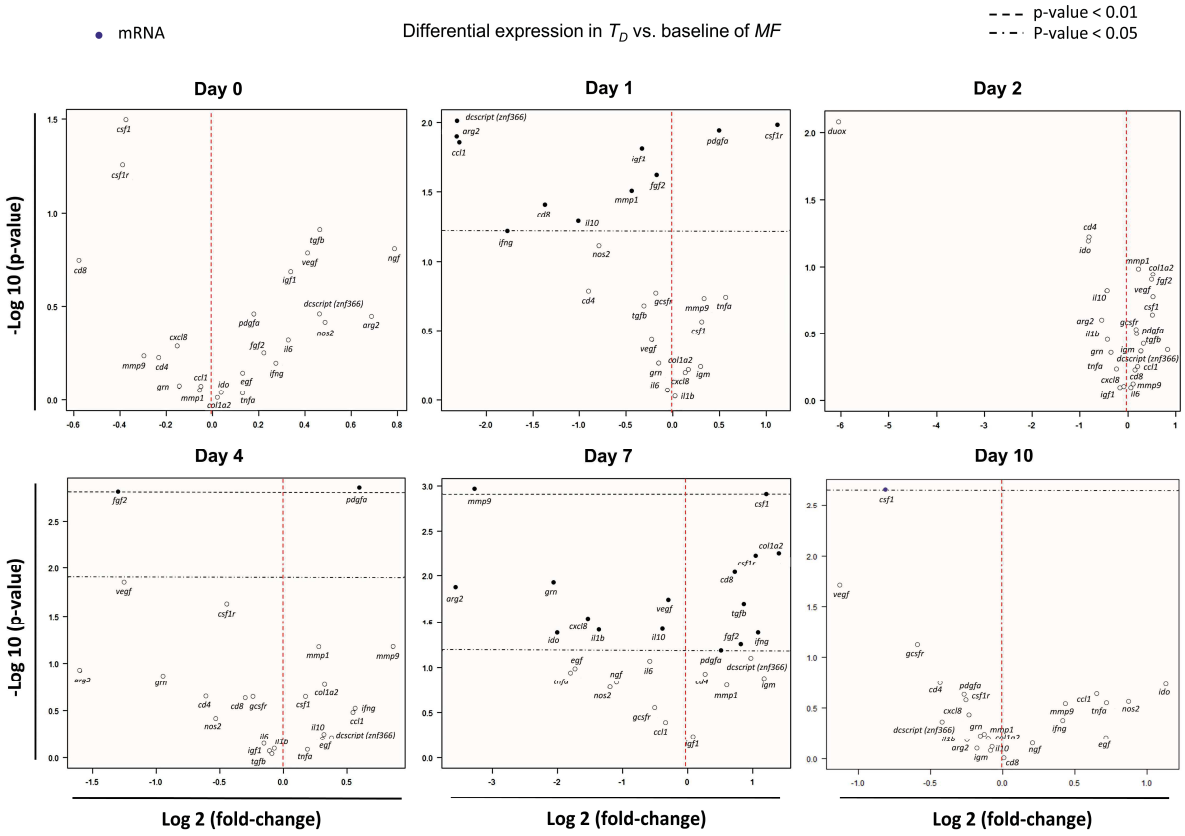

Figure 5.7. Differential gene expression in dynamic fever compared to baseline of mechanical fever. Volcano plots display each target gene's -log10 (*p*-value) and log2 fold-change. Highly statistically significant targets fall at the top of the plot, and highly differentially expressed genes fall to either side, with genes on the right side being upregulated in dynamic fever and those on the left side upregulated in mechanical fever. Gene expression analysis was performed using nCounter hybridized multiplex analysis system (Nanostring technologies) to quantify target mRNA counts in RNA extracted from wound tissue. T_D: dynamic fever; *MF*: mechanical fever.

Chapter VI

Discussion and future directions†

† Parts of this chapter have been published in

- Haddad, F.*, **Soliman, A. M.***, Wong, M. E., Albers, E. H., Semple, S. L., Torrealba, D., Heimroth, R. D., Nashiry, A., Tierney, K. B., & Barreda, D. R. (2023). Fever integrates antimicrobial defences, inflammation control, and tissue repair in a cold-blooded vertebrate. *eLife*, 12; e83644.
  * *Authors contributed equally to this work, and parts of this paper will be published in Haddad, F. thesis.*

6.1. Overview of findings

The conservation of fever across 550 million years of metazoan evolution [43] indicates a survival advantage, which happens to outweigh metabolic costs [578], increased risk for predation [38] and reduction in reproductive success [579]. This was supported by the expanding literature recounting survival advantages of febrile responses (refer to **1.4.2.3. Fever, survival and impact of antipyretics**); however, mechanisms underlying these contributions remain inadequately understood. The gaps in our understanding of fever biology are attributed to deficient experimental models adequately reiterating natural physiological processes driving and maintaining fever. In this study, I used a cold-blooded teleost fish behavioural fever model to examine febrile responses under host-driven dynamic thermoregulation, thus averting common limitations associated with mechanical hyperthermia and antipyretics use that can interrupt native thermoregulatory pathways. Challenging fish with *A. veronii* cutaneous infection induced a behavioural fever response associated with a preference for high temperature and lethargy behaviours (**Chapter III**). Confirmation of a behavioural fever response in our model was fundamental to link our observations to febrile responses.

The main focus of my thesis was to investigate the potential role of fever in restoring homeostasis upon infection via assessing its impact on tissue repair. Fever was found to improve overall wound healing when assessing wound pathology compared to basal acclimated temperature. A self-resolving *A. veronii* skin infection model allowed me to examine fever-induced changes during both inflammatory and proliferative phases of the repair process. Our findings show that fever is an important regulator of acute inflammation

induction and control. The earlier and more selective rather than stronger activation of innate antimicrobial programs against infection led to markedly quicker pathogen clearance (**Chapter IV**). These functional characteristics of fever were further integrated with effective resolution of inflammation and triggering of various tissue repair mechanisms that accelerated healing of damaged tissues and achieved efficient return to homeostasis (**Chapter IV**). In comparison to prevalent theories that assume global induction of immunity or rely on a shift away from those temperatures preferred by invading pathogens, this integrative approach is novel and represents a notable upgrade in refinement. Mechanically replicating the thermal preference of fish exerting behavioural fever showed some benefits but failed to recapitulate natural febrile response (**Chapter V**).

6.2. Behavioural fever in goldfish

Subsequent to using goldfish as a comparative ectothermic model to study fever, it was essential to characterize behavioural fever response in these animals. Goldfish were infected with *A. veronii* then added to ATPT to track their movements. A custom animal enclosure delivered a stable multi-day thermal gradient without using physical barriers that are known to affect behaviour [138,489]. This animal model, enclosure layout and automated continuous per-second tracking of animal locomotory patterns during the behavioural thermoregulation greatly improved analytical robustness and temporal resolution. The behavioural analysis revealed a distinct timeframe from 1 to 8 dpi with an overall trend of ~2.9°C increase in temperature preference of *A. veronii* infected fish when

compared to controls [490]. This was consistently observed in infected fish, while control fish displayed a high degree of variability within the same timeframe. Two lethargy behaviours, overlapping the window of high-temperature preference, were identified by a remarkably lower mean velocity and zone transitions in infected fish [490]. Outside the fever window, there were no significant differences in temperature preference, velocity and zone transitions between infected and control fish, with both groups demonstrating large variations temporally and across individual fish [490]. Collectively, behavioural analysis of *A. veronii* infected outbred population fish showed consistency in their preference for high temperature during a window of seven days. The period of increased thermal preference was further associated with two lethargy behaviours mimicking sickness behaviours of endotherms/humans.

Additional experiments revealing upregulation of pro-inflammatory cytokines and Hsps in the hypothalamic tissue and high levels of serum PGE2 in infected fish further confirmed the behavioural fever response [490]. Moreover, when infected fish were injected with ketorolac, a common antipyretic, they exhibited a temporary disruption of their behavioural thermoregulation [490]. These findings are in accordance with the previously reported common pathways of fever induction that involve COX2/PGE2 between cold- and warm-blooded vertebrates [18].

6.3. Fever promotes tissue repair

6.3.1. Contributions of fever to inflammatory phase of tissue healing

Increases in core body temperature are well-established to promote neutrophil accumulation, NADPH oxidase activity, and production rates of toxic superoxide anions [3,580]. Models of fever-range hyperthermia have associated these effects with higher serum concentrations of Il1, Tnfa, and Il6 [166,581], Gcsf-driven release of neutrophils from the hematopoietic bone marrow,[582] expansion of the circulating neutrophil pool [170,582] and increased endothelial barrier permeability of blood vessels [583], in addition to upregulation of *gmcsf*, *il8* and other CXC chemokines at the infection site [78,169]. However, these thermal increases have also been shown to promote collateral tissue injury [168,584]. This continues to be largely viewed as an inevitable cost of fever, where induction of immune defenses will undoubtedly drive accompanying inflammation-associated tissue injury [168,169]. Our results offer an alternative explanation, where fever-range hyperthermia partially recapitulates the regulatory capacity of fever on acute inflammation. Both fever and mechanical fever range-hyperthermia displayed accelerated kinetics of leukocyte recruitment and earlier control of pro-inflammatory cytokine expression. Though differences were observed in the induction of pro-resolution genes, and fever ultimately demonstrated a superior capacity to restore tissue integrity and homeostasis.

We also documented a clear shift from a ROS-dominant microbicidal response under euthermic and fever-range hyperthermia conditions to one dominated by NO production under fever. Yet, this inhibition in ROS production seemed contradictory to a well-established role of fever in pathogen resistance. Notably, reduced ROS activity does not

essentially have to result in compromised host defenses. Additionally, NO and downstream reactive nitrogen species (RNS) exert microbicidal or microbiostatic activities against a broad range of bacteria, viruses, yeasts, helminths, and protozoa [273]. In a murine *Pseudomonas aeruginosa* infection, NO enhanced bacterial clearance via an Atg7-mediated mechanism that further inhibited ROS production and limited oxidative stress, resulting in reduced lung injury and lower infection-associated mortality [558]. Other examples of antagonistic NO modulation of ROS responses during infection have also been described, some of which can be traced as far back as plants [273,275,555,585,586]. My results are consistent with these observations and offer a natural scenario where fever drives a shift in the NO-ROS balance, maintaining capabilities of microbial clearance to subvert infection while contributing to inflammation control and the re-establishment of a functional mucosal barrier.

Recent years have seen renewed interest in the links between thermoregulation and host defense, which extends to cooler temperatures [587,588]. This has led to a perceived functional dichotomy between fever and hypothermia. Although both reflect an animal's capacity to take advantage of thermoregulation to maintain fitness upon infection, fever drives elimination of invading microorganisms through microbicidal disease resistance, while hypothermia promotes tolerance to foster energy conservation and management of collateral inflammation-associated tissue damage [587,588]. Our results blur the line in this perceived dichotomy. We identified clear fever-embedded mechanisms that contributed to the maintenance of tissue integrity and would allow for energy conservation. These

contributions were prominent features through initial induction and subsequent resolution of acute inflammation and the following tissue repair mechanisms.

Fever promoted disease resistance via enhanced kinetics of leukocyte recruitment rather than augmenting the magnitude or duration of immune activation. Selective rather than global upregulation of immunity further decreased the potential for collateral damage often attributed to fever. Remarkably, microbicidal efficacy was still superior under fever, with *A. veronii* clearance achieved markedly faster than under thermally restricted basal conditions. Fever then showed greater efficiency in inflammation control. This was paired with novel contributions that actively promoted tissue repair instead of resilience to inflammatory damage. There was no induction of a hypothermic state at any point during our observation periods; instead, high-resolution positional tracking only showed a discrete, self-resolving fever response. Thus, fever actively engaged mechanisms that enhance protection, while also limiting pathology, controlling inflammation, and promoting tissue repair. Importantly, our findings do not dispute the previously described competition mechanisms between immunity and other maintenance programs that direct a transition towards tolerance under high pathogen loads [589]. Instead, they simply highlight the persistent and long-standing considerations placed on energy allocation and tissue integrity by an animal host at all stages of infection.

6.3.2. Contributions of fever to proliferative phase of tissue healing

To date, studies looking at the basis for host survival promoted by fever have focused on the activation of immune defense mechanisms [3]. The self-resolving nature of our teleost model allowed for characterization of immunological changes during the transition between inflammatory and proliferative phases of tissue repair, which necessitates resolution of inflammation. Indeed, evaluation of cellular responses subsequent to *A. veronii* infection showed marked differences in the control of leukocyte recruitment toward infection site. Early cellular recruitment and their rapid resolution during fever were consistent with accelerated kinetics of induction and control of pro-inflammatory cytokines. In contrast, slower kinetics of leukocyte recruitment was detected among T_{16} fish, which was associated with delayed upregulation of pro-inflammatory mediators. Thus, fever promoted an earlier pro-inflammatory period, which was further paired with more efficient resolution of inflammation based on inhibition of leukocyte recruitment, control of pro-inflammatory cytokine expression and induction of pro-resolution genes.

Wound pathology demonstrated a robust ability of T_D fish to heal wounds. By 2 dpi, T_D and T_{26} fish displayed accelerated kinetics of purulent exudate formation, which was similar to enhanced kinetics of leukocyte recruitment. The fastest progress was made by fish that were exerting dynamic fever, which showed early indications of advanced stages of wound healing. T_{16} and T_{26} wounds did not reach the same degrees of closure, in comparison. Thus, fish that were allowed to exert fever were able to clear infection and heal the damage to cutaneous barrier more quickly than fish that were kept in static 16°C or under fever-range mechanical hyperthermia.

Histopathological examination of wound sections further demonstrated earlier re-establishment of the basal epidermal layer and overlying layers of keratinocytes among T_D and T_{26} experimental groups. Among T_{16} fish, wound re-epithelialization occurred but was delayed. Regeneration of mucus-secreting cells, consistent with re-establishment of skin barrier functionality, was only observed in the T_D experimental group. Thus, fever promoted greater levels of wound repair and regained original structural features required for restoration of skin barrier functionality after cutaneous infection. The enhanced kinetics of re-epithelialization during fever was associated with significant upregulation of growth mediators involved in epidermis development and maturation.

Tissue repair advanced faster in wounds derived from T_D fish, with collagen deposition becoming evident as early as 4 dpi. For fish exerting fever, this further developed into more extensive, organized collagen deposition by 7 dpi. In comparison, slower progression was observed among T_{26} and T_{16} wounds based on the abundance and relative organization of collagen arrangements at wound area. Conversely, the absence of fever caused delayed resolution of inflammatory response, re-epithelialization and appearance of extracellular matrix components. In investigating the possible mechanisms underlying these observations, we examined fibroblast proliferation rate and gene expression of growth factors regulating collagen synthesis. Although there was a limited impact of febrile response on fibroblast proliferation, a remarkable upregulation of mediators engaged in fibroblast activation and collagen deposition was observed. Together, fever offers a natural strategy to harness the body's intrinsic repair mechanisms to enhance restoration of tissue integrity and homeostasis.

6.4. Mechanical replication of fever and tissue repair

Significant and beneficial contributions of fever to tissue repair postulated a question on the possibility of mechanically replicating febrile responses to attain similar effects of dynamic thermoregulation. My findings demonstrated advantageous healing properties induced by mechanical fever when compared to fish held at 16°C, yet it did not recapitulate all the repair benefits observed during dynamic fever. Although wound pathology revealed early signs of acute inflammation in both *MF* and T_D, there were differences in wound closure rate, which was largely induced by the sturdiness of dynamic fever in promoting reparative responses. Similarly, *MF* cleared pathogens at a surprisingly faster rate. These observations can be explained by parallels in the underlying molecular pathways regulating the early expression of pro-inflammatory mediators between dynamic and mechanical fever, as shown in the Nanostring analysis. Nevertheless, there was a delay in the downregulation of pro-inflammatory cytokines and substantial upregulation of *grn* and *mmp9* in mechanical fever. At the same time, I detected a remarkable decrease in mRNA levels of genes implicated in collagen synthesis that was, in contrast, significantly upregulated in dynamic fever. As a result, wound area demonstrated low collagen content in *MF* group, indicating delayed engagement of tissue repair pathways.

The results are partially similar to the findings of T_{26} group, where fish held at fixed high temperature failed to recap all the benefits demonstrated by fever. However, it appears that mechanical fever outperformed T_{26} in terms of re-epithelialization as demonstrated by

the emergence of mucus-secreting cells. This emphasizes the significance of distinct behavioural thermoregulations of infected fish, which are time and temperature specific. It also shows that a constant increase in housing temperature nullifies these conditions, eliminating some of the healing benefits. We revealed that natural dynamic fever has a greater intrinsic healing capacity than a mechanical replication of the thermal pattern of febrile responses. These observations can be explained by the ability of fever fish to freely choose their preferred temperature, which provided them with the flexibility to utilize higher temperatures to their benefit, thereby rapidly overcoming infection and returning to homeostasis. Moreover, additional positively contributing neuronal and metabolic factors activated only in dynamic fever could have contributed to these healing benefits.

6.5. Relevance

Herein, we revealed for the first time a superior intrinsic healing capacity of natural dynamic fever. Our findings present fever as an essential modulator of induction and resolution of acute inflammation. Moreover, it promotes restoration of tissue homeostasis via reducing inflammation-associated tissue damage and activating a variety of tissue repair pathways. Together, these observations offered an alternative approach for understating fever biology and its contribution to host survival. This integrative mechanism proposes a selective rather augmented activation of antimicrobial responses complemented by significant attributes to tissue healing. Collectively, my data underscores the crucial role of fever in host defense, which establishes it as a beneficial physiological and

immunomodulatory response. This, in turn, encourages further animal experiments and clinical trials looking into a possible review of the current unregulated use of antipyretics in suppressing mild fever. Additionally, these observations may open the door toward therapeutic applications that take advantage of the immune modulation induced by fever. Beyond human medicine, my research has meaningful implications for animal health. Among others, it has direct applicability in the aquaculture sector, where disease and a shift away from antibiotic use continue to risk its sustainability and that of wild fish stocks.

Furthermore, our results introduce fever as an integrative response modulating both inflammation and proliferation phases of tissue repair, thus achieving efficient return to homeostasis. This was evidenced by fever-induced enhancements in restoration of barrier integrity; thereby reducing time required for healing of damaged tissue and possible secondary infections. Additionally, improved pathogen clearance is likely associated with low risk of disease transmission, instituting novel applications for infectious diseases management. More studies are still required to test these potentials. Nevertheless, my thesis provides insights helping us better understand the long-standing role of fever in the modulation of acute inflammation and the repercussions of inhibiting moderate fever in veterinary and human medicine.

6.6. Future directions

My findings revealed an essential role of temperature rise in inducing some of fever's immunomodulatory and tissue repair effects, whereas other metabolic and neuronal factors

are also postulated to be involved. This was apparent in both mechanical fever and static 26°C groups that demonstrated some parallels yet failed to fully recapitulate fever's benefits. Additionally, truncation of fever's thermal pattern inhibited some of these advantages. Still, mechanisms of temperature sensing and thermal regulation of various biological processes during fever remain poorly understood. Regulatory machinery during febrile responses is activated at the molecular level, which likely necessitates the detection of temperature changes. Notably, recognition of thermal alterations in ectotherms is critical to protect the host against damages generated by detrimental environmental temperatures [590]. This was further evident by the fine control of thermoregulatory responses in infected fish, where thermal preference is provoked following thermal perception [66,93].

Recent reports suggested significant contributions of transient receptor potential (TRP) family to thermoregulations. These receptors are recognized as thermal receptors that can sense a wide range of hot and cold temperatures where they are directly activated to stimulate a variety of downstream signalling pathways [591,592]. An increased expression of vanilloids type of TRP (TRPV1) was linked to upregulation of pro-inflammatory cytokines and PGE2 in POA [109]. TRPV was also found to regulate behavioural fever via enhancing PGE2-activated EP3 receptors [109]. Additional studies are needed to characterize the possible role of TRP receptors as a part of functional mechanisms that ectothermic and endothermic vertebrates utilize to regulate fever-associated modulatory impact upon immune responses and tissue healing. Likewise, characterizing potential metabolic and neuronal factors activated during febrile responses would provide a better

understanding of fever's biology. This can be attained by examining the effects of applying metabolic inhibitors such as beta blockers during febrile responses.

In this study, I highlighted some of the upregulated growth mediators during febrile response controlling re-epithelialization and granulation tissue formation. Tissue repair is a complex biological process that integrates an intricate network of cytokines and crosstalk between immune and connective tissue cells. Therefore, further experiments are required to identify detailed pathways involved in regulating various tissue repair events contributing to faster wound healing during fever. The improved bacterial clearance shown in fish exerting behavioural fever indicated enhancements of innate immune mechanisms. Despite the marked alterations in the kinetics of inflammatory responses exemplified in this thesis, additional investigations on other possible aspects of immunomodulation with regard to, for example, adaptive immune responses induced by fever are encouraged.

References

1. Kluger, M.J. Is Fever Beneficial? *Yale J Biol Med* **1986**, *59*, 89–95.
2. Duffell, E. Curative Power of Fever. *The Lancet* **2001**, *358*, 1276.
3. Evans, S.S.; Repasky, E.A.; Fisher, D.T. Fever and the Thermal Regulation of Immunity: The Immune System Feels the Heat. *Nat Rev Immunol* **2015**, *15*, 335–349.
4. Harden, L.M.; Kent, S.; Pittman, Q.J.; Roth, J. Fever and Sickness Behavior: Friend or Foe? *Brain Behav Immunol* **2015**, *50*, 322–333.
5. Graham, N.M.; Burrell, C.J.; Douglas, R.M.; Debelle, P.; Davies, L. Adverse Effects of Aspirin, Acetaminophen, and Ibuprofen on Immune Function, Viral Shedding, and Clinical Status in Rhinovirus-Infected Volunteers. *J Infect Dis* **1990**, *162*, 1277–1282.
6. Zellner, M.; Hergovics, N.; Roth, E.; Jilma, B.; Spittler, A.; Oehler, R. Human Monocyte Stimulation by Experimental Whole Body Hyperthermia. *Wien Klin Wochenschr* **2002**, *114*, 102–107.
7. Atkins, E.; Bodel, P. Clinical Fever: Its History, Manifestations and Pathogenesis. *Fed Proc* **1979**, *38*, 57–63.
8. Roth, J.; Blatteis, C.M. Mechanisms of Fever Production and Lysis: Lessons from Experimental LPS Fever. *Compr Physiol* **2014**, *4*, 1563–1604.
9. Netea, M.G.; Kullberg, B.J.; Van der Meer, J.W. Circulating Cytokines as Mediators of Fever. *Clin Infect Dis* **2000**, *31 Suppl 5*, S178-184.
10. Nakamura, K. Central Circuitries for Body Temperature Regulation and Fever. *Am J Physiol Regul Integr Comp Physiol* **2011**, *301*, R1207-1228.
11. Vaughn, L.K.; Bernheim, H.A.; Kluger, M.J. Fever in the Lizard Dipsosaurus Dorsalis. *Nature* **1974**, *252*, 473–474.
12. Reynolds, W.W.; Casterlin, M.E.; COVERT, J.B. Behavioural Fever in Teleost Fishes. *Nature* **1976**, *259*, 41–42.
13. Burns, G.; Ramos, A.; Muchlinski, A. Fever Response in North American Snakes. *J Hepatol* **1996**, *30*, 133–139.
14. Merchant, M.; Williams, S.; Trosclair, P.L.; Elsey, R.M.; Mills, K. Febrile Response to Infection in the American Alligator (Alligator Mississippiensis). *Comp Biochem Physiol A Mol Integr Physiol* **2007**, *148*, 921–925.
15. Kluger, M.J. Fever in the Frog Hyla Cinerea. *J Thermal Biol* **1977**, *2*, 79–81.
16. Cabanac, M.; Laberge, F. Fever in Goldfish Is Induced by Pyrogens but Not by Handling. *Physiol Behav* **1998**, *63*, 377–379.

17. Reynolds, W.W.; Covert, J.B.; Casterlin, M.E. Febrile Responses of Goldfish Carassius Auratus (L.)to Aeromonas Hydrophila and to Escherichia Coli Endotoxin. *J Fish Dis* **1978**, *1*, 271–273.

18. Rakus, K.; Ronsmans, M.; Vanderplasschen, A. Behavioral Fever in Ectothermic Vertebrates. *Dev Comp Immunol* **2017**, *66*, 84–91.

19. Krafts, K.P. Tissue Repair. *Organogenesis* **2010**, *6*, 225–233.

20. Eming, S.A.; Krieg, T.; Davidson, J.M. Inflammation in Wound Repair: Molecular and Cellular Mechanisms. *J Invest Dermatol* **2007**, *127*, 514–525.

21. Eming, S.A.; Martin, P.; Tomic-Canic, M. Wound Repair and Regeneration: Mechanisms, Signaling, and Translation. *Sci Transl Med* **2014**, *6*, 265sr6.

22. Rodrigues, M.; Kosaric, N.; Bonham, C.A.; Gurtner, G.C. Wound Healing: A Cellular Perspective. *Physiol Rev* **2019**, *99*, 665–706.

23. Kratz, G.; Lake, M.; Gidlund, M. Insulin like Growth Factor-1 and-2 and Their Role in the Re-Epithelialisation of Wounds; Interactions with Insulin like Growth Factor Binding Protein Type 1. *Scand J Plast Reconstr Surg Hand Surg Suppl* **1994**, *28*, 107–112.

24. Haase, I.; Evans, R.; Pofahl, R.; Watt, F.M. Regulation of Keratinocyte Shape, Migration and Wound Epithelialization by IGF-1-and EGF-Dependent Signalling Pathways. *J Cell Sci* **2003**, *116*, 3227–3238.

25. Tsuboi, R.; Shi, C.-M.; Sato, C.; Cox, G.N.; Ogawa, H. Co-Administration of Insulin-like Growth Factor (IGF)-I and IGF-Binding Protein-1 Stimulates Wound Healing in Animal Models. *J Invest Dermatol* **1995**, *104*, 199–203.

26. Lee, R.H.; Efron, D.; Tantry, U.; Barbul, A. Nitric Oxide in the Healing Wound: A Time-Course Study. *J Surg Res* **2001**, *101*, 104–108.

27. Bao, P.; Kodra, A.; Tomic-Canic, M.; Golinko, M.S.; Ehrlich, H.P.; Brem, H. The Role of Vascular Endothelial Growth Factor in Wound Healing. *J Surg Res* **2009**, *153*, 347–358.

28. Kluger, M.J. Survival Value of Fever. In *Contributions to Thermal Physiology*; Szelényi, Z., Székely, M., Eds.; Pergamon, 1981; pp. 133–141 ISBN 978-0-08-027354-9.

29. Velnar, T.; Bailey, T.; Smrkolj, V. The Wound Healing Process: An Overview of the Cellular and Molecular Mechanisms. *J Int Med Res* **2009**, *37*, 1528–1542.

30. Janis, J.E.; Harrison, B. Wound Healing: Part I. Basic Science. *Plast Reconstr Surg* **2016**, *138*, 9S.

31. Stitt, J.T. Fever versus Hyperthermia. *Fed Proc* **1979**, *38*, 39–43.

32. Beard, R.M.; Day, M.W. Fever and Hyperthermia: Learn to Beat the Heat. *Nursing2023* **2008**, *38*, 28.

33. Simon, H.B. Hyperthermia. *N Engl J Med* **1993**, *329*, 483–487.

34. Mackowiak, P.A. Concepts of Fever. *Arch Internal Med* **1998**, *158*, 1870–1881.

35. Yarwood, C.E. Heat of Respiration of Injured and Diseased Leaves. *Phytopathology* **1953**, *43*, 675–681.

36. Whitrow, M. Wagner-Jauregg and Fever Therapy. *Med Hist* **1990**, *34*, 294–310.

37. Muchlinski, A.E. The Energetic Cost of the Fever Response in Three Species of Ectothermic Vertebrates. *Comp Biochem Physiol A Comp Physiol* **1985**, *81*, 577–579.

38. Otti, O.; Gantenbein-Ritter, I.; Jacot, A.; Brinkhof, M.W.G. Immune Response Increases Predation Risk. *Evolution* **2012**, *66*, 732–739.

39. Aronoff, D.M.; Neilson, E.G. Antipyretics: Mechanisms of Action and Clinical Use in Fever Suppression. *Am J Med* **2001**, *111*, 304–315.

40. Kiekkas, P.; Konstantinou, E.; Psychogiou, K.-S.; Tsampoula, I.; Stefanopoulos, N.; Bakalis, N. Nursing Personnel's Attitudes towards Fever and Antipyresis of Adult Patients: Cross-Sectional Survey. *J Clin Nurs* **2014**, *23*, 2949–2957.

41. Liu, E.; Lewis, K.; Al-Saffar, H.; Krall, C.M.; Singh, A.; Kulchitsky, V.A.; Corrigan, J.J.; Simons, C.T.; Petersen, S.R.; Musteata, F.M.; et al. Naturally Occurring Hypothermia Is More Advantageous than Fever in Severe Forms of Lipopolysaccharide- and Escherichia Coli-Induced Systemic Inflammation. *Am J Physiol Regul Integr Comp Physiol* **2012**, *302*, R1372-1383.

42. Polderman, K.H. Induced Hypothermia and Fever Control for Prevention and Treatment of Neurological Injuries. *Lancet* **2008**, *371*, 1955–1969.

43. Kluger, M.J. Phylogeny of Fever. *Fed Proc* **1979**, *38*, 30–34.

44. Blatteis, C.M.; Sehic, E.; Li, S. Pyrogen Sensing and Signaling: Old Views and New Concepts. *Clin Infect Dis* **2000**, *31*, S168–S177.

45. O'Neill, L.A.J.; Golenbock, D.; Bowie, A.G. The History of Toll-like Receptors — Redefining Innate Immunity. *Nat Rev Immunol* **2013**, *13*, 453–460.

46. Mogensen, T.H. Pathogen Recognition and Inflammatory Signaling in Innate Immune Defenses. *Clin Microbiol Rev* **2009**, *22*, 240–273.

47. Dinarello, C.A. Cytokines as Endogenous Pyrogens. *J Infect Dis* **1999**, *179 Suppl 2*, S294-304.

48. Luheshi, G.; Rothwell, N. Cytokines and Fever. *IAA* **1996**, *109*, 301–307.

49. Zetterström, M.; Sundgren-Andersson, A.K.; Ostlund, P.; Bartfai, T. Delineation of the Proinflammatory Cytokine Cascade in Fever Induction. *Ann N Y Acad Sci* **1998**, *856*, 48–52.

50. Hamzic, N.; Tang, Y.; Eskilsson, A.; Kugelberg, U.; Ruud, J.; Jönsson, J.-I.; Blomqvist, A.; Nilsberth, C. Interleukin-6 Primarily Produced by Non-Hematopoietic Cells Mediates the Lipopolysaccharide-Induced Febrile Response. *Brain Behav Immun* **2013**, *33*, 123–130.

51. Chai, Z.; Gatti, S.; Toniatti, C.; Poli, V.; Bartfai, T. Interleukin (IL)-6 Gene Expression in the Central Nervous System Is Necessary for Fever Response to Lipopolysaccharide or IL-1 Beta: A Study on IL-6-Deficient Mice. *J Exp Med* **1996**, *183*, 311–316.

52. Kozak, W.; Kluger, M.J.; Soszynski, D.; Conn, C.A.; Rudolph, K.; Leon, L.R.; Zheng, H. IL-6 and IL-1 Beta in Fever. Studies Using Cytokine-Deficient (Knockout) Mice. *Ann N Y Acad Sci* **1998**, *856*, 33–47.

53. Banks, W.A. Blood-Brain Barrier Transport of Cytokines: A Mechanism for Neuropathology. *Curr Pharm Des* **2005**, *11*, 973–984.

54. Roth, J.; Harré, E.-M.; Rummel, C.; Gerstberger, R.; Hübschle, T. Signaling the Brain in Systemic Inflammation: Role of Sensory Circumventricular Organs. *Front Biosci* **2004**, *9*, 290–300.

55. Nadjar, A.; Tridon, V.; May, M.J.; Ghosh, S.; Dantzer, R.; Amédée, T.; Parnet, P. NFkappaB Activates in Vivo the Synthesis of Inducible Cox-2 in the Brain. *J Cereb Blood Flow Metab* **2005**, *25*, 1047–1059.

56. Rummel, C.; Voss, T.; Matsumura, K.; Korte, S.; Gerstberger, R.; Roth, J.; Hübschle, T. Nuclear STAT3 Translocation in Guinea Pig and Rat Brain Endothelium during Systemic Challenge with Lipopolysaccharide and Interleukin-6. *J Comp Neurol* **2005**, *491*, 1–14.

57. Rummel, C.; Sachot, C.; Poole, S.; Luheshi, G.N. Circulating Interleukin-6 Induces Fever through a STAT3-Linked Activation of COX-2 in the Brain. *Am J Physiol Regul Integr Comp Physiol* **2006**, *291*, R1316-1326.

58. Rivest, S. Molecular Insights on the Cerebral Innate Immune System. *Brain Behav Immun* **2003**, *17*, 13–19.

59. Crack, P.J.; Bray, P.J. Toll-like Receptors in the Brain and Their Potential Roles in Neuropathology. *Immunol Cell Biol* **2007**, *85*, 476–480.

60. Engström, L.; Ruud, J.; Eskilsson, A.; Larsson, A.; Mackerlova, L.; Kugelberg, U.; Qian, H.; Vasilache, A.M.; Larsson, P.; Engblom, D.; et al. Lipopolysaccharide-Induced Fever Depends on Prostaglandin E2 Production Specifically in Brain Endothelial Cells. *Endocrinology* **2012**, *153*, 4849–4861.

61. Milton, A.S.; Wendlandt, S. Effects on Body Temperature of Prostaglandins of the A, E and F Series on Injection into the Third Ventricle of Unanaesthetized Cats and Rabbits. *J Physiol* **1971**, *218*, 325–336.

62. Ivanov, A.I.; Romanovsky, A.A. Prostaglandin E2 as a Mediator of Fever: Synthesis and Catabolism. *Front Biosci* **2004**, *9*, 1977–1993.

63. Blatteis, C.M.; Li, S.; Li, Z.; Feleder, C.; Perlik, V. Cytokines, PGE2 and Endotoxic Fever: A Re-Assessment. *Prostaglandins Other Lipid Mediat* **2005**, *76*, 1–18.

64. Yamagata, K.; Matsumura, K.; Inoue, W.; Shiraki, T.; Suzuki, K.; Yasuda, S.; Sugiura, H.; Cao, C.; Watanabe, Y.; Kobayashi, S. Coexpression of Microsomal-Type Prostaglandin E Synthase with Cyclooxygenase-2 in Brain Endothelial Cells of Rats during Endotoxin-Induced Fever. *J Neurosci* **2001**, *21*, 2669–2677.

65. Steiner, A.A.; Rudaya, A.Y.; Robbins, J.R.; Dragic, A.S.; Langenbach, R.; Romanovsky, A.A. Expanding the Febrigenic Role of Cyclooxygenase-2 to the Previously Overlooked Responses. *Am J Physiol Regul Integr Comp Physiol* **2005**, *289*, R1253-1257.

66. Boltana, S.; Rey, S.; Roher, N.; Vargas, R.; Huerta, M.; Huntingford, F.A.; Goetz, F.W.; Moore, J.; Garcia-Valtanen, P.; Estepa, A. Behavioural Fever Is a Synergic Signal Amplifying the Innate Immune Response. *Proc Royal Soc B Biol Sci* **2013**, *280*, 20131381.

67. Sanhueza, N.; Fuentes, R.; Aguilar, A.; Carnicero, B.; Vega, K.; Muñoz, D.; Contreras, D.; Moreno, N.; Troncoso, E.; Mercado, L.; et al. Behavioural Fever Promotes an Inflammatory Reflex Circuit in Ectotherms. *Int J Mol Sci* **2021**, *22*, 8860.

68. Oka, T. Prostaglandin E2 as a Mediator of Fever: The Role of Prostaglandin E (EP) Receptors. *Front Biosci* **2004**, *9*, 3046–3057.

69. Lazarus, M.; Yoshida, K.; Coppari, R.; Bass, C.E.; Mochizuki, T.; Lowell, B.B.; Saper, C.B. EP3 Prostaglandin Receptors in the Median Preoptic Nucleus Are Critical for Fever Responses. *Nat Neurosci* **2007**, *10*, 1131–1133.

70. Nakamura, K.; Matsumura, K.; Kaneko, T.; Kobayashi, S.; Katoh, H.; Negishi, M. The Rostral Raphe Pallidus Nucleus Mediates Pyrogenic Transmission from the Preoptic Area. *J Neurosci* **2002**, *22*, 4600–4610.

71. Saper, C.B.; Romanovsky, A.A.; Scammell, T.E. Neural Circuitry Engaged by Prostaglandins during the Sickness Syndrome. *Nat Neurosci* **2012**, *15*, 1088–1095.

72. Navarro, V.P.; Iyomasa, M.M.; Leite-Panissi, C.R.A.; Almeida, M.C.; Branco, L.G.S. New Role of the Trigeminal Nerve as a Neuronal Pathway Signaling Brain in Acute Periodontitis: Participation of Local Prostaglandins. *Pflugers Arch* **2006**, *453*, 73–82.

73. Romanovsky, A.A. Thermoregulatory Manifestations of Systemic Inflammation: Lessons from Vagotomy. *Auton Neurosci* **2000**, *85*, 39–48.

74. Gagge, A.P.; Stolwijk, J.A.J.; Hardy, J.D. Comfort and Thermal Sensations and Associated Physiological Responses at Various Ambient Temperatures. *Environ Res* **1967**, *1*, 1–20.

75. Craig, A.D.; Bushnell, M.C.; Zhang, E.T.; Blomqvist, A. A Thalamic Nucleus Specific for Pain and Temperature Sensation. *Nature* **1994**, *372*, 770–773.

76. Flouris, A.D. Functional Architecture of Behavioural Thermoregulation. *Eur J Appl Physiol* **2011**, *111*, 1–8.

77. Kappel, M.; Stadeager, C.; Tvede, N.; Galbo, H.; Pedersen, B.K. Effects of in Vivo Hyperthermia on Natural Killer Cell Activity, in Vitro Proliferative Responses and Blood Mononuclear Cell Subpopulations. *Clin Exp Immunol* **1991**, *84*, 175–180.

78. Lee, C.; Zhong, L.; Mace, T.A.; Repasky, E.A. Elevation in Body Temperature to Fever Range Enhances and Prolongs Subsequent Responsiveness of Macrophages to Endotoxin Challenge. *PLoS One* **2012**, *7*, e30077.

79. Munck, A.; Guyre, P.M.; Holbrook, N.J. Physiological Functions of Glucocorticoids in Stress and Their Relation to Pharmacological Actions. *Endocr Rev* **1984**, *5*, 25–44.

80. Chrousos, G.P. The Stress Response and Immune Function: Clinical Implications. The 1999 Novera H. Spector Lecture. *Ann N Y Acad Sci* **2000**, *917*, 38–67.

81. Elenkov, I.J.; Chrousos, G.P. Stress Hormones, Proinflammatory and Antiinflammatory Cytokines, and Autoimmunity. *Ann N Y Acad Sci* **2002**, *966*, 290–303.

82. Rohleder, N. Acute and Chronic Stress Induced Changes in Sensitivity of Peripheral Inflammatory Pathways to the Signals of Multiple Stress Systems --2011 Curt Richter Award Winner. *Psychoneuroendocrinology* **2012**, *37*, 307–316.

83. Saleh, E.; Moody, M.A.; Walter, E.B. Effect of Antipyretic Analgesics on Immune Responses to Vaccination. *Hum Vaccin Immunother* **2016**, *12*, 2391–2402.

84. Koufoglou, E.; Kourlaba, G.; Michos, A. Effect of Prophylactic Administration of Antipyretics on the Immune Response to Pneumococcal Conjugate Vaccines in Children: A Systematic Review. *Pneumonia* **2021**, *13*, 7.

85. Abdel Shaheed, C.; Beardsley, J.; Day, R.O.; McLachlan, A.J. Immunomodulatory Effects of Pharmaceutical Opioids and Antipyretic Analgesics: Mechanisms and Relevance to Infection. *Br J Clin Pharmacol* **2022**, *88*, 3114–3131.

86. Sherman, E.; Baldwin, L.; Fernandez, G.; Deurell, E. Fever and Thermal Tolerance in the Toad Bufo Marinus. *J Thermal Biol* **1991**, *16*, 297–301.

87. Bicego, K.C.; Steiner, A.A.; Antunes-Rodrigues, J.; Branco, L.G.S. Indomethacin Impairs LPS-Induced Behavioral Fever in Toads. *J Appl Physiol (1985)* **2002**, *93*, 512–516.

88. Richards-Zawacki, C.L. Thermoregulatory Behaviour Affects Prevalence of Chytrid Fungal Infection in a Wild Population of Panamanian Golden Frogs. *Proc Royal Soc B Biol Sci* **2010**, *277*, 519–528.

89. Hallman, G.M.; Ortega, C.E.; Towner, M.C.; Muchlinski, A.E. Effect of Bacterial Pyrogen on Three Lizard Species. *Comp Biochem Physiol A Comp Physiol* **1990**, *96*, 383–386.

90. Merchant, M.; Fleury, L.; Rutherford, R.; Paulissen, M. Effects of Bacterial Lipopolysaccharide on Thermoregulation in Green Anole Lizards (Anolis Carolinensis). *Vet Immunol Immunopathol* **2008**, *125*, 176–181.

91. Conover, A.E.; Cook, E.G.; Boronow, K.E.; Muñoz, M.M. Effects of Ectoparasitism on Behavioral Thermoregulation in the Tropical Lizards Anolis Cybotes (Squamata: Dactyloidae) and Anolis Armouri (Squamata: Dactyloidae). *Breviora* **2015**, *545*, 1–13.

92. Covert, J.B.; Reynolds, W.W. Survival Value of Fever in Fish. *Nature* **1977**, *267*, 43–45.

93. Rey, S.; Moiche, V.; Boltaña, S.; Teles, M.; MacKenzie, S. Behavioural Fever in Zebrafish Larvae. *Dev Comp Immunol* **2017**, *67*, 287–292.

94. Gräns, A.; Rosengren, M.; Niklasson, L.; Axelsson, M. Behavioural Fever Boosts the Inflammatory Response in Rainbow Trout Oncorhynchus Mykiss. *J Fish Biol* **2012**, *81*, 1111–1117.

95. Starks, P.T.; Blackie, C.A.; Seeley, T.D. Fever in Honeybee Colonies. *Naturwissenschaften* **2000**, *87*, 229–231.

96. Simone-Finstrom, M.; Foo, B.; Tarpy, D.R.; Starks, P.T. Impact of Food Availability, Pathogen Exposure, and Genetic Diversity on Thermoregulation in Honey Bees (Apis Mellifera). *J Insect Behav* **2014**, *27*, 527–539.

97. Satinoff, E.; McEwen, G.N.; Williams, B.A. Behavioral Fever in Newborn Rabbits. *Science* **1976**, *193*, 1139–1140.

98. Marx, J.; Hilbig, R.; Rahmann, H. Endotoxin and Prostaglandin E1 Fail to Induce Fever in a Teleost Fish. *Comp Biochem Physiol A Physiol* **1984**, *77*, 483–487.

99. Laburn, H.P.; Mitchell, D.; Kenedi, E.; Louw, G.N. Pyrogens Fail to Produce Fever in a Cordylid Lizard. *Am J Physiol* **1981**, *241*, R198-202.

100. Zurovsky, Y.; Mitchell, D.; Laburn, H. Pyrogens Fail to Produce Fever in the Leopard Tortoise Geochelone Pardalis. *Comp Biochem Physiol A Comp Physiol* **1987**, *87*, 467–469.

101. Zurovsky, Y.; Brain, T.; Laburn, H.; Mitchell, D. Pyrogens Fail to Produce Fever in the Snakes Psammophis Phillipsii and Lamprophis Fuliginosus. *Comp Biochem Physiol A Comp Physiol* **1987**, *87*, 911–914.

102. Bicego, K.C.; Barros, R.C.H.; Branco, L.G.S. Physiology of Temperature Regulation: Comparative Aspects. *Comp Biochem Physiol A Mol Integr Physiol* **2007**, *147*, 616–639.

103. Casterlin, M.E.; Reynolds, W.W. Behavioral Fever in Anuran Amphibian Larvae. *Life Sci* **1977**, *20*, 593–596.

104. Monagas, W.R.; Gatten, R.E. Behavioural Fever in the Turtles Terrapene Carolina and Chrysemys Picta. *J Thermal Biol* **1983**, *8*, 285–288.

105. Ortega, C.E.; Stranc, D.S.; Casal, M.P.; Hallman, G.M.; Muchlinski, A.E. A Positive Fever Response in Agama Agama and Sceloporus Orcutti (Reptilia: Agamidae and Iguanidae). *J Comp Physiol B* **1991**, *161*, 377–381.

106. Reynolds, W.W. Fever and Antipyresis in the Bluegill Sunfish, Lepomis Macrochirus. *Comp Biochem Physiol C Comp Pharmacol* **1977**, *57*, 165–167.

107. Bernheim, H.A.; Kluger, M.J. Fever and Antipyresis in the Lizard Dipsosaurus Dorsalis. *Am J Physiol* **1976**, *231*, 198–203.

108. Murphy, P.J.; St-Hilaire, S.; Corn, P.S. Temperature, Hydric Environment, and Prior Pathogen Exposure Alter the Experimental Severity of Chytridiomycosis in Boreal Toads. *Dis Aquat Organ* **2011**, *95*, 31–42.

109. Boltana, S.; Sanhueza, N.; Donoso, A.; Aguilar, A.; Crespo, D.; Vergara, D.; Arriagada, G.; Morales-Lange, B.; Mercado, L.; Rey, S.; et al. The Expression of TRPV Channels, Prostaglandin E2 and pro-Inflammatory Cytokines during Behavioural Fever in Fish. *Brain Behav Immun* **2018**, *71*, 169–181.

110. do Amaral, J.P.S.; Marvin, G.A.; Hutchison, V.H. The Influence of Bacterial Lipopolysaccharide on the Thermoregulation of the Box Turtle Terrapene Carolina. *Physiol Biochem Zool* **2002**, *75*, 273–282.

111. Bernheim, H.A.; Kluger, M.J. Endogenous Pyrogen-like Substance Produced by Reptiles. *J Physiol* **1977**, *267*, 659–666.

112. Myhre, K.; Cabanac, M.; Myhre, G. Fever and Behavioural Temperature Regulation in the Frog Rana Esculenta. *Acta Physiol Scand* **1977**, *101*, 219–229.

113. Cabanac, M. Fever in the Leech,Nephelopsis Obscura (Annelida). *J Comp Physiol B* **1989**, *159*, 281–285.

114. Cabanac, M.; Hammel, T.; Hardy, J.D. Tiliqua Scincoides: Temperature-Sensitive Units in Lizard Brain. *Science* **1967**, *158*, 1050–1051.

115. Nelson, D.O.; Prosser, C.L. Effect of Preoptic Lesions on Behavioral Thermoregulation of Green Sunfish, Lepomis Cyanellus, and of Goldfish, Carassius Auratus. *J Comp Physiol* **1979**, *129*, 193–197.

116. Prosser, C.L.; Nelson, D.O. The Role of Nervous Systems in Temperature Adaptation of Poikilotherms. *Annu Rev Physiol* **1981**, *43*, 281–300.

117. Bicego, K.C.; Branco, L.G.S. Discrete Electrolytic Lesion of the Preoptic Area Prevents LPS-Induced Behavioral Fever in Toads. *J Exp Biol* **2002**, *205*, 3513–3518.

118. Hutchison, V.H.; Erskine, D.J. Thermal Selection and Prostaglandin E1 Fever in the Salamander Necturus Maculosus. *Herpetologica* **1981**, 195–198.

119. Bernheim, H.A.; Kluger, M.J. Fever: Effect of Drug-Induced Antipyresis on Survival. *Science* **1976**, *193*, 237–239.

120. Haesemeyer, M. Thermoregulation in Fish. *Mol Cell Endocrinol* **2020**, *518*, 110986.

121. Dickson, K.A.; Graham, J.B. Evolution and Consequences of Endothermy in Fishes. *Physiol Biochem Zool* **2004**, *77*, 998–1018.

122. Block, B.A.; Finnerty, J.R.; Stewart, A.F.R.; Kidd, J. Evolution of Endothermy in Fish: Mapping Physiological Traits on a Molecular Phylogeny. *Science* **1993**, *260*, 210–214.

123. Golovanov, V.K. The Ecological and Evolutionary Aspects of Thermoregulation Behavior on Fish. *J. Ichthyol.* **2006**, *46*, S180–S187.

124. Tattersall, G.J.; Leite, C.A.C.; Sanders, C.E.; Cadena, V.; Andrade, D.V.; Abe, A.S.; Milsom, W.K. Seasonal Reproductive Endothermy in Tegu Lizards. *Sci Adv* **2016**, *2*, e1500951.

125. Hutchison, V.H.; Dowling, H.G.; Vinegar, A. Thermoregulation in a Brooding Female Indian Python, Python Molurus Bivittatus. *Science* **1966**, *151*, 694–696.

126. Block, B.A.; Finnerty, J.R. Endothermy in Fishes: A Phylogenetic Analysis of Constraints, Predispositions, and Selection Pressures. *Environ Biol Fish* **1994**, *40*, 283–302.

127. Bernal, D.; Donley, J.M.; Shadwick, R.E.; Syme, D.A. Mammal-like Muscles Power Swimming in a Cold-Water Shark. *Nature* **2005**, *437*, 1349–1352.

128. Bernal, D.; Dickson, K.A.; Shadwick, R.E.; Graham, J.B. Review: Analysis of the Evolutionary Convergence for High Performance Swimming in Lamnid Sharks and Tunas. *Comp Biochem Physiol A Mol Integr Physiol* **2001**, *129*, 695–726.

129. Carey, F.G.; Teal, J.M.; Kanwisher, J.W. The Visceral Temperatures of Mackerel Sharks (Lamnidae). *Physiol Zool* **1981**, *54*, 334–344.

130. Carey, F.G.; Teal, J.M. Heat Conservation in Tuna Fish Muscle. *Proc Natl Acad Sci U S A* **1966**, *56*, 1464–1469.

131. Block, B.A. Chapter 11 - Endothermy in Fish: Thermogenesis, Ecology and Evolution. In *Biochemistry and Molecular Biology of Fishes*; Hochachka, P.W., Mommsen, T.P., Eds.; Phylogenetic and biochemical perspectives; Elsevier, 1991; Vol. 1, pp. 269–311.

132. Block, B.A. Structure of the Brain and Eye Heater Tissue in Marlins, Sailfish, and Spearfishes. *J Morphol* **1986**, *190*, 169–189.

133. Tullis, A.; Block, B.A.; Sidell, B.D. Activities of Key Metabolic Enzymes in the Heater Organs of Scombroid Fishes. *J Exp Biol* **1991**, *161*, 383–403.

134. Carey, F.G. A Brain Heater in the Swordfish. *Science* **1982**, *216*, 1327–1329.

135. Brill, R.W. Selective Advantages Conferred by the High Performance Physiology of Tunas, Billfishes, and Dolphin Fish. *Comparative Biochemistry and Physiology Part A: Physiology* **1996**, *113*, 3–15.

136. Holland, K.N.; Brill, R.W.; Chang, R.K.C.; Sibert, J.R.; Fournier, D.A. Physiological and Behavioural Thermoregulation in Bigeye Tuna (Thunnus Obesus). *Nature* **1992**, *358*, 410–412.

137. Wegner, N.C.; Snodgrass, O.E.; Dewar, H.; Hyde, J.R. Whole-Body Endothermy in a Mesopelagic Fish, the Opah, Lampris Guttatus. *Science* **2015**, *348*, 786–789.

138. Rakus, K.; Ronsmans, M.; Forlenza, M.; Boutier, M.; Piazzon, M.C.; Jazowiecka-Rakus, J.; Gatherer, D.; Athanasiadis, A.; Farnir, F.; Davison, A.J.; et al. Conserved Fever Pathways across Vertebrates: A Herpesvirus Expressed Decoy TNF-α Receptor Delays Behavioral Fever in Fish. *Cell Host Microbe* **2017**, *21*, 244–253.

139. Kurosawa, S.; Kobune, F.; Okuyama, K.; Sugiura, A. Effects of Antipyretics in Rinderpest Virus Infection in Rabbits. *J Infect Dis* **1987**, *155*, 991–997.

140. Kluger, M.J.; Vaughn, L.K. Fever and Survival in Rabbits Infected with Pasteurella Multocida. *J Physiol* **1978**, *282*, 243–251.

141. Vaughn, L.K.; Veale, W.L.; Cooper, K.E. Antipyresis: Its Effect on Mortality Rate of Bacterially Infected Rabbits. *Brain Res Bull* **1980**, *5*, 69–73.

142. Miert, A. s. j. p. a. m. V.; Duin, C.Th.V.; Busser, F. j. m.; Periea, N.; Ingh, T.S.G. a. M.V.D.; Neys-Backers, M.H.H.D. The Effect of Flurbiprofen, a Potent Non-Steroidal Anti-Inflammatory Agent, upon Trypanosoma Vivax Infection in Goats. *J Vet Pharmacol Ther* **1978**, *1*, 69–76.

143. Bryant, R.E.; Hood, A.F.; Hood, C.E.; Koenig, M.G. Factors Affecting Mortality of Gram-Negative Rod Bacteremia. *Arch Internal Med* **1971**, *127*, 120–128.

144. Weinstein, M.P.; Iannini, P.B.; Stratton, C.W.; Eickhoff, T.C. Spontaneous Bacterial Peritonitis. A Review of 28 Cases with Emphasis on Improved Survival and Factors Influencing Prognosis. *Am J Med* **1978**, *64*, 592–598.

145. Henriksen, D.P.; Havshøj, U.; Pedersen, P.B.; Laursen, C.B.; Jensen, H.K.; Brabrand, M.; Lassen, A.T. Hospitalized Acute Patients with Fever and Severe Infection Have Lower Mortality than Patients with Hypo- or Normothermia: A Follow-up Study. *QJM* **2016**, *109*, 473–479.

146. Sundén-Cullberg, J.; Rylance, R.; Svefors, J.; Norrby-Teglund, A.; Björk, J.; Inghammar, M. Fever in the Emergency Department Predicts Survival of Patients With Severe Sepsis and Septic Shock Admitted to the ICU. *Crit Care Med* **2017**, *45*, 591–599.

147. Wu, C.; Chen, X.; Cai, Y.; Xia, J.; Zhou, X.; Xu, S.; Huang, H.; Zhang, L.; Zhou, X.; Du, C.; et al. Risk Factors Associated With Acute Respiratory Distress Syndrome and Death in Patients With Coronavirus Disease 2019 Pneumonia in Wuhan, China. *JAMA Intern Med* **2020**, *180*, 934–943.

148. Earn, D.J.D.; Andrews, P.W.; Bolker, B.M. Population-Level Effects of Suppressing Fever. *Proc Biol Sci* **2014**, *281*, 20132570.

149. Ryan, M.; Levy, M.M. Clinical Review: Fever in Intensive Care Unit Patients. *Crit Care* **2003**, *7*, 221–225.

150. Schulman, C.I.; Namias, N.; Doherty, J.; Manning, R.J.; Li, P.; Elhaddad, A.; Lasko, D.; Amortegui, J.; Dy, C.J.; Dlugasch, L. The Effect of Antipyretic Therapy upon Outcomes in Critically Ill Patients: A Randomized, Prospective Study. *Surg Infect* **2005**, *6*, 369–375.

151. Brandts, C.H.; Ndjavé, M.; Graninger, W.; Kremsner, P.G. Effect of Paracetamol on Parasite Clearance Time in Plasmodium Falciparum Malaria. *Lancet* **1997**, *350*, 704–709.

152. Doran, T.F.; De Angelis, C.; Baumgardner, R.A.; Mellits, E.D. Acetaminophen: More Harm than Good for Chickenpox? *J Pediatr* **1989**, *114*, 1045–1048.

153. Voiriot, G.; Philippot, Q.; Elabbadi, A.; Elbim, C.; Chalumeau, M.; Fartoukh, M. Risks Related to the Use of Non-Steroidal Anti-Inflammatory Drugs in Community-Acquired Pneumonia in Adult and Pediatric Patients. *J Clin Med* **2019**, *8*, E786.

154. Kushimoto, S.; Gando, S.; Saitoh, D.; Mayumi, T.; Ogura, H.; Fujishima, S.; Araki, T.; Ikeda, H.; Kotani, J.; Miki, Y.; et al. The Impact of Body Temperature Abnormalities on the Disease Severity and Outcome in Patients with Severe Sepsis: An Analysis from a Multicenter, Prospective Survey of Severe Sepsis. *Crit Care* **2013**, *17*, R271.

155. Young, P.J.; Saxena, M.; Beasley, R.; Bellomo, R.; Bailey, M.; Pilcher, D.; Finfer, S.; Harrison, D.; Myburgh, J.; Rowan, K. Early Peak Temperature and Mortality in Critically Ill Patients with or without Infection. *Intensive Care Med* **2012**, *38*, 437–444.

156. DuPONT, H.L.; Spink, W.W. Infections Due to Gram-Negative Organisms: An Analysis of 860 Patients with Bacteremia at the University of Minnesota Medical Center, 1958–1966. *Medicine* **1969**, *48*, 307–332.

157. Schortgen, F.; Clabault, K.; Katsahian, S.; Devaquet, J.; Mercat, A.; Deye, N.; Dellamonica, J.; Bouadma, L.; Cook, F.; Beji, O.; et al. Fever Control Using External Cooling in Septic Shock: A Randomized Controlled Trial. *Am J Respir Crit Care Med* **2012**, *185*, 1088–1095.

158. Niven, D.J.; Stelfox, H.T.; Laupland, K.B. Antipyretic Therapy in Febrile Critically Ill Adults: A Systematic Review and Meta-Analysis. *J Crit Care* **2013**, *28*, 303–310.

159. Kluger, M.J.; Ringler, D.H.; Anver, M.R. Fever and Survival. *Science* **1975**, *188*, 166–168.

160. Green, M.H.; Vermeulen, C.W. Fever and the Control of Gram-Negative Bacteria. *Res Microbiol* **1994**, *145*, 269–272.

161. Lwoff, A. From Protozoa to Bacteria and Viruses. Fifty Years with Microbes (André Lwoff). *Annu Rev Microbiol* **1971**, *25*, 1–26.

162. Robert, V.A.; Casadevall, A. Vertebrate Endothermy Restricts Most Fungi as Potential Pathogens. *J Infect Dis* **2009**, *200*, 1623–1626.

163. Avunje, S.; Kim, W.-S.; Oh, M.-J.; Choi, I.; Jung, S.-J. Temperature-Dependent Viral Replication and Antiviral Apoptotic Response in Viral Haemorrhagic Septicaemia Virus (VHSV)-Infected Olive Flounder (Paralichthys Olivaceus). *Fish Shellfish Immunol* **2012**, *32*, 1162–1170.

164. Osawa, E.; Muschel, L.H. STUDIES RELATING TO THE SERUM RESISTANCE OF CERTAIN GRAM-NEGATIVE BACTERIA. *J Exp Med* **1964**, *119*, 41–51.

165. Casadevall, A. Thermal Restriction as an Antimicrobial Function of Fever. *PLoS Pathog* **2016**, *12*, e1005577.

166. Jiang, Q.; Cross, A.S.; Singh, I.S.; Chen, T.T.; Viscardi, R.M.; Hasday, J.D. Febrile Core Temperature Is Essential for Optimal Host Defense in Bacterial Peritonitis. *Infect Immun* **2000**, *68*, 1265–1270.

167. Soehnlein, O.; Lindbom, L. Phagocyte Partnership during the Onset and Resolution of Inflammation. *Nat Rev Immunol* **2010**, *10*, 427–439.

168. Rice, P.; Martin, E.; He, J.-R.; Frank, M.; DeTolla, L.; Hester, L.; O'Neill, T.; Manka, C.; Benjamin, I.; Nagarsekar, A. Febrile-Range Hyperthermia Augments Neutrophil

Accumulation and Enhances Lung Injury in Experimental Gram-Negative Bacterial Pneumonia. *J Immunol* **2005**, *174*, 3676–3685.

169. Hasday, J.D.; Garrison, A.; Singh, I.S.; Standiford, T.; Ellis, G.S.; Rao, S.; He, J.-R.; Rice, P.; Frank, M.; Goldblum, S.E.; et al. Febrile-Range Hyperthermia Augments Pulmonary Neutrophil Recruitment and Amplifies Pulmonary Oxygen Toxicity. *Am J Pathol* **2003**, *162*, 2005–2017.

170. Capitano, M.L.; Nemeth, M.J.; Mace, T.A.; Salisbury-Ruf, C.; Segal, B.H.; McCarthy, P.L.; Repasky, E.A. Elevating Body Temperature Enhances Hematopoiesis and Neutrophil Recovery after Total Body Irradiation in an IL-1-, IL-17-, and G-CSF-Dependent Manner. *Blood* **2012**, *120*, 2600–2609.

171. Singh, I.S.; Gupta, A.; Nagarsekar, A.; Cooper, Z.; Manka, C.; Hester, L.; Benjamin, I.J.; He, J.-R.; Hasday, J.D. Heat Shock Co-Activates Interleukin-8 Transcription. *Am J Respir Cell Mol Biol* **2008**, *39*, 235–242.

172. Tulapurkar, M.E.; Almutairy, E.A.; Shah, N.G.; He, J.; Puche, A.C.; Shapiro, P.; Singh, I.S.; Hasday, J.D. Febrile-Range Hyperthermia Modifies Endothelial and Neutrophilic Functions to Promote Extravasation. *Am J Respir Cell Mol Biol* **2012**, *46*, 807–814.

173. Keitelman, I.A.; Sabbione, F.; Shiromizu, C.M.; Giai, C.; Fuentes, F.; Rosso, D.; Ledo, C.; Miglio Rodriguez, M.; Guzman, M.; Geffner, J.R.; et al. Short-Term Fever-Range Hyperthermia Accelerates NETosis and Reduces Pro-Inflammatory Cytokine Secretion by Human Neutrophils. *Front Immunol* **2019**, *10*, 2374.

174. Khan, I.U.; Brooks, G.; Guo, N.N.; Chen, J.; Guo, F. Fever-Range Hyperthermia Promotes CGAS-STING Pathway and Synergizes DMXAA-Induced Antiviral Immunity. *Int J Hyperthermia* **2021**, *38*, 30–37.

175. Knippertz, I.; Stein, M.F.; Dörrie, J.; Schaft, N.; Müller, I.; Deinzer, A.; Steinkasserer, A.; Nettelbeck, D.M. Mild Hyperthermia Enhances Human Monocyte-Derived Dendritic Cell Functions and Offers Potential for Applications in Vaccination Strategies. *Int J Hyperthermia* **2011**, *27*, 591–603.

176. Postic, B.; DeAngelis, C.; Breinig, M.K.; Ho, M. Effect of Temperature on the Induction of Interferons by Endotoxin and Virus. *J Bacteriol* **1966**, *91*, 1277–1281.

177. Hatzfeld-Charbonnier, A.S.; Lasek, A.; Castera, L.; Gosset, P.; Velu, T.; Formstecher, P.; Mortier, L.; Marchetti, P. Influence of Heat Stress on Human Monocyte-Derived Dendritic Cell Functions with Immunotherapeutic Potential for Antitumor Vaccines. *J Leukoc Biol* **2007**, *81*, 1179–1187.

178. Peng, J.C.; Hyde, C.; Pai, S.; O'Sullivan, B.J.; Nielsen, L.K.; Thomas, R. Monocyte-Derived DC Primed with TLR Agonists Secrete IL-12p70 in a CD40-Dependent Manner under Hyperthermic Conditions. *J Immunother* **2006**, *29*, 606–615.

179. Ostberg, J.R.; Kaplan, K.C.; Repasky, E.A. Induction of Stress Proteins in a Panel of Mouse Tissues by Fever-Range Whole Body Hyperthermia. *Int J Hyperthermia* **2002**, *18*, 552–562.

180. Ulvmar, M.H.; Werth, K.; Braun, A.; Kelay, P.; Hub, E.; Eller, K.; Chan, L.; Lucas, B.; Novitzky-Basso, I.; Nakamura, K.; et al. The Atypical Chemokine Receptor CCRL1 Shapes Functional CCL21 Gradients in Lymph Nodes. *Nat Immunol* **2014**, *15*, 623–630.

181. Schumann, K.; Lämmermann, T.; Bruckner, M.; Legler, D.F.; Polleux, J.; Spatz, J.P.; Schuler, G.; Förster, R.; Lutz, M.B.; Sorokin, L.; et al. Immobilized Chemokine Fields and Soluble Chemokine Gradients Cooperatively Shape Migration Patterns of Dendritic Cells. *Immunity* **2010**, *32*, 703–713.

182. Amend, D.F. Prevention and Control of Viral Diseases of Salmonids. *J Fish Res Bd Can* **1976**, *33*, 1059–1066.

183. Plumb, J.A. Effects of Temperature on Mortality of Fingerling Channel Catfish (Ictalurus Punctatus) Experimentally Infected with Channel Catfish Virus. *J Fish Res Bd Can* **1973**, *30*, 568–570.

184. Boltana, S.; Aguilar, A.; Sanhueza, N.; Donoso, A.; Mercado, L.; Imarai, M.; Mackenzie, S. Behavioral Fever Drives Epigenetic Modulation of the Immune Response in Fish. *Front Immunol* **2018**, *9*, 1241.

185. Brem, H.; Tomic-Canic, M. Cellular and Molecular Basis of Wound Healing in Diabetes. *J Clin Invest* **2007**, *117*, 1219–1222.

186. Wynn, T.A.; Vannella, K.M. Macrophages in Tissue Repair, Regeneration, and Fibrosis. *Immunity* **2016**, *44*, 450–462.

187. Broughton, G.I.; Janis, J.E.; Attinger, C.E. Wound Healing: An Overview. *Plast Reconstr Surg* **2006**, *117*, 1e.

188. DiPietro, L.A. Angiogenesis and Wound Repair: When Enough Is Enough. *J Leukoc Biol* **2016**, *100*, 979–984.

189. Holzer-Geissler, J.C.J.; Schwingenschuh, S.; Zacharias, M.; Einsiedler, J.; Kainz, S.; Reisenegger, P.; Holecek, C.; Hofmann, E.; Wolff-Winiski, B.; Fahrngruber, H.; et al. The Impact of Prolonged Inflammation on Wound Healing. *Biomedicines* **2022**, *10*, 856.

190. Zhao, R.; Liang, H.; Clarke, E.; Jackson, C.; Xue, M. Inflammation in Chronic Wounds. *Int J Mol Sci* **2016**, *17*, 2085.

191. Jung, K.; Covington, S.; Sen, C.K.; Januszyk, M.; Kirsner, R.S.; Gurtner, G.C.; Shah, N.H. Rapid Identification of Slow Healing Wounds. *Wound Repair Regen* **2016**, *24*, 181–188.

192. Guo, S. al; DiPietro, L.A. Factors Affecting Wound Healing. *J Dental Res* **2010**, *89*, 219–229.

193. Jensen, L.B.; Wahli, T.; McGurk, C.; Eriksen, T.B.; Obach, A.; Waagbø, R.; Handler, A.; Tafalla, C. Effect of Temperature and Diet on Wound Healing in Atlantic Salmon (Salmo Salar L.). *Fish Physiol Biochem* **2015**, *41*, 1527–1543.

194. Cai, W.; Kumar, S.; Navaneethaiyer, U.; Caballero-Solares, A.; Carvalho, L.A.; Whyte, S.K.; Purcell, S.L.; Gagne, N.; Hori, T.S.; Allen, M.; et al. Transcriptome Analysis of Atlantic Salmon (Salmo Salar) Skin in Response to Sea Lice and Infectious Salmon Anemia Virus Co-Infection Under Different Experimental Functional Diets. *Front Immunol* **2022**, *12*.

195. Roh, J.S.; Sohn, D.H. Damage-Associated Molecular Patterns in Inflammatory Diseases. *Immune Netw* **2018**, *18*, e27.

196. Medzhitov, R.; Janeway Jr, C. Innate Immunity. *N Engl J Med* **2000**, *343*, 338–344.

197. Abdallah, F.; Mijouin, L.; Pichon, C. Skin Immune Landscape: Inside and Outside the Organism. *Mediators Inflamm* **2017**, *2017*, 5095293.

198. Shi, Y.; Evans, J.E.; Rock, K.L. Molecular Identification of a Danger Signal That Alerts the Immune System to Dying Cells. *Nature* **2003**, *425*, 516–521.

199. Weathington, N.M.; van Houwelingen, A.H.; Noerager, B.D.; Jackson, P.L.; Kraneveld, A.D.; Galin, F.S.; Folkerts, G.; Nijkamp, F.P.; Blalock, J.E. A Novel Peptide CXCR Ligand Derived from Extracellular Matrix Degradation during Airway Inflammation. *Nat Med* **2006**, *12*, 317–323.

200. Van der Vliet, A.; Janssen-Heininger, Y.M.W. Hydrogen Peroxide as a Damage Signal in Tissue Injury and Inflammation: Murderer, Mediator, or Messenger? *J Cell Biochem* **2014**, *115*, 427–435.

201. Yamaguchi, A.; Botta, E.; Holinstat, M. Eicosanoids in Inflammation in the Blood and the Vessel. *Front Pharmacol* **2022**, *13*.

202. Bianchi, M.E. DAMPs, PAMPs and Alarmins: All We Need to Know about Danger. *J Leukoc Biol* **2007**, *81*, 1–5.

203. Li, D.; Wu, M. Pattern Recognition Receptors in Health and Diseases. *Sig Transduct Target Ther* **2021**, *6*, 1–24.

204. Kumar, H.; Kawai, T.; Akira, S. Toll-like Receptors and Innate Immunity. *Biochem Biophys Res Commun* **2009**, *388*, 621–625.

205. Kaisho, T.; Akira, S. Toll-like Receptor Function and Signaling. *J Allergy Clin Immunol* **2006**, *117*, 979–987.

206. Lansdown, A.B.G. Calcium: A Potential Central Regulator in Wound Healing in the Skin. *Wound Repair Regen* **2002**, *10*, 271–285.

207. Dinarello, C.A. Historical Review of Cytokines. *Eur J Immunol* **2007**, *37*, S34–S45.

208. Barrientos, S.; Stojadinovic, O.; Golinko, M.S.; Brem, H.; Tomic-Canic, M. Growth Factors and Cytokines in Wound Healing. *Wound Repair Regen* **2008**, *16*, 585–601.

209. Soliman, A.M.; Barreda, D.R. Acute Inflammation in Tissue Healing. *Int J Mol Sci* **2023**, *24*, 641.

210. Gethin, G. Understanding the Inflammatory Process in Wound Healing. *Br J Community Nurs* **2012**, *17*, S17–S22.

211. Weissenbach, M.; Clahsen, T.; Weber, C.; Spitzer, D.; Wirth, D.; Vestweber, D.; Heinrich, P.C.; Schaper, F. Interleukin-6 Is a Direct Mediator of T Cell Migration. *Eur J Immunol* **2004**, *34*, 2895–2906.

212. Wright, H.L.; Cross, A.L.; Edwards, S.W.; Moots, R.J. Effects of IL-6 and IL-6 Blockade on Neutrophil Function in Vitro and in Vivo. *Rheumatology (Oxford)* **2014**, *53*, 1321–1331.

213. Lin, Z.-Q.; Kondo, T.; Ishida, Y.; Takayasu, T.; Mukaida, N. Essential Involvement of IL-6 in the Skin Wound-Healing Process as Evidenced by Delayed Wound Healing in IL-6-Deficient Mice. *J Leukoc Biol* **2003**, *73*, 713–721.

214. Martins-Green, M.; Petreaca, M.; Wang, L. Chemokines and Their Receptors Are Key Players in the Orchestra That Regulates Wound Healing. *Adv Wound Care (New Rochelle)* **2013**, *2*, 327–347.

215. Frangogiannis, N.G. Chemokines in Ischemia and Reperfusion. *Thromb Haemost* **2007**, *97*, 738–747.

216. Miller, M.D.; Krangel, M.S. The Human Cytokine I-309 Is a Monocyte Chemoattractant. *Proc Natl Acad Sci U S A* **1992**, *89*, 2950–2954.

217. D'Ambrosio, D.; Iellem, A.; Bonecchi, R.; Mazzeo, D.; Sozzani, S.; Mantovani, A.; Sinigaglia, F. Cutting Edge: Selective Up-Regulation of Chemokine Receptors CCR4 and CCR8 upon Activation of Polarized Human Type 2 Th Cells. *J Immunol* **1998**, *161*, 5111–5115.

218. Wang, J.; Knaut, H. Chemokine Signaling in Development and Disease. *Development* **2014**, *141*, 4199–4205.

219. Jin, T.; Xu, X.; Hereld, D. Chemotaxis, Chemokine Receptors and Human Disease. *Cytokine* **2008**, *44*, 1–8.

220. Gerard, C.; Rollins, B.J. Chemokines and Disease. *Nat Immunol* **2001**, *2*, 108–115.

221. Proudfoot, A.E.I.; Handel, T.M.; Johnson, Z.; Lau, E.K.; LiWang, P.; Clark-Lewis, I.; Borlat, F.; Wells, T.N.C.; Kosco-Vilbois, M.H. Glycosaminoglycan Binding and Oligomerization Are Essential for the in Vivo Activity of Certain Chemokines. *Proc Natl Acad Sci U S A* **2003**, *100*, 1885–1890.

222. Olson, T.S.; Ley, K. Chemokines and Chemokine Receptors in Leukocyte Trafficking. *Am J Physiol Regul Integr Comp Physiol* **2002**, *283*, R7-28.

223. Russo, R.C.; Garcia, C.C.; Teixeira, M.M.; Amaral, F.A. The CXCL8/IL-8 Chemokine Family and Its Receptors in Inflammatory Diseases. *Expert Rev Clin Immunol* **2014**, *10*, 593–619.

224. Ridiandries, A.; Tan, J.T.M.; Bursill, C.A. The Role of Chemokines in Wound Healing. *Int J Mol Sci* **2018**, *19*, 3217.

225. Zaja-Milatovic, S.; Richmond, A. CXC Chemokines and Their Receptors: A Case for a Significant Biological Role in Cutaneous Wound Healing. *Histol Histopathol* **2008**, *23*, 1399–1407.

226. Abkowitz, J.L.; Robinson, A.E.; Kale, S.; Long, M.W.; Chen, J. Mobilization of Hematopoietic Stem Cells during Homeostasis and after Cytokine Exposure. *Blood* **2003**, *102*, 1249–1253.

227. Zarbock, A.; Ley, K.; McEver, R.P.; Hidalgo, A. Leukocyte Ligands for Endothelial Selectins: Specialized Glycoconjugates That Mediate Rolling and Signaling under Flow. *Blood* **2011**, *118*, 6743–6751.

228. Ley, K.; Laudanna, C.; Cybulsky, M.I.; Nourshargh, S. Getting to the Site of Inflammation: The Leukocyte Adhesion Cascade Updated. *Nat Rev Immunol* **2007**, *7*, 678–689.

229. Phillipson, M.; Heit, B.; Colarusso, P.; Liu, L.; Ballantyne, C.M.; Kubes, P. Intraluminal Crawling of Neutrophils to Emigration Sites: A Molecularly Distinct Process from Adhesion in the Recruitment Cascade. *J Exp Med* **2006**, *203*, 2569–2575.

230. Wang, S.; Voisin, M.-B.; Larbi, K.Y.; Dangerfield, J.; Scheiermann, C.; Tran, M.; Maxwell, P.H.; Sorokin, L.; Nourshargh, S. Venular Basement Membranes Contain Specific Matrix Protein Low Expression Regions That Act as Exit Points for Emigrating Neutrophils. *J Exp Med* **2006**, *203*, 1519–1532.

231. de Oliveira, S.; Rosowski, E.E.; Huttenlocher, A. Neutrophil Migration in Infection and Wound Repair: Going Forward in Reverse. *Nat Rev Immunol* **2016**, *16*, 378–391.

232. Gillitzer, R.; Goebeler, M. Chemokines in Cutaneous Wound Healing. *J Leukoc Biol* **2001**, *69*, 513–521.

233. Su, Y.; Richmond, A. Chemokine Regulation of Neutrophil Infiltration of Skin Wounds. *Adv Wound Care (New Rochelle)* **2015**, *4*, 631–640.

234. Lämmermann, T. In the Eye of the Neutrophil Swarm-Navigation Signals That Bring Neutrophils Together in Inflamed and Infected Tissues. *J Leukoc Biol* **2016**, *100*, 55–63.

235. Kolaczkowska, E.; Kubes, P. Neutrophil Recruitment and Function in Health and Inflammation. *Nat Rev Immunol* **2013**, *13*, 159–175.

236. Ellis, S.; Lin, E.J.; Tartar, D. Immunology of Wound Healing. *Curr Dermatol Rep* **2018**, *7*, 350–358.

237. Wilgus, T.A.; Roy, S.; McDaniel, J.C. Neutrophils and Wound Repair: Positive Actions and Negative Reactions. *Adv Wound Care (New Rochelle)* **2013**, *2*, 379–388.

238. Moor, A.N.; Vachon, D.J.; Gould, L.J. Proteolytic Activity in Wound Fluids and Tissues Derived from Chronic Venous Leg Ulcers. *Wound Repair Regen* **2009**, *17*, 832–839.

239. Degradation of the Epidermal-Dermal Junction by Proteolytic Enzymes from Human Skin and Human Polymorphonuclear Leukocytes. *J Exp Med* **1984**, *160*, 1027–1042.

240. Pirilä, E.; Korpi, J.T.; Korkiamäki, T.; Jahkola, T.; Gutierrez-Fernandez, A.; Lopez-Otin, C.; Saarialho-Kere, U.; Salo, T.; Sorsa, T. Collagenase-2 (MMP-8) and Matrilysin-2 (MMP-26) Expression in Human Wounds of Different Etiologies. *Wound Repair Regen* **2007**, *15*, 47–57.

241. Butin-Israeli, V.; Bui, T.M.; Wiesolek, H.L.; Mascarenhas, L.; Lee, J.J.; Mehl, L.C.; Knutson, K.R.; Adam, S.A.; Goldman, R.D.; Beyder, A.; et al. Neutrophil-Induced Genomic Instability Impedes Resolution of Inflammation and Wound Healing. *J Clin Invest* **2019**, *129*, 712–726.

242. Borregaard, N.; Cowland, J.B. Granules of the Human Neutrophilic Polymorphonuclear Leukocyte. *Blood* **1997**, *89*, 3503–3521.

243. Reeves, E.P.; Lu, H.; Jacobs, H.L.; Messina, C.G.M.; Bolsover, S.; Gabella, G.; Potma, E.O.; Warley, A.; Roes, J.; Segal, A.W. Killing Activity of Neutrophils Is Mediated through Activation of Proteases by K+ Flux. *Nature* **2002**, *416*, 291–297.

244. Segel, G.B.; Halterman, M.W.; Lichtman, M.A. The Paradox of the Neutrophil's Role in Tissue Injury. *J Leukoc Biol* **2011**, *89*, 359–372.

245. Ma, Y.; Yabluchanskiy, A.; Iyer, R.P.; Cannon, P.L.; Flynn, E.R.; Jung, M.; Henry, J.; Cates, C.A.; Deleon-Pennell, K.Y.; Lindsey, M.L. Temporal Neutrophil Polarization Following Myocardial Infarction. *Cardiovasc Res* **2016**, *110*, 51–61.

246. Elliott, M.R.; Koster, K.M.; Murphy, P.S. Efferocytosis Signaling in the Regulation of Macrophage Inflammatory Responses. *J Immunol* **2017**, *198*, 1387–1394.

247. Devalaraja, R.M.; Nanney, L.B.; Du, J.; Qian, Q.; Yu, Y.; Devalaraja, M.N.; Richmond, A. Delayed Wound Healing in CXCR2 Knockout Mice. *J Invest Dermatol* **2000**, *115*, 234–244.

248. Dovi, J.V.; He, L.-K.; DiPietro, L.A. Accelerated Wound Closure in Neutrophil-Depleted Mice. *J Leukoc Biol* **2003**, *73*, 448–455.

249. Nishio, N.; Okawa, Y.; Sakurai, H.; Isobe, K. Neutrophil Depletion Delays Wound Repair in Aged Mice. *Age (Dordr)* **2008**, *30*, 11–19.

250. Tseng, C.W.; Liu, G.Y. Expanding Roles of Neutrophils in Aging Hosts. *Curr Opin Immunol* **2014**, *29*, 43–48.

251. Minutti, C.M.; Knipper, J.A.; Allen, J.E.; Zaiss, D.M.W. Tissue-Specific Contribution of Macrophages to Wound Healing. *Semin Cell Dev Biol* **2017**, *61*, 3–11.

252. Yanez, D.A.; Lacher, R.K.; Vidyarthi, A.; Colegio, O.R. The Role of Macrophages in Skin Homeostasis. *Pflugers Arch Eur J Physiol* **2017**, *469*, 455–463.

253. Xuan, W.; Qu, Q.; Zheng, B.; Xiong, S.; Fan, G.-H. The Chemotaxis of M1 and M2 Macrophages Is Regulated by Different Chemokines. *J Leukoc Biol* **2015**, *97*, 61–69.

254. DiPietro, L.A.; Polverini, P.J.; Rahbe, S.M.; Kovacs, E.J. Modulation of JE/MCP-1 Expression in Dermal Wound Repair. *Am J Pathol* **1995**, *146*, 868–875.

255. Novak, M.L.; Koh, T.J. Macrophage Phenotypes during Tissue Repair. *J Leukoc Biol* **2013**, *93*, 875–881.

256. Murray, P.J.; Allen, J.E.; Biswas, S.K.; Fisher, E.A.; Gilroy, D.W.; Goerdt, S.; Gordon, S.; Hamilton, J.A.; Ivashkiv, L.B.; Lawrence, T.; et al. Macrophage Activation and Polarization: Nomenclature and Experimental Guidelines. *Immunity* **2014**, *41*, 14–20.

257. Stout, R.D.; Jiang, C.; Matta, B.; Tietzel, I.; Watkins, S.K.; Suttles, J. Macrophages Sequentially Change Their Functional Phenotype in Response to Changes in Microenvironmental Influences. *J Immunol* **2005**, *175*, 342–349.

258. Slauch, J.M. How Does the Oxidative Burst of Macrophages Kill Bacteria? Still an Open Question. *Mol Microbiol* **2011**, *80*, 580–583.

259. Gordon, S. Alternative Activation of Macrophages. *Nat Rev Immunol* **2003**, *3*, 23–35.

260. Kim, S.Y.; Nair, M.G. Macrophages in Wound Healing: Activation and Plasticity. *Immunol Cell Biol* **2019**, *97*, 258–267.

261. Goren, I.; Allmann, N.; Yogev, N.; Schürmann, C.; Linke, A.; Holdener, M.; Waisman, A.; Pfeilschifter, J.; Frank, S. A Transgenic Mouse Model of Inducible Macrophage Depletion: Effects of Diphtheria Toxin-Driven Lysozyme M-Specific Cell Lineage Ablation on Wound Inflammatory, Angiogenic, and Contractive Processes. *Am J Pathol* **2009**, *175*, 132–147.

262. Mirza, R.; DiPietro, L.A.; Koh, T.J. Selective and Specific Macrophage Ablation Is Detrimental to Wound Healing in Mice. *Am J Pathol* **2009**, *175*, 2454–2462.

263. Hart, P.H.; Jones, C.A.; Finlay-Jones, J.J. Monocytes Cultured in Cytokine-Defined Environments Differ from Freshly Isolated Monocytes in Their Responses to IL-4 and IL-10. *J Leukoc Biol* **1995**, *57*, 909–918.

264. D'Autréaux, B.; Toledano, M.B. ROS as Signalling Molecules: Mechanisms That Generate Specificity in ROS Homeostasis. *Nat Rev Mol Cell Biol* **2007**, *8*, 813–824.

265. Lennicke, C.; Cochemé, H.M. Redox Metabolism: ROS as Specific Molecular Regulators of Cell Signaling and Function. *Mol Cell* **2021**, *81*, 3691–3707.

266. Lambeth, J.D. NOX Enzymes and the Biology of Reactive Oxygen. *Nat Rev Immunol* **2004**, *4*, 181–189.

267. Babior, B.M.; Lambeth, J.D.; Nauseef, W. The Neutrophil NADPH Oxidase. *Arch Biochem Biophys* **2002**, *397*, 342–344.

268. Donkó, Á.; Péterfi, Z.; Sum, A.; Leto, T.; Geiszt, M. Dual Oxidases. *Philos Trans R Soc Lond B Biol Sci* **2005**, *360*, 2301–2308.

269. Forteza, R.; Salathe, M.; Miot, F.; Forteza, R.; Conner, G.E. Regulated Hydrogen Peroxide Production by Duox in Human Airway Epithelial Cells. *Am J Respir Cell Mol Biol* **2005**, *32*, 462–469.

270. Förstermann, U.; Sessa, W.C. Nitric Oxide Synthases: Regulation and Function. *Eur Heart J* **2012**, *33*, 829–837.

271. Hodgkinson, J.W.; Grayfer, L.; Belosevic, M. Biology of Bony Fish Macrophages. *Biology (Basel)* **2015**, *4*, 881–906.

272. Radi, R. Peroxynitrite, a Stealthy Biological Oxidant. *J Biol Chem* **2013**, *288*, 26464–26472.

273. Wink, D.A.; Hines, H.B.; Cheng, R.Y.; Switzer, C.H.; Flores-Santana, W.; Vitek, M.P.; Ridnour, L.A.; Colton, C.A. Nitric Oxide and Redox Mechanisms in the Immune Response. *J Leukoc Biol* **2011**, *89*, 873–891.

274. De Groote, M.A.; Fang, F.C. NO Inhibitions: Antimicrobial Properties of Nitric Oxide. *Clin Infect Dis* **1995**, *21 Suppl 2*, S162-165.

275. Graham, D.B.; Jasso, G.J.; Mok, A.; Goel, G.; Ng, A.C.Y.; Kolde, R.; Varma, M.; Doench, J.G.; Root, D.E.; Clish, C.B.; et al. Nitric Oxide Engages an Anti-Inflammatory Feedback Loop Mediated by Peroxiredoxin 5 in Phagocytes. *Cell Rep* **2018**, *24*, 838–850.

276. Kubes, P.; Suzuki, M.; Granger, D.N. Nitric Oxide: An Endogenous Modulator of Leukocyte Adhesion. *Proc Natl Acad Sci U S A* **1991**, *88*, 4651–4655.

277. Henrotin, Y.E.; Zheng, S.X.; Deby, G.P.; Labasse, A.H.; Crielaard, J.M.; Reginster, J.Y. Nitric Oxide Downregulates Interleukin 1beta (IL-1beta) Stimulated IL-6, IL-8, and Prostaglandin E2 Production by Human Chondrocytes. *J Rheumatol* **1998**, *25*, 1595–1601.

278. Mao, K.; Chen, S.; Chen, M.; Ma, Y.; Wang, Y.; Huang, B.; He, Z.; Zeng, Y.; Hu, Y.; Sun, S.; et al. Nitric Oxide Suppresses NLRP3 Inflammasome Activation and Protects against LPS-Induced Septic Shock. *Cell Res* **2013**, *23*, 201–212.

279. Witte, M.B.; Barbul, A. Role of Nitric Oxide in Wound Repair. *Am J Surg* **2002**, *183*, 406–412.

280. Headland, S.E.; Norling, L.V. The Resolution of Inflammation: Principles and Challenges. *Seminar Immunol* **2015**, *27*, 149–160.

281. Fullerton, J.N.; Gilroy, D.W. Resolution of Inflammation: A New Therapeutic Frontier. *Nat Rev Drug Discov* **2016**, *15*, 551–567.

282. Bratton, D.L.; Henson, P.M. Neutrophil Clearance: When the Party Is over, Clean-up Begins. *Trends Immunol* **2011**, *32*, 350–357.

283. Jun, J.-I.; Kim, K.-H.; Lau, L.F. The Matricellular Protein CCN1 Mediates Neutrophil Efferocytosis in Cutaneous Wound Healing. *Nat Commun* **2015**, *6*, 7386.

284. Ji, J.; Fan, J. Neutrophil in Reverse Migration: Role in Sepsis. *Front Immunol* **2021**, *12*.

285. Chen, W.Y.J.; Rogers, A.A. Recent Insights into the Causes of Chronic Leg Ulceration in Venous Diseases and Implications on Other Types of Chronic Wounds. *Wound Repair Regen* **2007**, *15*, 434–449.

286. Zhao, H.; Li, W.; Lu, Z.; Sheng, Z.; Yao, Y. The Growing Spectrum of Anti-Inflammatory Interleukins and Their Potential Roles in the Development of Sepsis. *J Interferon Cytokine Res* **2015**, *35*, 242–251.

287. Arango Duque, G.; Descoteaux, A. Macrophage Cytokines: Involvement in Immunity and Infectious Diseases. *Front Immunol* **2014**, *5*.

288. Demidova-Rice, T.N.; Hamblin, M.R.; Herman, I.M. Acute and Impaired Wound Healing: Pathophysiology and Current Methods for Drug Delivery, Part 1: Normal and Chronic Wounds: Biology, Causes, and Approaches to Care. *Adv Skin Wound Care* **2012**, *25*, 304–314.

289. Diegelmann, R.F.; Evans, M.C. Wound Healing: An Overview of Acute, Fibrotic and Delayed Healing. *Front Biosci* **2004**, *9*, 283–289.

290. Mast, B.A.; Schultz, G.S. Interactions of Cytokines, Growth Factors, and Proteases in Acute and Chronic Wounds. *Wound Repair Regen* **1996**, *4*, 411–420.

291. Kandhwal, M.; Behl, T.; Singh, S.; Sharma, N.; Arora, S.; Bhatia, S.; Al-Harrasi, A.; Sachdeva, M.; Bungau, S. Role of Matrix Metalloproteinase in Wound Healing. *Am J Transl Res* **2022**, *14*, 4391–4405.

292. Pedersen, M.E.; Vuong, T.T.; Rønning, S.B.; Kolset, S.O. Matrix Metalloproteinases in Fish Biology and Matrix Turnover. *Matrix Biol* **2015**, *44–46*, 86–93.

293. Barrick, B.; Campbell, E.J.; Owen, C.A. Leukocyte Proteinases in Wound Healing: Roles in Physiologic and Pathologic Processes. *Wound Repair Regen* **1999**, *7*, 410–422.

294. Saarialho-Kere, U.K. Patterns of Matrix Metalloproteinase and TIMP Expression in Chronic Ulcers. *Arch Dermatol Res* **1998**, *290 Suppl*, S47-54.

295. Soehnlein, O.; Steffens, S.; Hidalgo, A.; Weber, C. Neutrophils as Protagonists and Targets in Chronic Inflammation. *Nat Rev Immunol* **2017**, *17*, 248–261.

296. Thamm, O.C.; Koenen, P.; Bader, N.; Schneider, A.; Wutzler, S.; Neugebauer, E.A.; Spanholtz, T.A. Acute and Chronic Wound Fluids Influence Keratinocyte Function Differently. *Int Wound J* **2015**, *12*, 143–149.

297. Stojadinovic, O.; Pastar, I.; Vukelic, S.; Mahoney, M.G.; Brennan, D.; Krzyzanowska, A.; Golinko, M.; Brem, H.; Tomic-Canic, M. Deregulation of Keratinocyte Differentiation and Activation: A Hallmark of Venous Ulcers. *J Cell Mol Med* **2008**, *12*, 2675–2690.

298. Cha, J.; Kwak, T.; Butmarc, J.; Kim, T.-A.; Yufit, T.; Carson, P.; Kim, S.-J.; Falanga, V. Fibroblasts from Non-Healing Human Chronic Wounds Show Decreased Expression of Big-H3, a TGF-β Inducible Protein. *J Dermatol Sci* **2008**, *50*, 15–23.

299. Clark, R.A.; Lanigan, J.M.; DellaPelle, P.; Manseau, E.; Dvorak, H.F.; Colvin, R.B. Fibronectin and Fibrin Provide a Provisional Matrix for Epidermal Cell Migration during Wound Reepithelialization. *J Invest Dermatol* **1982**, *79*, 264–269.

300. Donaldson, D.J.; Mahan, J.T. Fibrinogen and Fibronectin as Substrates for Epidermal Cell Migration during Wound Closure. *J Cell Sci* **1983**, *62*, 117–127.

301. Baum, C.L.; Arpey, C.J. Normal Cutaneous Wound Healing: Clinical Correlation with Cellular and Molecular Events. *Dermatol Surg* **2005**, *31*, 674–686.

302. Rohani, M.G.; Parks, W.C. Matrix Remodeling by MMPs during Wound Repair. *Matrix Biol* **2015**, *44–46*, 113–121.

303. Rousselle, P.; Braye, F.; Dayan, G. Re-Epithelialization of Adult Skin Wounds: Cellular Mechanisms and Therapeutic Strategies. *Adv Drug Deliv Rev* **2019**, *146*, 344–365.

304. Santoro, M.M.; Gaudino, G. Cellular and Molecular Facets of Keratinocyte Reepithelization during Wound Healing. *Exp Cell Res* **2005**, *304*, 274–286.

305. Werner, S.; Krieg, T.; Smola, H. Keratinocyte-Fibroblast Interactions in Wound Healing. *J Invest Dermatol* **2007**, *127*, 998–1008.

306. Pastar, I.; Stojadinovic, O.; Yin, N.C.; Ramirez, H.; Nusbaum, A.G.; Sawaya, A.; Patel, S.B.; Khalid, L.; Isseroff, R.R.; Tomic-Canic, M. Epithelialization in Wound Healing: A Comprehensive Review. *Adv Wound Care* **2014**, *3*, 445–464.

307. Kaltalioglu, K.; Coskun-Cevher, S. A Bioactive Molecule in a Complex Wound Healing Process: Platelet-Derived Growth Factor. *Int J Dermatol* **2015**, *54*, 972–977.

308. Xu, J.; Lamouille, S.; Derynck, R. TGF-β-Induced Epithelial to Mesenchymal Transition. *Cell Res* **2009**, *19*, 156–172.

309. Li, J.; Chen, J.; Kirsner, R. Pathophysiology of Acute Wound Healing. *Clin Dermatol* **2007**, *25*, 9–18.

310. Xue, M.; Jackson, C.J. Extracellular Matrix Reorganization During Wound Healing and Its Impact on Abnormal Scarring. *Adv Wound Care (New Rochelle)* **2015**, *4*, 119–136.

311. Mathew-Steiner, S.S.; Roy, S.; Sen, C.K. Collagen in Wound Healing. *Bioengineering (Basel)* **2021**, *8*, 63.

312. Wilkinson, H.N.; Hardman, M.J. Wound Healing: Cellular Mechanisms and Pathological Outcomes. *Open Biol 10*, 200223.

313. Driskell, R.R.; Lichtenberger, B.M.; Hoste, E.; Kretzschmar, K.; Simons, B.D.; Charalambous, M.; Ferron, S.R.; Herault, Y.; Pavlovic, G.; Ferguson-Smith, A.C.; et al. Distinct Fibroblast Lineages Determine Dermal Architecture in Skin Development and Repair. *Nature* **2013**, *504*, 277–281.

314. Singhal, P.K.; Sassi, S.; Lan, L.; Au, P.; Halvorsen, S.C.; Fukumura, D.; Jain, R.K.; Seed, B. Mouse Embryonic Fibroblasts Exhibit Extensive Developmental and Phenotypic Diversity. *PNAS* **2016**, *113*, 122–127.

315. Phan, S.H. Biology of Fibroblasts and Myofibroblasts. *Proc Am Thorac Soc* **2008**, *5*, 334–337.

316. Fries, K.M.; Blieden, T.; Looney, R.J.; Sempowski, G.D.; Silvera, M.R.; Willis, R.A.; Phipps, R.P. Evidence of Fibroblast Heterogeneity and the Role of Fibroblast Subpopulations in Fibrosis. *Clin Immunol Immunopathol* **1994**, *72*, 283–292.

317. Gurtner, G.C.; Werner, S.; Barrandon, Y.; Longaker, M.T. Wound Repair and Regeneration. *Nature* **2008**, *453*, 314–321.

318. Eilken, H.M.; Adams, R.H. Dynamics of Endothelial Cell Behavior in Sprouting Angiogenesis. *Curr Opin Cell Biol* **2010**, *22*, 617–625.

319. Tonnesen, M.G.; Feng, X.; Clark, R.A.F. Angiogenesis in Wound Healing. *J Investig Dermatol Symp Proc* **2000**, *5*, 40–46.

320. Gerhardt, H.; Golding, M.; Fruttiger, M.; Ruhrberg, C.; Lundkvist, A.; Abramsson, A.; Jeltsch, M.; Mitchell, C.; Alitalo, K.; Shima, D.; et al. VEGF Guides Angiogenic Sprouting Utilizing Endothelial Tip Cell Filopodia. *J Cell Biol* **2003**, *161*, 1163–1177.

321. Covassin, L.D.; Villefranc, J.A.; Kacergis, M.C.; Weinstein, B.M.; Lawson, N.D. Distinct Genetic Interactions between Multiple Vegf Receptors Are Required for

Development of Different Blood Vessel Types in Zebrafish. *Proc Natl Acad Sci* **2006**, *103*, 6554–6559.

322. Ruhrberg, C.; Gerhardt, H.; Golding, M.; Watson, R.; Ioannidou, S.; Fujisawa, H.; Betsholtz, C.; Shima, D.T. Spatially Restricted Patterning Cues Provided by Heparin-Binding VEGF-A Control Blood Vessel Branching Morphogenesis. *Genes Dev.* **2002**, *16*, 2684–2698.

323. Siekmann, A.F.; Lawson, N.D. Notch Signalling and the Regulation of Angiogenesis. *Cell Adhes Migr* **2007**, *1*, 104–105.

324. Govinden, R.; Bhoola, K.D. Genealogy, Expression, and Cellular Function of Transforming Growth Factor-Beta. *Pharmacol Ther* **2003**, *98*, 257–265.

325. Haddad, G.; Hanington, P.C.; Wilson, E.C.; Grayfer, L.; Belosevic, M. Molecular and Functional Characterization of Goldfish (Carassius Auratus L.) Transforming Growth Factor Beta. *Dev Comp Immunol* **2008**, *32*, 654–663.

326. Chang, Z.; Kishimoto, Y.; Hasan, A.; Welham, N.V. TGF-B3 Modulates the Inflammatory Environment and Reduces Scar Formation Following Vocal Fold Mucosal Injury in Rats. *Dis Model Mech* **2014**, *7*, 83–91.

327. Levine, J.H.; Moses, H.L.; Gold, L.I.; Nanney, L.B. Spatial and Temporal Patterns of Immunoreactive Transforming Growth Factor Beta 1, Beta 2, and Beta 3 during Excisional Wound Repair. *Am J Pathol* **1993**, *143*, 368–380.

328. Lichtman, M.K.; Otero-Vinas, M.; Falanga, V. Transforming Growth Factor Beta (TGF-β) Isoforms in Wound Healing and Fibrosis. *Wound Repair Regen* **2016**, *24*, 215–222.

329. Kiritsi, D.; Nyström, A. The Role of TGFβ in Wound Healing Pathologies. *Mech Ageing Dev* **2018**, *172*, 51–58.

330. Kiwanuka, E.; Junker, J.; Eriksson, E. Harnessing Growth Factors to Influence Wound Healing. *Clin Plast Surg* **2012**, *39*, 239–248.

331. Annes, J.P.; Munger, J.S.; Rifkin, D.B. Making Sense of Latent TGFbeta Activation. *J Cell Sci* **2003**, *116*, 217–224.

332. Li, M.O.; Wan, Y.Y.; Sanjabi, S.; Robertson, A.-K.L.; Flavell, R.A. Transforming Growth Factor-Beta Regulation of Immune Responses. *Annu Rev Immunol* **2006**, *24*, 99–146.

333. Reibman, J.; Meixler, S.; Lee, T.C.; Gold, L.I.; Cronstein, B.N.; Haines, K.A.; Kolasinski, S.L.; Weissmann, G. Transforming Growth Factor Beta 1, a Potent Chemoattractant for Human Neutrophils, Bypasses Classic Signal-Transduction Pathways. *Proc Natl Acad Sci U S A* **1991**, *88*, 6805–6809.

334. Wei, H.; Yin, L.; Feng, S.; Wang, X.; Yang, K.; Zhang, A.; Zhou, H. Dual-Parallel Inhibition of IL-10 and TGF-B1 Controls LPS-Induced Inflammatory Response via NF-KB Signaling in Grass Carp Monocytes/Macrophages. *Fish Shellfish Immunol* **2015**, *44*, 445–452.

335. Yang, M.; Wang, X.; Chen, D.; Wang, Y.; Zhang, A.; Zhou, H. TGF-B1 Exerts Opposing Effects on Grass Carp Leukocytes: Implication in Teleost Immunity, Receptor Signaling and Potential Self-Regulatory Mechanisms. *PLoS One* **2012**, *7*, e35011.

336. Puolakkainen, P.A.; Reed, M.J.; Gombotz, W.R.; Twardzik, D.R.; Abrass, I.B.; Sage, H.E. Acceleration of Wound Healing in Aged Rats by Topical Application of Transforming Growth Factor-Beta(1). *Wound Repair Regen* **1995**, *3*, 330–339.

337. Werner, S.; Grose, R. Regulation of Wound Healing by Growth Factors and Cytokines. *Physiol Rev* **2003**, *83*, 835–870.

338. Mustoe, T.A.; Pierce, G.F.; Thomason, A.; Gramates, P.; Sporn, M.B.; Deuel, T.F. Accelerated Healing of Incisional Wounds in Rats Induced by Transforming Growth Factor-β. *Science* **1987**, *237*, 1333–1336.

339. Nugent, M.A.; Iozzo, R.V. Fibroblast Growth Factor-2. *Int J Biochem Cell Biol* **2000**, *32*, 115–120.

340. Robson, M.C. The Role of Growth Factors in the Healing of Chronic Wounds. *Wound Repair Regen* **1997**, *5*, 12–17.

341. Ohura, T.; Nakajo, T.; Moriguchi, T.; Oka, H.; Tachi, M.; Ohura Jr., N.; Nogami, R.; Murayama, S. Clinical Efficacy of Basic Fibroblast Growth Factor on Pressure Ulcers: Case-Control Pairing Study Using a New Evaluation Method. *Wound Repair Regen* **2011**, *19*, 542–551.

342. Hayashida, K.; Akita, S. Quality of Pediatric Second-Degree Burn Wound Scars Following the Application of Basic Fibroblast Growth Factor: Results of a Randomized, Controlled Pilot Study. *Ostomy Wound Manage* **2012**, *58*, 32.

343. Kan, M.; Wang, F.; Xu, J.; Crabb, J.W.; Hou, J.; McKeehan, W.L. An Essential Heparin-Binding Domain in the Fibroblast Growth Factor Receptor Kinase. *Science* **1993**, *259*, 1918–1921.

344. Bikfalvi, A.; Klein, S.; Pintucci, G.; Rifkin, D.B. Biological Roles of Fibroblast Growth Factor-2*. *Endocr Rev* **1997**, *18*, 26–45.

345. Horowitz, A.; Simons, M. Regulation of Syndecan-4 Phosphorylation in Vivo *. *J Biol Chem* **1998**, *273*, 10914–10918.

346. Sogabe, Y.; Abe, M.; Yokoyama, Y.; Ishikawa, O. Basic Fibroblast Growth Factor Stimulates Human Keratinocyte Motility by Rac Activation. *Wound Repair Regen* **2006**, *14*, 457–462.

347. Sasaki, T. The Effects of Basic Fibroblast Growth Factor and Doxorubicin on Cultured Human Skin Fibroblasts: Relevance to Wound Healing. *J Dermatol* **1992**, *19*, 664–666.

348. Nanney, L.B. Epidermal and Dermal Effects of Epidermal Growth Factor during Wound Repair. *J Invest Dermatol* **1990**, *94*, 624–629.

349. Brown, G.L.; Nanney, L.B.; Griffen, J.; Cramer, A.B.; Yancey, J.M.; Curtsinger, L.J.; Holtzin, L.; Schultz, G.S.; Jurkiewicz, M.J.; Lynch, J.B. Enhancement of Wound Healing by Topical Treatment with Epidermal Growth Factor. *N Engl J Med* **1989**, *321*, 76–79.

350. Tsang, M.W.; Wong, W.K.R.; Hung, C.S.; Lai, K.-M.; Tang, W.; Cheung, E.Y.N.; Kam, G.; Leung, L.; Chan, C.W.; Chu, C.M.; et al. Human Epidermal Growth Factor Enhances Healing of Diabetic Foot Ulcers. *Diabetes Care* **2003**, *26*, 1856–1861.

351. Fernández-Montequín, J.I.; Valenzuela-Silva, C.M.; Díaz, O.G.; Savigne, W.; Sancho-Soutelo, N.; Rivero-Fernández, F.; Sánchez-Penton, P.; Morejón-Vega, L.; Artaza-Sanz, H.; García-Herrera, A.; et al. Intra-Lesional Injections of Recombinant Human Epidermal Growth Factor Promote Granulation and Healing in Advanced Diabetic Foot Ulcers: Multicenter, Randomised, Placebo-Controlled, Double-Blind Study. *Int Wound J* **2009**, *6*, 432–443.

352. Oda, K.; Matsuoka, Y.; Funahashi, A.; Kitano, H. A Comprehensive Pathway Map of Epidermal Growth Factor Receptor Signaling. *Mol Syst Biol* **2005**, *1*, 2005.0010.

353. Yamakawa, S.; Hayashida, K. Advances in Surgical Applications of Growth Factors for Wound Healing. *Burns Trauma* **2019**, *7*, s41038-019-0148–1.

354. Lazaro, J. l.; Izzo, V.; Meaume, S.; Davies, A. h.; Lobmann, R.; Uccioli, L. Elevated Levels of Matrix Metalloproteinases and Chronic Wound Healing: An Updated Review of Clinical Evidence. *J Wound Care* **2016**, *25*, 277–287.

355. Wang, H.S.; Chard, T. IGFs and IGF-Binding Proteins in the Regulation of Human Ovarian and Endometrial Function. *J Endocrinol* **1999**, *161*, 1–13.

356. Edmondson, S.R.; Thumiger, S.P.; Werther, G.A.; Wraight, C.J. Epidermal Homeostasis: The Role of the Growth Hormone and Insulin-like Growth Factor Systems. *Endocr Rev* **2003**, *24*, 737–764.

357. LeRoith, D.; Yakar, S. Mechanisms of Disease: Metabolic Effects of Growth Hormone and Insulin-like Growth Factor 1. *Nat Rev Endocrinol* **2007**, *3*, 302–310.

358. Gartner, M.H.; Benson, J.D.; Caldwell, M.D. Insulin-like Growth Factors I and II Expression in the Healing Wound. *J Surg Res* **1992**, *52*, 389–394.

359. Semenova, E.; Koegel, H.; Hasse, S.; Klatte, J.E.; Slonimsky, E.; Bilbao, D.; Paus, R.; Werner, S.; Rosenthal, N. Overexpression of MIGF-1 in Keratinocytes Improves

Wound Healing and Accelerates Hair Follicle Formation and Cycling in Mice. *Am J Pathol* **2008**, *173*, 1295–1310.

360. Shen, S.; Alt, A.; Wertheimer, E.; Gartsbein, M.; Kuroki, T.; Ohba, M.; Braiman, L.; Sampson, S.R.; Tennenbaum, T. PKCdelta Activation: A Divergence Point in the Signaling of Insulin and IGF-1-Induced Proliferation of Skin Keratinocytes. *Diabetes* **2001**, *50*, 255–264.

361. Antoniades, H.N.; Galanopoulos, T.; Neville-Golden, J.; Kiritsy, C.P.; Lynch, S.E. Expression of Growth Factor and Receptor MRNAs in Skin Epithelial Cells Following Acute Cutaneous Injury. *Am J Pathol* **1993**, *142*, 1099–1110.

362. Rappolee, D.A.; Mark, D.; Banda, M.J.; Werb, Z. Wound Macrophages Express TGF-Alpha and Other Growth Factors in Vivo: Analysis by MRNA Phenotyping. *Science* **1988**, *241*, 708–712.

363. Cook, J.J.; Haynes, K.M.; Werther, G.A. Mitogenic Effects of Growth Hormone in Cultured Human Fibroblasts. Evidence for Action via Local Insulin-like Growth Factor I Production. *J Clin Invest* **1988**, *81*, 206–212.

364. Heldin, C.-H.; Westermark, B. Mechanism of Action and In Vivo Role of Platelet-Derived Growth Factor. *Physiol Rev* **1999**, *79*, 1283–1316.

365. Uutela, M.; Wirzenius, M.; Paavonen, K.; Rajantie, I.; He, Y.; Karpanen, T.; Lohela, M.; Wiig, H.; Salven, P.; Pajusola, K.; et al. PDGF-D Induces Macrophage Recruitment, Increased Interstitial Pressure, and Blood Vessel Maturation during Angiogenesis. *Blood* **2004**, *104*, 3198–3204.

366. Rhee, S.; Grinnell, F. P21-Activated Kinase 1: Convergence Point in PDGF- and LPA-Stimulated Collagen Matrix Contraction by Human Fibroblasts. *J Cell Biol* **2006**, *172*, 423–432.

367. Stavri, G.T.; Hong, Y.; Zachary, I.C.; Breier, G.; Baskerville, P.A.; Ylä-Herttuala, S.; Risau, W.; Martin, J.F.; Erusalimsky, J.D. Hypoxia and Platelet-Derived Growth Factor-BB Synergistically Upregulate the Expression of Vascular Endothelial Growth Factor in Vascular Smooth Muscle Cells. *FEBS Lett* **1995**, *358*, 311–315.

368. Steed, D.L. Clinical Evaluation of Recombinant Human Platelet-Derived Growth Factor for the Treatment of Lower Extremity Ulcers. *Plast Reconstr Surg* **2006**, *117*, 143S.

369. Margolis, D.J.; Cromblehome, T.; Herlyn, M.; Cross, P.; Weinberg, L.; Filip, J.; Propert, K. Clinical Protocol. Phase I Trial to Evaluate the Safety of H5.020CMV.PDGF-b and Limb Compression Bandage for the Treatment of Venous Leg Ulcer: Trial A. *Hum Gene Ther* **2004**, *15*, 1003–1019.

370. Margolis, D.J.; Crombleholme, T.; Herlyn, M. Clinical Protocol: Phase I Trial to Evaluate the Safety of H5. 020CMV. PDGF-B for the Treatment of a Diabetic Insensate Foot Ulcer. *Wound Repair Regen* **2000**, *8*, 480–493.

371. Liu, Z.; Wu, H.; Huang, S. Role of NGF and Its Receptors in Wound Healing (Review). *Exp Ther Med* **2021**, *21*, 1–9.

372. Gostynska, N.; Pannella, M.; Rocco, M.L.; Giardino, L.; Aloe, L.; Calzà, L. The Pleiotropic Molecule NGF Regulates the in Vitro Properties of Fibroblasts, Keratinocytes, and Endothelial Cells: Implications for Wound Healing. *Am J Physiol Cell Physiol* **2020**, *318*, C360–C371.

373. Liu, Z.; Cao, Y.; Liu, G.; Yin, S.; Ma, J.; Liu, J.; Zhang, M.; Wang, Y. P75 Neurotrophin Receptor Regulates NGF-Induced Myofibroblast Differentiation and Collagen Synthesis through MRTF-A. *Exp Cell Res* **2019**, *383*, 111504.

374. Troullinaki, M.; Alexaki, V.-I.; Mitroulis, I.; Witt, A.; Klotzsche-von Ameln, A.; Chung, K.-J.; Chavakis, T.; Economopoulou, M. Nerve Growth Factor Regulates Endothelial Cell Survival and Pathological Retinal Angiogenesis. *J Cell Mol Med* **2019**, *23*, 2362–2371.

375. Frade, J.M.; Barde, Y.A. Nerve Growth Factor: Two Receptors, Multiple Functions. *Bioessays* **1998**, *20*, 137–145.

376. Tron, V.A.; Coughlin, M.D.; Jang, D.E.; Stanisz, J.; Sauder, D.N. Expression and Modulation of Nerve Growth Factor in Murine Keratinocytes (PAM 212). *J Clin Invest* **1990**, *85*, 1085–1089.

377. Murase, K.; Murakami, Y.; Takayanagi, K.; Furukawa, Y.; Hayashi, K. Human Fibroblast Cells Synthesize and Secrete Nerve Growth Factor in Culture. *Biochem Biophys Res Commun* **1992**, *184*, 373–379.

378. Matsuda, H.; Koyama, H.; Sato, H.; Sawada, J.; Itakura, A.; Tanaka, A.; Matsumoto, M.; Konno, K.; Ushio, H.; Matsuda, K. Role of Nerve Growth Factor in Cutaneous Wound Healing: Accelerating Effects in Normal and Healing-Impaired Diabetic Mice. *J Exp Med* **1998**, *187*, 297–306.

379. Nakagaki, O.; Miyoshi, H.; Sawada, T.; Atsumi, T.; Kondo, T.; Atsumi, T. Epalrestat Improves Diabetic Wound Healing via Increased Expression of Nerve Growth Factor. *Exp Clin Endocrinol Diabetes* **2013**, *121*, 84–89.

380. Emanueli, C.; Salis, M.B.; Pinna, A.; Graiani, G.; Manni, L.; Madeddu, P. Nerve Growth Factor Promotes Angiogenesis and Arteriogenesis in Ischemic Hindlimbs. *Circulation* **2002**, *106*, 2257–2262.

381. Kanu, L.N.; Ciolino, J.B. Nerve Growth Factor as an Ocular Therapy: Applications, Challenges, and Future Directions. *Semin Ophthalmol* **2021**, *36*, 224–231.

382. Keck, P.J.; Hauser, S.D.; Krivi, G.; Sanzo, K.; Warren, T.; Feder, J.; Connolly, D.T. Vascular Permeability Factor, an Endothelial Cell Mitogen Related to PDGF. *Science* **1989**, *246*, 1309–1312.

383. Berse, B.; Brown, L.F.; Van de Water, L.; Dvorak, H.F.; Senger, D.R. Vascular Permeability Factor (Vascular Endothelial Growth Factor) Gene Is Expressed Differentially in Normal Tissues, Macrophages, and Tumors. *MBoC* **1992**, *3*, 211–220.

384. Uchida, K.; Uchida, S.; Nitta, K.; Yumura, W.; Marumo, F.; Nihei, H. Glomerular Endothelial Cells in Culture Express and Secrete Vascular Endothelial Growth Factor. *Am J Physiol-Renal Physiol* **1994**, *266*, F81–F88.

385. Banks, R.E.; Forbes, M.A.; Kinsey, S.E.; Stanley, A.; Ingham, E.; Walters, C.; Selby, P.J. Release of the Angiogenic Cytokine Vascular Endothelial Growth Factor (VEGF) from Platelets: Significance for VEGF Measurements and Cancer Biology. *Br J Cancer* **1998**, *77*, 956–964.

386. Nissen, N.N.; Polverini, P.; Koch, A.E.; Volin, M.V.; Gamelli, R.L.; DiPietro, L.A. Vascular Endothelial Growth Factor Mediates Angiogenic Activity during the Proliferative Phase of Wound Healing. *Am J Pathol* **1998**, *152*, 1445.

387. de Vries, C.; Escobedo, J.A.; Ueno, H.; Houck, K.; Ferrara, N.; Williams, L.T. The Fms-Like Tyrosine Kinase, a Receptor for Vascular Endothelial Growth Factor. *Science* **1992**, *255*, 989–991.

388. Peters, K.G.; De Vries, C.; Williams, L.T. Vascular Endothelial Growth Factor Receptor Expression during Embryogenesis and Tissue Repair Suggests a Role in Endothelial Differentiation and Blood Vessel Growth. *Proc Natl Acad Sci* **1993**, *90*, 8915–8919.

389. Ji, R.C. Macrophages Are Important Mediators of Either Tumor- or Inflammation-Induced Lymphangiogenesis. *Cell Mol Life Sci* **2012**, *69*, 897–914.

390. Habeck, H.; Odenthal, J.; Walderich, B.; Maischein, H.; Schulte-Merker, S.; Tübingen 2000 screen consortium Analysis of a Zebrafish VEGF Receptor Mutant Reveals Specific Disruption of Angiogenesis. *Curr Biol* **2002**, *12*, 1405–1412.

391. Goishi, K.; Klagsbrun, M. Vascular Endothelial Growth Factor and Its Receptors in Embryonic Zebrafish Blood Vessel Development. *Curr Top Dev Biol* **2004**, *62*, 127–152.

392. Gong, B.; Liang, D.; Chew, T.-G.; Ge, R. Characterization of the Zebrafish Vascular Endothelial Growth Factor A Gene: Comparison with Vegf-A Genes in Mammals and Fugu. *Biochim Biophys Acta* **2004**, *1676*, 33–40.

393. Sveen, L.; Karlsen, C.; Ytteborg, E. Mechanical Induced Wounds in Fish – a Review on Models and Healing Mechanisms. *Rev Aquaculture* **2020**, *12*, 2446–2465.

394. Groff, J.M. Cutaneous Biology and Diseases of Fish. *Vet Clin North Am Exot Anim Pract* **2001**, *4*, 321–411.

395. Fontenot, D.K.; Neiffer, D.L. Wound Management in Teleost Fish: Biology of the Healing Process, Evaluation, and Treatment. *Vet Clin North Am Exot Anim Pract* **2004**, *7*, 57–86.

396. Richardson, R.; Slanchev, K.; Kraus, C.; Knyphausen, P.; Eming, S.; Hammerschmidt, M. Adult Zebrafish as a Model System for Cutaneous Wound-Healing Research. *J Invest Dermatol* **2013**, *133*, 1655–1665.

397. Abram, Q.H.; Dixon, B.; Katzenback, B.A. Impacts of Low Temperature on the Teleost Immune System. *Biology* **2017**, *6*, 39.

398. Quilhac, A.; Sire, J.Y. Spreading, Proliferation, and Differentiation of the Epidermis after Wounding a Cichlid Fish, Hemichromis Bimaculatus. *Anat Rec* **1999**, *254*, 435–451.

399. Bucke, D. The Anatomy and Histology of the Alimentary Tract of the Carnivorous Fish the Pike Esox Lucius L. *J Fish Biol* **1971**, *3*, 421–431.

400. Velmurugan, B.; Selvanayagam, M.; Cengiz, E.I.; Unlu, E. Histopathological Changes in the Gill and Liver Tissues of Freshwater Fish, Cirrhinus Mrigala Exposed to Dichlorvos. *Braz arch biol technol* **2009**, *52*, 1291–1296.

401. Toutou, M.M.; Osman, A. laa G.M.; Farrag, M.M.S.; Badrey, A.E.A.; Moustafa, M.A. Growth Performance, Feed Utilization and Gut Histology of Monosex Nile Tilapia (Oreochromis Niloticus) Fed with Varying Levels of Pomegranate (Punica Granatum) Peel Residues. *Aquac Aquar Conserv Legis* **2019**, *12*, 298–309.

402. Richardson, R.; Metzger, M.; Knyphausen, P.; Ramezani, T.; Slanchev, K.; Kraus, C.; Schmelzer, E.; Hammerschmidt, M. Re-Epithelialization of Cutaneous Wounds in Adult Zebrafish Combines Mechanisms of Wound Closure in Embryonic and Adult Mammals. *Development* **2016**, *143*, 2077–2088.

403. Caraguel, F.; Bessonov, N.; Demongeot, J.; Dhouailly, D.; Volpert, V. Wound Healing and Scale Modelling in Zebrafish. *Acta Biotheor* **2016**, *64*, 343–358.

404. Ceballos-Francisco, D.; Cordero, H.; Guardiola, F.A.; Cuesta, A.; Esteban, M.Á. Healing and Mucosal Immunity in the Skin of Experimentally Wounded Gilthead Seabream (Sparus Aurata L). *Fish Shellfish Immunol* **2017**, *71*, 210–219.

405. Banerjee, T.K.; Mittal, A.K. Histopathological Studies on the Repair of the Excised Skin Wounds of the Air-Breathing Scalyfish Channa Striata (Bloch). *Curr Sci* **1999**, *77*, 1067–1075.

406. Sveen, L.R.; Timmerhaus, G.; Krasnov, A.; Takle, H.; Handeland, S.; Ytteborg, E. Wound Healing in Post-Smolt Atlantic Salmon (Salmo Salar L.). *Sci Rep* **2019**, *9*, 3565.

407. Leibovich, S.; Ross, R. The Role of the Macrophage in Wound Repair. A Study with Hydrocortisone and Antimacrophage Serum. *Am J Pathol* **1975**, *78*, 71.

408. Ortega, S.; Ittmann, M.; Tsang, S.H.; Ehrlich, M.; Basilico, C. Neuronal Defects and Delayed Wound Healing in Mice Lacking Fibroblast Growth Factor 2. *Proc Natl Acad Sci U S A* **1998**, *95*, 5672–5677.

409. Fernández-Bravo, A.; Figueras, M.J. An Update on the Genus Aeromonas: Taxonomy, Epidemiology, and Pathogenicity. *Microorganisms* **2020**, *8*, 129.

410. Janda, J.M.; Abbott, S.L. The Genus Aeromonas: Taxonomy, Pathogenicity, and Infection. *Clin Microbiol Rev* **2010**, *23*, 35–73.

411. Monette, S.; Dallaire, A.D.; Mingelbier, M.; Groman, D.; Uhland, C.; Richard, J.-P.; Paillard, G.; Johannson, L.M.; Chivers, D.P.; Ferguson, H.W.; et al. Massive Mortality of Common Carp (Cyprinus Carpio Carpio) in the St. Lawrence River in 2001: Diagnostic Investigation and Experimental Induction of Lymphocytic Encephalitis. *Vet Pathol* **2006**, *43*, 302–310.

412. Elliott, D.G.; Shotts, E.B. Aetiology of an Ulcerative Disease in Goldfish Carassius Auratus (L.): Microbiological Examination of Diseased Fish from Seven Locations. *J Fish Dis* **1980**, *3*, 133–143.

413. Vivekanandhan, G.; Savithamani, K.; Hatha, A. a. M.; Lakshmanaperumalsamy, P. Antibiotic Resistance of Aeromonas Hydrophila Isolated from Marketed Fish and Prawn of South India. *Int J Food Microbiol* **2002**, *76*, 165–168.

414. Havixbeck, J.J.; Rieger, A.M.; Wong, M.E.; Hodgkinson, J.W.; Barreda, D.R. Neutrophil Contributions to the Induction and Regulation of the Acute Inflammatory Response in Teleost Fish. *J Leukoc Biol* **2016**, *99*, 241–252.

415. Sun, J.; Zhang, X.; Gao, X.; Jiang, Q.; Wen, Y.; Lin, L. Characterization of Virulence Properties of Aeromonas Veronii Isolated from Diseased Gibel Carp (Carassius Gibelio). *Int J Mol Sci* **2016**, *17*, 496.

416. Shameena, S.S.; Kumar, K.; Kumar, S.; Kumar, S.; Rathore, G. Virulence Characteristics of Aeromonas Veronii Biovars Isolated from Infected Freshwater Goldfish (Carassius Auratus). *Aquaculture* **2020**, *518*, 734819.

417. Austin, B.; Austin, D.A.; Munn, C.B. *Bacterial Fish Pathogens: Disease of Farmed and Wild Fish*; Springer, 2007; ISBN 978-1-4020-6068-7.

418. Wiklund, T.; Dalsgaard, I. Occurrence and Significance of Atypical Aeromonas Salmonicida in Non-Salmonid and Salmonid Fish Species: A Review. *Dis Aquat Organ* **1998**, *32*, 49–69.

419. Bernoth, E.-M.; Ellis, A.E.; Midtlyng, P.J.; Olivier, G.; Smith, P. *Furunculosis: Multidisciplinary Fish Disease Research*; Elsevier, 1997; ISBN 0-08-053222-5.

420. Lewbart, G.A. Bacteria and Ornamental Fish. In Proceedings of the Seminars in Avian and Exotic Pet Medicine; Elsevier, 2001; Vol. 10, pp. 48–56.

421. Gustafson, C.E.; Thomas, C.J.; Trust, T.J. Detection of Aeromonas Salmonicida from Fish by Using Polymerase Chain Reaction Amplification of the Virulence Surface Array Protein Gene. *Appl Environ Microbiol* **1992**, *58*, 3816–3825.

422. Tanrikul, T.T.; Dinçtürk, E. A New Outbreak in Sea Bass Farming in Turkey: Aeromonas Veronii. *J Hell Vet* **2021**, *72*, 3051–3058.

423. Raj, N.S.; Swaminathan, T.R.; Dharmaratnam, A.; Raja, S.A.; Ramraj, D.; Lal, K.K. Aeromonas Veronii Caused Bilateral Exophthalmia and Mass Mortality in Cultured Nile Tilapia, Oreochromis Niloticus (L.) in India. *Aquaculture* **2019**, *512*, 734278.

424. Cipriano, R.C.; Bullock, G.L. *Furunculosis and Other Diseases Caused by Aeromonas Salmonicida*; National Fish Health Research Laboratory, 2001; ISBN 1259–1261.

425. Parker, J.L.; Shaw, J.G. Aeromonas Spp. Clinical Microbiology and Disease. *J Infect* **2011**, *62*, 109–118.

426. Edberg, S.C.; Browne, F.A.; Allen, M.J. Issues for Microbial Regulation: Aeromonas as a Model. *Crit Rev Microbiol* **2007**, *33*, 89–100.

427. Kelly, K.A.; Koehler, J.M.; Ashdown, L.R. Spectrum of Extraintestinal Disease Due to Aeromonas Species in Tropical Queensland, Australia. *Clin Infect Dis* **1993**, *16*, 574–579.

428. Spadaro, S.; Berselli, A.; Marangoni, E.; Romanello, A.; Colamussi, M.V.; Ragazzi, R.; Zardi, S.; Volta, C.A. Aeromonas Sobria Necrotizing Fasciitis and Sepsis in an Immunocompromised Patient: A Case Report and Review of the Literature. *J Med Case Reports* **2014**, *8*, 315.

429. Nosenko, M.A.; Ambaryan, S.G.; Drutskaya, M.S. Proinflammatory Cytokines and Skin Wound Healing in Mice. *Mol Biol* **2019**, *53*, 653–664.

430. Frank, J.; Born, K.; Barker, J.H.; Marzi, I. In Vivo Effect of Tumor NecrosisFactor Alpha on Wound Angiogenesis AndEpithelialization. *Eur J Trauma* **2003**, *29*, 208–219.

431. Dudeck, J.; Froebel, J.; Kotrba, J.; Lehmann, C.H.K.; Dudziak, D.; Speier, S.; Nedospasov, S.A.; Schraven, B.; Dudeck, A. Engulfment of Mast Cell Secretory Granules on Skin Inflammation Boosts Dendritic Cell Migration and Priming Efficiency. *J Allergy Clin Immunol* **2019**, *143*, 1849-1864.e4.

432. Kawasaki, Y.; Zhang, L.; Cheng, J.-K.; Ji, R.-R. Cytokine Mechanisms of Central Sensitization: Distinct and Overlapping Role of Interleukin-1beta, Interleukin-6, and Tumor Necrosis Factor-Alpha in Regulating Synaptic and Neuronal Activity in the Superficial Spinal Cord. *J Neurosci* **2008**, *28*, 5189–5194.

433. Werner, S.; Peters, K.G.; Longaker, M.T.; Fuller-Pace, F.; Banda, M.J.; Williams, L.T. Large Induction of Keratinocyte Growth Factor Expression in the Dermis during Wound Healing. *Proc Natl Acad Sci U S A* **1992**, *89*, 6896–6900.

434. Tang, A.; Gilchrest, B.A. Regulation of Keratinocyte Growth Factor Gene Expression in Human Skin Fibroblasts. *J Dermatol Sci* **1996**, *11*, 41–50.

435. Lee, P.; Gund, R.; Dutta, A.; Pincha, N.; Rana, I.; Ghosh, S.; Witherden, D.; Kandyba, E.; MacLeod, A.; Kobielak, K.; et al. Stimulation of Hair Follicle Stem Cell Proliferation through an IL-1 Dependent Activation of ΓδT-Cells. *Elife* **2017**, *6*, e28875.

436. de Oliveira, S.; Reyes-Aldasoro, C.C.; Candel, S.; Renshaw, S.A.; Mulero, V.; Calado, Â. Cxcl8 (Interleukin-8) Mediates Neutrophil Recruitment and Behavior in the Zebrafish Inflammatory Response. *J Immunol* **2013**, *190*, 4349–4359.

437. Das, S.T.; Rajagopalan, L.; Guerrero-Plata, A.; Sai, J.; Richmond, A.; Garofalo, R.P.; Rajarathnam, K. Monomeric and Dimeric CXCL8 Are Both Essential for In Vivo Neutrophil Recruitment. *PLOS ONE* **2010**, *5*, e11754.

438. Paccaud, J.P.; Schifferli, J.A.; Baggiolini, M. NAP-1/IL-8 Induces up-Regulation of CR1 Receptors in Human Neutrophil Leukocytes. *Biochem Biophys Res Commun* **1990**, *166*, 187–192.

439. Cowland, J.B.; Borregaard, N. Granulopoiesis and Granules of Human Neutrophils. *Immunol Rev* **2016**, *273*, 11–28.

440. Yang, R.; Masters, A.R.; Fortner, K.A.; Champagne, D.P.; Yanguas-Casás, N.; Silberger, D.J.; Weaver, C.T.; Haynes, L.; Rincon, M. IL-6 Promotes the Differentiation of a Subset of Naive CD8+ T Cells into IL-21-Producing B Helper CD8+ T Cells. *J Exp Med* **2016**, *213*, 2281–2291.

441. Bosurgi, L.; Cao, Y.G.; Cabeza-Cabrerizo, M.; Tucci, A.; Hughes, L.D.; Kong, Y.; Weinstein, J.S.; Licona-Limon, P.; Schmid, E.T.; Pelorosso, F.; et al. Macrophage Function in Tissue Repair and Remodeling Requires IL-4 or IL-13 with Apoptotic Cells. *Science* **2017**, *356*, 1072–1076.

442. McFarland-Mancini, M.M.; Funk, H.M.; Paluch, A.M.; Zhou, M.; Giridhar, P.V.; Mercer, C.A.; Kozma, S.C.; Drew, A.F. Differences in Wound Healing in Mice with Deficiency of IL-6 versus IL-6 Receptor. *J Immunol* **2010**, *184*, 7219–7228.

443. Luckett, L.R.; Gallucci, R.M. Interleukin-6 (IL-6) Modulates Migration and Matrix Metalloproteinase Function in Dermal Fibroblasts from IL-6KO Mice. *Br J Dermatol* **2007**, *156*, 1163–1171.

444. Gallucci, R.M.; Sugawara, T.; Yucesoy, B.; Berryann, K.; Simeonova, P.P.; Matheson, J.M.; Luster, M.I. Interleukin-6 Treatment Augments Cutaneous Wound Healing in Immunosuppressed Mice. *J Interferon Cytokine Res* **2001**, *21*, 603–609.

445. Brown, L.F.; Yeo, K.T.; Berse, B.; Yeo, T.K.; Senger, D.R.; Dvorak, H.F.; van de Water, L. Expression of Vascular Permeability Factor (Vascular Endothelial Growth Factor) by Epidermal Keratinocytes during Wound Healing. *J Exp Med* **1992**, *176*, 1375–1379.

446. Schoenborn, J.R.; Wilson, C.B. Regulation of Interferon-γ During Innate and Adaptive Immune Responses. In *Advances in Immunology*; Academic Press, 2007; Vol. 96, pp. 41–101.

447. Saraiva, M.; Vieira, P.; O'Garra, A. Biology and Therapeutic Potential of Interleukin-10. *J Exp Med* **2019**, *217*, e20190418.

448. White, L.A.; Mitchell, T.I.; Brinckerhoff, C.E. Transforming Growth Factor Beta Inhibitory Element in the Rabbit Matrix Metalloproteinase-1 (Collagenase-1) Gene Functions as a Repressor of Constitutive Transcription. *Biochim Biophys Acta* **2000**, *1490*, 259–268.

449. Evrard, S.M.; d'Audigier, C.; Mauge, L.; Israël-Biet, D.; Guerin, C.L.; Bieche, I.; Kovacic, J.C.; Fischer, A.-M.; Gaussem, P.; Smadja, D.M. The Profibrotic Cytokine Transforming Growth Factor-B1 Increases Endothelial Progenitor Cell Angiogenic Properties. *J Thromb Haemost* **2012**, *10*, 670–679.

450. Ramirez, H.; Patel, S.B.; Pastar, I. The Role of TGFβ Signaling in Wound Epithelialization. *Adv Wound Care (New Rochelle)* **2014**, *3*, 482–491.

451. Koh, T.J.; DiPietro, L.A. Inflammation and Wound Healing: The Role of the Macrophage. *Expert Rev Mol Med* **2011**, *13*, e23.

452. Kreisel, D.; Nava, R.G.; Li, W.; Zinselmeyer, B.H.; Wang, B.; Lai, J.; Pless, R.; Gelman, A.E.; Krupnick, A.S.; Miller, M.J. In Vivo Two-Photon Imaging Reveals Monocyte-Dependent Neutrophil Extravasation during Pulmonary Inflammation. *Proc Natl Acad Sci U S A* **2010**, *107*, 18073–18078.

453. Sorokin, L. The Impact of the Extracellular Matrix on Inflammation. *Nat Rev Immunol* **2010**, *10*, 712–723.

454. Davies, L.C.; Jenkins, S.J.; Allen, J.E.; Taylor, P.R. Tissue-Resident Macrophages. *Nat Immunol* **2013**, *14*, 986–995.

455. Ferrante, C.J.; Leibovich, S.J. Regulation of Macrophage Polarization and Wound Healing. *Adv Wound Care* **2012**, *1*, 10–16.

456. Ogle, M.E.; Segar, C.E.; Sridhar, S.; Botchwey, E.A. Monocytes and Macrophages in Tissue Repair: Implications for Immunoregenerative Biomaterial Design. *Exp Biol Med (Maywood)* **2016**, *241*, 1084–1097.

457. Leitinger, N.; Schulman, I.G. Phenotypic Polarization of Macrophages in Atherosclerosis. *Arterioscler Thromb Vasc Biol* **2013**, *33*, 1120–1126.

458. Spiller, K.L.; Anfang, R.R.; Spiller, K.J.; Ng, J.; Nakazawa, K.R.; Daulton, J.W.; Vunjak-Novakovic, G. The Role of Macrophage Phenotype in Vascularization of Tissue Engineering Scaffolds. *Biomaterials* **2014**, *35*, 4477–4488.

459. Filardy, A.A.; Pires, D.R.; Nunes, M.P.; Takiya, C.M.; Freire-de-Lima, C.G.; Ribeiro-Gomes, F.L.; DosReis, G.A. Proinflammatory Clearance of Apoptotic Neutrophils Induces an IL-12lowIL-10high Regulatory Phenotype in Macrophages. *J Immunol* **2010**, *185*, 2044–2050.

460. Hesketh, M.; Sahin, K.B.; West, Z.E.; Murray, R.Z. Macrophage Phenotypes Regulate Scar Formation and Chronic Wound Healing. *Int J Mol Sci* **2017**, *18*, 1545.

461. Rőszer, T. Understanding the Mysterious M2 Macrophage through Activation Markers and Effector Mechanisms. *Mediators Inflamm* **2015**, *2015*, 816460.

462. Zizzo, G.; Hilliard, B.A.; Monestier, M.; Cohen, P.L. Efficient Clearance of Early Apoptotic Cells by Human Macrophages Requires M2c Polarization and MerTK Induction. *J Immunol* **2012**, *189*, 3508–3520.

463. Wang, Q.; Ni, H.; Lan, L.; Wei, X.; Xiang, R.; Wang, Y. Fra-1 Protooncogene Regulates IL-6 Expression in Macrophages and Promotes the Generation of M2d Macrophages. *Cell Res* **2010**, *20*, 701–712.

464. Duluc, D.; Delneste, Y.; Tan, F.; Moles, M.-P.; Grimaud, L.; Lenoir, J.; Preisser, L.; Anegon, I.; Catala, L.; Ifrah, N.; et al. Tumor-Associated Leukemia Inhibitory Factor and IL-6 Skew Monocyte Differentiation into Tumor-Associated Macrophage-like Cells. *Blood* **2007**, *110*, 4319–4330.

465. Atri, C.; Guerfali, F.Z.; Laouini, D. Role of Human Macrophage Polarization in Inflammation during Infectious Diseases. *Int J Mol Sci* **2018**, *19*, E1801.

466. Shapouri-Moghaddam, A.; Mohammadian, S.; Vazini, H.; Taghadosi, M.; Esmaeili, S.-A.; Mardani, F.; Seifi, B.; Mohammadi, A.; Afshari, J.T.; Sahebkar, A. Macrophage Plasticity, Polarization, and Function in Health and Disease. *J Cell Physiol* **2018**, *233*, 6425–6440.

467. Havixbeck, J.J.; Rieger, A.M.; Churchill, L.J.; Barreda, D.R. Neutrophils Exert Protection in Early Aeromonas Veronii Infections through the Clearance of Both Bacteria and Dying Macrophages. *Fish Shellfish Immunol* **2017**, *63*, 18–30.

468. Myrick, C.A.; Folgner, D.K.; Cech Jr, J.J. An Annular Chamber for Aquatic Animal Preference Studies. *Trans Am Fish* **2004**, *133*, 427–433.

469. Xu, Z.; Parra, D.; Gómez, D.; Salinas, I.; Zhang, Y.A.; Jørgensen, L. von G.; Heinecke, R.D.; Buchmann, K.; LaPatra, S.; Sunyer, J.O. Teleost Skin, an Ancient Mucosal Surface That Elicits Gut-like Immune Responses. *PNAS* **2013**, *110*, 13097–13102.

470. Granja, A.G.; Leal, E.; Pignatelli, J.; Castro, R.; Abós, B.; Kato, G.; Fischer, U.; Tafalla, C. Identification of Teleost Skin CD8α+ Dendritic-like Cells, Representing a Potential Common Ancestor for Mammalian Cross-Presenting Dendritic Cells. *J Immunol* **2015**, *195*, 1825–1837.

471. Leal, E.; Granja, A.G.; Zarza, C.; Tafalla, C. Distribution of T Cells in Rainbow Trout (Oncorhynchus Mykiss) Skin and Responsiveness to Viral Infection. *PLOS ONE* **2016**, *11*, e0147477.

472. Soliman, A.M.; Yoon, T.; Wang, J.; Stafford, J.L.; Barreda, D.R. Isolation of Skin Leukocytes Uncovers Phagocyte Inflammatory Responses During Induction and Resolution of Cutaneous Inflammation in Fish. *Front Immunol* **2021**, *12*, 725063.

473. Katzenback, B.A.; Belosevic, M. Isolation and Functional Characterization of Neutrophil-like Cells, from Goldfish (Carassius Auratus L.) Kidney. *Dev Comp Immunol* **2009**, *33*, 601–611.

474. Neumann, N.F.; Barreda, D.R.; Belosevic, M. Generation and Functional Analysis of Distinct Macrophage Sub-Populations from Goldfish (Carassius Auratus L.) Kidney Leukocyte Cultures. *Fish Shellfish Immunol* **2000**, *10*, 1–20.

475. Ra□, X.; Huang, X.; Zh□u, Z.; Lin, X. An Impr□vement □f the 2ˆ(–Delta Delta CT) Method for Quantitative Real-Time Polymerase Chain Reaction Data Analysis. *Biostat Bioinforma Biomath* **2013**, *3*, 71–85.

476. Grayfer, L.; Walsh, J.G.; Belosevic, M. Characterization and Functional Analysis of Goldfish (Carassius Auratus L.) Tumor Necrosis Factor-Alpha. *Dev Comp Immunol* **2008**, *32*, 532–543.

477. Oladiran, A.; Beauparlant, D.; Belosevic, M. The Expression Analysis of Inflammatory and Antimicrobial Genes in the Goldfish (Carassius Auratus L.) Infected with Trypanosoma Carassii. *Fish Shellfish Immunol* **2011**, *31*, 606–613.

478. Grayfer, L.; Hodgkinson, J.W.; Hitchen, S.J.; Belosevic, M. Characterization and Functional Analysis of Goldfish (Carassius Auratus L.) Interleukin-10. *Mol Immunol* **2011**, *48*, 563–571.

479. Rieger, A.M.; Barreda, D.R. Antimicrobial Mechanisms of Fish Leukocytes. *Dev Comp Immunol* **2011**, *35*, 1238–1245.

480. Schairer, D.O.; Chouake, J.S.; Nosanchuk, J.D.; Friedman, A.J. The Potential of Nitric Oxide Releasing Therapies as Antimicrobial Agents. *Virulence* **2012**, *3*, 271–279.

481. Wink, D.A.; Mitchell, J.B. Chemical Biology of Nitric Oxide: Insights into Regulatory, Cytotoxic, and Cytoprotective Mechanisms of Nitric Oxide. *Free Radic Biol Med* **1998**, *25*, 434–456.

482. Wink, D.A.; Kasprzak, K.S.; Maragos, C.M.; Elespuru, R.K.; Misra, M.; Dunams, T.M.; Cebula, T.A.; Koch, W.H.; Andrews, A.; Allen, J.S. DNA Deaminating Ability and Genotoxicity of Nitric Oxide and Its Progenitors. *Science* **1991**, *254*, 1001–1003.

483. Laval, F.; Wink, D.A.; Laval, J. A Discussion of Mechanisms of NO Genotoxicty: Implication of Inhibition of DNA Repair Proteins. In *Reviews of Physiology Biochemistry and Pharmacology, Volume 131: Special Issue on Membrane-Mediated Cellular Responses: The Roles of Reactive Oxygens, NO, CO, II*; Reviews of Physiology, Biochemistry and Pharmacology; Springer: Berlin, Heidelberg, 1997; pp. 175–191 ISBN 978-3-540-49585-7.

484. Deupree, S.M.; Schoenfisch, M.H. Morphological Analysis of the Antimicrobial Action of Nitric Oxide on Gram-Negative Pathogens Using Atomic Force Microscopy. *Acta Biomater* **2009**, *5*, 1405–1415.

485. Shi, H.P.; Efron, D.T.; Most, D.; Tantry, U.S.; Barbul, A. Supplemental Dietary Arginine Enhances Wound Healing in Normal but Not Inducible Nitric Oxide Synthase Knockout Mice. *Surgery* **2000**, *128*, 374–378.

486. Nussler, A.K.; Billiar, T.R. Inflammation, Immunoregulation, and Inducible Nitric Oxide Synthase. *J Leukoc Biol* **1993**, *54*, 171–178.

487. Dash, S.; Das, S.K.; Samal, J.; Thatoi, H.N. Epidermal Mucus, a Major Determinant in Fish Health: A Review. *Iran J Vet Res* **2018**, *19*, 72–81.

488. Laplante, A.F.; Moulin, V.; Auger, F.A.; Landry, J.; Li, H.; Morrow, G.; Tanguay, R.M.; Germain, L. Expression of Heat Shock Proteins in Mouse Skin during Wound Healing. *J Histochem Cytochem* **1998**, *46*, 1291–1301.

489. Brown, C.; Laland, K.; Krause, J. Fish Cognition and Behaviour. In *Fish Cognition and Behavior*; John Wiley & Sons, Ltd, 2011; pp. 1–9 ISBN 978-1-4443-4253-6.

490. Haddad, F.; Soliman, A.M.; Wong, M.E.; Albers, E.H.; Semple, S.L.; Torrealba, D.; Heimroth, R.D.; Nashiry, A.; Tierney, K.B.; Barreda, D.R. Fever Integrates Antimicrobial Defences, Inflammation Control, and Tissue Repair in a Cold-Blooded Vertebrate. *eLife* **2023**, *12*, e83644.

491. Vadivelu, N.; Gowda, A.M.; Urman, R.D.; Jolly, S.; Kodumudi, V.; Maria, M.; Taylor, R.; Pergolizzi, J.V. Ketorolac Tromethamine - Routes and Clinical Implications. *Pain Pract* **2015**, *15*, 175–193.

492. Rooks, W.H. The Pharmacologic Activity of Ketorolac Tromethamine. *Pharmacotherapy* **1990**, *10*, 30S-32S.

493. Baevsky, R.H.; Nyquist, S.N.; Roy, M.N.; Smithline, H.A. Antipyretic Effectiveness of Intravenous Ketorolac Tromethamine. *J Emerg Med* **2004**, *26*, 407–410.

494. Horne, J.H. Furunculosis in Trout and the Importance of Carriers in the Spread of the Disease. *J Hyg (Lond)* **1928**, *28*, 67–78.

495. Deodhar, L.P.; Saraswathi, K.; Varudkar, A. Aeromonas Spp. and Their Association with Human Diarrheal Disease. *J Clin Microbiol* **1991**, *29*, 853–856.

496. Graf, J. Symbiosis of Aeromonas Veronii Biovar Sobria and Hirudo Medicinalis, the Medicinal Leech: A Novel Model for Digestive Tract Associations. *Infect Immun* **1999**, *67*, 1–7.

497. Krzymińska, S.; Kaznowski, A.; Chodysz, M. Aeromonas Spp. Human Isolates Induce Apoptosis of Murine Macrophages. *Curr Microbiol* **2009**, *58*, 252–257.

498. Janda, J.M.; Duffey, P.S. Mesophilic Aeromonads in Human Disease: Current Taxonomy, Laboratory Identification, and Infectious Disease Spectrum. *Rev Infect Dis* **1988**, *10*, 980–997.

499. Deng, Q.; Huttenlocher, A. Leukocyte Migration from a Fish Eye's View. *J Cell Sci* **2012**, *125*, 3949–3956.

500. Nguyen-Chi, M.; Phan, Q.T.; Gonzalez, C.; Dubremetz, J.-F.; Levraud, J.-P.; Lutfalla, G. Transient Infection of the Zebrafish Notochord with E. Coli Induces Chronic Inflammation. *Dis Model Mech* **2014**, *7*, 871–882.

501. Ozer, A.; Altuntas, C.Z.; Bicer, F.; Izgi, K.; Hultgren, S.J.; Liu, G.; Daneshgari, F. Impaired Cytokine Expression, Neutrophil Infiltration and Bacterial Clearance in Response to Urinary Tract Infection in Diabetic Mice. *Pathog Dis* **2015**, *73*.

502. Boxio, R.; Bossenmeyer-Pourié, C.; Steinckwich, N.; Dournon, C.; Nüsse, O. Mouse Bone Marrow Contains Large Numbers of Functionally Competent Neutrophils. *J Leukoc Biol* **2004**, *75*, 604–611.

503. Furze, R.C.; Rankin, S.M. Neutrophil Mobilization and Clearance in the Bone Marrow. *Immunology* **2008**, *125*, 281–288.

504. Rankin, S.M. The Bone Marrow: A Site of Neutrophil Clearance. *J Leukoc Biol* **2010**, *88*, 241–251.

505. Yoo, S.K.; Huttenlocher, A. Spatiotemporal Photolabeling of Neutrophil Trafficking during Inflammation in Live Zebrafish. *J Leukoc Biol* **2011**, *89*, 661–667.

506. Rosenzweig, J.A.; Chopra, A.K. Modulation of Host Immune Defenses by Aeromonas and Yersinia Species: Convergence on Toxins Secreted by Various Secretion Systems. *Front Cell Infect Microbiol* **2013**, *3*.

507. Wang, J.; Kubes, P. A Reservoir of Mature Cavity Macrophages That Can Rapidly Invade Visceral Organs to Affect Tissue Repair. *Cell* **2016**, *165*, 668–678.

508. Guilliams, M.; Scott, C.L. Does Niche Competition Determine the Origin of Tissue-Resident Macrophages? *Nat Rev Immunol* **2017**, *17*, 451–460.

509. Milich, L.M.; Ryan, C.B.; Lee, J.K. The Origin, Fate, and Contribution of Macrophages to Spinal Cord Injury Pathology. *Acta Neuropathol* **2019**, *137*, 785–797.

510. Young, A.; McNaught, C.-E. The Physiology of Wound Healing. *Surgery (Oxford)* **2011**, *29*, 475–479.

511. Singer, A.J.; Clark, R.A. Cutaneous Wound Healing. *N Engl J Med* **1999**, *341*, 738–746.

512. Barbul, A.; Shawe, T.; Rotter, S.M.; Efron, J.E.; Wasserkrug, H.L.; Badawy, S.B. Wound Healing in Nude Mice: A Study on the Regulatory Role of Lymphocytes in Fibroplasia. *Surgery* **1989**, *105*, 764–769.

513. Barbul, A.; Breslin, R.J.; Woodyard, J.P.; Wasserkrug, H.L.; Efron, G. The Effect of in Vivo T Helper and T Suppressor Lymphocyte Depletion on Wound Healing. *Ann Surg* **1989**, *209*, 479–483.

514. Lei, Y.; Wang, K.; Deng, L.; Chen, Y.; Nice, E.C.; Huang, C. Redox Regulation of Inflammation: Old Elements, a New Story. *Med Res Rev* **2015**, *35*, 306–340.

515. Medzhitov, R. Recognition of Microorganisms and Activation of the Immune Response. *Nature* **2007**, *449*, 819–826.

516. Zamboni, D.S.; Rabinovitch, M. Nitric Oxide Partially Controls Coxiella Burnetii Phase II Infection in Mouse Primary Macrophages. *Infect Immun* **2003**, *71*, 1225–1233.

517. Johann, A.M.; von Knethen, A.; Lindemann, D.; Brüne, B. Recognition of Apoptotic Cells by Macrophages Activates the Peroxisome Proliferator-Activated Receptor- γ and Attenuates the Oxidative Burst. *Cell Death Differ* **2006**, *13*, 1533–1540.

518. Rieger, A.M.; Konowalchuk, J.D.; Grayfer, L.; Katzenback, B.A.; Havixbeck, J.J.; Kiemele, M.D.; Belosevic, M.; Barreda, D.R. Fish and Mammalian Phagocytes Differentially Regulate Pro-Inflammatory and Homeostatic Responses In Vivo. *PLOS ONE* **2012**, *7*, e47070.

519. Esmann, L.; Idel, C.; Sarkar, A.; Hellberg, L.; Behnen, M.; Möller, S.; van Zandbergen, G.; Klinger, M.; Köhl, J.; Bussmeyer, U.; et al. Phagocytosis of Apoptotic Cells by Neutrophil Granulocytes: Diminished Proinflammatory Neutrophil Functions in the Presence of Apoptotic Cells. *J Immunol* **2010**, *184*, 391–400.

520. Kuijpers, T.; Lutter, R. Inflammation and Repeated Infections in CGD: Two Sides of a Coin. *Cell Mol Life Sci* **2012**, *69*, 7–15.

521. Flannagan, R.S.; Cosío, G.; Grinstein, S. Antimicrobial Mechanisms of Phagocytes and Bacterial Evasion Strategies. *Nat Rev Microbiol* **2009**, *7*, 355–366.

522. Pacelli, R.; Wink, D.A.; Cook, J.A.; Krishna, M.C.; DeGraff, W.; Friedman, N.; Tsokos, M.; Samuni, A.; Mitchell, J.B. Nitric Oxide Potentiates Hydrogen Peroxide-Induced Killing of Escherichia Coli. *J Exp Med* **1995**, *182*, 1469–1479.

523. Rubbo, H.; Radi, R.; Trujillo, M.; Telleri, R.; Kalyanaraman, B.; Barnes, S.; Kirk, M.; Freeman, B.A. Nitric Oxide Regulation of Superoxide and Peroxynitrite-Dependent Lipid Peroxidation. Formation of Novel Nitrogen-Containing Oxidized Lipid Derivatives. *J Biol Chem* **1994**, *269*, 26066–26075.

524. Martin, P.; Leibovich, S.J. Inflammatory Cells during Wound Repair: The Good, the Bad and the Ugly. *Trends in Cell Biol* **2005**, *15*, 599–607.

525. Loynes, C.A.; Martin, J.S.; Robertson, A.; Trushell, D.M.; Ingham, P.W.; Whyte, M.K.; Renshaw, S.A. Pivotal Advance: Pharmacological Manipulation of Inflammation Resolution during Spontaneously Resolving Tissue Neutrophilia in the Zebrafish. *J Leukoc Biol* **2010**, *87*, 203–212.

526. Fadok, V.A.; Bratton, D.L.; Konowal, A.; Freed, P.W.; Westcott, J.Y.; Henson, P.M. Macrophages That Have Ingested Apoptotic Cells in Vitro Inhibit Proinflammatory Cytokine Production through Autocrine/Paracrine Mechanisms Involving TGF-Beta, PGE2, and PAF. *J Clin Invest* **1998**, *101*, 890–898.

527. Gonzalez, A.C. de O.; Costa, T.F.; Andrade, Z. de A.; Medrado, A.R.A.P. Wound Healing - A Literature Review. *An Bras Dermatol* **2016**, *91*, 614–620.

528. Yun, T.; Shin, S.; Bang, K.; Lee, M.; Cho, J.-A.; Baek, M. Skin Wound Healing Rate in Fish Depends on Species and Microbiota. *Int J Mol Sci* **2021**, *22*, 7804.

529. Bennett, I.L.; Nicastri, A. Fever as a Mechanism of Resistance. *Bacteriol Rev* **1960**, *24*, 16–34.

530. Medzhitov, R. Origin and Physiological Roles of Inflammation. *Nature* **2008**, *454*, 428–435.

531. Sugimoto, M.A.; Sousa, L.P.; Pinho, V.; Perretti, M.; Teixeira, M.M. Resolution of Inflammation: What Controls Its Onset? *Front Immunol* **2016**, *7*, 160.

532. Neumann, N.F.; Stafford, J.L.; Barreda, D.; Ainsworth, A.J.; Belosevic, M. Antimicrobial Mechanisms of Fish Phagocytes and Their Role in Host Defense. *Dev Comp Immunol* **2001**, *25*, 807–825.

533. Bogdan, C. Nitric Oxide Synthase in Innate and Adaptive Immunity: An Update. *Trends Immunol* **2015**, *36*, 161–178.

534. Singh, S.; Young, A.; McNaught, C.-E. The Physiology of Wound Healing. *Surgery (Oxford)* **2017**, *35*, 473–477.

535. De Muynck, L.; Van Damme, P. Cellular Effects of Progranulin in Health and Disease. *J Mol Neurosci* **2011**, *45*, 549.

536. Xu, D.; Suenaga, N.; Edelmann, M.J.; Fridman, R.; Muschel, R.J.; Kessler, B.M. Novel MMP-9 Substrates in Cancer Cells Revealed by a Label-Free Quantitative Proteomics Approach. *Mol Cell Proteomics* **2008**, *7*, 2215–2228.

537. Sehgal, A.; Irvine, K.M.; Hume, D.A. Functions of Macrophage Colony-Stimulating Factor (CSF1) in Development, Homeostasis, and Tissue Repair. *Semin Immunol* **2021**, *54*, 101509.

538. Hoelzinger, D.B.; Smith, S.E.; Mirza, N.; Dominguez, A.L.; Manrique, S.Z.; Lustgarten, J. Blockade of CCL1 Inhibits T Regulatory Cell Suppressive Function Enhancing Tumor Immunity without Affecting T Effector Responses. *J Immunol* **2010**, *184*, 6833–6842.

539. Fallarino, F.; Grohmann, U.; You, S.; McGrath, B.C.; Cavener, D.R.; Vacca, C.; Orabona, C.; Bianchi, R.; Belladonna, M.L.; Volpi, C.; et al. The Combined Effects of Tryptophan Starvation and Tryptophan Catabolites Down-Regulate T Cell Receptor ζ-Chain and Induce a Regulatory Phenotype in Naive T Cells. *J Immunol* **2006**, *176*, 6752–6761.

540. Sharma, M.D.; Baban, B.; Chandler, P.; Hou, D.-Y.; Singh, N.; Yagita, H.; Azuma, M.; Blazar, B.R.; Mellor, A.L.; Munn, D.H. Plasmacytoid Dendritic Cells from Mouse Tumor-Draining Lymph Nodes Directly Activate Mature Tregs via Indoleamine 2,3-Dioxygenase. *J Clin Invest* **2007**, *117*, 2570–2582.

541. McLoughlin, R.M.; Witowski, J.; Robson, R.L.; Wilkinson, T.S.; Hurst, S.M.; Williams, A.S.; Williams, J.D.; Rose-John, S.; Jones, S.A.; Topley, N. Interplay between IFN-Gamma and IL-6 Signaling Governs Neutrophil Trafficking and Apoptosis during Acute Inflammation. *J Clin Invest* **2003**, *112*, 598–607.

542. Ishida, Y.; Kondo, T.; Takayasu, T.; Iwakura, Y.; Mukaida, N. The Essential Involvement of Cross-Talk between IFN-γ and TGF-β in the Skin Wound-Healing Process. *J Immunol* **2004**, *172*, 1848–1855.

543. Kanno, E.; Tanno, H.; Masaki, A.; Sasaki, A.; Sato, N.; Goto, M.; Shisai, M.; Yamaguchi, K.; Takagi, N.; Shoji, M.; et al. Defect of Interferon γ Leads to Impaired Wound Healing through Prolonged Neutrophilic Inflammatory Response and Enhanced MMP-2 Activation. *Int J Mol Sci* **2019**, *20*, 5657.

544. Lee, B.N.R.; Chang, H.-K.; Son, Y.S.; Lee, D.; Kwon, S.-M.; Kim, P.-H.; Cho, J.-Y. IFN-γ Enhances the Wound Healing Effect of Late EPCs (LEPCs) via BST2-Mediated Adhesion to Endothelial Cells. *FEBS Lett* **2018**, *592*, 1705–1715.

545. Gu, X.; Shen, S.; Huang, C.; Liu, Y.; Chen, Y.; Luo, L.; Zeng, Y.; Wang, A. Effect of Activated Autologous Monocytes/Macrophages on Wound Healing in a Rodent Model of Experimental Diabetes. *Diabetes Res Clin Pract* **2013**, *102*, 53–59.

546. desJardins-Park, H.E.; Foster, D.S.; Longaker, M.T. Fibroblasts and Wound Healing: An Update. *Regen Med* **2018**, *13*, 491–495.

547. Enoch, S.; Leaper, D.J. Basic Science of Wound Healing. *Surgery (Oxford)* **2008**, *26*, 31–37.

548. Bernheim, H.; Bodel, P.; Askenase, P.; Atkins, E. Effects of Fever on Host Defense Mechanisms after Infection in the Lizard Dipsosaurus Dorsalis. *Br J Exp Pathol* **1978**, *59*, 76.

549. O'Grady, N.P.; Barie, P.S.; Bartlett, J.G.; Bleck, T.; Carroll, K.; Kalil, A.C.; Linden, P.; Maki, D.G.; Nierman, D.; Pasculle, W. Guidelines for Evaluation of New Fever in Critically Ill Adult Patients: 2008 Update from the American College of Critical Care Medicine and the Infectious Diseases Society of America. *Crit Care Med* **2008**, *36*, 1330–1349.

550. Laupland, K.B. Fever in the Critically Ill Medical Patient. *Crit Care Med* **2009**, *37*, S273-278.

551. Launey, Y.; Nesseler, N.; Mallédant, Y.; Seguin, P. Clinical Review: Fever in Septic ICU Patients--Friend or Foe? *Crit Care* **2011**, *15*, 222.

552. Lin, C.; Zhang, Y.; Zhang, K.; Zheng, Y.; Lu, L.; Chang, H.; Yang, H.; Yang, Y.; Wan, Y.; Wang, S.; et al. Fever Promotes T Lymphocyte Trafficking via a Thermal Sensory Pathway Involving Heat Shock Protein 90 and A4 Integrins. *Immunity* **2019**, *50*, 137-151.e6.

553. Evans, S.S.; Wang, W.C.; Bain, M.D.; Burd, R.; Ostberg, J.R.; Repasky, E.A. Fever-Range Hyperthermia Dynamically Regulates Lymphocyte Delivery to High Endothelial Venules. *Blood* **2001**, *97*, 2727–2733.

554. Wei, X.Q.; Charles, I.G.; Smith, A.; Ure, J.; Feng, G.J.; Huang, F.P.; Xu, D.; Muller, W.; Moncada, S.; Liew, F.Y. Altered Immune Responses in Mice Lacking Inducible Nitric Oxide Synthase. *Nature* **1995**, *375*, 408–411.

555. Coleman, J.W. Nitric Oxide in Immunity and Inflammation. *Int Immunopharmacol* **2001**, *1*, 1397–1406.

556. Gutierrez, H.H.; Nieves, B.; Chumley, P.; Rivera, A.; Freeman, B.A. Nitric Oxide Regulation of Superoxide-Dependent Lung Injury: Oxidant-Protective Actions of Endogenously Produced and Exogenously Administered Nitric Oxide. *Free Radic Biol Med* **1996**, *21*, 43–52.

557. Hopkins, N.; Gunning, Y.; O'Croinin, D.F.; Laffey, J.G.; McLoughlin, P. Anti-Inflammatory Effect of Augmented Nitric Oxide Production in Chronic Lung Infection. *J Pathol* **2006**, *209*, 198–205.

558. Li, X.; Ye, Y.; Zhou, X.; Zhao, K.; Huang, C.; Wu, M. Atg7 Enhances Host Defense against Infection via Down-Regulation of Superoxide but up-Regulation of Nitric Oxide. *J Immunol* **2015**, *194*, 1112–1121.

559. Anderson, C.; Roberts, R. A Comparison of the Effects of Temperature on Wound Healing in a Tropical and a Temperate Teleost. *J Fish Biol* **1975**, *7*, 173–182.

560. Ang, J.; Pierezan, F.; Kim, S.; Heckman, T.I.; Sebastiao, F.A.; Yazdi, Z.; Abdelrazek, S.M.R.; Soto, E. Use of Topical Treatments and Effects of Water Temperature on Wound Healing in Common Carp (Cyprinus Carpio). *J Zoo Wildl Med* **2021**, *52*, 103–116.

561. Melling, A.C.; Ali, B.; Scott, E.M.; Leaper, D.J. Effects of Preoperative Warming on the Incidence of Wound Infection after Clean Surgery: A Randomised Controlled Trial. *Lancet* **2001**, *358*, 876–880.

562. Plattner, O.; Akca, O.; Herbst, F.; Arkilic, C.F.; Függer, R.; Barlan, M.; Kurz, A.; Hopf, H.; Werba, A.; Sessler, D.I. The Influence of 2 Surgical Bandage Systems on Wound Tissue Oxygen Tension. *Arch Surg* **2000**, *135*, 818–822.

563. Danno, K.; Mori, N.; Toda, K.; Kobayashi, T.; Utani, A. Near-Infrared Irradiation Stimulates Cutaneous Wound Repair: Laboratory Experiments on Possible Mechanisms. *Photodermatol Photoimmunol Photomed* **2001**, *17*, 261–265.

564. Hartel, M.; Hoffmann, G.; Wente, M.N.; Martignoni, M.E.; Büchler, M.W.; Friess, H. Randomized Clinical Trial of the Influence of Local Water-Filtered Infrared A Irradiation on Wound Healing after Abdominal Surgery. *Br J Surg* **2006**, *93*, 952–960.

565. Derwin, R.; Patton, D.; Avsar, P.; Strapp, H.; Moore, Z. The Impact of Topical Agents and Dressing on PH and Temperature on Wound Healing: A Systematic, Narrative Review. *Int Wound J 19*, 1397–1408.

566. Khan, A.A.; Banwell, P.E.; Bakker, M.C.; Gillespie, P.G.; McGrouther, D.A.; Roberts, A.H. Topical Radiant Heating in Wound Healing: An Experimental Study in a Donor Site Wound Model*. *Int Wound J* **2004**, *1*, 233–240.

567. Kojima, Y.; Ono, K.; Inoue, K.; Takagi, Y.; Kikuta, K.; Nishimura, M.; Yoshida, Y.; Nakashima, Y.; Matsumae, H.; Furukawa, Y.; et al. Progranulin Expression in Advanced Human Atherosclerotic Plaque. *Atherosclerosis* **2009**, *206*, 102–108.

568. Ashcroft, G.S.; Lei, K.; Jin, W.; Longenecker, G.; Kulkarni, A.B.; Greenwell-Wild, T.; Hale-Donze, H.; McGrady, G.; Song, X.Y.; Wahl, S.M. Secretory Leukocyte Protease Inhibitor Mediates Non-Redundant Functions Necessary for Normal Wound Healing. *Nat Med* **2000**, *6*, 1147–1153.

569. Ito, H.; Ando, T.; Ogiso, H.; Arioka, Y.; Saito, K.; Seishima, M. Inhibition of Indoleamine 2,3-Dioxygenase Activity Accelerates Skin Wound Healing. *Biomaterials* **2015**, *53*, 221–228.

570. Caldwell, R.B.; Toque, H.A.; Narayanan, S.P.; Caldwell, R.W. Arginase: An Old Enzyme with New Tricks. *Trends Pharmacol Sci* **2015**, *36*, 395–405.

571. Popovic, P.J.; Zeh, H.J., III; Ochoa, J.B. Arginine and Immunity. *J Nutr* **2007**, *137*, 1681S-1686S.

572. Saleh, R.; Lee, M.-C.; Khiew, S.H.; Louis, C.; Fleetwood, A.J.; Achuthan, A.; Förster, I.; Cook, A.D.; Hamilton, J.A. CSF-1 in Inflammatory and Arthritic Pain Development. *J Immunol* **2018**, *201*, 2042–2053.

573. Li, Y.; Jalili, R.B.; Ghahary, A. Accelerating Skin Wound Healing by M-CSF through Generating SSEA-1 and -3 Stem Cells in the Injured Sites. *Sci Rep* **2016**, *6*, 28979.

574. Zhang, M.-Z.; Yao, B.; Yang, S.; Jiang, L.; Wang, S.; Fan, X.; Yin, H.; Wong, K.; Miyazawa, T.; Chen, J.; et al. CSF-1 Signaling Mediates Recovery from Acute Kidney Injury. *J Clin Invest* **2012**, *122*, 4519–4532.

575. Kawahara, Y.; Nakase, Y.; Isomoto, Y.; Matsuda, N.; Amagase, K.; Kato, S.; Takeuchi, K. Role of Macrophage Colony-Stimulating Factor (M-CSF)-Dependent Macrophages in Gastric Ulcer Healing in Mice. *J Physiol Pharmacol* **2011**, *62*, 441–448.

576. Wu, L.; Yu, Y.L.; Galiano, R.D.; Roth, S.I.; Mustoe, T.A. Macrophage Colony-Stimulating Factor Accelerates Wound Healing and Upregulates TGF-Beta1 MRNA Levels through Tissue Macrophages. *J Surg Res* **1997**, *72*, 162–169.

577. Raja, S.K.; Garcia, M.S.; Isseroff, R.R. Wound Re-Epithelialization: Modulating Keratinocyte Migration in Wound Healing. *Front Biosci* **2007**, *12*, 2849–2868.

578. Hasday, J.D.; Thompson, C.; Singh, I.S. Fever, Immunity, and Molecular Adaptations. *Compr Physiol* **2014**, *4*, 109–148.

579. Graham, J.L.; Mady, R.P.; Greives, T.J. Experimental Immune Activation Using a Mild Antigen Decreases Reproductive Success in Free-Living Female Dark-Eyed Juncos (Junco Hyemalis). *Can J Zool* **2017**, *95*, 263–269.

580. Souabni, H.; Wien, F.; Bizouarn, T.; Houée-Levin, C.; Réfrégiers, M.; Baciou, L. The Physicochemical Properties of Membranes Correlate with the NADPH Oxidase Activity. *Biochim Biophys Acta Gen Subj* **2017**, *1861*, 3520–3530.

581. Ostberg, J.R.; Repasky, E.A. Comparison of the Effects of Two Different Whole Body Hyperthermia Protocols on the Distribution of Murine Leukocyte Populations. *Int J Hyperthermia* **2000**, *16*, 29–43.

582. Ellis, G.S.; Carlson, D.E.; Hester, L.; He, J.-R.; Bagby, G.J.; Singh, I.S.; Hasday, J.D. G-CSF, but Not Corticosterone, Mediates Circulating Neutrophilia Induced by Febrile-Range Hyperthermia. *J Appl Physiol (1985)* **2005**, *98*, 1799–1804.

583. Shah, N.G.; Tulapurkar, M.E.; Damarla, M.; Singh, I.S.; Goldblum, S.E.; Shapiro, P.; Hasday, J.D. Febrile-Range Hyperthermia Augments Reversible TNF-α-Induced Hyperpermeability in Human Microvascular Lung Endothelial Cells. *Int J Hyperthermia* **2012**, *28*, 627–635.

584. Lipke, A.B.; Matute-Bello, G.; Herrero, R.; Kurahashi, K.; Wong, V.A.; Mongovin, S.M.; Martin, T.R. Febrile-Range Hyperthermia Augments Lipopolysaccharide-

Induced Lung Injury by a Mechanism of Enhanced Alveolar Epithelial Apoptosis. *J Immunol* **2010**, *184*, 3801–3813.

585. Fang, F.C. Antimicrobial Reactive Oxygen and Nitrogen Species: Concepts and Controversies. *Nat Rev Microbiol* **2004**, *2*, 820–832.

586. Kolbert, Z.; Barroso, J.B.; Brouquisse, R.; Corpas, F.J.; Gupta, K.J.; Lindermayr, C.; Loake, G.J.; Palma, J.M.; Petřivalský, M.; Wendehenne, D.; et al. A Forty Year Journey: The Generation and Roles of NO in Plants. *Nitric Oxide* **2019**, *93*, 53–70.

587. Steiner, A.A.; Romanovsky, A.A. Energy Trade-Offs in Host Defense: Immunology Meets Physiology. *Trends Endocrinol Metab* **2019**, *30*, 875–878.

588. Wang, A.; Medzhitov, R. Counting Calories: The Cost of Inflammation. *Cell* **2019**, *177*, 223–224.

589. Romanovsky, A.A.; Székely, M. Fever and Hypothermia: Two Adaptive Thermoregulatory Responses to Systemic Inflammation. *Med Hypotheses* **1998**, *50*, 219–226.

590. Boltaña, S.; Sanhueza, N.; Aguilar, A.; Gallardo-Escarate, C.; Arriagada, G.; Valdes, J.A.; Soto, D.; Quiñones, R.A. Influences of Thermal Environment on Fish Growth. *Ecol Evol* **2017**, *7*, 6814–6825.

591. Feng, Q. Temperature Sensing by Thermal TRP Channels: Thermodynamic Basis and Molecular Insights. *Curr Top Membr* **2014**, *74*, 19–50.

592. Song, K.; Wang, H.; Kamm, G.B.; Pohle, J.; Reis, F. de C.; Heppenstall, P.; Wende, H.; Siemens, J. The TRPM2 Channel Is a Hypothalamic Heat Sensor That Limits Fever and Can Drive Hypothermia. *Science* **2016**, *353*, 1393–1398.